



<https://theses.gla.ac.uk/>

Theses Digitisation:

<https://www.gla.ac.uk/myglasgow/research/enlighten/theses/digitisation/>

This is a digitised version of the original print thesis.

Copyright and moral rights for this work are retained by the author

A copy can be downloaded for personal non-commercial research or study,
without prior permission or charge

This work cannot be reproduced or quoted extensively from without first
obtaining permission in writing from the author

The content must not be changed in any way or sold commercially in any
format or medium without the formal permission of the author

When referring to this work, full bibliographic details including the author,
title, awarding institution and date of the thesis must be given

Enlighten: Theses

<https://theses.gla.ac.uk/>
research-enlighten@glasgow.ac.uk

**Effects of increased dosage of the *Plp* gene:
a study in transgenic mice**

A thesis presented to the Faculty of Veterinary Medicine,
University of Glasgow

for the degree of
Doctor of Philosophy

September 1997

©

Thomas James Anderson

ProQuest Number: 10992042

All rights reserved

INFORMATION TO ALL USERS

The quality of this reproduction is dependent upon the quality of the copy submitted.

In the unlikely event that the author did not send a complete manuscript and there are missing pages, these will be noted. Also, if material had to be removed, a note will indicate the deletion.



ProQuest 10992042

Published by ProQuest LLC (2018). Copyright of the Dissertation is held by the Author.

All rights reserved.

This work is protected against unauthorized copying under Title 17, United States Code
Microform Edition © ProQuest LLC.

ProQuest LLC.
789 East Eisenhower Parkway
P.O. Box 1346
Ann Arbor, MI 48106 – 1346

GLASGOW
UNIVERSITY
LIBRARY

Abstract

The *Plp* gene encodes two proteins (proteolipid protein and DM20), by alternative splicing of the primary transcript, that between them account for greater than 50% of total myelin protein in the central nervous system. Though the proteolipid protein is thought to have a structural role in the compaction of the myelin sheath the role of the DM20 protein isoform remains uncertain but is speculated to involve oligodendrocyte development. The *Plp* gene has been strongly conserved during evolution, and across species, and it is well recognised that its mutation is involved with dysmyelination. It has become increasingly clear that as well as mutations altering the nucleotide sequence being associated with disease that duplications of the gene locus, without nucleotide changes, are also significant in disease aetiopathogenesis in man. This project describes the phenotypic consequences of extra copies of the *Plp* gene on two lines of transgenic mice (#66 and #72) in relation to myelin gene expression.

Mice homozygous for the two transgenic cassettes dysmyelinate, though they are affected to different degrees. The level of *Plp* gene transcription is of a similar order to wild type litter mates suggesting that this is not a consequence of insufficient gene transcription. There is an increase in the total glial cell density during development suggesting a change in the dynamics of the glial cell population. Oligodendrocytes in these mice appear to be compromised in their ability to elaborate a myelin sheath. The myelin sheath that is formed is normally compacted.

Myelination in mice hemizygous for the two transgenic cassettes is indistinguishable from their wild type litter mates, though there is evidence for an increase in the total glial cell density during development. However, as hemizygous mice age they develop tract specific neurodegeneration which exhibits a specific temporal progression. This process is characterised by the development of abnormal myelin loops and an axonopathy. Eventually there is extensive demyelination but it primarily affects tracts with narrower fibres. Close examination of the homozygous mice demonstrated that they also develop demyelination, superimposed on the dysmyelinated background, which contributes to the characteristics of their phenotype.

As an incidental observation these transgenes were shown to lead to the incorporation of the PLP isoform in compact myelin of the peripheral nervous system. Further evaluation of this phenomenon indicated that Schwann cells from these transgenic mice are capable of differential targeting of the PLP and DM20

protein isoforms. This has potential implications for the trafficking of these two protein isoforms in oligodendrocytes.

To
Pamela and Robert who have been faced with far greater challenges in
life than I
and
my parents for not asking why

List of Contents

Abstract.....	i
Dedication.....	iii
List of Contents	iv
List of Figures.....	xii
List of Tables.....	xvi
Declaration	xvii
Acknowledgements	xviii
1. Introduction	1
1.1 Background.....	2
1.2 Myelination.....	3
1.2.1 The composition and structure of myelin.....	3
1.2.2 The <i>Plp</i> gene locus	12
1.2.3 Regulation of <i>Plp</i> gene expression and co-ordinate expression of the myelin genes.....	16
1.2.4 The relationship between axons and glia in development of the myelin sheath.....	23
1.3 Abnormal development and loss of myelin.....	24
1.3.1 Dysmyelination and demyelination in the CNS	24
1.3.2 Naturally occurring mutants with abnormal myelination.....	26
1.4 Experimental strategies for the manipulation of myelination	34
1.4.1 Expression of cloned genes	34
1.4.2 Methods of creating transgenic animals	35
1.4.3 Other genetically engineered myelin mutants	39

1.5 Aims of thesis	39
2. Materials and Methods - General Techniques.....	42
2.1 Tissue fixation and processing	43
2.1.1 Fixatives	43
2.1.2 Fixation techniques.....	43
2.2 Processing.....	44
2.2.1 Paraffin wax processing	44
2.2.2 Resin processing.....	44
2.2.3 Cryo-preservation.....	44
2.2.4 Preparation of sections	45
2.3 Staining techniques.....	45
2.3.1 Light microscopy.....	45
2.3.2 Electron microscopy.....	46
2.4 Microbiological manipulations.....	46
2.4.1 Bacterial media.....	46
2.4.2 Competent cell preparation.....	47
2.4.3 Transformations.....	47
2.4.4 Plasmid preparations	48
2.5 Isolation and manipulation of nucleic acids	48
2.5.1 Isolation of nucleic acids from tissues.....	48
2.5.2 Polymerase chain reaction (PCR).....	52
2.5.3 Southern transfer	52
2.5.4 Analysis of transcripts	55

2.6 <i>Analysis of proteins</i>	60
2.6.1 Isolation of protein from tissue.....	60
2.6.2 Western blotting	60
2.7 <i>Preparation of radiolabelled probes</i>	61
2.7.1 Isolation of DNA fragments from agarose gels.....	61
2.7.2 Radiolabelling.....	61
2.8 <i>In situ</i> hybridisation (ISH).....	62
2.8.1 ³⁵ S riboprobes.....	62
2.8.2 ISH protocol	63
2.9 Immunocytochemistry	68
2.9.1 Tissue sections.....	68
2.9.2 Teased fibres.....	72
2.10 Morphometry	72
2.10.1 Glial cell quantification	72
2.10.2 Myelin thickness.....	73
2.10.3 Myelin density	74
2.11 Statistical methods.....	74
2.12 Image recording.....	74
2.12.1 Photomicrographs.....	74
2.12.2 Immunofluorescent photography.....	74
2.12.3 Confocal microscopy	74
2.12.4 Electronmicroscopy	75
2.12.5 Image presentation.....	75

2.13 Growth of mice.....	75
3. Materials and methods - Genotyping and breeding of transgenic mice.....	76
3.1 Introduction	77
3.2 genomic DNA extraction (gDNA)	77
3.2.1 QuiAMP gDNA extraction.....	78
3.3 PCR genotyping.....	79
3.3.1 #66 and #72 mice.....	79
3.3.2 <i>Plp</i> Tag1 and <i>Dm20</i> Tag2 mice.....	79
3.3.3 <i>Plp</i> ^{<i>j</i>} carrier females.....	79
3.4 Southern blot assessment of #66 and #72 transgene zygosity.....	80
3.4.1 gDNA digestion.....	80
3.4.2 Southern transfer	80
3.4.3 Hybridisation probes	80
3.5 Breeding of transgenic mice and <i>Plp</i> ^{<i>j</i>} crosses.....	81
3.6 Discussion.....	82
4. Late onset neurodegeneration in mice hemizygous for the #66 and #72 transgenes.....	89
4.1 Background.....	90
4.2 Aims	90
4.3 Methods	90
4.3.1 Mouse breeding	91
4.3.2 Preparation of tissue	91
4.3.3 Histopathology	91
4.3.4 Immunocytochemistry.....	91

4.3.5 Myelin morphometry, ultrastructure of myelin and glial cells.....	93
4.3.6 Glial cell quantification	93
4.3.7 Dead cell density	93
4.3.8 Transcript analysis.....	93
4.3.9 CNS protein analysis	94
4.4 Results	94
4.4.1 Phenotypic characteristics	95
4.4.2 Pathology of neurodegeneration.....	95
4.4.3 Glial cell density.....	97
4.4.4 Dead cell density	97
4.4.5 Myelin morphometry.....	97
4.4.6 Oligodendrocyte and axon ultrastructure	98
4.4.7 Gene expression.....	98
4.4.8 Summary.....	100
4.5 Discussion.....	101
5. Dysmyelination and demyelination in mice homozygous for #66 and #72 transgene cassettes.....	134
5.1 Background.....	135
5.2 Aims	135
5.3 Methods	135
5.4 Results for homozygous #72 transgenic mice	136
5.4.1 Phenotypic characteristics	136
5.4.2 Neuropathology	136
5.4.3 Glial cell density.....	137

5.4.4 Dead cell density	137
5.4.5 Myelin morphometry	137
5.4.6 Ultrastructure of oligodendrocytes and myelin	137
5.4.7 Gene expression.....	138
5.4.8 Summary of the phenotype of homozygous #72 mice	139
5.5 Results for homozygous #66 transgenic mice	140
5.5.1 Phenotypic characteristics	140
5.5.2 Neuropathology	140
5.5.3 Total glial cell density	141
5.5.4 Dead cell density	141
5.5.5 Myelin morphometry	141
5.5.6 Ultrastructure of oligodendrocytes and myelin	142
5.5.7 Gene expression.....	142
5.5.8 Summary of the phenotype of homozygous #66 mice	143
5.6 Discussion.....	144
6. Expression of <i>Plp</i> transgenes in the peripheral nervous system	171
6.1 Background.....	172
6.2 Aims	173
6.3 Methods	173
6.3.1 Mouse breeding	174
6.3.2 Immunocytochemistry	174
6.3.3 Transplant studies	174
6.3.4 Ultrastructure of myelin	175

6.3.5 Transcript analysis by RT-PCR.....	175
6.4 Results	176
6.4.1 Immunocytochemistry	176
6.4.2 Nerve transplantation study.....	176
6.4.3 Morphology	177
6.4.4 RT-PCR	177
6.5 Discussion.....	177
7. General discussion	191
8. Appendix	200
8.1 Fixatives	201
8.1.1 Buffered neutral formaldehyde, 4% (BNF).....	201
8.1.2 Karnovsky`s modified fixative (paraformaldehyde/glutaraldehyde 4%/5%).....	201
8.1.3 Periodate-lysine-paraformaldehyde.....	202
8.2 Tissue processing protocols.....	202
8.2.1 Paraffin wax processing	202
8.2.2 Resin processing.....	203
8.3 Mounting media.....	204
8.3.1 Araldite resin	204
8.4 Staining protocols and stains	204
8.4.1 Haematoxylin and eosin	204
8.4.2 haematoxylin	205
8.4.3 Staining of tissues for electronmicroscopy.....	206
8.5 Buffers	208

8.5.1 Tris buffered saline.....	208
8.5.2 Gel running buffer	208
8.5.3 SSC (Sodium chloride / sodium citrate) x20.....	209
8.5.4 TE	210
8.6 Loading dyes	210
8.7 Bacteriological media.....	210
8.7.1 Luria-Bertani medium	210
8.7.2 SOC medium	210
9. Abbreviations:.....	212
10. References	216

List of Figures

Figure 1. Proposed models for the orientation of PLP/DM20 within the myelin lipid bilayer.....	8
Figure 2. Schematic diagram illustrating the arrangement of some of the other major myelin proteins in CNS and PNS myelin.....	10
Figure 3. Organisation of the <i>Plp</i> gene. (a) The arrangement of exons (with sizes) and introns..	14
Figure 4. Semi-quantitative RT-PCR analysis of <i>Plp:Dm20</i> ratios in spinal cord....	20
Figure 5. Example of gDNA digested with <i>Bam</i> HI run out on a 0.7% agarose gel immediately prior to Southern transfer.....	54
Figure 6. Methylene blue stained northern filter.....	59
Figure 7. Generation of the PLP-1 probe for <i>in-situ</i> hybridisation.	67
Figure 8. Assessment of the quality of gDNA	83
Figure 9. The position of primers to produce a transgene specific product from genomic DNA.....	84
Figure 10. Products of PCR reactions used for identification of #66/#72, <i>Plp</i> Tag1 and <i>Dm20</i> Tag2 transgenes	86
Figure 11. Identification of <i>Plp</i> ^{plp} carrier females by PCR of gDNA and subsequent <i>Dde</i> I digest.....	87
Figure 12. Examples of autoradiographs of Southern blots using probe B6.....	88
Figure 13. Schematic diagram of digests for the liberation of DNA fragments used for northern hybridisation.....	108
Figure 14. Body weight of mice hemizygous for #66 and #72 transgenes	109
Figure 15. Transverse sections of brain from aged wild type and hemizygous #66 and #72 mice.....	110
Figure 16. Tract specific distribution of lesions in the development of demyelination in #66 and #72 hemizygous mice	111

Figure 17. Vacuolation of the grey and white matter in a hemizygous #72 mouse stained for PLP/DM20.....	114
Figure 18. Corrected total glial cell density in cervical cord white matter	115
Figure 19. Corrected white matter total glial cell count in cervical cord.....	116
Figure 20. Microglia in area of neurodegeneration in aged hemizygous mouse....	117
Figure 21. Dead cell densities in the white matter of cervical cord in 20 day hemizygous #66 and #72 mice and their wild type litter mates.	118
Figure 22. Morphometric analysis of myelin in the cervical cord of hemizygous #66 and #72 mice at P20 and P60	119
Figure 23. Electronmicrograph of the early changes associated with hemizygosity for the #66 and #72 transgenes.....	121
Figure 24. Electronmicrograph of the late changes associated with hemizygosity for the #66 and #72 transgenes.....	122
Figure 25. Electronmicrograph of the abnormalities of the inner tongue of an oligodendrocyte from a mouse hemizygous for the #66 transgen.....	124
Figure 26. Immunostaining for myelin proteins and phosphorylated NF-H (SMI-31) in areas of neurodegeneration in aged hemizygous #66 and #72 mice	125
Figure 27. Microgliosis and astrocytosis in aged mice hemizygous for #66 and #72 transgenes	127
Figure 28. T cells in the brain of mice hemizygous for the #72 transgene.	129
Figure 29. Expression of myelin genes in 20 day and aged mice and their wild type littermates showing autoradiographs of northern hybridisation, RT-PCR and western analysis.....	131
Figure 30. <i>In-situ</i> hybridisation (PLP-1) of transverse sections of brains from hemizygous mice	133
Figure 31. Body weights of homozygous #66 and #72 mice and wild type mice..	148
Figure 32. Abnormalities of myelination in homozygous #66 and #72 mice	149
Figure 33. Total glial cell density in homozygous #66 and # 72mice.....	153

Figure 34. Total glial cell numbers in white matter in homozygous #66 and # 72 mice	154
Figure 35. Estimates of dead cells in cervical cords of #66 and #72 homozygous mice at P20.	155
Figure 36. Myelin morphometry in #66 and #72 homozygous mice at P20 and P60	156
Figure 37. Electronmicrograph of the ultrastructure of myelin from the ventral columns of a homozygous #72 mouse.....	159
Figure 38. Electronmicrograph of spinal cord white matter at P20	160
Figure 39. Electronmicrographs of spinal cord white matter at P60 in #72 homozygous mice.....	161
Figure 40. Electronmicrograph of spinal cord white matter of a homozygous #66 (P3) mouse.....	163
Figure 41. Electronmicrograph of spinal cord white matter of a wild type (P3) mouse.....	165
Figure 42. Ultrastructure of developing (P10) homozygous #66 oligodendrocyte and myelin	166
Figure 43. MBP immunostaining showing reduced immunoreactivity at P60 in thoracic cord reflecting the reduced amount of myelin present.	168
Figure 44. Transcription of the <i>Plp</i> (PLP-1) and <i>Mobp</i> genes in homozygous #66 and #72 mice at P20.	169
Figure 45. <i>In-situ</i> hybridisation with PLP-1 of cervical cord from homozygous #66 and #72 mice and wild type.....	170
Figure 46. PLP/DM20 and P ₀ immunostaining in wild type CNS and PNS.	181
Figure 47. Immunostaining of PNS myelin in a homozygous #72 mouse.....	183
Figure 48. The distribution of <i>Plp</i> transgene derived PLP/DM20 (green) proteins in the <i>Plp^{plp}/Y</i> PNS.	184
Figure 49. Unmerged confocal images of paraffin sections of sciatic nerve double stained for PLP/DM20 and P ₀	187

Figure 50. Unmerged confocal images of paraffin sections of sciatic nerve from a nude mouse that received a graft of sciatic nerve from a homozygous #72 mouse, double stained for PLP/DM20 and P ₀	188
Figure 51. Electronmicrographs of PNS myelin sheaths from the ventral nerve roots of a wild type mouse and a homozygous #72 litter mate at 60 days	189
Figure 52. RT-PCR data illustrating the behaviour of <i>Plp</i> transgenes on a wild type and <i>Plp</i> ^l <i>Plp</i> backgrounds.	190
Figure 53. Northern hybridisation analysis of <i>Plp</i> gene transcription in #66 and #72 mice at P20.	194

List of Tables

Table 1. Summary of naturally occurring <i>Plp</i> mutant animals and mutations found in man	33
Table 2. Primer pairs used for transcript analysis.	58
Table 3. Antibodies, sources, dilutions and links used in PAP immunostaining.	70
Table 4. Antibodies, sources, dilutions and links used in fluorescent immunostaining.	71
Table 5. Summary of PCR primers used for the genotyping of transgenic and <i>Plp^{jp}</i> mice.	85
Table 6. Antibodies, dilutions, sources and links used in immunostaining for microglia and T cells in mice hemizygous for #66 and #72 transgenes.....	107

Declaration

I, Thomas James Anderson, do hereby declare that the carried work out in this thesis is original, was carried out by myself or with due acknowledgement, and has not been presented for the award of a degree at any other University.

Acknowledgements

I would like to thank my supervisor, Professor Ian Griffiths, and Dr Paul Montague for supporting me through this project and challenging me to think about how to approach questions. Their continued interest and considered guidance is truly appreciated.

This project has benefited from the skilled assistance of the technical staff of the Applied Neurobiology Group who have provided tuition, assistance (particularly in tissue preparation) and most importantly their understanding. I would like to thank Jennifer Barrie, Mailise McCulloch, Evangelos Kyriakides, Douglas Kirkam, Eilidh McPhee and Nan Deary. Douglas Kirkham was responsible for the western analysis presented in Figure 29, page 131.

I have been supported in my studies by a Scholarship from the University of Glasgow Faculty of Veterinary Medicine, to which I will always be grateful for this unique opportunity. These studies were pursued under the auspices of a succession of Departmental Heads for whom I am grateful for continuing to encourage and support me: Professor Neil Gorman, Dr Mike Harvey and Professor David Bennett. I will always be grateful to Neil Gorman for encouraging me in my career. Likewise, I will also always be grateful to Dr Martin Sullivan for being my conscience.

Many of the images in this thesis have been taken by Alan May, whose skill as a photographer has contributed greatly to the quality of the illustrations. The electronmicrographs were taken by Professor Ian Griffiths. Images were scanned by Susan Cain and Viki Dale of the Faculty of Veterinary Medicine.

I would also like to acknowledge the assistance of Dr Linda Terry of the Department of Veterinary Pathology, Royal (Dick) School of Veterinary Studies, University of Edinburgh in establishing the immunostaining for leukocyte markers. I also appreciate the advice from Professor Stuart Reid on approaching statistical analysis and interpretation.

I would like to acknowledge the staff of the Animal House for their skill in caring for the mouse colonies and helping me keep it organised.

The post-graduate students lot is improved by working within a supportive environment, such as I have found in the Applied Neurobiology Group. I would like to acknowledge the support and friendship of Dr Peter Dickinson, Dr Christine Thomson and Dr Demetrius Vouyiouklis. I would also like to thank my fellow students for putting up with me: Pamela Johnston, Helen King and Donald Yool.

Lastly, I would like to thank Pete for his support and friendship and Pamela for believing in me.

1. Introduction

1.1 Background

Diseases involving the perturbation of myelin are responsible for a significant degree of morbidity and mortality in the human and animal populations and furthering their understanding is an important feature of biomedical research. The use of animal models has featured strongly in advancing understanding and the investigation of a new neurological phenotype potentially offers to yield further information. Through the understanding of the abnormalities associated with gene dysfunction that result in abnormal myelination not only can inferences be made about probable gene function but experimental models of disease can be developed.

The stimulation for the work presented in this thesis, a study of perturbed myelination related to increased gene dosage of the *Plp* gene, stems from the unexpected development of a neurological phenotype in transgenic mice harbouring extra copies of the *Plp* gene. These mice were created as part of a larger experiment to address the rescue of the *Plp*⁰ phenotype, using an approach similar to that which had been successful with the shiverer (*Mbp*^{shi}) mouse. This hypomyelinating mutant has a deletion of the myelin basic protein (MBP) gene, encoding for the second most abundant family of proteins in CNS myelin, and was phenotypically rescued by transgenic complementation.

Two lines of transgenic mice complemented with extra copies of the wild type *Plp* gene were generated by Readhead *et al*'s original experiments, with line #66 carrying a greater number of gene copies than #72 and it was the homozygous #66 mice that exhibited neurological abnormalities. The initial study of the homozygous #66 mice confirmed that they were dysmyelinated which contrasted with the initial data on homozygous #72 which described these mice as minimally dysmyelinated, implying a gradation in phenotypic severity apparently related to gene dosage. These observations justified further study to explore the development of the two phenotypes in relation to the progress of myelination and *Plp* gene expression. As these studies proceeded continuing behavioural studies on the mice revealed a late onset neurological phenotype in homozygous #72 mice and in both hemizygous #66 and #72 mice. These observations broadened the study to include characterising the late onset phenotype, in which demyelination and an axonopathy were prominent features.

Though point mutations resulting in qualitative changes in the *Plp* gene were well recognised in causing perturbations of myelination the development of an abnormal

phenotype following the introduction of extra copies of a wild type gene (a quantitative change) was hardly recognised. This observation suggested that abnormalities of myelination could stem from causes other than the presence of an abnormal myelin protein.

The unexpected observation of the incorporation of the PLP/DM20 protein isoforms into the myelin of the peripheral nervous system (PNS) became the basis of a separate study into the behaviour of *Plp* transgenes in the PNS. This was further expanded by introducing *Plp* and *Dm20* minigenes to assess the contribution of the two isoform messages and products to this phenomenon.

Though at the time of creation of the #66 and #72 mice *Plp* gene dosage was only suspected as being involved in the aetiopathogenesis of disease this picture was to change as the project developed and gene dosage is now recognised to be a major factor in the development of Pelizaeus-Merzbacher disease (PMD), the human clinical syndrome for which the *Plp* mutants are good animal models. As the genetic analysis of pedigrees affected by PMD has developed it has become clearer that there is a wide spectrum of disease associated with a large and expanding group of mutations of the *Plp* gene locus.

The purpose of the introduction is to put the #66 and ##72 transgenic mice in the context of current thoughts on myelin biology and the consequences of mutation of the *Plp* gene.

1.2 Myelination

1.2.1 The composition and structure of myelin

The following description of myelin refers in the main to that found in the mammalian central nervous system (CNS), with references to PNS myelin to highlight the similarities and differences. Myelin, however, is a specialised feature of vertebrates and there are significant differences in protein composition between phyla, some of these differences and their possible significance is explored in 1.2.2.1.1 Phylogenetic evolution of the *Plp* gene (page 13).

1.2.1.1 The myelin sheath

The myelin sheath is a specialised development of the cell membrane elaborated and maintained by specialised, tissue specific cells. In the CNS these are oligodendrocytes and in the PNS the myelin forming Schwann cells (MFSC).

The myelin sheath surrounds axons in a multi-layer lamellar structure. Examination by electronmicroscopy (EM) demonstrates that the structure has a regular periodicity, made up of the major dense line (MDL) representing the apposition of the cytoplasmic surfaces and intra-period (IPL) which represents the apposition of the extracellular surfaces (Raine, 1984).

The presence of the myelin sheath allows the saltatory conduction of impulses thus facilitating transmission (both in terms of speed and energy consumption) and reducing the volume of axon required for fast conduction. The emergence of this structure during evolution was necessary for the development of the integrated function of the vertebrate nervous system (Rogers *et al.*, 1997).

Abnormalities of this structure due to either abnormal development (dysmyelination) or loss (demyelination) almost invariably have a profound effect on the function of the nervous system and the viability of the organism (see 1.3.1 Dysmyelination and demyelination in the CNS, page 24).

1.2.1.2 Comparison of CNS and PNS myelin

The myelin of the two divisions of the nervous system share many similarities, though several notable differences exist as they are products of different cell types in different nervous tissue environments. One of the most notable differences is the relationship between these two myelinating cells and the number of axons they ensheath. Oligodendrocytes are capable of myelinating segments of multiple axons and up to 60 may be supported by one cell, though the relationship between axon diameter and number of sheaths supported is complex (Szuchet, 1995). Conversely the Schwann cell myelinates only one axonal internode (Bunge and Fernandez-Valle, 1995). Occasionally oligodendrocytes with a Schwann cell like relationship to an individual axon are found in the developing spinal cord (Remahl & Hildebrand, 1990).

The nature of the lamellar structure is similar but the periodicity is different (CNS 10.5-11.5nm c.f. PNS 11.5-12.7nm) and CNS sheaths are thinner compared to those of the PNS for a given axonal diameter (Fraher, 1992). Schwann cells, unlike oligodendrocytes, have a basal lamina and the myelin sheath is formed from the soma of the cell whilst oligodendrocytes are not as tightly apposed to the axon (Bunge and Fernandez-Valle, 1995; Szuchet, 1995).

Compaction of the myelin sheath excludes the majority of the cytoplasm from the final structure although cytoplasmic domains do remain in both the CNS and PNS and they form a continuous cytoplasmic network that completely surrounds the

compacted regions. These are the paranodes and the Schmidt-Lanterman incisures (SLI) in the PNS (Colman *et al.*, 1996) and the lateral loops and longitudinal incisure in the CNS (Raine, 1984).

The protein composition of CNS and PNS myelin differs. Some proteins are common to both CNS and PNS myelin (for example MBP, myelin-associated glycoprotein (MAG) and 2',3'-cyclic nucleotide 3'-phosphodiesterase (CNP)). However, the proportions may differ e.g. the amount of MBP is lower in the PNS as compared to the CNS (5-15% c.f. 30% (Lees and Brostoff, 1984)). Myelin-associated oligodendrocyte basic protein (MOBP), myelin oligodendrocyte protein (MOG), oligodendrocyte-myelin glycoprotein (Ompg) are specific to the oligodendrocyte and thus the CNS (Holz *et al.*, 1996). P₀ is Schwann cell specific and detected only in the PNS (Suter, 1997). PMP22, previously thought to be exclusive to the PNS, has been localised to CNS motor neurones, though it has not been shown to be a constituent of CNS myelin (Parmantier *et al.*, 1995). The putative structure of PMP22 shares similarities with those proposed for PLP (see Figure 1, pages 8-9 and Figure 2, page 10) and it has been speculated that they have similar functions (Suter & Snipes, 1995).

1.2.1.3 The composition of central nervous system myelin

Myelin is a heterogeneous combination of proteins and lipids. A small number of constituents make up the bulk of myelin, with many of the proteins being myelin specific.

1.2.1.3.1 Lipids

Lipids make up the 70% of the dry weight of myelin (Norton and Cammer, 1984). No lipids are specific to myelin but the high proportions of galactosphingolipids, cerebroside (galactosylceramide) and sulphatide are a characteristic of myelin. Cerebroside is the most myelin specific of these lipids and is an oligodendrocyte specific marker in the CNS (Raff *et al.*, 1978).

1.2.1.3.2 Proteins

1.2.1.3.2.1 The myelin proteolipid proteins (PLP/DM20)

Proteolipids are not specific to myelin and are a general feature of the cell membranes of plants and animals and are characterised by their solubility in organic solvents, particularly chloroform/methanol mixtures (Folch & Lees, 1951). Myelin has two specific proteolipids, termed proteolipid protein (PLP) and DM20. PLP is

the major CNS myelin protein representing approximately 50% of myelin protein (Lees and Brostoff, 1984). PLP has no specific activity that can be measured to quantify its presence and is thus detected immunologically. It has been important to demonstrate that with such techniques there is no cross reactivity with non-neural proteolipids or other myelin proteins, such as MBP (Macklin *et al.*, 1982).

The PLP and DM20 protein isoforms are alternative splice products of the *Plp* gene and are size separated on a sodium dodecyl sulphate (SDS) polyacrylamide gels. PLP has an apparent molecular mass of ~24KDa and DM20 is so called because of its apparent molecular mass of ~20KDa. The actual masses are greater: PLP ~30kda; DM20 ~26.5KDa (Nave *et al.*, 1987; Stoffel *et al.*, 1983).

PLP consists of 276 amino acid residues and is highly hydrophobic, with the amino acid residues that confer this behaviour grouped into four domains, which are separated by hydrophilic domains (Lees and Brostoff, 1984). *In vivo* the hydrophobic nature of the protein is increased by acetylation with long chain fatty acids at four of the cysteine residues in PLP but only two in DM20 (Weimbs & Stoffel, 1992). Acylation is a dynamic process that occurs in myelin and is possibly related to maintenance (Bizzozero & Good, 1991). DM20 is generated from an alternate 5' splice site in exon 3 which results in a protein 35 amino acids shorter (amino acids 116-150) but otherwise identical to PLP (Nave *et al.*, 1987). The PLP-specific region of the protein is highly charged and hydrophilic.

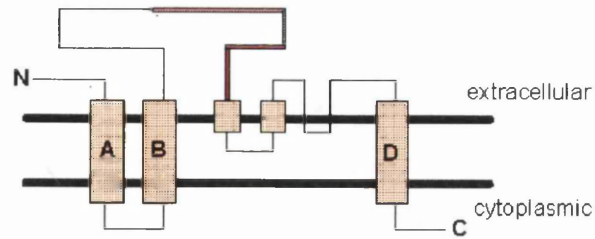
The orientation of the PLP/DM20 protein isoforms within the lipid bilayer has yet to be elucidated partially because of technical difficulties due its integral position within this structure. Models have been inferred based on considerations of available evidence, some of which is contradictory, and the similarity to other known structural proteins. These models are summarised in Figure 1 (pages 8-9). A common feature of these models is a number of transmembrane domains, with the major differences between models being the positions of the N and C terminals and the PLP specific region. For comparison a schematic representations of some of the other major myelin proteins are presented in Figure 2 (page 10).

The most recent studies place both terminals on the cytoplasmic surface, though only the C-terminus has been specifically located (Konola *et al.*, 1992). The extracellular nature of domains proposed by Laursen (1984), Popot *et al* (Popot *et al.*, 1991) and Wiembs and Stoffel (1992) are supported by the work of Greer *et al* (1996) and Gow *et al* (1997). The residues 103-116, which are adjacent to the PLP specific region, have been shown to be at the MDL (Sobel *et al.*, 1994) suggesting

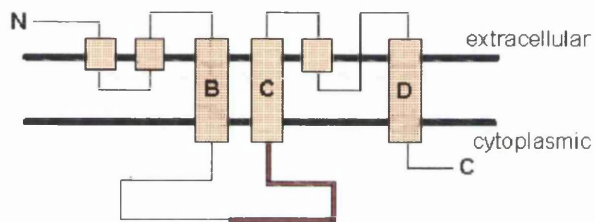
that the PLP specific region is probably also on the cytoplasmic surface. DM20 has been proposed to share the topology of PLP (Gow *et al.*, 1997).

The contribution of PLP to the IPL of compact myelin is documented where it is postulated to be an adhesive strut (Duncan *et al.*, 1987). This concept is supported by the perturbations of the IPL in myelin mutants (see 1.3.2.1 Animal models, page 26) and knockout mice (Klugmann *et al.*, 1997). It has been suggested that PLP may also be involved in the generation of the MDL (Kitagawa *et al.*, 1993; Duncan *et al.*, 1987).

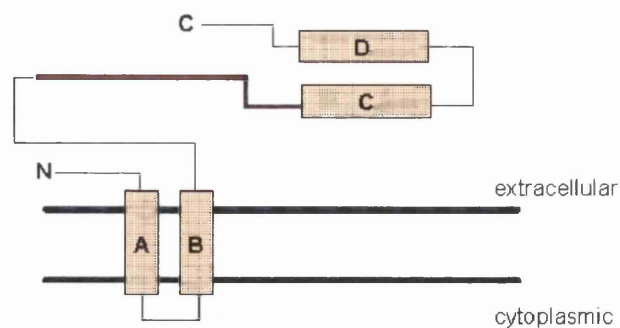
A full evaluation of the functions of PLP and DM20 has yet to be completed. The high degree of conservation of the amino acid sequences across diverse species and through evolution (see 1.2.2.1.1 Phylogenetic evolution of the *Plp* gene, page 13) is suggestive of a fundamental and crucial role for the protein-protein interactions of these products of the *Plp* gene locus. Analysis of the evolution of this gene suggests the hydrophobic transmembrane domains exhibit the strongest conservation, suggesting the arrangement of these regions within the membrane are critical and very sensitive to disruption. PLP forms hexamers under certain conditions (Smith *et al.*, 1984) and such an assembly could be sensitive to disruptive changes. Examination of the DM-like family of proteins shows similarity with channel forming regions of the nicotinic acetylcholine receptor and glutamate receptor macromolecular complexes (Kitagawa *et al.*, 1993) (also see 1.2.2.1.1 Phylogenetic evolution of the *Plp* gene, page 13). The proposed structure of the PLP/DM20 protein isoforms places them in a heterogeneous group of membrane bound 'four helix bundle' proteins (Nave, 1996). There are several other myelin proteins (PMP22, OSP and the connexins) with a similar topology (Gow *et al.*, 1997) (also see Figure 2, page 10). Whether the PLP/DM20 proteins are members of the group of proteins, described by Wright and Tomlinson (1994), with four-transmembrane regions and having ion-channel properties is yet to be resolved. Other authors have presented evidence that PLP may form pores and be involved in ion transport (Knapp, 1996). There is also a considerable body of data suggesting roles other than that of structural proteins for the products of the *Plp* gene, pointing in particular for a role for DM20 in oligodendrocyte development (Montague and Griffiths, 1997).



(a)

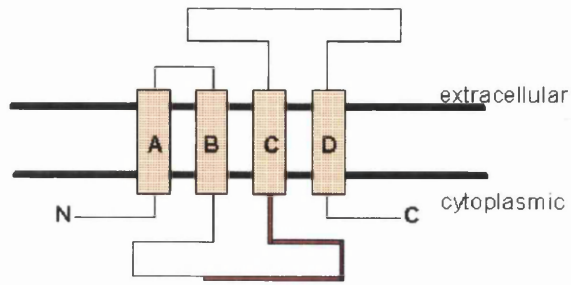


(b)

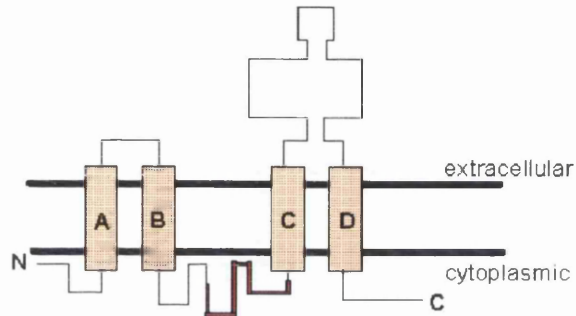


(c)

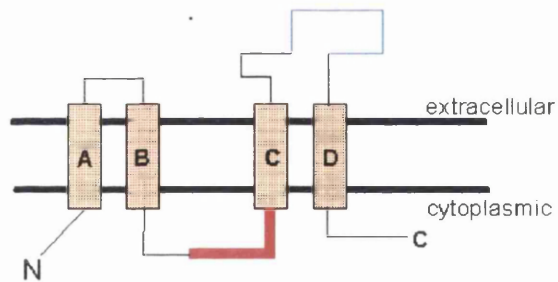
Figure 1. Proposed models for the orientation of PLP/DM20 within the myelin lipid bilayer. The proposed hydrophobic transmembranous domains are shaded (brown). The PLP specific segment is in red. (a) Stoffel *et al* (1984); (b) Laursen *et al* (1984); (c) Hudson *et al* (1989).



(d)



(e)



(f)

Figure 1 (continued). Proposed models for the orientation of PLP/DM20 within the myelin lipid bilayer. (d) Popot *et al* (1991); (e) Weimbs and Stoffel (1992); (f) Gow *et al* (1997). The blue line represents a region of the C-D loop that the authors postulate may be significant in PLP-PLP interactions and also part of the epitope recognised by B cells.

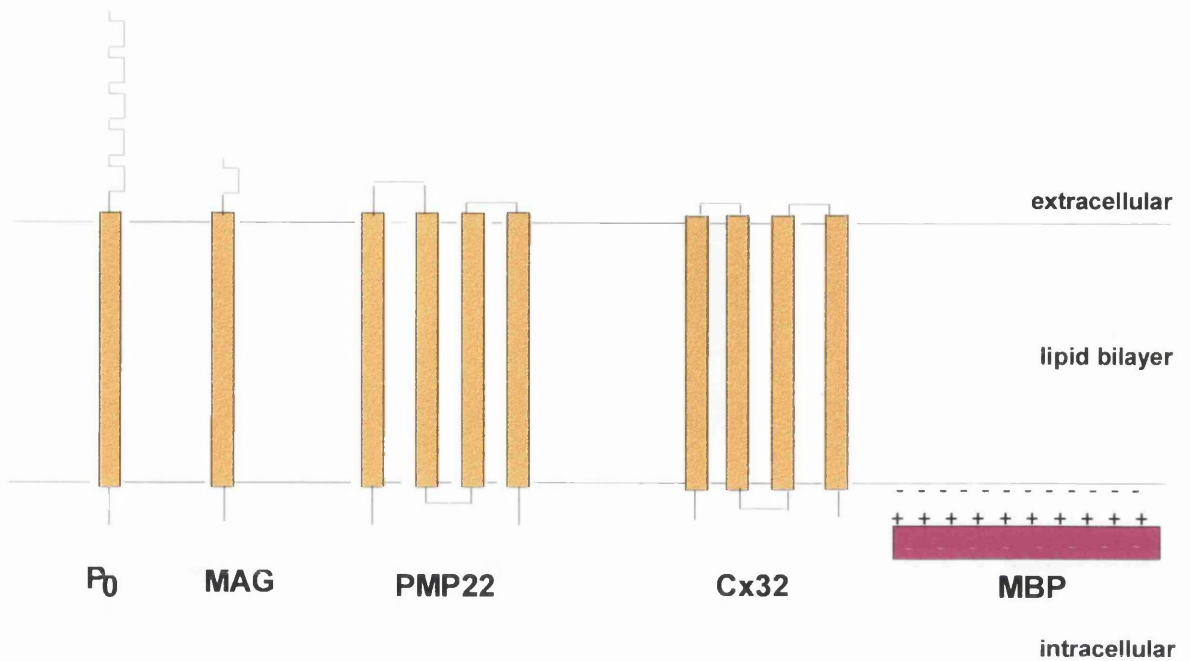


Figure 2. Schematic diagram illustrating the arrangement of some of the other major myelin proteins in CNS and PNS myelin (hydrophobic regions thought to be transmembranous domains are represented by an orange filled box). P₀ and MAG are both monotopic proteins whilst PMP22 and connexin 32 (Cx32) are polytopic, with four transmembranous domains (Snipes & Suter, 1995). MBP does not cross the lipid bilayer and appears to lie on its intracellular surface (Smith, 1992), where it is proposed to interact with the negative charge of the phosphate groups on the lipid bilayer's inner surface.

1.2.1.3.2.2 Myelin basic protein (MBP)

MBP is the other major CNS protein representing ~ 30% of total myelin. Differential gene splicing produces a family of related proteins which in rodents consists of four isoforms (Campagnoni, 1988). MBP is associated with the MDL of compact myelin (Nave, 1996) but its isoforms have different developmental profiles including expression during embryogeny, suggesting a role distinct to that of a structural component of myelin (Nakajima *et al.*, 1993). Recently a regulatory role has been suggested for one of the MBP isoforms, MBPexII, as it is preferentially targeted to the nucleus (Pedraza *et al.*, 1997).

1.2.1.3.2.3 Myelin associated glycoprotein (MAG)

MAG is predominantly found in the periaxonal regions of the CNS myelin sheath and very little is found in compact myelin (Trapp, 1990). It is specific to myelinating cells and member of the Ig superfamily and thus probably has adhesive properties (Nave, 1996). Two message isoforms are produced which show developmental regulation (Kirchhoff *et al.*, 1997). There are two protein isoforms designated L-MAG (large) and S-MAG (small) (Quarles *et al.*, 1992). These isoforms have different patterns of expression in the CNS, with L-MAG being associated with active myelination and S-MAG associated with mature myelin (Minuk & Braun, 1996). In the PNS S-MAG is the major isoform expressed during development (Nave, 1996). These different patterns of regulation of the two isoforms implies a functional difference between the isoforms but though a number are postulated none has been specifically attributed to either isoform (Minuk & Braun, 1996).

1.2.1.3.2.4 2',3'-cyclic nucleotide 3'-phosphodiesterase (CNP)

The enzyme CNP is expressed by developing oligodendrocytes (Scherer *et al.*, 1994). It is localised beneath the oligodendrocyte surface membrane and within cytoplasmic domains of the myelin sheath (De Angelis & Braun, 1996) rather than in compact myelin. It exists as two isoforms of 44 and 48kD (Campagnoni, 1988) which are differentially expressed during development (Scherer *et al.*, 1994). The specific substrate and action are uncertain but the evidence suggests roles in maintenance of the myelin sheath and oligodendrocyte differentiation (Gravel *et al.*, 1996; Trapp, 1990).

1.2.1.3.2.5 Myelin-oligodendrocyte basic protein (MOBP)

The MOBPs are a recently identified family of myelin proteins and are currently being actively characterised. MOBP message is the third most abundant mRNA species, after PLP and MBP (Yamamoto *et al.*, 1994). A number of isoforms are produced, one of which (MOBP81) is associated with development (Holz *et al.*, 1996). The MOBP family are small basic proteins of between 69 and 99 amino acids in length, which are identical from residues 1 to 68 and thus vary at the C-terminal. The expression of one abundant isoform occurs in conjunction with myelin compaction suggesting a late role in myelination and a possible role in myelin compaction (Montague *et al.*, 1997).

1.2.1.3.2.6 other minor protein constituents of CNS myelin

CNS myelin contains small amounts of other myelin specific proteins which are currently of uncertain significance. These include: myelin/oligodendrocyte glycoprotein (MOG); oligodendrocyte-myelin glycoprotein (OMpg); myelin-oligodendrocyte specific protein (MOSP) (Montague and Griffiths, 1997). Recently a new oligodendrocyte protein oligodendrocyte-specific protein (OSP) has been described (Bronstein *et al.*, 1996). The small amounts of these proteins present in myelin is not necessarily a reflection of their functional significance, which will become clearer as they are further characterised. As the recent identification of MOBP and OSP illustrates there are likely to be other proteins as yet uncharacterised.

1.2.2 The *Plp* gene locus

1.2.2.1 The organisation of the *Plp* gene

The single *Plp* gene locus is located on the X-chromosome (at Xq21.33-22 in man) (Mattei *et al.*, 1986; Willard & Riordan, 1985). It is a complex transcriptional unit encoding for at least two protein isoforms. The molecular architecture is summarised in Figure 3, page 14. It is greater than 17Kb in size and is considered to comprise seven exons and six introns, though an eighth exon has been proposed by Kamholz *et al.* (1992). In rodents two transcription initiation sites have been described, at nucleotides -130 and -160, but there is heterogeneity around the major initiation point between these sites (Macklin *et al.*, 1987; Bradley & Jenkison, 1973). The *Plp* gene has three polyadenylation sites resulting in heterogeneous population of mRNAs, with three major transcripts observed: 1.5-1.6Kb; 2.4-2.6Kb and 3.0-3.4Kb. The proportions of these transcripts varies between species and on northern hybridisation the following patterns are observed: the rat has a major band

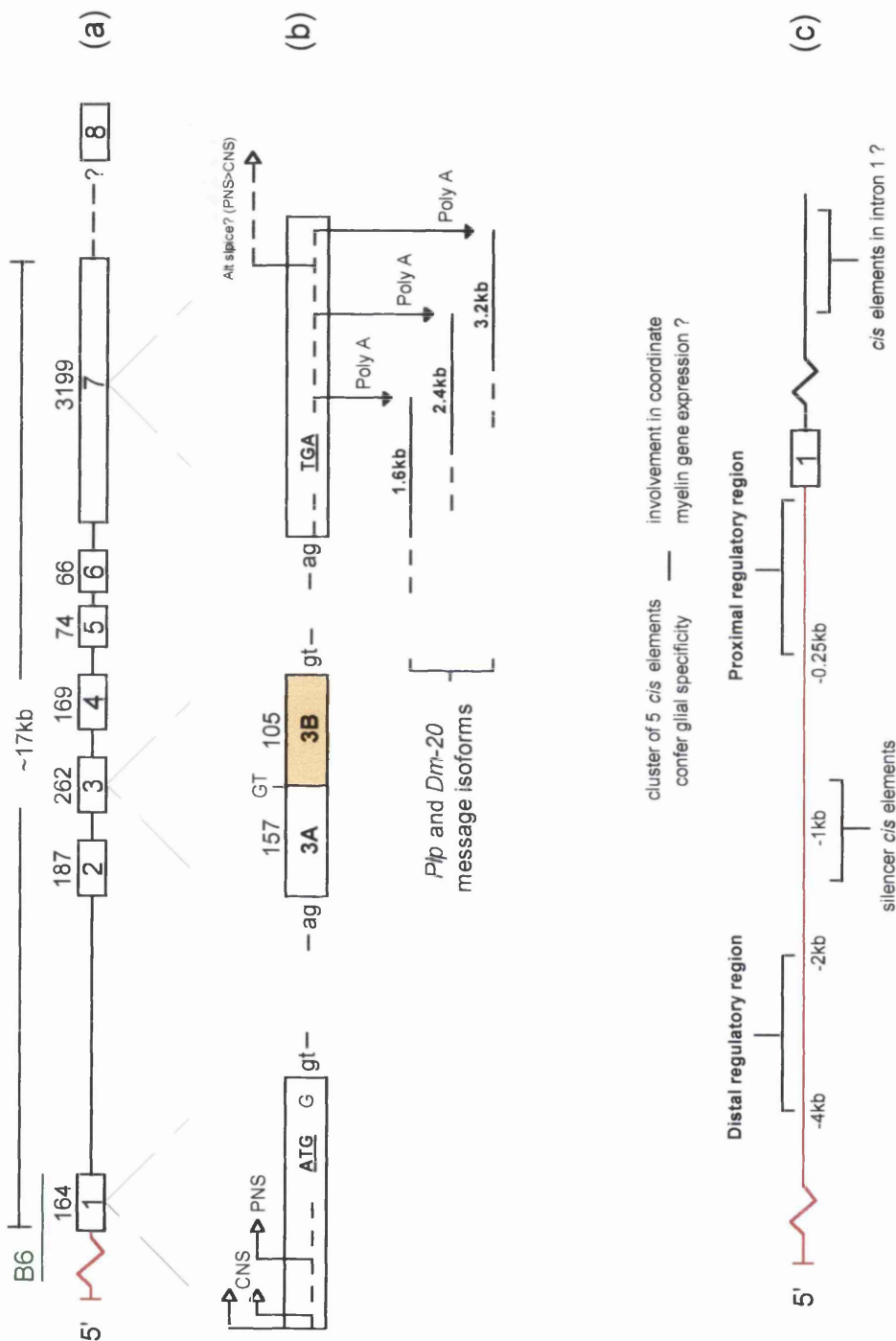


Figure 3. Organisation of the mouse *Plp* gene. (a) The arrangement of exons (with sizes) and introns. The position of the B6 fragment used in Southern analysis is marked (green). A ? is placed by exon 8 as this has only been reported in one study; (b) Sequences controlling message isoform synthesis. Exon 3 contains the alternate splice site giving rise to the *Dm-20* isoform in which exon 3B (shaded) is deleted from the final transcript; (c) A putative regulatory map encompassing the 5' non-coding region (red) and intron 1.

PLP-like proteins appear to have developed about 400 million years ago, before the evolution of tetrapods, in the CNS myelin of *Sarcopterygii* fish (lung fish) and the Coelacanth (Waehneltd & Malotka, 1989; Waehneltd *et al.*, 1986). However, DM20 appears to be a relatively recent development as fish (Colman *et al.*, 1996) and amphibia (Schliess & Stoffel, 1991) do not express a DM20 protein and a *Dm20* message cannot be detected in *Xenopus* (Nave *et al.*, 1993). Neither the DM-like or M6 genes contain the PLP-specific segment. These observations support the idea that the present vertebrate *Plp* gene has developed from a duplication of one of the DM-like genes and the acquisition of the PLP-specific segment (Colman *et al.*, 1996). Other postulations for the generation of DM20 are a *de novo* mutation creating a splice site in exon 3 of a *Plp* like gene in post-amphibian tetrapods (Schliess & Stoffel, 1991), or alternatively the loss of the splice site in amphibia.

Expression of the DM-like gene family appears to have a greater diversity of tissue expression than the *Plp* gene. Though M6b is expressed in developing glia (Yan *et al.*, 1996) it is also expressed in neurones whilst M6a is expressed in developing neurones, renal tubules, olfactory epithelium and choroid plexus (Yan *et al.*, 1993). DM α and γ are expressed in shark white matter tracts whilst DM β is expressed in neurones, kidney and choroid plexus but not white matter (Kitagawa *et al.*, 1993). The early appearance of the M6 message in mouse CNS suggests a role in the development of a number of neural cell types (Yan *et al.*, 1996).

The question as to why PLP, a tetraspan protein, appears to have replaced P₀, a monotopic protein, in myelin compaction remains unresolved and intriguing.

1.2.2.2 Developmental expression of the *Plp* gene in the CNS

This data has been accrued from a range of species, various areas of the CNS and using a range of experimental techniques with varying sensitivities. Data also vary between descriptions of gene activity describing the presence of transcript, product or both. However, general patterns of gene transcription and translation can be deduced.

Plp/Dm20 transcripts have been documented in embryonic nervous tissue including brain (Ikenaka *et al.*, 1992), spinal cord (Timsit *et al.*, 1995; Timsit *et al.*, 1992), and PNS (Yu *et al.*, 1994; Timsit *et al.*, 1995; Timsit *et al.*, 1992) (also see 1.2.3.3 Expression of the *Plp* gene in the PNS, page 23). The first myelin sheaths are seen at E18 in the mouse and thus such transcripts are in tissues in which the oligodendroglia are immature and non-myelinating. The *Dm20* transcript is the sole/predominant transcript at this stage. Expression in non-neural tissue types has been shown to be predominately *Dm20*, with both transcript and protein being

described in some organs (Pribyl *et al.*, 1996). Likewise, in the PNS transcripts are also predominantly *Dm20*. The significance of these *Dm20* transcripts has not been established but in consideration with other observations lends credence to the idea of a developmental role for the gene products and in particular for *Dm20*.

There is controversy over the cell types responsible for the *Plp* gene transcripts in embryonic CNS tissue and progenitors of other cell types have been proposed as expressing these transcripts (Dickinson *et al.*, 1996; Richardson *et al.*, 1997; Timsit *et al.*, 1995; Yu *et al.*, 1994). This arises from difficulties in confident identification of the immature cells shown by *in situ* hybridisation to express *Plp/Dm20*. There is a lack of a robust marker for early committed oligodendroblasts and there is the possibility that expressing cells may be pluripotential (Williams *et al.*, 1991). However, some of these *Dm20* positive cells have been identified as being of the O2-A lineage and thus destined to ultimately differentiate into oligodendrocytes (Dickinson *et al.*, 1996).

In mice the *Plp/Dm20* message isoform population is *Dm20* dominant from E12-E16, equivalent from E17-P1 and is characterised by a *Plp* dominance (3:1) during myelination and myelin maintenance (Figure 4, page 20). After myelination starts and during myelin maintenance the *Plp* isoform is the dominant message and PLP protein is the dominant isoform.

1.2.3 Regulation of *Plp* gene expression and co-ordinate expression of the myelin genes

1.2.3.1 Regulation of *Plp* gene expression

Proteins are the effectors of eukaryotic cell activity and the genes that encode for them and are transcribed by the RNA polymerase II (PolII) transcriptional machinery. The co-ordinated flow of information from DNA to protein requires a complex regulatory circuit to achieve the appropriate spatial and temporal expression in co-ordination with other genes and their products. The product of transcription, termed nascent or pre-mRNA, is subject to further processing, including splicing, that influences the final mRNA population. The *Plp* gene is one of the spectrum of cellular and viral genes that are transcribed by the PolII transcriptional machinery for which the major step determining the level of mRNA is the control of initiation and thus the amounts of nascent product produced.

The current paradigm of the basic mechanisms in the control of transcription of PolII genes involves regions of gDNA sequence, termed *cis*-elements, that are recognised by a heterogeneous group of molecules termed *trans*-factors. The final

levels of protein may be influenced at other stages in the process including alternative splicing of the nascent RNA, changes RNA half life, control of translation and post-translational influences on cellular trafficking. It is important to note that message levels cannot be used as a measure of protein levels.

1.2.3.1.1.1 Transcription of the *Plp* gene

As described in 1.2.2.2 Developmental expression of the *Plp* gene in the CNS (page 15) the absolute amounts and ratios of the *Plp* and *Dm20* messages are developmentally regulated. The regulatory circuit responsible for the co-ordination of these events is complex. *Plp* gene regulation has been demonstrated (or inferred) to be effected at the levels of transcription, translation and post-translation (Montague and Griffiths, 1997). Many of these experimental regimes have studied elements of the *Plp* gene in isolation and the interpretation of such studies must be cautious as in such circumstances the behaviour of such isolated elements may be unregulated. Further problems arise from the diversity of techniques that have been employed and the use *in vitro* tissue cultures systems, particularly the use of stable cell lines the existence of which implies changes from *in vivo* gene regulation.

There are three broad areas of interest in the regulation of the *Plp* gene: the developmental changes in message ratios; the transcriptional burst of activity associated with myelination; the co-ordination of *Plp* gene expression in relation to other myelin genes.

Nuclear run-off assays (Cook *et al.*, 1992) demonstrated that the *Plp* gene is regulated principally at the level of transcription. This is in common with other myelin genes such as MBP (Cook *et al.*, 1992), and typical of genes transcribed by the PolII transcriptional machinery.

There has been intense activity directed towards identifying the potential *cis*-elements of the gene locus related to transcriptional control. Sequence analysis of the 1.5Kb upstream of the translation start codon (+1) demonstrates areas of remarkable conservation between mouse, rat and man (Janz & Stoffel, 1993). This is about 95% between -250 and +100, falling to about 50% further upstream and suggests evolutionary conservation of a region and the presence of putative *cis*-elements. Physical techniques (footprint and gel shift) and functional analysis (transfection studies and the creation of transgenic mice) have been used to confirm putative *cis*-elements and identify the associated *trans*-factors. Positive (Berndt *et al.*, 1992) and negative *cis*-regulatory elements (Nave & Lemke, 1991) have been identified in the 5' non-coding region and possibly in intron 1 (Wight *et al.*, 1993).

Tissue specific expression for genes from other systems has also been associated with enhancers in both 5' regions and introns (Lefebvre *et al.*, 1996).

In this upstream region there are two copies of the sequence AAGGGGAGGAGA, which is conserved between mouse, rat and man (-63 to -75) and has complementarity to sequences found in the 5' regions of other myelin genes (see 1.2.3.2 Co-ordinate expression of the CNS myelin genes, page 21), (Hudson *et al.*, 1996)). This sequence lies within a purine rich element of 44 purines residing on one strand (Berndt *et al.*, 1992). This element is in a region of the *Plp* gene promoter that confers maximal expression of the *Plp* gene in a variety of transfected cells and its function is sensitive to mutation (Hudson *et al.*, 1996). It is recognised by factors that are ubiquitous (Sp1) and others that are tissue specific (a brain enriched 66Kda protein with similarities to an ETS domain) (Janz & Stoffel, 1993). The ETS domain is important in glial cell development in invertebrates (Hudson *et al.*, 1996) but is also seen in neural precursors (Charron *et al.*, 1995). Another putative glial specific elements has been identified at -118 which is also found in other myelin genes (Berndt *et al.*, 1992).

A range of factors have been shown to increase *Plp* gene transcription. These include thyroid hormones, steroids, retinoic acid, PDGF (Grinspan *et al.*, 1993) and cAMP (Nave & Lemke, 1991). The thyroid hormone response element is present in both the 5' region and exon 1 presenting the possibility of both transcriptional and post-transcriptional control (Gao *et al.*, 1997) (also see 1.2.3.2 Co-ordinate expression of the CNS myelin genes, page 21). Steroids have conflicting effects *in vivo* (negative (Tsuneishi *et al.*, 1991)) and *in vitro* (positive (Zhu *et al.*, 1994)). Retinoic acid has been demonstrated to increase message half life (Zhu *et al.*, 1994) and also has a role in early differentiation of oligodendrocytes (Fraichard *et al.*, 1995; Barres *et al.*, 1994). Expression of the *Plp* gene is also modulated by signals from other components of nervous tissue for example axons (Scherer *et al.*, 1992; Kidd *et al.*, 1990) (see 1.2.4 The relationship between axons and glia in development of the myelin sheath, page 23).

Genes responsible for *trans*-factors that are required for glial differentiation have been identified in *Drosophilla* and there are also genes for *trans*-factors that are important for glial development after cells are committed to the glial lineage (Hudson *et al.*, 1996). *Trans*-factors that have been described include myelin transcription factor 1 (MyT1), which is a zinc finger transcription factor, the expression of which is strongly associated with oligodendrocyte development and which binds to a site in the *Plp* gene promoter (Armstrong *et al.*, 1995) and other

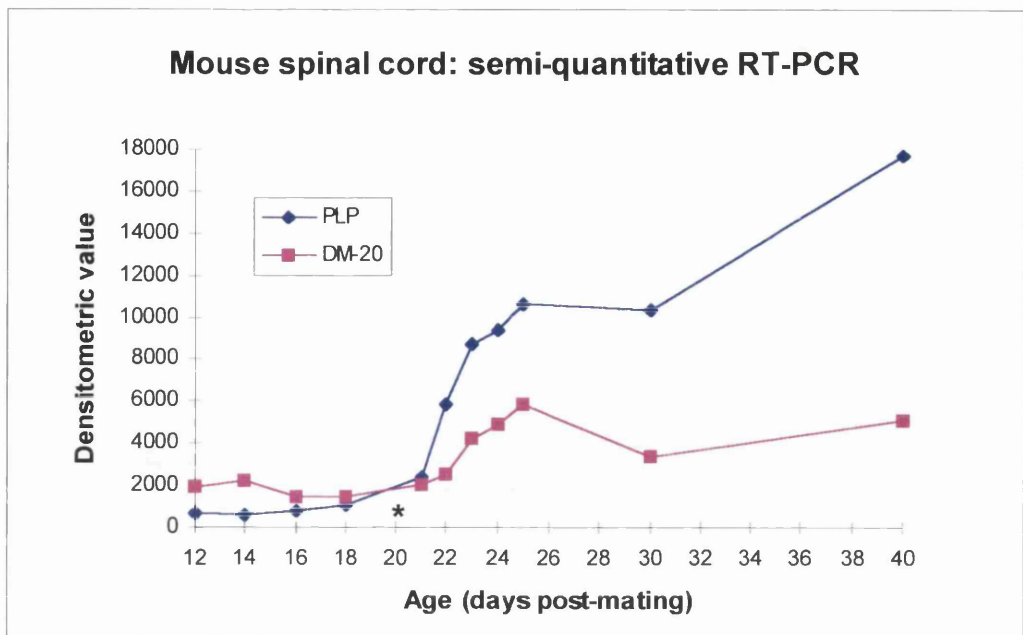
myelin genes (Hudson *et al.*, 1996). Currently the control of these early steps in the regulation of vertebrate *Plp* gene expression are poorly understood.

1.2.3.1.1.2 Post-transcriptional regulation

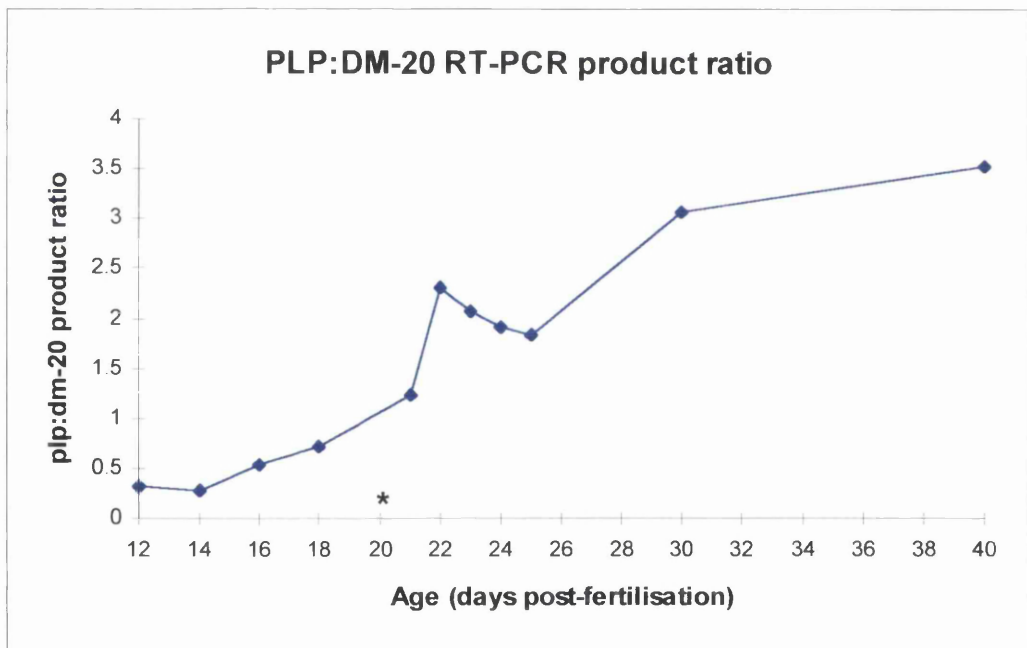
The varying ratios in the *Plp* and *Dm20* message isoforms observed during development is achieved by varying the use of the two potential splice sites in exon 3, one of which is internal and the other is at the 3' exon/intron boundary (Figure 3, page 14). Both sites show a similar degree of complementarity with U1 small nuclear ribonucleoproteins (snRNP), which form an RNA duplex with the 5' splice site, an early regulatory event in the formation of the spliceosome (Montague and Griffiths, 1997). It has been suggested that the selection of the distal site is the default pathway for spliceosome assembly (Montague and Griffiths, 1997). Selection of a particular site is also related to the relative and absolute amounts of SR proteins which vary between tissues (Zahler & Roth, 1995), a mechanism by which both temporal and cell specificity may be enhanced. Hudson *et al.* (1996) suggest that the embryonic expression of *Dm20* message may represent loose transcriptional control at this early stage of development, as a consequence of the requirements of regulation at later stages, and imply that the message observed does not necessarily have physiological significance.

1.2.3.1.2 Post-translational events

The *Plp* and *Dm20* mRNAs are translated on the rough endoplasmic reticulum (RER) and the proteins follow the secretory pathway passing through the Golgi apparatus en route to the cell membrane (Gow *et al.*, 1994). *In vitro* studies suggest that in developing oligodendrocytes these proteins are stored for a period before assembly into myelin (Dubois-Dalcq *et al.*, 1986), however, *in vivo* studies show that translocation can take as little as 30 minutes (Colman *et al.*, 1982). Transport to the cell membrane is in association with the micro-tubular apparatus possibly in association with other myelin components (Brown *et al.*, 1993; Trapp, 1990). Membrane proteins are recycled and enter the endocytic pathway for eventual degradation. It is likely that interactions with other cell types are important in modulating any differences in trafficking between the two isoforms (Montague and Griffiths, 1997).



a)



b)

Figure 4. Semi-quantitative RT-PCR analysis of *Plp:Dm20* ratios in spinal cord. a) densitometric analysis of RT-PCR products illustrates marked up-regulation of the *Plp* gene coinciding with the change to predominance of the *Plp* message isoform around P1; b) Increasing predominance of the *Plp* isoform in post-natal life is seen in the *Plp:Dm20* transcript ratios rising from greater than 1 to 3.5 by P20. Gestation length was approximately 20 days in the strain of mice studied and approximate point of birth is marked on the graphs (*). From Dickinson, 1995, Figure 20, page 99 (with permission).

The PLP and DM20 protein isoforms undergo two post-translational modifications which are losing the N-residue (Milner *et al.*, 1985) and becoming acylated. The lack of an amino terminal leader sequence, a feature of some but not all transmembranous proteins, suggests that targeting is by an internal signal. The first 13 amino acids may contain a topogenic signal sufficient for membrane incorporation (Wight *et al.*, 1993) (also see 6.5 Discussion, page 177). However, Gow *et al* (1994) demonstrated that transfected COS-7 cells are able to translocate PLP and DM20 through their secretory pathways suggesting that glial specific elements are not essential for correct folding and transport.

The complex topography of the oligodendrocyte with multiple processes supplying internodes of different sizes with potentially differing requirements suggests a sophisticated system for ensuring appropriate delivery. These mechanisms in relation to the PLP/DM20 protein isoforms are unknown. The local translation of *Mbp* mRNA at the periphery of the cell, which may be regulated by local requirements for myelin components, has been suggested to be a potential regulator of PLP/DM20 transport (Hudson *et al.*, 1996). Some transfection studies have suggested that both PLP and DM20 must be present for incorporation to occur (Sinoway *et al.*, 1994) but other studies, using different cell types do not support this (Montague, unpublished observations). The experiments of Sinoway *et al* (1994) suggest that the two proteins form a complex reminiscent of adhesive proteins such as P₀ and cadherin, concentrated at regions of cell-cell contact.

1.2.3.2 Co-ordinate expression of the CNS myelin genes

The ability of oligodendrocyte to both elaborate and maintain a myelin sheath requires the co-ordinated activity of many genes encoding both structural proteins and those involved in the mechanisms of intracellular transport. The mechanisms behind this achievement are only just being answered.

No “master” gene has been identified that orchestrates the expression of the CNS myelin genes, as for example the *Pax-6* gene is thought to have a pivotal role in lens formation (Schedl *et al.*, 1996). Co-ordination is not achieved by a unique *trans*-factor that regulates each individual gene but through a complex, and potentially more flexible system, involving the interaction of a cohort of specific and ubiquitous factors. A *cis*-structure (see above) has been identified to be common to the *Mbp*, *Mag* and *Omg* genes and the glial specific JC virus (Hudson *et al.*, 1996). There are also homologues of *cis*-elements found in the *Plp* gene in other myelin genes. The thyroid response element illustrates how common *cis*-elements may be involved in co-ordinate but temporally specific expression of myelin genes. Both the *Mbp* and

Plp genes are modulated by thyroid hormone and have the similar hormone response elements in their promoters. However, the two genes have different co-transcription factors binding to the element and it is the developmental profile of these co-factors that mirrors specific gene activity (Hudson *et al.*, 1996). The *Plp* gene also shares a co-factor with another group of genes modulated by thyroid hormone that are related to the production of liposomes, an organelle important in lipid metabolism (Hudson *et al.*, 1996).

1.2.3.3 Expression of the *Plp* gene in the PNS

Initially the *Plp* gene was thought to be expressed exclusively in the CNS. It is now well established that it is transcribed in a number of other tissues including cells of the PNS (Griffiths *et al.*, 1995). In all PNS cell types *Dm20* message isoform and DM20 protein are predominant. Transcription occurs in both non-myelin forming Schwann cell (NMFSC) and MFSC and the product is localised to cytoplasmic domains and is not generally detected in PNS myelin (see 6 Expression of *Plp* transgenes in the peripheral nervous system, page 171). The DM20 protein isoform is also detectable in the perineuronal satellite cells of the spinal cord, cranial and autonomic ganglia and in the ensheathing cells of the olfactory nerve layer of the olfactory bulb (Dickinson *et al.*, 1997).

The functional significance if any of *Plp* gene expression in the PNS is unknown. It is notable that it is expressed in cells that do not produce myelin. Developmental studies show that regulation of the *Plp* gene is not related to PNS myelination (Griffiths *et al.*, 1995; Kamholz *et al.*, 1992; Stahl *et al.*, 1990). *Dm20* is strongly expressed in the embryo at a point when Schwann cell precursors are actively mitotic and motile and not expressing myelin protein genes (Griffiths *et al.*, 1995). Observations by Kamholz and others (1992) concur with the *Plp* gene not being part of co-ordinate myelin gene expression in the PNS. For example, in sciatic nerves undergoing Wallerian degeneration PNS myelin proteins are markedly downregulated whilst *Plp* gene transcription is minimally affected (Kamholz *et al.*, 1992).

The reasons for these differences in *Plp* gene expression between the PNS and CNS are not known. Different transcription start sites are used in Schwann cells compared with oligodendrocytes and may thus represent different promoter sites in these cell types implying a response to different combinations of *trans*-factors (Kamholz *et al.*, 1992). PNS myelin has a different composition from CNS myelin and it has been proposed that the physical association of these proteins excludes PLP from participating in myelin assembly (Kamholz *et al.*, 1992) (see 6 Expression

of *Plp* transgenes in the peripheral nervous system, page 171). The converse relationship between the two isoforms in the PNS, as compared to the CNS, may result in conditions that are stoichiometrically unfavourable for insertion (see 1.2.3.1.2 Post-translational events, page 19). The purported lack of acylation of the PLP/DM20 isoproteins in Schwann cells (Agrawal & Agrawal, 1991), refuted by Tetzloff and Bissozero (1993), has been suggested as being significant, though acylation probably develops within myelin.

These observations, though not providing a mechanistic reason for *Plp* gene expression in the PNS, support the growing consensus that DM20 has a separate, but as yet undefined, role in development and that this may not be confined to the oligodendrocyte.

1.2.4 The relationship between axons and glia in development of the myelin sheath

The development and maintenance of the organs of eukaryotic organisms is dependent on the interaction of disparate groups of cell types. In the CNS the oligodendrocyte should be considered in relation to the cell it ensheathes - the neurone and its axon- and the other glia, in particular the astrocyte.

A number of features of the formation of the myelin sheath demonstrate the importance of the influence of the axon over whether it is ensheathed and the properties of any myelin sheath that does form (reviewed by Doyle and Colman (1993), Waxman and Black (1995)). The formation of the sheath in relation to thickness (the number of myelin turns) and the length of the internode is a function of the axon diameter and as the majority of oligodendrocytes ensheath multiple internodes of axons of varying diameters this is very suggestive of local factors influencing the properties of distal regions of oligodendrocyte processes. Though the precise mechanism by which oligodendrocyte processes are attracted to axons and stimulated to ensheath them remains unclear it is evident that a sequential cascade of gene expression encompassing a variety of gene groups, including adhesion and structural genes, is essential for the formation of a functional myelin sheath. Oligodendrocytes that fail to ensheath an axon undergo apoptosis illustrating the importance of this relationship in their continued survival and development (Trapp *et al.*, 1997).

This establishment of the close association between oligodendrocyte and axon influences the ultrastructure of axons and glial cells. In the axon there are influences on both membrane structures (e.g. ion channels) and axoplasmal contents

(e.g. packing of neurofilaments). The loss of myelin results in the loss of this axonal organisation (Rosenbluth, 1995).

1.3 Abnormal development and loss of myelin

1.3.1 Dysmyelination and demyelination in the CNS

Myelin is both elaborated and maintained by oligodendrocytes and perturbations of cell development, metabolism or death are likely lead to myelin abnormalities.

The inability to elaborate a compact myelin sheath is referred to as dysmyelination and consequently is a feature of abnormal development. The essential features are hypomyelination due to failure of myelin production, often with concomitant abnormalities of any myelin elaborated (see 1.3.2 Naturally occurring mutants, page 26). Myelin debris is not usually a feature. Though dysmyelination has been associated with mutations of the myelin genes the mechanisms underlie the failure of the system are poorly understood. Dysmyelination also may be associated with mutations in genes encoding for proteins other than the specific myelin genes. For example, the quaking (*qk*) mouse has is a deletion in chromosome 17 affecting a signal transduction and activator of RNA protein (STAR protein), which is proposed to affect the alternative splicing of myelin specific protein(s) (Ebersole *et al.*, 1996).

Demyelination, the loss of formed myelin with relative preservation of the axon, is the final common pathway of multiple aetiologies including the effects of toxic chemicals, trauma, viruses, etc. and the end-stage of a considerable number of inflammatory and non-inflammatory diseases. The initiation of breakdown is poorly understood and is the potential key to a number of significant conditions, for example multiple sclerosis (MS). Both the oligodendrocyte and the myelin sheath are potential targets. Myelin potentially may be lost due to a failure of the oligodendrocyte to maintain the sheath or the sheath may be attacked directly. Oligodendrocyte metabolism can be affected by exogenous chemicals (Blakemore, 1984) and factors produced by cells (cytokines, reactive oxygen species (ROS), nitric oxide (NO))(Cuzner & Norton, 1996; Sun *et al.*, 1995; Rodriguez *et al.*, 1994). Demyelination is often associated with a change, often inflammatory in character, in the local cell population. Cells may be exogenous to the CNS arriving in the circulation but there also may be local proliferation of microglia and astrocytes. Cytokines released from activated cells, for example TNF α , are also significant in modulating other local events that may contribute to the process. In viral infections the virus itself may damage the oligodendrocyte or possibly render it susceptible to attack by CD⁺ T cells (Rodriguez *et al.*, 1994). It is the macrophage

lineage cells that are currently thought to be the pivotal cells in inflammatory disease, though their role may vary (Rodriguez *et al.*, 1994; Sun *et al.*, 1995; Cuzner & Norton, 1996; Dijkstra *et al.*, 1992). The myelin sheath may be attacked directly by macrophages in experimental allergic encephalomyelitis (EAE) and MS (Dijkstra *et al.*, 1992). Opsonisation increases the susceptibility of myelin to attack by stimulated macrophages. There also exists the possibility of myelin damage by enzymes released during “frustrated” phagocytosis by macrophages unable to internalise intact myelin (Cuzner & Norton, 1996).

Predictably the first manifestation of dysfunction resulting in an inability to maintain the myelin sheath would be an abnormality of the inner tongue, this being the most distal part of the oligodendrocyte cytoplasm. This phenomenon of a “dying back oligodendrogliaopathy” is observed in some intoxications (Blakemore, 1984), in the demyelinating form of Theiler’s virus infection and more controversially in early cases of MS (Allen and Kirk, 1997; Rodriguez *et al.*, 1994). Histologically the first stages of demyelination are vesiculation and swelling of the myelin sheath, with splitting of the IPL and potentially the development of vacuoles (Blakemore, 1984). Myelin changes following administration of toxic chemicals, such as hexachlorophene or triethyl tin, may be limited to vacuolation which is reversible, implying that exposure of myelin constituents does not necessarily result in demyelination (Ludwin, 1995). However, in many circumstances once myelin breakdown is initiated there appears to be a common pathway of destruction. The exposed myelin proteins and lipids are exposed to endogenous enzymes, which may derive from inflammatory cells or from the circulation through an incompetent blood-brain-barrier. In the CNS microglia/macrophages may be an important source of such enzymes. The final removal of myelin debris is by phagocytic cells, predominantly macrophages and microglia, though myelin debris can be observed in astrocytes (Cuzner & Norton, 1996).

1.3.1.1 Demyelination in mice due to viral infection

Demyelination is a recognised sequela to a range of viral infections in mice. Viruses from a range of unrelated groups are implicated. These infections must be considered when animals are not maintained in a specific pathogen free environments. In stable populations such infections can be enzootic.

1.3.1.1.1 Mouse hepatitis virus (MHV)

The possible consequences of infection with this corona virus are reviewed by Fujiwara (1994). It is extremely contagious and can be transmitted in tissue grafts. Infection is the norm in multipurpose breeding facilities and in most

immunocompetent mice the effects are sub-clinical (Lindsey *et al.*, 1991). Potentially the virus may cause enteric, hepatic, respiratory and neurological disease. Susceptibility varies with viral tropism and between mouse strains. Demyelinating disease results from the infection of oligodendrocytes, which can be persistent and latent. MHV is well recognised as having effects on experimental responses and the potential effects are wide ranging but those pertinent to neurological disease include activating natural killer cells and affecting phagocytic responses.

1.3.1.1.2 Toga virus

Toga virus infection is usually a meningitis with severe mononuclear cell infiltration and perivascular cuffing. A late demyelinating condition of white matter can arise as the result of the infection of oligodendrocytes (Lindsey *et al.*, 1991).

1.3.1.1.3 Picornavirus (Theiler's murine encephalomyelitis virus-TMEV)

The possible consequences of infection with this picornavirus are reviewed by (Lipton *et al.*, 1994). Usually infection is innocuous causing an asymptomatic gut infection but occasionally will enter the CNS resulting in flaccid paralysis (Theiler's disease). Some strains, if given by intra-cranial injection, produce an acute myelitis followed by a chronic, inflammatory demyelinating condition in which the virus is thought to persist in the oligodendrocytes and other glia. This manifestation is characterised by weight loss, abnormal gait, tremor, ataxia, poor righting reflex, urine staining, priapism and death. There is a variation in susceptibility between mouse strains.

1.3.2 Naturally occurring mutants with abnormal myelination

1.3.2.1 Animal models

The inherent advantages of animal models as research tools for investigating the function of the *Plp* gene has resulted in intense activity to both characterise naturally occurring examples and with the recent advantages in recombinant DNA technology, create specific types of mutant (see 1.4.2 Methods of creating transgenic animals, page 35).

Mutants have been characterised in a number of species and these are summarised in Table 1 (page 33). The mutations are all point mutations and with the exception of Plp^jP have a single amino acid substitution in a variety of exons. They result in primarily non-conservative amino acid substitutions but surprisingly there is a conservative substitution (Plp^jP-msd) (Hudson and Nadon, 1992) (there is also an

example of a conservative amino acid substitution in Pelizaeus-Merzbacher disease). In *Plp^{jP}* there is mutation at the 3' acceptor site of intron 4 which results in the deletion of exon 5 from the mRNA, a frame shift and a truncated product with an altered carboxy-terminus (Nave *et al.*, 1987).

The general phenotype of the animal *Plp* gene mutants is neurological dysfunction related to hypomyelination, with the severity of disease varying between mutants. Hypomyelination in these mutants is a function of abnormal development and thus it is considered to be dysmyelination (see 1.3.1 Dysmyelination and demyelination, page 24). The primary features of the phenotypes are an early onset of generalised tremor and ataxia. The more severely affected mutants (*Plp^{jP}*, *Plp^{jP4}*, *md* rat) seizure and die prior to adulthood. The less severely affected phenotypes (*Plp^{jP-rsh}*, *sh-pup* and *Pt* rabbit) do not seizure, attain maturity and can reproduce. In *Plp^{jP-rsh}* the tremor ameliorates with age and becomes confined to the hind limbs during ambulation.

The degree of hypomyelination varies between mutants and is most severe in the mutants with the most profound disease. Occasional thin, poorly compacted myelin sheaths are found in the severe mutants, which fail to immunostain for PLP (Schwab & Bartholdi, 1996). In *md* rat and *Plp^{jP}* there are abnormalities of the intraperiod line (IP) (Duncan *et al.*, 1989; Duncan *et al.*, 1987). The less severe mutants have thicker myelin sheaths (negative for PLP immunostaining) and in *Pt* rabbit they increase with age, suggesting a delay in the process of myelination as well as a reduction in the amount of myelin formed (Tosic *et al.*, 1993).

Numbers of mature oligodendrocyte are profoundly reduced in the severely affected mutants. However, numbers are approximately normal during myelination in *Plp^{jP}* (Ghandour & Skoff, 1988). However, the population distribution is skewed to the more immature phenotype, which undergo an increased rate of apoptosis reducing the number of potential myelinating cells (Skoff, 1995). Increased mitotic rates of immature glia have been observed (Skoff, 1982) and there is an increase in transcription of glycerol phosphate dehydrogenase, an early marker of oligodendrocytes (Macklin *et al.*, 1991). In *sh pup* there is a reduction in mature oligodendrocytes but this is apparently not due to cell death (Nadon & Duncan, 1996). Reduced oligodendrocyte numbers are not a feature of *Plp^{jP-rsh}* and *Pt* rabbit (Tosic *et al.*, 1993; Schneider *et al.*, 1992). These two mutants show normal (increased in *Plp^{jP--rsh}*) numbers of cells, though there is delayed maturation (Tosic *et al.*, 1993). The oligodendrocytes of these two mutants do not undergo an increased rate of apoptosis (Schneider *et al.*, 1992; Tosic *et al.*, 1994). A moderate

to severe astrocytosis is a feature of the myelin mutants and abnormalities in astrocyte cell cycle and metabolism have been described (Knapp & Skoff, 1993).

Mutations of the *Plp* gene are associated with perturbations not only its transcription and translation but also of other genes expressed by oligodendrocytes, with the *Mbp* gene being the most studied example. In the *Plp^{jp}* mouse brain, *Plp* transcripts are similar to wild type at 3 days but there is no upregulation, as seen in wild type during myelination, and by 20 days levels are about 5% of normal. *Mbp* message levels also fails to show a developmental increase in *Plp^{jp}* and at 20 days are about 6% of wild type (Macklin *et al.*, 1991; Gardinier *et al.*, 1986). In *sh pup* the transcription of myelin specific genes is reduced but there is a delayed peak mirroring wild type in the spinal cord (Nadon & Duncan, 1996). Assessment of *Mbp* gene expression shows that there is a relative increase in the isoforms associated with immature oligodendrocytes, a reduction in those associated with maturity (Kerner & Carson, 1984) and the cellular distribution of protein also suggests cell immaturity (Shiota *et al.*, 1991). The *Cnp* and *Mag* genes also have an altered pattern of expression (Yanagisawa & Quarles, 1986).

In *Plp^{jp-rsh}*, *Pt* rabbit and *sh pup* the changes in *Plp* gene transcripts levels and ratios differ from those of mutants such as *Plp^{jp}*. Though there is also a reduction in the amount of *Plp* message and product, this is not as uniform across the two isoforms. There is a significant change in the ratio of DM20/PLP protein isoforms and the PLP dominance is lost (Tosic *et al.*, 1994; Mitchell *et al.*, 1992). In *Pt* rabbit the DM20/PLP ratio is increased from 0.70 to 1.14 at 8 weeks (Tosic *et al.*, 1994). In *Plp^{jp-rsh}* the amount of DM20 synthesised in some tissues is similar to wild type (Mitchell *et al.*, 1992). An increase in the DM20/PLP ratio is also observed in *sh pup* and *Plp^{jp-msd}*, which are intermediate in severity between *Plp^{jp}* and *Plp^{jp-rsh}* (Yanagisawa *et al.*, 1987). It is this relative maintenance of the levels of the DM20 protein isoform in these mutants that is postulated to ameliorate the phenotype and suggests a role other than as structural protein for DM20 (Schneider *et al.*, 1992).

The levels of myelin gene mRNA and protein observed in CNS tissues of severely affected mutants, such as *Plp^{jp}* and *Plp^{jp-msd}*, may in part reflect the preponderance of immature cells in the population of the oligodendrocytes. As discussed above in *Plp^{jp}* mouse there is skew in maturity of the oligodendrocyte population and the majority of oligodendrocytes die about 2-3 days before they might be expected to elaborate significant amounts of myelin (Vermeesch *et al.*, 1990). In *Plp^{jp-rsh}* oligodendrocytes persistently express markers associated with an immature phenotype and the elaboration of myelin is delayed. Whether the few *Plp^{jp}*

oligodendrocytes that reach maturity elaborate *Plp* gene derived proteins *in vivo* is controversial. That such oligodendrocytes can elaborate myelin, albeit abnormal, can be observed in *Plp^{jP}* spinal cord where a proportion of axons have some myelin (Duncan *et al.*, 1989). Generally there is no positive immunostaining for wild type PLP as many of these antibodies recognise epitopes that would be absent in the truncated *Plp^{jP}* protein. A number of authors have reported failed attempts to purify a *Plp^{jP}* PLP protein from brain (Benjamins *et al.*, 1994; Sorg *et al.*, 1986). One group report a single band (~23kDa) on Western analysis, which is recognised by PLP antibodies and not by antibodies to the C-terminal, a region which is predicted to be altered in *Plp^{jP}* (1994). Recently Knapp *et al* (1996) have demonstrated the production of a protein recognised by antibodies that recognise an epitope specific to the truncated *Plp^{jP}* protein. This protein was also recognised by antibodies that recognise epitopes that should be common to the wild type and *Plp^{jP}* PLP protein isoform.

1.3.2.2 The consequences of mutant *Plp* alleles for carrier females

X-linked diseases predominantly affect males, with in many diseases apparently unaffected females carrying the affected allele and passing it onto the next generation. In normal females there is inactivation of one of the pair of X chromosomes in each somatic cell and theoretically the mean overall contribution of each X-chromosome is 50%, though ratios of 60:40 and greater are common (Willard, 1995). Quantification of oligodendrocyte numbers in females heterozygous for the *Plp^{jP}* allele suggests that there is a reduction in oligodendrocytes (Skoff & Ghandour, 1995) that progresses with time (Griffiths, unpublished data). Phenotypic signs do not develop which may be due to compensation with unaffected oligodendrocytes elaborating more myelin (Skoff & Ghandour, 1995). Females of the less severe mutants (for example *sh pup* and *Plp^{jP}-rsh*) can show mild phenotypic changes implying improved survivability of mutant oligodendrocytes. Abnormalities have also been noted in some females from human pedigrees with muscular dystrophy (Belmont, 1996) and PMD (see below). Control of X-inactivation may be influenced by other genes and may explain why individual carrier females occasionally have phenotypic signs in contrast to the majority (Belmont, 1996).

1.3.2.3 Human diseases associated with the *Plp* gene

1.3.2.3.1 Pelizaeus-Merzbacher disease / X-linked spastic paraplegia

Pelizaeus-Merzbacher disease is a rare disorder characterised by profound hypomyelination, due to dysmyelination, the consequences of which are severe

neurological disease, with early mortality in the majority of patients. There is both inter and intra-family heterogeneity in the clinical course of the disease and until recently this caused difficulty in the classification of some candidate cases. Clinical classification is related to the severity of disease and is of some value in assessing the impact of the underlying genetic abnormalities. The classification system of Seitelberger is often referred to but this has now been shown to include diseases not associated with the *Plp* gene locus (Hodes *et al.*, 1993).

This condition is considered to be X-linked (indeed this is a requirement of some classification systems), however, PMD like disease does occur in females associated with *Plp* mutations (Hodes *et al.*, 1995) and late onset neurological disease has been observed in female carriers (Nance *et al.*, 1993). For further discussion see 1.3.2.3.2 *PMD-like* disease in females, page 32. *De novo* cases also arise where X-linkage cannot be determined.

PMD was first described at the turn of this century but it was not until the late 1980s that linkage with the *Plp* locus was established (Trofatter *et al.*, 1989; Hudson *et al.*, 1989). *Plp* polymorphisms are rare (Mimault *et al.*, 1995; Boespflug-Tanguy *et al.*, 1994) and the first linkage of PMD to the *Plp* gene was established by specifically screening the *Plp* gene of an affected family for point mutations (Hudson *et al.*, 1989). An expanding range of principally exonic mutations is described with only two families sharing a specific mutation (Pratt *et al.*, 1995; Otterbach *et al.*, 1993) (see Table 1, page 33). Initially the significance of *Plp* mutation in the aetiology of PMD was uncertain, though extensive analysis of PMD pedigrees had revealed a spectrum of mutations affecting the exonic regions, these represented only about one in four or five pedigrees (Hodes & Dlouhy, 1996). However, tight linkage of PMD in families without demonstrable exonic mutations to the *Plp* gene locus has been confirmed by Boespflug-Tanguy and others (1994). The potential involvement of duplication of the *Plp* gene in the aetiopathogenesis of PMD, initially reported by Cremers and others (1987) and reinforced by Ellis and Malcolm (1994), was an important step in refining the molecular basis of PMD pedigrees.

Techniques that identify changes in the coding sequence, for example single strand conformational polymorphism analysis (SSCP), will not identify duplications and thus there has been an expansion in the techniques used to investigate pedigrees. Initially this involved blotting techniques (Ellis & Malcolm, 1994) but a PCR based technology is now described (Inoue *et al.*, 1996). The proportion of PMD cases demonstrating duplication is increasing as more pedigrees are suitably investigated (Hodes & Dlouhy, 1996). It is likely that duplication will represent the largest group of mutations associated with PMD.

PMD is a disease of development. However, in the early literature there is one pedigree (Camp & Lowenberg, 1941; Lowenberg & Hill, 1933) and a number of rare *de novo* cases where PMD-like disease has been described in adults (Bruyn *et al.*, 1985). This association is on clinicopathological grounds as these cases predate mutational analysis of the *Plp* gene. They differ on features of pathology and affect both males and females. Some cases share similarities with SPG2 (see below). The inclusion of these cases in the description of PMD has been controversial but new instances of such disease can now be assessed to see whether they have *Plp* mutations. Two pedigrees with known *Plp* mutations contain individual carrier females who have exhibited late-onset neurodegenerative disorders. One family had a deletion (Raskind *et al.*, 1991) and one a point mutation in (Nance *et al.*, 1993).

The X-linked hereditary spastic paraplegias (HSP) are rare diseases that form a subgroup of a heterogeneous clinical classification, many of unknown aetiology, termed the hereditary ataxias and paraplegias (Harding, 1983). They are characterised by spastic paraplegia, but latterly the arms may be affected, and are sub-classified according to whether individuals exhibit other neurological signs (The so called complicated form). They were assigned to potential genes and linkage analysis undertaken: spastic paraplegia gene 1 (SPG1) for the complicated form and SPG2 for the uncomplicated form. Cases of SPG2 are rarer than those SPG1 (Cambi *et al.*, 1996). Linkage analysis showed that SPG2 was allelic to the *Plp* gene (Cambi *et al.*, 1996). SPG1 was mapped to both the *Plp* and *L1cam* (at Xq28) gene loci (Bonneau *et al.*, 1993). Further examination of the clinical manifestation of cases SPG1 linked to the *Plp* gene suggest they lack features seen in diseases associated with *Lcam1*. The product of the *Lcam1* gene locus is a neural cell adhesion molecule (Jouet *et al.*, 1994). In SPG1 the associated neurological disease may develop concurrently with the spastic paraplegia, or may develop at a later, variable date (Saugier-Verber *et al.*, 1994). Though SPG1 has not been specifically linked to *Plp* gene duplication it is suspected (Cambi *et al.*, 1996). Other dominant spastic paraplegias have been demonstrated to be linked to other chromosomes (Kobayashi *et al.*, 1996).

The pathology of these diseases is poorly described as they are rare and most patients have a reasonably normal lifespan. As the association with the *Plp* gene is only recently described its status in many of the cases described is unknown. The pathology is likely to involve demyelination, as the onset is after myelination should be well advanced or complete.

The nosology of PMD/X-SPG has changed, moving from clinical criteria to a genetic basis by linkage with the *Plp* gene, which has linked these two previously

separate clinical entities. This has expanded the clinical definition of PMD and clinicians are looking at a broader group of patients for *Plp* gene mutations (Hodes & Dlouhy, 1996). These two diseases confirm the heterogeneity of phenotype caused by mutation of the *Plp* locus also observed in the animal models. Indeed, as can be seen from the above, the clinical classification of some pedigrees has been difficult due to the similarity of the clinical findings in “mild” PMD and SPG2 (Hodes *et al.*, 1993).

1.3.2.3.2 PMD-like disease in females

Since the first description of a PMD pedigree by Merzbacher in 1910 there have been occasional cases of affected females described. Affected individuals have been members of large pedigrees, with typical or atypical PMD, and *de novo* cases. These cases, and the *de novo* cases in particular, have posed problems of classification as their inclusion challenged the proposed X-linked status of PMD (though there are precedents for disease in carrier females in other X-linked diseases - see below). Though some cases of PMD-like disease in females may be due to other aetiologies resulting in a similar phenotype, demonstration of *Plp* gene mutations in affected females has confirmed the involvement of the *Plp* gene in this group of patients (Hodes *et al.*, 1995; Hodes *et al.*, 1993).

There are two phenotypes seen in females associated with *Plp* gene mutation. The early onset disease that parallels that seen in male children and a late-onset condition which presumably represents demyelination.

Early onset disease is likely to be due to predominant expression of the mutant allele. There are at least four recognised explanations for phenotypic expression of X-linked disease in females (Willard, 1995): Turner’s syndrome which has a 45 XO karyotype and a female phenotype; a female with two mutated genes, a very unlikely situation, in human pedigrees; skewing of X-chromosome inactivation (extreme lyonisation) favouring the survival of cells carrying the mutant allele; uniparental disomy.

Late-onset disease suggests that cells with an active mutant allele are present and that the product of this allele perturbs the maintenance of the myelin sheath. It has also been proposed that the myelin elaborated is in some way abnormal and ultimately is lost (Ellis & Malcolm, 1994). It is also possible that the mutant allele is expressed by cells other than oligodendrocytes, explaining their longevity, and that the activity of the mutant gene leads to late-onset perturbations in other cell types.

Species	Allele designation	Nature of mutation
mouse	<i>Plp^{jP}</i>	missense at splice site 3' exon 4, frameshift, truncated C-terminal
	<i>Plp^{jP}-msd</i>	missense, exon 6
	<i>Plp^{jP}-rsh</i>	missense, exon 4
	<i>Plp^{jP}-4j</i>	missense, exon 2
rabbit	<i>pt</i>	missense, exon 2
rat	<i>md</i>	missense, exon 2
dog	<i>sh-pup</i>	missense, exon 2
man	PMD	missense, exons 2, 3, 4, 5, 6
		nonsense, exon 3B
		deletions (partial exon 1, 3, 4, and total)
		frameshifts,
		duplications
		silent, exon 3, 4
		insertion exon 7 and 3' untranslated
		others (no exonic mutations, may have duplications)
	SPG 2	missense, exon 3B
		missense, exon 4 (equivalent to <i>Plp^{jP}-rsh</i>)

Table 1. Summary of naturally occurring *Plp* mutant animals and mutations found in man. (*sh-pup* and *pt* rabbit have a mutation affecting the same base pair but have a different substitution).

1.3.2.4 Hereditary motor and sensory neuropathies (HMSN) of the PNS

As discussed above PMP22 is a probable homologue of PLP in the PNS (1.2.1.2 Comparison of CNS and PNS myelin, page 4). Thus the consequences of mutation in this gene are of interest in the study of *Plp* gene mutations.

Charcot-Marie-Tooth disease 1A (CMT1A), a sub-group of the HMSN, and the associated syndromes hereditary neuropathy with liability to pressure palsies (HNPP) and Dejerine-Sottas disease (DSD) are due to mutations of the PMP22 gene (chromosome 17) (Thomas *et al.*, 1996). They all exhibit demyelination (with or without remyelination) of the peripheral nerves though they are clinically and pathologically distinct. DSD has the most severe phenotype and HNPP the mildest.

In general the association of mutation with phenotype is quite strong with duplication of PMP22 resulting in CMT1A and deletion in HNPP, with DSD due to point mutations. The picture is slightly complicated by rare cases of point mutations with phenotypes of both HNPP or CMT1A. It also must be remembered that these are clinical groupings and thus diseases with similar phenotypes may be due to mutations affecting other genes (Thomas *et al.*, 1996).

1.4 Experimental strategies for the manipulation of myelination

As described above a wide variety of natural mutant animals with mutations of the *Plp* gene have been identified and have proved to be invaluable research tools. However, to address questions about specific mutations recombinant DNA technology techniques have been utilised to dissect aspects of *Plp* gene function.

1.4.1 Expression of cloned genes

A natural development of the evolution of recombinant DNA techniques was the wish to study the properties of cloned genetic material in living systems. Methods for introducing eukaryotic genes into prokaryotic cells (transformation), though successful in achieving high levels of transcription, are of limited value because of the lack of post-translational modification, problems with folding and secretion (Harvey *et al.*, 1992).

The introduction of foreign genes into mammalian cells in culture (transfection) is a widely used, flexible approach that has been extensively used in the study of the *Plp*

gene. Exogenous DNA constructs can be expressed either transiently or incorporated into the endogenous DNA to give stable transfectants. The use of cell lines allows the expression of genes in controlled conditions. The availability of a wide range of cell lines allows the behaviour of cloned genes to be studied within and without their normal cellular environments. Cell culture transfection results must be interpreted with care because of the abnormal cellular environment and should be examined in the context of *in-vivo* studies.

1.4.2 Methods of creating transgenic animals

To study the properties of a gene in relation to the development and maintenance of a tissue within an organism requires the stable manipulation of the genome of an appropriate animal.

The creation of transgenic organisms is now an important tool in many fields of biology and their uses and applications are wide and varied. There are broadly two approaches to the stable integration of exogenous DNA into the genome: pro-nuclear injection and gene targeting by homologous recombination in embryonic stem (ES) cells. The selection of technique is reflected by the ambition of the experiment. In general pro-nuclear injection is used to complement the genome with extra gene copies and homologous recombination to target a gene with specific mutations.

1.4.2.1 Pro-nuclear injection

The purified DNA construct is injected directly into the pro-nucleus of donor eggs. Currently there is no control over the number of integration events, the number of gene copies involved per integration event (constructs tend to be integrated as variable chains of head-to-tail concatomers) and position within the genome. The efficiency of the technique in the number of transgenic animals born is relatively low, even in laboratories experienced in the technique (Kollias and Grosveld, 1992). Transgenic animals are identified by Southern blotting or PCR. Occasionally integration occurs after the first division and the resulting animal is a mosaic thus transgenic animals are test mated to establish whether there has been integration into germ cells.

The behaviour of transgenes should be interpreted in the light of the limitations of the technique. The behaviour of a specific construct is potentially influenced by a number of factors including number of copies in the integrated cassette, chromosomal location (position effect) and possible influences of modifying loci (Wilkins, 1990; Clark *et al.*, 1994). These influences can be ameliorated by careful

construct design and it is possible to produce transgenic animals with transgenes having copy number dependent activity apparently free of position effects (Clark *et al.*, 1994). The production of a number of different lines from the same original experiment, thus almost certainly with different areas of integration, can be useful in assessing a transgenic cassette in relation to these concerns. The nature of transgene integration means there is the potential for random disruption of genes with the possibility of an unexpected phenotype related to insertional mutagenesis. This can give rise to a phenotype characterised by neurological abnormalities (Orlan *et al.*, 1994).

1.4.2.2 Homologous recombination in embryonic stem (ES) cells

The basis of this approach is the phenomenon of homologous recombination of exogenous DNA with homologous chromosomal sequences. This allows the targeting of specific sequences and thus the ability to engineer changes in a gene locus by introducing sequences with specific mutations.

This technique has been pioneered in mice where the ES cells are derived from the inner cell mass of mouse blastocyst. Though they are at a later stage of development than the cell type used in pro-nuclear injection they are pluripotent and have the potential to contribute to all cell types of the chimera that develops after their introduction into blastocysts. ES cells represent a convenient cell type in which to introduce targeting vectors as they can be maintained in their pluripotent state in tissue culture. The exogenous DNA can be introduced by a number of techniques including nuclear injection and electroporation. Homologous recombination events are relatively rare and random integration is possible, thus the design of selection markers to allow the identification of successful clones is an important part of vector design.

ES technology has been used extensively to engineer null alleles of selected genes (the so called “knockout”). This technology is routinely available and many facilities offer a custom service to the scientific community (P. Montague, personal communication).

1.4.2.3 Application of transgenic animals to the investigation of *Plp* gene function

Transgenic animals models have been created that address a number of aspects of *Plp* gene regulation and function. These include: transgenes with increased copy number of the wild type gene (see below); gene knockouts (Klugmann *et al.*, 1997; Boison & Stoffel, 1994); minigenes that code for individual *Plp* and *Dm20* protein

isoforms (Johnson *et al.*, 1995; Mastronardi *et al.*, 1993); a *Lac-z* fusion gene (Wight *et al.*, 1993); and as tool for tracking transplanted glial cells (Gout *et al.*, 1991). The *Plp* gene is X-linked and all the *Plp* gene transgenics produced by pro-nuclear injection have autosomal integration sites and thus the transgenes exhibit a simple Mendelian autosomal pattern of inheritance.

The main thrust behind the creation of the *Plp* gene derived transgenic mice currently described has been as part of larger experimental programmes directed towards the “rescue” of *Plp⁰* mice by gene complementation. These experiments were stimulated by the success of rescuing the hypomyelinating phenotype of the MBP mutant *sh* mouse by transgenic complementation of the *sh* genome with extra copies of the wildtype MBP gene (Readhead *et al.*, 1987). The experimental strategies for *Plp⁰* mice differ in that the initial complementation with extra copies of the gene was of wild type mice and attempting the rescue of *Plp⁰* offspring by mating (Kagawa *et al.*, 1994; Readhead *et al.*, 1994). However, the *Dm20* minigene mice described in the literature have been developed expressly to explore the role of DM20 protein isoform (Johnson *et al.*, 1995).

1.4.2.3.1 *Plp* transgenic mice with extra copies of the wild type *Plp* gene

There are currently two groups of mice with transgenic cassettes conferring extra copies of the wild type murine *Plp* gene: #66 and #72, in which the pro-nuclear injection using the same construct has resulted in two different integration events representing 7 (#66) and 3 (#72) copies per haploid genome (Readhead *et al.*, 1994); 4e in which there are two copies per haploid genome (Inoue *et al.*, 1996; Kagawa *et al.*, 1994). It was thus in independent experiments that mice with a neurological phenotype was observed. In both instances this involved the breeding of founder mice (#66 and 4e) to produce homozygous individuals. In both lines affected individuals were noticeable from the time of ambulation as being affected by a tremor, developed seizures and died prematurely. In both lines Southern hybridisation analysis linked the mutant phenotype to homozygosity for the transgene.

The transgenic cassettes used to produce these two groups of mice were developed independently from different clones of the *Plp* gene, and though both contain the 7 exons and 6 introns of the wild type gene they differ significantly in the amount of flanking sequence information they incorporate. The constructs differ primarily in the amount of 5' sequence, with 4e containing a considerably larger region (4e 20Kb c.f. #66/72 3.5Kb), with a relatively small difference at the 3' end (4e 4Kb c.f. #66/72 ~6Kb).

Both groups confirmed the sequence of the their transgenes was unaltered. The transgenes ability to produce the wild type PLP/DM20 protein isoforms was confirmed by expressing the transgenes on a male *Plp^{fl}/P* background on which positive immunostaining with antibodies to the C-terminal region confirms the presence of wild type protein isoforms.

1.4.2.4 Evidence that increased *Plp* gene dosage affects myelination

The nature of the pathology underlying the phenotype in both these homozygous mice was confirmed to be dysmyelination. The existence of two independent examples of increased wild type *Plp* gene dosage leading to perturbation of myelination provides useful corroboration that the dysmyelinating phenotype is an effect of the increase in *Plp* gene dosage, as opposed to a feature of the transgenic cassette or a function of the site of integration. Though they are conceptually are very similar there are a number of similarities and differences.

The constructs are both based on the wild type *Plp* gene, though cloned from different DNA libraries and into different backgrounds. Both constructs contain the 7 exons and associated introns but differ markedly in the amount of flanking sequences, particularly in the 5' region, which contains many putative regulatory regions (see 1.2.3.1 Regulation of *Plp* gene expression, page 16).

The phenotypic abnormalities of *4e* mice are apparently more severe than those of the homozygous #66 and #72 mice. Other changes seem more pronounced e.g. oligodendrocytes in *4e* mice show more dramatic ultrastructural abnormalities than homozygous #66 mice. Most interestingly, regarding the work presented in this thesis hemizygous *4e* mice relatively quickly develop demyelination a process which was not recognised in the #66 and #72 lines at the inception of this project.

In contrast the effect on myelination of the *Plp* related minigenes that have been created is variable. The only *Plp* cDNA construct results in no detectable phenotypic abnormalities (Nadon *et al.*, 1994), even after extended periods of observation of 18-24 months (personal observation). There are two groups of DM20 minigene, one based on the construct described by Nadon *et al* (1994) and the other based on a construct described by Mastronardi *et al* (1993), both have which have been used to produce a range of transgenic mice with different numbers of intergrates. Of these only one, ND4 carrying ~70 copies of the transgene (Johnson *et al.*, 1995; Mastronardi *et al.*, 1993), is related to a phenotype in which there is late onset CNS demyelination. This is associated with an increase in DM20 and a reduction in PLP with the total amount of proteolipid proteins much reduced. These changes are detected before demyelination is observed. A transgene with the

same construct, but containing fewer copies (ND3), induces similar abnormalities in the relative amounts of the PLP and DM20 protein isoforms but does not associated with demyelination in homozygous mice (Johnson *et al.*, 1995).

All the *Plp* minigene constructs have 5' sequence derived from human clones and have between 2.9Kb (Johnson *et al.*, 1995; Mastronardi *et al.*, 1993) to 4.2Kb (Nadon *et al.*, 1994) but do not include any *Plp* gene intronic sequence. The *lac-z* fusion gene transgenic construct includes 2.4Kb human 5' sequence and the *Plp* gene intron 1 (Wight *et al.*, 1993). The lack of dysmyelination associated with these constructs implies that extra copies of these transcriptionally important sites is not related to dysmyelination.

Considering this spectrum of *Plp* gene related transgenic mice suggests that there is a role for increased *Plp* gene dosage to influence myelination.

1.4.3 Other genetically engineered myelin mutants

The transgenic approach is a popular and versatile one and has been used to address the aspects of gene regulation and function for a number of other myelin genes. Transgenic animals with extra copies of wild type genes have been created for *Cnp* (Gravel *et al.*, 1996) and *Pmp22* (Huxley *et al.*, 1996; Sereda *et al.*, 1996) and extra copies of anti-sense constructs in *Mbp* (Ikenaka & Kagawa, 1995), *Mog* (Jaquet *et al.*, 1996) and *Pmp22* (Maycox *et al.*, 1997). The creation of null alleles has been examined for *Cgt* (UDP-galactose:ceramide galactosyl-transferase (CGT), resulting in failure GalC synthesis) (Coetzee *et al.*, 1996) and P_0 (Giese *et al.*, 1992).

1.5 Aims of thesis

The observation that increased *Plp* gene dosage was related to a dysmyelinating phenotype was an unexpected and exciting finding. The development of a phenotype associated with increased gene dosage is a relatively unusual occurrence and in this case there were strong links to the emerging story of the importance of gene dosage in Pelizaeus-Merzbacher disease in man.

The availability of the two lines of *Plp* gene transgenic mice (#66 and #72) afforded the opportunity to compare and contrast the development of CNS myelination. At the time of the projects inception it was unclear whether mice homozygous for the #72 transgene developed significant neurological dysfunction, though subtle abnormalities of myelin sheaths were documented. When it became clear that a delayed phenotype did develop in homozygous #72 mice this delayed onset implied

other aetiopathological features other than the recognised mild dysmyelination. Likewise it was unclear whether mice hemizygous for the #66 and #72 transgenes would develop a neurological abnormalities as they were phenotypically unremarkable in early adulthood.

Techniques for the identification of the lines of transgenic mice studied in this project were described but not established in the Applied Neurobiology Group. The first task was to establish these techniques within the laboratory so that mice bred could be reliably identified.

The initial aim was to document the development of dysmyelination in homozygous #66 and #72. Techniques that had previously developed in the Applied Neurobiology Group for the study of other dysmyelinating mutants were applicable to this task. This included studying the nature of the developing glial cell population, combining total white matter glial cell counts from a representative area of CNS white matter with *in-situ* hybridisation to assess the adequacy oligodendrocyte population. The presence of myelin proteins was documented by immunocytochemistry using a panel of appropriate antibodies the validity of which had been well established by work in this group and elsewhere. The quality and quantity of myelin was assessed for the same region in which the glial cell population was quantified. Steady state levels of mRNA for the *Plp* and other myelin genes were assessed by northern hybridisation to put the observed dysmyelination in the context of myelin gene activity. Examination of early quantitative data suggested that generation of sufficient data points for rigorous statistical assessment was outwith the technical resources of this project and data collection was made with the goal of identifying trends that may be present.

The observation of a late onset neurological phenotype in mice hemizygous for these two transgenic cassettes was approached by initially detailing early development and comparing this to wild type littermates to assess whether there was evidence of dysmyelination. This involved collection of similar classes of data during myelination and early adulthood to that outlined above for homozygous mice. The variable age of onset of phenotypic abnormalities with the lack of a quantitative measure of phenotypic progression made the collection of data from animals of equivalent phenotypic status difficult. Consequently, in this initial study of this late onset neurodegenerative phenotype the aim was to confirm that this was indeed a late onset phenomenon and illustrate qualitatively the features of the neurodegeneration.

A separate aspect of this project developed from the incidental observation of PLP/DM20 immunostaining in PNS myelin in mice homozygous for the #72 transgene. Though the *Plp* gene is known to be translated in Schwann cells it is generally accepted that it is not incorporated into myelin. The distribution of PLP/DM20 was examined in relation to the major myelin protein P₀ using confocal microscopy. To study the transcription of the *Plp* gene and the distribution of the two protein isoforms in the PNS the transgenes were introduced onto a male *Plp^{flp}* background on which there was the potential to differentiate the wild type product of the transgenes from the *Plp^{flp}* message and product. The availability of *Plp* and *Dm20* minigenes extended this work by allowing the assessment of the distribution of the two protein isoforms in this model.

In summary the overall aims of this project were to establish the nature of the phenotypes associated with increased dosage of the *Plp* gene and put these in context of phenotypic consequences already described for *Plp* gene mutations.

2. Materials and Methods - General Techniques

The details of the preparation of all fixatives, stains, buffers, bacterial media, etc. are given in the 8 Appendix (page 200). The specific page number is given in the text.

Solutions were sterilised as appropriate. Bulk solutions were autoclaved. Small volumes, and fluids that could not be autoclaved were filter sterilised using a Flowpore 0.45µm filter (Biomedicals Ltd.).

2.1 Tissue fixation and processing

2.1.1 Fixatives

2.1.1.1 Buffered neutral formaldehyde, 4% (BNF)

This fixative was used for the preservation of tissues destined for *in situ* hybridisation, immunocytochemistry and routine haematoxylin and eosin (H and E) staining. See page 201.

2.1.1.2 Karnovsky's modified fixative (paraformaldehyde/glutaraldehyde 4%/5%)

This fixative was used for the preservation of tissues destined for light and electron microscopy as well as immunocytochemistry using resin sections. See page 201.

2.1.1.3 Periodate-lysine-paraformaldehyde

This fixative was used for the preservation of tissues destined for staining with the microglia marker and T cell markers. See page 202.

2.1.2 Fixation techniques

2.1.2.1 Immersion

Teased sciatic nerve preparations were immersion fixed prior to immunofluorescent staining (see 2.9.2 Teased fibres, page 72).

2.1.2.2 Cardiac perfusion

All perfusions were undertaken in a fume cupboard. Each mouse was handled with a separate pair of latex gloves. All mice over 10 days of age were killed in a carbon dioxide chamber. Mice under this age were killed in a halothane (Fluothane, Mallinkrodt Veterinary) chamber.

Immediately following death the carcass was sexed, weighed and pinned out on a cork board in dorsal recumbency. Tails were isolated from the board by a fresh piece of aluminium foil. The root of the tail was clamped with haemostats and the tail severed with a new scalpel blade. The tail sample was stored at -20°C until required.

The skin of the thorax was removed and the contents exposed by dividing the diaphragm, incising through the ribs on either side and reflecting the ribs and sternum. The right atrium was nicked and the perfusion carried out by instilling solutions into the left ventricle via either a 21 or 25 gauge hypodermic needle, depending on body size.

The blood was flushed from the circulation with 0.85% saline. This was followed by the fixative. All solutions were injected from a syringe by another operator. The volumes used were dependent on the size of the carcass and varied between ~20-60ml.

2.2 Processing

2.2.1 Paraffin wax processing

Tissues for paraffin wax embedding was processed using a Shandon Elliot automatic tissue processor (Histokinette). For processing protocol see page 202.

Tissues were blocked out in paraffin wax at 60°C .

2.2.2 Resin processing

Samples were processed for araldite resin embedding using a Lynx *el* microscopy tissue processor (Leica). For processing protocol see page 203.

2.2.3 Cryo-preservation

Cryo-preservation was used for tissues destined for immunofluorescent immunocytochemistry and *in-situ* hybridisation.

Nervous tissue was dissected from the freshly killed carcass and immediately immersed in “Tissue-Tek” OCT compound (Miles Inc.) in foil boats. The foil boats were immersed in isopentane which was cooled with liquid nitrogen. Once frozen the foil was removed and the block double wrapped (to limit dehydration) in “Sealon film” (Fuji) and stored at -20°C . Muscles were maintained in tension, covered in talcum powder to reduce ice artefact, and snap frozen in liquid nitrogen.

Tissues from animals perfused with periodate-lysine-paraformaldehyde were also cryo-preserved. Immediately following perfusion tissues were removed and further immersion fixed in the buffer for 4-6 hours at 4⁰C. They were cryo-protected by immersing overnight in 20% sucrose before being frozen in OCT as above.

2.2.4 Preparation of sections

2.2.4.1 Paraffin-embedded tissue

Paraffin-embedded tissue sections were cut on a Biocut 2035 microtome (Leica) at 6µm for ISH and routine stains and left overnight at 60⁰C.

2.2.4.2 Cryo-preserved tissue

OCT-embedded cryo-sections were cut on an OTF cryostat (Bright Instrument Company) at 15µm for ISH and immunocytochemistry and stored at -20⁰C.

2.2.4.3 Resin sections

Sections for light microscopy were cut at 1µm on a Ultracut E ultratome (Reichert-Jung) and mounted on plain sulphuric acid-treated slides.

2.2.4.4 Ultra-thin sections for electronmicroscopy

Sections for electronmicroscopy were cut at ~70nm (ultratome see above) and mounted on 200 mesh-3.06mm diameter copper grids.

2.2.4.5 Teased sciatic nerves

Whole nerves were taken immediately after death and teased in PBS, on poly-L-lysine coated slides, to separate the fibres. Prepared fibres were air dried and processed promptly.

2.3 Staining techniques

2.3.1 Light microscopy

2.3.1.1 Haematoxylin and eosin (H and E)

Sections from paraffin blocks were routinely stained with H and E to assess tissue quality. For details of technique see page 204. Sections were mounted in DPX (BDH).

2.3.1.2 Haematoxylin

ISH sections were counterstained with haematoxylin following autoradiography. For details of technique see page 204. Sections were dehydrated and mounted as for H and E staining.

2.3.1.3 Methylene blue/azur II

Resin sections were routinely stained with methylene blue/azur II (page 207). Slides were heated on a hot plate to 60°C and flooded with stain for 10-30 secs followed by rinsing in running tap water. Slides were dried overnight on the hot plate and mounted in DPX (BDH).

2.3.2 Electron microscopy

Ultra thin sections of araldite embedded tissue were mounted on copper grids and stained with uranyl acetate and lead citrate for electron microscopy. Details see page 205.

2.4 Microbiological manipulations

2.4.1 Bacterial media

2.4.1.1 Luria-Bertani (LB) medium

This nutrient broth was used for culturing bacteria. For details see page 210.

2.4.1.2 SOC medium

This enriched broth was used for the growth of transformed competent cells. For details see page 210.

2.4.1.3 Ampicillin LB agar plates

LB agar plates were prepared at a concentration of 1.2% by the addition of 12g agar (Agar bacteriological, Oxoid) per litre of LB medium prior to autoclaving. The mix was cooled to ~ 50°C before ampicillin was added (100µg ml⁻¹). Approximately 30ml LB agar was poured into each 90mm plate. Plates were stored at 4°C. Plates were dried before use in the 37°C incubator for 2 hrs to reduce “sweating” and smearing, which interfere with plating and reduce colony separation.

2.4.2 Competent cell preparation

Competent cells were prepared from JM101 *Esherichia coli* bacteria (supE, thi, $\nabla(lac-proAB)$, [F', *traD36*, *proAB*, *lacI9ZVM15*]) (Pharmacia Biotech) maintained on M9 thiamine agarose plates as single colony cultures. Cultures were replated every 6-8 weeks to maintain the population as a single clone with the required properties.

To ensure that the culture consisted of a single clone a single colony was inoculated into a 10ml LB broth and cultured overnight at 37⁰C at 200rpm in an orbital incubator (Gallenkamp). One ml of the overnight culture was inoculated into 100ml LB broth and incubated under the same conditions for 1.5~2 hrs, until the optical density at 600nm was between 0.2-0.3, thus ensuring that the cell density did not exceed 10⁸ cells ml⁻¹. At this concentration the bacterial population will be in the exponential part of its growth phase and thus consist mostly of viable cells. For operational reasons the bacteria were precipitated by centrifuging the broth as 3 ~ 33ml aliquots in 40ml sterile, chilled, polypropylene tubes (Becton Dickinson) followed by and incubation on ice for 20 mins. Bacteria were recovered by centrifugation at 5000rpm (JA-20 rotor) for 10 mins at 4⁰C and followed by removal of the supernatant to leave the pelleted cells. The pelleted cells were gently reconstituted in 50ml of chilled sterile 100mM magnesium chloride and recovered as in the previous step. After reconstitution as before the pelleted cells were incubated on ice with occasional agitation for 1 hr. The cell were recover cells as above and reconstitute in 10ml ice cold sterile 100mM calcium chloride with 15% (V/V) glycerol. Aliquots were placed into 1.5ml eppendorf vials and snap frozen in liquid nitrogen and stored at -70⁰C. Aliquots were stored for a minimum of 24 hrs prior to use.

2.4.3 Transformations

All cultures were performed in the presence of ampicillin.

Transformations were performed in sterile 40ml polypropylene tubes pre-chilled on ice. To allow for variations in preparations acquired from other laboratories two transformations were performed at nominal 0.1 μ g and 1 μ g of DNA, made up to 100 μ l with TE buffer (page 209). An aliquot of competent cells was slowly thawed. A 100 μ l aliquot of cells was added to each DNA sample, swirled gently to mix and incubated on ice for 30 mins. The cells were heat shocked at 42⁰C for 45 secs and rapidly transferred to ice for a further 2 mins, after which 800 μ l of SOC medium was added. Cultures were incubated in an orbital incubator at 100rpm for 60 mins

at 37⁰C, after which 200µl aliquots were plated out on LB agar plates and incubated overnight at 37⁰C.

2.4.4 Plasmid preparations

Plasmid DNA was isolated from the host bacteria using QIAfilter midi kit (Qiagen). This protocol is based on the alkaline lysis procedure (Birnboim & Doly, 1979) with lysis of the bacterial cell wall using the detergent SDS and sodium hydroxide. The lysis time is optimised to release the maximal amount of plasmid DNA with the minimal amount of degradation. In the neutralisation conditions the plasmid DNA preferentially renatures whilst the longer chromosomal DNA is precipitated, with the denatured proteins and cell debris. Plasmid DNA is further purified by preferential binding to a column followed by elution in TE buffer.

All cultures were performed in the presence of ampicillin. Cultures were made of single colonies of the appropriate transformed bacteria grown on LB plates. Bacteria were initially cultured in seeder broths of 5ml LB broth, in 50ml tubes (Becton Dickinson) to allow adequate aeration, at 37⁰C in an orbital incubator for ~2 hours. Aliquots of the seeder broth (250µl) were added to 12.5ml LB broth in a 50ml tube and cultured overnight at 37⁰C in an orbital shaker at 220rpm. Cultures were placed on ice, to keep the bacterial population within the log phase of growth, until extraction was undertaken. A 25ml culture yielded ~80-100µg of plasmid DNA.

2.5 Isolation and manipulation of nucleic acids

2.5.1 Isolation of nucleic acids from tissues

2.5.1.1 Extraction of genomic DNA from mouse tails

2.5.1.1.1 Tail tipping

Tissue from live animals was collected under anaesthesia. Mice were anaesthetised in a chamber using halothane (Fluothane, Mallinkrodt Veterinary), the tail tip removed with a scalpel and the wound cauterised. Tissue was stored at -20⁰C. Tissue could be stored at this temperature in excess of one year and yield good quality gDNA (see Figure 8, page 83).

2.5.1.1.2 Preparation of genomic DNA

See 3.2 genomic DNA extraction page 77

2.5.1.1.3 Preparation of RibonucleaseA (RNaseA)

Lyophilised bovine pancreatic enzyme (NBL Gene Sciences Limited) was resuspended in 10mM Tris pH 7.5, 15mM sodium chloride at 20mg/ml. Remaining DNase activity was removed by heating the solution in a water bath at 100⁰C for 15 mins. The solution was cooled slowly to room temperature, aliquoted and stored at -20⁰C.

2.5.1.1.4 Preparation of proteinase K

Proteinase K was supplied lyophilised with the QuiAMP kit. It was reconstituted in SDW at 20mg/ml and stored at -20⁰C in small aliquots. Any remaining after defrosting was discarded.

2.5.1.2 The isolation and storage of RNA

2.5.1.2.1 Tissue storage

Tissues were removed immediately after death, placed in freezer tubes (Nucleon) and snap frozen in liquid nitrogen. The majority of tissues were stored in liquid nitrogen freezers, with a small number being stored at -70⁰C.

2.5.1.2.2 Isolation of RNA

RNA was isolated from fresh frozen tissues using RNazol B (Biotech Laboratories Inc.) following the manufacturer's instructions. This is a modification of the one step method described by Chomczynski and Sacchi (1987). RNazolB contains guanidinium and phenol/chloroform in a monophasic solution. This technique is based on RNA forming complexes with guanidinium and water, keeping it in the aqueous phase, whilst DNA in this environment loses its hydrophilic properties and is sequestered in the phenol/chloroform phase with the protein.

All plastic-ware and apparatus were treated with 0.1% di-ethyl pyrocarbonate (DEPC). Apparatus was soaked in the solution overnight. Pipette tips and eppendorf vials were soaked overnight, oven dried and autoclaved. Distilled water prepared with DEPC was autoclaved to remove remaining DEPC, as this may interfere with downstream applications.

All nervous tissue samples were homogenised by tituration through sterile hypodermic needles of decreasing sizes (21-27 gauge) in the presence of the appropriate amount of RNazol B. Organs were crushed initially in a sterile pestle and mortar in the presence of liquid nitrogen. This was homogenised in a Dounce homogeniser in the presence of the appropriate amount of RNazol B.

A one tenth volume of ice cold chloroform was added to the homogenate and this was vortexed for 15secs and allowed to sit on ice for 15 minutes. The sample was centrifuged for 15 minutes at 12,000g at 4⁰C and the upper aqueous phase was removed and retained.

The RNA was precipitated by adding an equal volume of isopropanol to the aqueous phase. In situations where >1µg was anticipated this was left on ice for 15 mins. Samples with expected yields of <1µg were precipitated at -20⁰C overnight. The RNA was pelleted by centrifuging for 15 minutes at 12,000g at 4⁰C.

An alternative technique for the precipitation of small amounts of RNA the Paint Pellet (Novagen) system was used. Paint Pellet is a fluorescent-dye labelled carrier that encourages precipitation of nucleic acids and labels the resulting pellet allowing easy visualisation with UV light. RNA was precipitated in the presence of sodium acetate and 2 volumes of ethanol with 2µl Paint pellet. The sample was vortexed briefly and incubated at room temperature for 2 minutes. Samples were recovered at 12,000g at room temperature for 5 mins to pull down the RNA.

Pellets were washed with 800µl 75% ethanol/DEPC-treated sterile distilled water (SDW). After further centrifugation the pellet was air dried for 5 minutes and reconstituted in an appropriate volume of DEPC-treated SDW. The RNA concentration was measured as described below. Samples were stored at -70⁰C.

2.5.1.3 Quantification of nucleic acid

Nucleic acid samples, with the exception of the small amounts extracted from sciatic nerves and fragments extracted from gels, were quantified using a GeneQuant RNA/DNA calculator (Pharmacia Biotech). A spectrophotometer cell with a minimum volume of 70µl ensured that the minimal amount of nucleic acid was discarded during quantification. Working concentrations were a mean of two readings, of different dilutions, that were within 10% of each other.

The concentration of small quantities of nucleic acid was estimated by gel analysis against varying aliquots of an appropriate sample of known concentration. Alternatively, in the absence of an appropriate sample for quantifying small amounts of DNA samples were run out against aliquots of a low DNA mass ladder (Life Sciences, Paisley).

2.5.1.4 Nucleic acid electrophoresis

2.5.1.4.1 Agarose gels

Routine analysis of both DNA and RNA was performed on 0.7-2% agarose gels in a Tris acetate EDTA (TAE buffer). 0.7% agarose was used for the analysis of gDNA; 1% for the analysis of RNA; 1.3% for the separation of digested plasmids; 2% for the analysis of PCR products. Samples of RNA were examined on a denaturing gel if there was doubt about their integrity.

Gels were cast from ultra pure electrophoresis grade agarose (Life Sciences, Paisley). The agarose was melted in the presence of TAE buffer (see page 208). Ethidium bromide (from a stock at 10mg ml^{-1}) was added to the cooled gel to give a final concentration of $\sim 4\mu\text{g ml}^{-1}$. Samples were loaded with a 6x gel loading buffer (page 210). Gels were run in TAE buffer.

Gels were viewed with a "Fotoprep I" ultraviolet (UV) transilluminator (Fotodyne Inc.) and photographed using a Polaroid MP4 land camera (Polaroid) on Polaroid 667 (ASA 3000) film through a Wratten 22A filter (Kodak). Alternatively analytical gels were recorded using the ImageDoc Gel Documentation system (Scotlab) consisting of a high performance CDC video camera (COHU), UVT-28M UV transilluminator (Herotech) and a UP890CE video graphic thermal printer (Sony).

2.5.1.4.2 Denaturing agarose gels

Denaturing gels were used for gel separation of RNA populations prior to northern transfer. The addition of formaldehyde prevents the formation of secondary structures that would interfere with the migration of RNA species. One percent agarose gels (ultra pure electrophoresis grade agarose (Life Sciences, Paisley) were made in a formaldehyde/MOPS environment (see 8.5.2.2 *MOPS x10*, page 209). The buffering capacity of the MOPS buffer comes from both the sodium acetate and the 3-(N-morpholino) propanesulphonic acid (MOPS) (which is used in preference to Tris as it does not react with the formaldehyde).

Gels were cast by melting the agarose in MOPS buffer and allowing it to cool to $\sim 60^{\circ}\text{C}$ before adding 40% formaldehyde, to give a final formaldehyde concentration of 6.4% (w/v).

2.5.2 Polymerase chain reaction (PCR)

The same basic protocol was used for all primer pairs, with specific variations of magnesium chloride concentration and cycle number depending on individual primer pairs and the ambition of the experiment.

Primers were obtained as pairs and sourced from the same manufacturer (Cruachem, Glasgow).

2.5.2.1 PCR core programme

Samples were initially denatured at 94⁰C for 90 secs. The step cycle consisted of an annealing period of 45 secs at 55⁰C, an extension period of 60 secs at 72⁰C and a denaturation period of 45 secs at 94⁰C. The step cycle was varied according to the requirements of specific primer pairs (details with specific primer pairs). The final cycle consisted of an extended annealing period of 60 secs at 55⁰C and an extended extension period of 5 mins at 72⁰C. The extended extension period was shown to significantly increase the product yield. PCR products were harvested by careful pipetting from beneath the oil layer.

2.5.2.2 Genomic PCR

Amplifications for genotyping were performed either on the Perkin Elmer DNA thermal cycler or a PHC-3 (Techne). Reactions were carried out in 50µl volumes, in 0.5ml eppendorfs, and overlaid with 50µl of molecular biology grade mineral oil (Sigma) to prevent evaporation. Reactions contained 100ng target, 0.2mM dNTPs, 0.3µM of the forward and reverse primers (see 3.3 PCR genotyping, page 79), the specific concentration of magnesium chloride and were performed in the presence of 2.5U Taq polymerase (Bioline) with the manufacturers ammonium buffer. The addition of ammonium sulphate decreases the incidence of non-specific primer annealing by destabilising weak hydrogen bonding. Thirty cycles were used for all primer pairs with the exception of the primer pair used to identify the *Plp* and *Dm20* minigene mice, which required 39 cycles to produce a robust *Dm20* signal.

2.5.3 Southern transfer

2.5.3.1 Gel preparation

A mid-gel system (Model H3-SET, Anachem) giving a gel 15x13cm, approximately 100ml in volume, was used to provide wells of a suitable size within a gel of appropriate thickness for Southern transfer. The digested gDNA samples were run on 0.7% agarose gels (see 2.5.1.4 Nucleic acid electrophoresis, page 51) in

conjunction with suitable size markers. A photographic record was kept to aid interpretation of the autoradiograph (Figure 5, page 54).

The size separated gDNA fragments were denatured by soaking the gel in 0.5M sodium hydroxide/1.5M sodium chloride for 30 mins on a slowly shaking platform. The gel was neutralised in 1.5M sodium chloride/0.5M Tris pH7.4 to enhance binding of the nucleic acids to the transfer filter, which is reduced in environments >pH9.0.

2.5.3.2 Transfer

Transfer was achieved using a vacuum blotter (model 785, Bio-Rad) in a high salt environment (10xSSC, see page 209) onto a nylon filter (Hybond-N, Amersham). Transfer was for 90 minutes with a vacuum equivalent to 5 inches of mercury. After transfer filters were washed in 2xSSC to remove gel fragments and blotted dry. Nucleic acids were immobilised by UV cross-linking using an XL-100 (Spectronics Corporation).

2.5.3.3 Hybridisation

Pre-hybridisation and hybridisation were undertaken in a hybridisation oven with rotisserie (Micro-4, Hybaid) using Rapid-hyb buffer (Amersham). Volume of hybridisation buffer depended on size of the hybridisation bottle and the number of filters hybridised. Oven, bottles and hybridisation buffer were preheated to 65⁰C. Pre-hybridisation was for a minimum of 3 hrs. Probe was added to the hybridisation buffer and hybridisation was carried out over night at 65⁰C.

2.5.3.4 Stringency washing

Filters were washed to remove non-specifically bound probe. All stringency washes were in conducted at 65⁰C and 0.1% SDS in a sealed container in a shaking waterbath. The first two washes were in 2xSSC for 30 minutes. The second two washes were of increased in stringency, being in 0.1xSSC, with the first wash being for 30 mins. At this point filters were monitored and on the basis of the level of activity the final wash was conducted for between 30 mins and overnight. A final wash in 0.1%xSSC was conducted briefly at room temperature to remove the SDS.

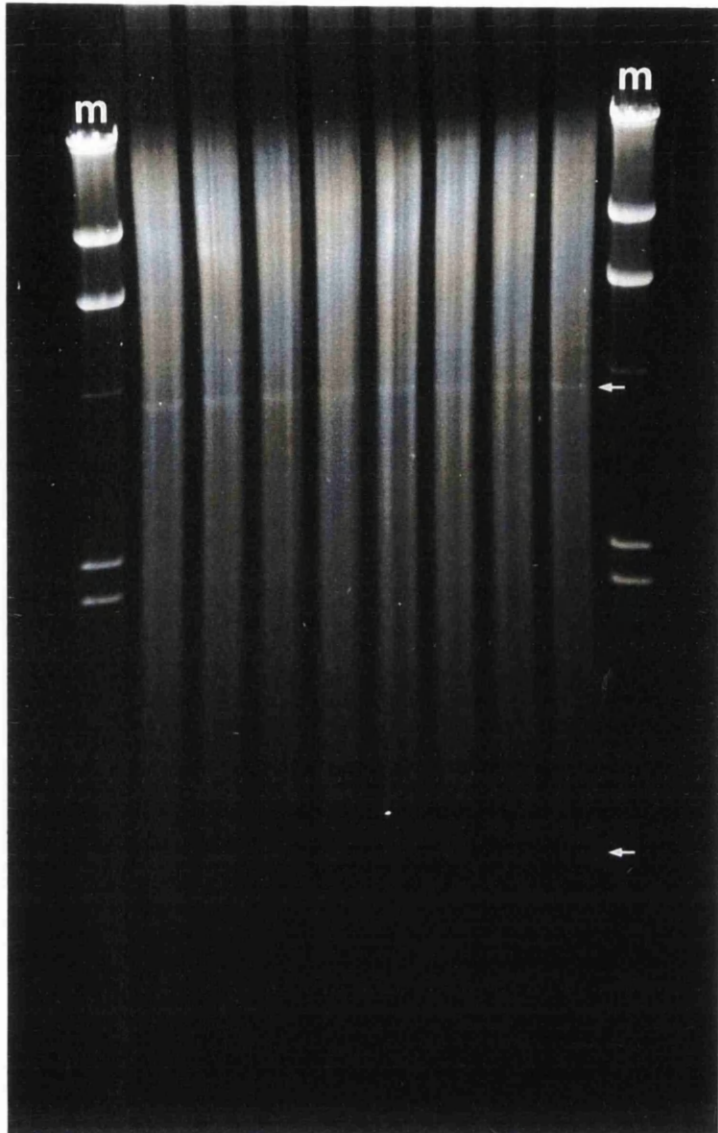


Figure 5. Example of gDNA digested with *Bam*HI run out on a 0.7% agarose gel immediately prior to Southern transfer. Arrows indicate the position of satellite bands, an indication of satisfactory gDNA digestion. Marker (m) λ *Hind*III.

2.5.3.5 Development

Hybridised filters were blotted dry (but not allowed to completely dry to prevent irreversible probe binding) and sealed in plastic bags. Autoradiography was performed using Cronex 10S film (DuPont) at -70°C . Films were developed using a Cronex-130 (DuPont) automatic processor.

2.5.4 Analysis of transcripts

2.5.4.1 Reverse transcription polymerase chain reaction (RT-PCR).

2.5.4.1.1 Design of novel PCR primers

This was undertaken using the Genetics Computing Group Wisconsin Package (Version 8)¹. Sequences were obtained from GenBank and EMBL. PCR primers were designed using the Extension programmes². The particular programme used for PCR primers was "PRIMA".

2.5.4.1.2 cDNA preparation

First strand cDNAs were synthesised from $2\mu\text{g}$ of total RNA, given availability. RNA was initially denatured at 65°C for 5 mins and quenched on ice. Reactions proceeded in the presence of $3\mu\text{g}$ random primers (Life Sciences, Paisley), 0.5mM dNTPs, 10mM dithiothrietol and 20U RNasin (Promega) for 30 mins at 37°C followed by 60 mins at 42°C using 400U Moloney murine leukaemia virus (M-MLV) reverse transcriptase (Life Sciences, Paisley) in the manufacturer's buffer. Reactions were terminated with the addition of 500mM EDTA to give a concentration of 12.5mM . The product was ethanol precipitated in the presence of 0.3M sodium acetate pH5.2 by adding 2 volumes of cold ethanol and incubating for 1 hr at -20°C . The product was pelleted by centrifugation at $12,000\text{g}$ for 30 mins. Excess salt was removed with a 70% ethanol wash and the pellet air dried for 5 mins. The product was reconstituted in SDW at $25\text{ng}\ \mu\text{l}^{-1}$. For cDNA preparations

¹ Program Manual for the Wisconsin Package, Version 8, August 1994, Genetics Computer Group, 575 Science Drive, Madison, Wisconsin, USA 53711

² Program Manual for the EGCG Package, Peter Rice, The Sanger Centre, Hinxton Hall, Cambridge, CB10 1RQ, England

from RNAs extracted from sciatic nerve the Paint Pellet technique was used to maximise the yield (see 2.5.1.2.2 Isolation of RNA page 49).

2.5.4.1.3 RT-PCR

These experiments were carried out exclusively on the DNA thermal cycler (Perkin Elmer) to reduce variability in results. This semi-quantitative procedure is based on the generation of a product from a constitutively expressed gene that acts as an internal control for invariant temporal expression. Cyclophilin (Danielson *et al.*, 1988) primers were used for parallel experiments to control for target and gel loading.

Reactions were performed in 25 μ l volumes in 0.5ml eppendorf vials overlaid with 50 μ l molecular biology grade mineral oil (Sigma). The target was 12.5ng of cDNA and this was amplified with 1.25U Taq DNA polymerase (Bioline) in the manufacturer's ammonium buffer in the presence of 0.2mM dNTPs and 0.3 μ M each of the forward and reverse primers. The concentration of magnesium chloride was optimised for each primer pair. Cycle assays were performed and a cycle number within the linear range used for subsequent experiments. The core PCR cycle is described in 2.5.2.1 PCR core programme (page 52). The primer pairs used for transcript analysis are described in Table 2 (page 58).

2.5.4.2 Northern blotting

This technique was used to compare the steady state levels of specific mRNA populations within the general mRNA pool of various tissues. RNA was extracted and quantified as in 2.5.1.2.2 Isolation of RNA (page 49).

2.5.4.2.1 Equipment preparation

All plastics were prepared as above. The mid-gel rig was soaked overnight in 0.5% DEPC water and dried without being rinsed.

2.5.4.2.2 Sample preparation

RNA samples were defrosted and kept on ice. Aliquots of 5 μ g were made up to a total volume of 10 μ l with DEPC treated water to which 31.12 μ l of denaturing buffer (page 209) was added. Samples were denatured by heating to 65⁰C for 5 minutes and 5 μ l of northern loading buffer (page 210) was added.

2.5.4.2.3 Gel conditions

A 100 ml 1% agarose denaturing gel was prepared as described in 2.5.1.4.2 Denaturing agarose gels (page 51). The MOPS buffer was changed once during the run as the heat generated during electrophoresis leads to buffer denaturation. The gel was washed 3x for 5 mins in DW to remove formaldehyde and equilibrated with transfer buffer by soaking for between 10 and 45 minutes.

2.5.4.2.4 Transfer

Transfer was as for Southern blots (see 2.5.3.2 Transfer page 53). Filters were stored between sheets of filter paper.

2.5.4.2.5 Methylene blue staining

To assess integrity and equality of transfer of RNA filters were stained with methylene blue. Filters were bathed in 5% acetic acid for 15 mins in a shaking water bath and stained by soaking in methylene blue for 10 mins. Staining was highlighted by removing the background staining by washing the filter in DW followed by air drying. The filter was photographed (see 2.5.1.4.1 Agarose gels page 51) using a green filter (Figure 6, page 59). Methylene blue readily identifies the ribosomal RNA species 28S and 18S, which migrate at approximately 5.1Kb and 1.9Kb respectively (Nyberg-Hansen, 1964). The position of these was marked by creating pinpricks, these can be identified on an autoradiograph due to non-specific binding, thus allowing estimation of the size of hybridised species.

2.5.4.2.6 Hybridisation

See 2.5.3.3 Hybridisation, page 53.

2.5.4.2.7 Stringency washing

See 2.5.3.4 Stringency washing, page 53.

2.5.4.2.8 Development

See 2.5.3.5 Development, page 55.

Primer target	Forward primer (5') sense	Reverse primer (3') anti-sense	Product length (bp)
<i>Plp</i> gene transcripts exons 2-exon 4	5'-gCTCTCACTggTACAGAA-3'	5'-TACATTCTTggCATCAgCgCAgAgACTgC-3'	506 <i>Plp</i> 401 <i>Dm20</i>
<i>Plp</i> gene transcripts exons 2-5 transgene specific on <i>Plp^{IP}</i> background	5'-gTggATgTggACATgAAg-3'	5'-ATggACAgAAggTTggAg-3'	583 <i>Plp</i> 478 <i>Dm20</i>
cyclophylin gene transcripts	5'-ACCCCACCgTgTTCTTCgAC-3'	5'-CATTIgccATGGACAAgATG-3'	300
<i>P₀</i> gene transcripts	5'-CCAgTgAATgggTCTCAGAT-3'	5'-TgCCgTTgTCACTgTAgTCT-3'	210

Table 2. Primer pairs used for transcript analysis.

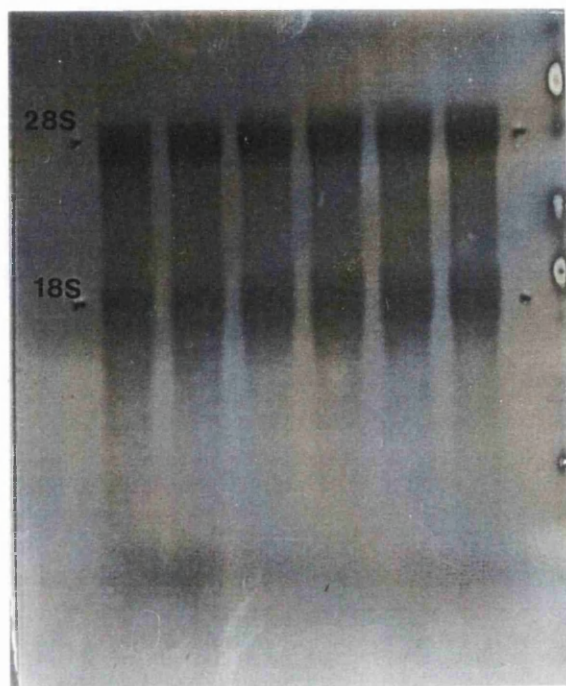


Figure 6. Methylene blue stained northern filter. The 18S and 28S bands can be seen clearly. They have been marked with pinpricks to aid subsequent analysis of the autoradiograph and represent ~ 1.9Kb and 5.1Kb respectively.

2.6 Analysis of proteins

2.6.1 Isolation of protein from tissue

Protein was isolated from whole mouse brains by homogenisation in 0.1M Tris (pH6.8) and 1mM N α -p- tosyl-L-lysine chloro-methyl ketone (TLCK) to which 2% SDS was added and the samples boiled for 5 minutes. The samples were centrifuged at 13,000g for 5 minutes in a Heraeus Biofuge at 4⁰C, the supernatant retained and stored at -20⁰C. Total protein concentration was measured using the BCA Assay (Pierce). DTT was added to give a final concentration of 40mM.

2.6.2 Western blotting

Aliquots (100 μ g) were resolved on a 5-17.5% gradient SDS-polyacrylamide gel with a 2.5% stacking gel. Electrophoretic transfer of the separated proteins onto Hybond ECL nitrocellulose membrane (Amersham Life Sciences) was performed at 200mA for 4 hours at 4⁰C in a transblot cell (Bio-Rad).

Immunodetection was accomplished using enhanced chemiluminescence (ECL). Non-specific binding was blocked by overnight treatment in Tris buffered saline (pH7.6) containing 5% dried milk, 0.2% gelatin and 0.1% Tween 20. The ECL nitrocellulose membrane was treated with the primary antibody, anti-PLP C-terminus (PLP226), at 1: 5000 for 60 minutes at room temperature, followed by extensive washing in the blocking buffer. The membrane was incubated in the secondary antibody, goat anti-rabbit IgG conjugated with peroxidase (Sigma), at 1:5000 for 60 minutes at room temperature, followed by extensive washing with the blocking buffer and a final rinse in Tris buffered saline (pH7.6). The ECL nitrocellulose membrane was incubated in equal volumes of luminol enhancer solution and stable peroxide solution (Pierce Chemical Co.) for five minutes at room temperature. The membrane was wrapped in Saran wrap and exposed to X-omat imaging film (Kodak) in a radiography cassette for 30 seconds. The film was developed using an automatic processor (DuPont Cronex CX-130).

2.7 Preparation of radiolabelled probes

2.7.1 Isolation of DNA fragments from agarose gels

The digested plasmid DNA was run out on a 1.3% agarose gel (see 2.5.1.4.1 Agarose gels page 51) to separate the fragment of interest from associated plasmid DNA. The region of interest was excised and the DNA fragment extracted from the gel slice using the QIAEX II Gel Extraction kit (Qiagen). This is a spin column system and is based on the QIAEX II silica particles that absorb DNA in a high salt environment from which it can be subsequently eluted in low salt conditions.

The gel slice was incubated in 3x its volume in buffer QX1 at 50⁰C in the presence of 10µl of QuiexII silica beads for 10 mins, with frequent vortexing. In these conditions the agarose melts and the nucleic acids are selectively absorbed onto the QuiexII beads. The beads were pelleted and the supernatant removed. The beads were resuspended by vortexing for 30 secs in a further 500µl of QX1, this wash removing further traces of agarose. Two similar washes in 500µl buffer PE, a high salt/ethanol buffer, removes final traces of salts. Traces of ethanol were allowed to evaporate as the pellet was air dried for 10 mins. The final step was to elute the DNA which was achieved by vortexing for 30 secs in SDW. Eluted DNA fragments were stored at -20⁰C.

2.7.2 Radiolabelling

DNA fragments were radiolabelled using High Prime (Boehringer-Mannheim) an optimised mixture of random oligonucleotide primers, dNTPs, Klenow enzyme in 5x buffer and glycerol. This kit is optimised for the use of radioactive dCTP. The use of random primers produces a mixed population of labelled fragments complementary to the 3`-5` strand.

The DNA fragment, usually 100ng, was made up to 11µl in SDW, denatured for 10 mins at 100⁰C and quenched on ice. To this was added 4µl High Prime and 5µl α³²P dCTP (Amersham) and the mixture thoroughly mixed. The labelling reaction was performed at 37⁰C for 10 mins at which time it was quenched by the addition of 0.2M EDTA to give a final concentration of 10mM EDTA. Labelled mixtures were stored at 4⁰C until the removal of unincorporated nucleotides (see below).

2.7.2.1 Removal of unincorporated nucleotides

Unincorporated nucleotides were removed by passing the labelled mixture through a Nick column (Pharmacia Biotech) containing Sephadex[®] G-50 beads. The eluted labelled DNA fragment was stored at -20°C until use.

2.8 *In situ* hybridisation (ISH)

2.8.1 ³⁵S riboprobes

A ³⁵S riboprobe was generated which was complementary to a sequence common to both *Plp* and *Dm20* mRNA, using the SP6/T7 Transcription kit (Boehringer-Mannheim). This probe, termed PLP-1, was generated from a 0.8kb cDNA containing mainly the coding region cloned into pGEM 4 (Promega) (Milner *et al.*, 1985) (see Figure 7, page 67). The plasmid was linearised using *Bam*HI (Life Sciences, Paisley), the digestion being confirmed by analytical gel analysis, ethanol precipitated and reconstituted at a final concentration of 500ng μl^{-1} . The choice of restriction enzyme was influenced by the need to generate a 5' overhang as 3' overhangs may cause aberrant transcript generation.

A 20 μl labelling reaction contained the following: 1-2 μg linearised plasmid DNA, 1.0 μl each of the nucleotides (ATP, GTP, UTP (10mM in Tris buffer), 5.0 μl (50 μCi) ³⁵S αCTP (specific activity 37Tbq mM^{-1} ; <1000Ci mM^{-1} ; Amersham), 2.0 μl 10x transcription buffer, 1.0 μl RNase inhibitor (20U μl^{-1}) in a final volume of 20 μl in DEPC SDW. The mixture was incubated at 37°C for 30 mins after the addition of 1.0 μl of T7 RNA polymerase (20U μl^{-1}). An additional 1.0 μl enzyme was added and the incubation extended for a further 30 mins. Template was digested by the addition of 2.0 μl DNase (10U μl^{-1} , RNase free) and incubated for a further 15 mins. The product was phenol-chloroform extracted and a further extraction made after the addition of a further 22 μl DEPC SDW. The RNA was precipitated with 7.5M ammonium acetate, a 5.0 μl aliquot was set aside (A) and the product pelleted by centrifugation and a 5.0 μl of the supernatant set aside (B). The RNA pellet was reconstituted in 100 μl DEPC SDW and 5.0 μl was set aside (C). The riboprobe was reprecipitated overnight in ethanol. The aliquots A, B and C were placed in 5ml Ecoscint (National Diagnostics).

The Ecoscint vials were counted on a LS 1801 scintillation counter (Beckman). Vial A represents total isotope; B represents unincorporated isotope; C represents incorporated isotope. Percentage incorporation was calculated from the ratio of B/A. Isotope incorporated into RNA in the form of the riboprobe, was calculated

from a standard formula and it was reconstituted in 0.01M DTT at a concentration of $1.0\text{ng } \mu\text{l}^{-1} \text{ kb}^{-1}$. Probe was stored at -20°C and used within 6-8 weeks.

Probes were prepared by Dr P. Dickinson.

2.8.2 ISH protocol

The basic procedure was as described by Cox *et al* (Cox *et al.*, 1984) and modified by Wilkinson *et al* (Wilkinson *et al.*, 1987). Pre-treatment involves several steps which maximise the accessibility of the target to the probe whilst maintaining the tissue morphology. Proteinase K treatment removes protein bound to the target whilst acetylation decreases non-specific binding due to electrostatic interactions between basic proteins and the probe (Hayashi, 1978). Hybridisation is undertaken in low stringency conditions to favour hybrid formation with the unbound probe removed by the higher stringency washes. An RNase step is included to remove single stranded RNA.

2.8.2.1 Preparation of apparatus

2.8.2.1.1 RNase treatment of glassware

To minimise RNase activity all glassware and slides were soaked in 6.0% sulphuric acid/6% potassium dichromate overnight, rinsed in tap water for 2-4 hrs, rinsed in DW, immersed in 0.01% DEPC SDW overnight, oven dried at 60°C and baked at 180°C for 4 hrs loosely wrapped in foil. Eppendorf vials and pipette tips were treated as described in 2.5.4.2.1 Equipment preparation (page 56).

2.8.2.1.2 Preparation of coverslips

The coverslips used to cover sections during hybridisation were soaked in 1M hydrochloric acid for 30 mins, rinsed 3x in DW and air dried. Cleaned coverslips were immersed in Repelcoat (BDH) for 20 mins, rinsed 2x in DW and baked at 130°C for 90 mins. The siliconisation with Repelcoat was included to reduce probe binding.

2.8.2.1.3 Preparation of APES coated slides

Cleaned slides were coated with 3-aminopropyltriethoxy-silane (APES) (Sigma). Slides were washed in the detergent Decon 90 (5%) (Decon Lab Ltd) to remove grease overnight, washed well in DW and oven dried wrapped in foil. In a fumehood slides were soaked in 0.25% APES in methylated spirit for 2 mins

followed by 0.01% DEPC SDW for 2 mins prior to oven drying wrapped in foil. Slides were stored at room temperature.

2.8.2.2 Preparation of tissue

In situ hybridisation was performed on 6µm tissue sections from BNF perfused / paraffin wax embedded tissue (see 2.2.4.1 Paraffin-embedded tissue page 45) on APES slides and 15µm unfixed cryo-preserved tissue (see 2.2.3 Cryo-preservation page 44) also on APES slides.

2.8.2.3 Pre-treatment

Slides were passed through the following solutions:

- | | | | |
|-----|--|--------------------------|---|
| 1) | xylene | 10 mins | paraffin embedded sections only |
| 2) | absolute alcohol | 5 mins | paraffin embedded sections only |
| 3) | methylated spirit | 5 mins | paraffin embedded sections only |
| 4) | 0.85% saline | 5 mins | |
| 5) | PBS | 5 mins | |
| 6) | 4% paraformaldehyde
(in PBS) | 20 mins | |
| 7) | PBS rinse | 5 mins (x ²) | |
| 8) | proteinase K* | 7.5 mins | paraffin embedded sections only |
| 9) | 4% paraformaldehyde
(in PBS) | 5 mins | only proteinase K treated sections |
| 10) | 0.1M triethanolamine
+625µl acetic
anhydride | 5 mins | performed in fumehood using
magnetic stirrer |
| 11) | add further 625µl acetic
anhydride | further 5
mins | |
| 12) | PBS rinse | 5 mins | |
| 13) | 0.85% saline | 5 mins | |

- 1) 75ml ethanol, 162.5ml DW, 12.5ml 30 secs
6M ammonium acetate
- 2) 150ml ethanol, 87.5ml DW, 12.5ml 30 secs
6M ammonium acetate
- 3) 200ml ethanol, 37.5ml DW, 12.5ml 30 secs
6M ammonium acetate
- 4) 237.5ml ethanol, 12.5ml 6M 30secs
ammonium acetate

Slides were rinsed in absolute alcohol for 2 mins, air dried.

2.8.2.6 Autoradiography

Slides were exposed to Cronex (DuPont) autoradiography film in a radiography cassette overnight at room temperature. The intensity of the image determined the subsequent exposure to photographic emulsion. Slides were dipped in a solution of Ilford K5 emulsion in a 1:1 ratio with DW containing 1.0% glycerol at 42⁰C. Slides were air dried for 4-6 hrs and stored at 4⁰C in light tight boxes, containing a sachet of silica gel, for a period of 1-2 days. The slides were developed by immersion in D19 developer (Kodak) at 18⁰C for 3-5 mins. This was stopped by immersion in 1% acetic acid/1% glycerol. Slides were fixed in 30% sodium thiosulphate for 8 mins and washed in water for 20-30 mins in the dark before air drying.

Sections were counterstained with haematoxylin (see 2.3.1.2 Haematoxylin, page 46) dehydrated and mounted.

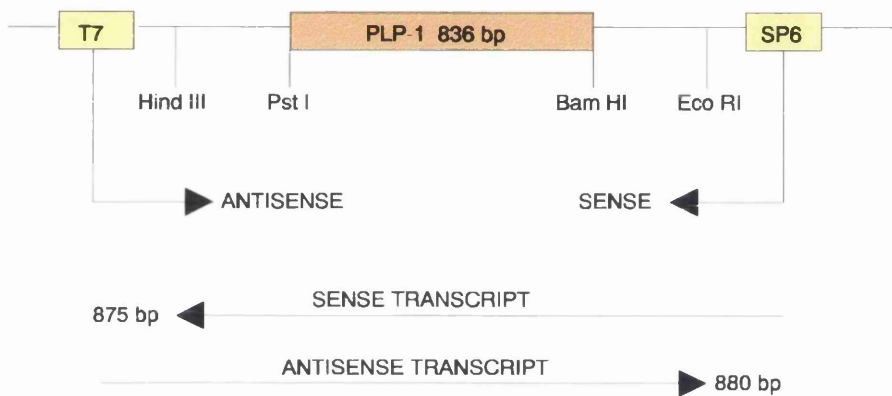


Figure 7. Generation of the PLP-1 probe for *in-situ* hybridisation. The use of the T7 promoter produces an α -sense sequence which will hybridise with mRNA in the tissue. The fragment recognises both the *Plp* and *Dm20* message isoforms.

2.9 Immunocytochemistry

2.9.1 Tissue sections

All incubations with antibodies and links where sections were bathed in small volumes of fluid were performed in a humidifying chamber. Control sections were included where the primary antibody was omitted and replaced with PBS. Tissue sections were cut as described in 2.2.4 Preparation of sections (page 45).

2.9.1.1 Peroxidase anti-peroxidase (PAP)

The primary antibodies, sources, dilutions and links used for PAP immunostaining are summarised in Table 3 (page 70) with the exception of the antibodies used for the demonstration of microglia and T cell sub types, which are summarised in 4.3.4 Immunocytochemistry (page 91).

2.9.1.1.1 Paraffin wax embedded tissue

Sections were hydrated:

- | | | |
|----|----------------------------------|-------|
| 1) | xylene | 2 min |
| 2) | absolute alcohol | 2 min |
| 3) | methylated spirit | 2 min |
| 4) | water | 2 min |
| 5) | Lugols iodine | 1 min |
| 6) | water | 1 min |
| 7) | 5% sodium thiosulphate
(hypo) | 1 min |
| 8) | water | |

Endogenous peroxidase activity was quenched by immersing slides in 3% hydrogen peroxidase (in absolute alcohol) for 30 minutes followed by a wash in running water for 30 mins. Non-specific binding was blocked by incubating in 10% normal goat

serum (NGS) in PBS for 2 hr at room temperature. Sections were incubated in the primary antibody in 1% NGS in PBS overnight at 4⁰C.

Sections were adjusted to room temperature and washed for 30 mins in PBS (six changes) followed by the link antibody in 1% NGS at room temperature for 1 hr. Excess antibody was removed by washing in PBS for 30 mins (6 changes) and the sections incubated in the PAP complex for 30 mins at room temperature. Excess was removed by washing in PBS for 30 minutes (6 changes). The chromogen was developed in filtered 0.1M phosphate buffer (pH7.3) containing 0.5mg/ml 3,4,4',4',-tetraminobiphenyl hydrochloride (DAB) and 0.003% hydrogen peroxide until the required colour intensity had been achieved (30s-5 mins). Sections were washed in running water, dehydrated and mounted in DPX (BDH).

2.9.1.1.2 Resin embedded tissue

Resin was removed by immersing slides in sodium ethoxide (50% ripened sodium ethoxide in 50% absolute alcohol) for 30 mins after which they were examined by microscopy to ensure that this had been achieved. Sections were washed in absolute alcohol for 30 mins (six changes) and running water for 30 mins. Endogenous peroxidase activity was quenched with 3% hydrogen peroxide in water. Further steps were as above. After development of the DAB reaction, sections were osmicated in 1% osmium, to intensify the colour product, for 1 min before washing, dehydrating and mounting in DPX.

2.9.1.2 Immunofluorescence

The antibodies, their source, dilutions and links used in fluorescent immunostaining are summarised in Table 4 page 71. Secondary antibodies labelled with fluorescein isothiocyanate (FITC) and Texas red (TXR) were used and sections examined by epifluorescence. FITC absorbs light with a wavelength 495nm and emits it at 525nm which can be visualised as green light using a blue filter. The TXR labelled conjugate absorbs light at 596nm and emits it at 620nm which can be visualised as red light using a green filter.

Primary antibody	Dilution	Source	Link	PAP complex	Source
rabbit anti-MBP (polyclonal)	1:400	Dr J.M. Matthieu, Lausanne, Switzerland	goat-anti rabbit (1:10)	rabbit (1:40)	ICN
rabbit anti- PLP/DM20 (PLP- CT) (polyclonal)	1:600	Professor N.P. Groome, Univeristy of Oxford	goat-anti rabbit (1:10)	rabbit (1:40)	ICN
(amino acids 271- 276)					
rabbit anti-GFAP (bovine) (polyclonal)	1:1000	DAKO	goat-anti rabbit (1:10)	rabbit (1:40)	ICN
mouse anti-SMI-31 (monoclonal)	1:1500	Affinity Research Products	goat-anti mouse (1:10)	mouse (1:1250)	Sigma
rabbit anti-MAG 253 (polyclonal)	1:500	Professor N.P. Groome, Univeristy of Oxford	goat-anti rabbit (1:10)	rabbit (1:40)	ICN

Table 3. Antibodies, sources, dilutions and links used in PAP immunostaining. All link antibodies were sourced from Sigma.

Primary antibody	Dilution	Source	Secondary antibody	Dilution
rabbit anti-PLP/DM20 CT (aa 271-276) (polyclonal)	1:600	Prof. N.P. Groome, Oxford, UK	goat-ant rabbit-IgG (H+L)-FITC human/mouse absorbed	1:80
rabbit anti PLP specific (aa 117-129) (polyclonal)	1:600	Dr. J.C. Nusbaum, Strasbourg, France	goat-ant rabbit-IgG (H+L)-FITC human/mouse absorbed	1:80
mouse anti-P ₀ (monoclonal) PO7, clone 18	1:500	Dr Archelos, Würzburg, FDR	goat-ant mouse-IgG ₁ (H+L)-TXR human/mouse absorbed	1:75
mouse anti-SMI 31 phosphorylated NF-H (monoclonal)	1:1500	Affinity Research Products	goat-ant mouse-IgG ₁ (H+L)-TXR human/mouse absorbed	1:75

Table 4. Antibodies, sources, dilutions and links used in fluorescent immunostaining. FITC fluorescein isothiocyanate; TXR Texas red. All secondary antibodies were obtained from Southern Biotech.

2.9.1.2.1 Cryo-sections

Sections were allowed to warm to room temperature, dry and washed in PBS for 10 mins, to remove the embedding medium. Sections were fixed in 4% paraformaldehyde at room temperature for 20 mins, rinsed in PBS, followed by methanol at -20°C for 10 mins and 2x 5 minute washes in PBS. Incubation in the primary antibody, in 1% NGS, was for 1 hr at room temperature or overnight at 4°C . Sections were washed 6x 5 mins in PBS and the secondary antibody applied for 30 mins at room temperature. After a final thorough wash with 3x 5 mins in PBS followed by 5 mins in running water sections were mounted in Citifluor (UCK Chem Lab), to prevent fading, and stored in the dark at 4°C .

2.9.1.2.2 Paraffin wax embedded sections

Sections were hydrated as in 2.9.1.1.1 Paraffin wax embedded tissue (page 68). The sections were not further fixed and immunostaining and mounting was as described above.

2.9.2 Teased fibres

2.9.2.1 Immunofluorescence

Prepared fibres were fixed in fresh 4% paraformaldehyde for 20 mins at 4°C , rinsed briefly in PBS, followed by 10 mins in methanol at -20°C . Sections were incubated in primary antibody in 1% NGS for 1 hr at room temperature. Excess antibody was removed by washing in PBS for 20 minutes. Sections were incubated in secondary antibody for 30 minutes, rinsed in water and mounted as above.

2.10 Morphometry

2.10.1 Glial cell quantification

All cell counting was performed on $1\mu\text{m}$ resin-embedded sections of cervical cord at the level of approximately C2, stained with methylene blue/azur II. Counting was performed with a 6.3x eyepiece in combination with a 100x oil immersion lens with a 100 square graticule (Graticules Ltd.). The area selected was the ventral columns immediately adjacent to the ventro-median fissure and its continuation onto the ventral surface of the cord. Only cells in which the nucleus was sectioned were counted. Between 400-600 cells were counted, depending on the animals age, with

a minimum of 12 μ m between sections to prevent individual nuclei being counted more than once. Counts were made of all glial cells and precursors with categorisation made on morphological characteristics. Endothelial cells were not counted. Longitudinal sections taken from the cord immediately caudal to the counting area were used to estimate the mean and maximum nuclear lengths. Areas of sections were calculated from Polaroid light microscopy images using Sigma Scan/Image measurement software (Jandel Scientific Software) and SummaSketch III graphics tablet (Summagraphics). Corrected total cell glial counts and glial densities were calculated using Abercrombie's formula as discussed by Sturrock (1983). Three animals were counted for each age and transgenic status. The results were plotted using Graphpad Prism software (Graphpad Software Inc.).

2.10.1.1.1 Dead cell density

The dead cell density was estimated by counting pyknotic nuclei distributed throughout the white matter of the cord section. For each mouse two sections, separated by 12 μ m, were counted and the mean calculated. Though the type of cell cannot be ascertained it is well recognised that during development of the CNS a large proportion of such dead cells represent glial cells of which the majority are oligodendrocytes (Vela *et al.*, 1996).

2.10.2 Myelin thickness

Araldite blocks used for cell counting were trimmed and ultra-thin sections prepared for electron microscopy (2.2.4.4 Ultra-thin sections page 45 and 2.3.2 Electron microscopy page 46). Random fields from the ventral columns were photographed at approximately 5000x and printed at 2x magnification. Calibration was achieved by photographing a diffraction grating of known size for each set of prints.

Myelin and axons were outlined using a graphics pad to generate the total area of axon and myelin and axon area (software/hardware as above). A total of 150-180 myelinated axons were measured for each mouse. This data was used to derive (Excel 5, Microsoft) diameters of circles with equivalent areas and thus the notional myelin thickness. The derived myelin thickness and equivalent axonal diameter allowed the derivation of the *g* value (*g* is defined as the ratio of axon diameter to that of the axon plus sheath).

To examine the relationship between axon diameter and *g* value the data for mice of the same age and zygosity was pooled.

2.10.3 Myelin density

These measurements were performed by point counting of the electron-micrographs using a method described by Williams (1977). Squares of 2cm^2 were used giving a total of 64 possible intercepts per electron-micrograph with 10-12 photographs being counted per animal. The myelin to axon ratio was calculated from the contacts made with myelin sheath or axon.

2.11 Statistical methods

In general, the results for experimental groups were summarised graphically by three data points. In most instances the small group sizes limited the applicability of complex statistical analysis, but by presenting all the data points comments on general trends can be made. Comparisons were made referring to the median. The median was selected as it is less susceptible to distortion by out lying values. In populations with a normal distribution the median and mean have the same value. Occasionally only two data points were available for a group and interpretation was limited to commenting on any apparent trend. Experimental groups with sufficient data were compared using the non-parametric two tailed Mann-Whitney test. This test ranks the data and makes a statement on the significance of the mixing of the distributions of ranked values from the two groups. Throughout this thesis, statistical significance was set at the 5 percent level (i.e. $P < 0.05$).

2.12 Image recording

2.12.1 Photomicrographs

Photographs of histological sections were taken on a Olympus Vanox-S. Dark field images of ISH sections were captured on a stage illuminated by a Fibre-Lite Series 180 (Doran Jenner Industries, Inc.).

2.12.2 Immunofluorescent photography

Photographs were taken using a Reichart-Jung Diastar photomicroscope with epifluorescence (Model 2090).

2.12.3 Confocal microscopy

The confocal system was a MRC600 (BioRad). This data output from this system is in the form computer graphic files and the images presented are from these original data files.

2.12.4 Electronmicroscopy

The electronmicroscope was an AEI EM6B.

2.12.5 Image presentation

Suitable images were scanned from transparencies using a Coolscan II (Nikon) and the images printed on a Epson Stylus Color 800. Images of epifluorescence are not suitable for this process and have been printed from transparencies.

2.13 Growth of mice

Mice were weighed immediately after being killed.

Body weight as a measure of development is a parameter that is straightforward to obtain. The information must be considered in the light of the variables that have been demonstrated to affect weight gain, many of which are pertinent to this study. The following general features have been identified as having significant effects on weight gain (Cunliffe-Beamer and Les, 1987): age of dam; age of sire; parity of dam; size of litter; availability of food; etc.

3. Materials and Methods - Genotyping and breeding of transgenic mice

3.1 Introduction

The transgenic status of the mice described in the following chapters was confirmed using a combination of data including: phenotype, observations on pathological features, PCR data and Southern blotting.

3.2 genomic DNA extraction (gDNA)

The selection of a procedure to be adopted for routine gDNA extraction was influenced by the potential downstream ambition of semi-quantitative Southern analysis, and its requirements for reproducibility and high quality. Another criterion in the selection of a technique for gDNA extraction was its suitability for simultaneous handling of multiple extractions.

As a base line, the traditional technique of cell lysis and deproteinisation by phenol-chloroform extraction was assessed. Tissues were incubated at 55°C in buffers based on SDS (to lyse cell membranes) and proteinase K to denature proteins (including DNases) and EDTA (which also inhibits DNases). This was followed by protein extraction using phenol-chloroform and an alcohol precipitation of nucleic acids. A number of extraction buffers, varying in SDS and EDTA content, were assessed. Though high molecular weight gDNA with good digestibility and consistent quantification could be obtained using this system it proved time consuming and less reliable when used with large numbers of samples. There are also inherent problems associated with working with and disposing of phenol.

Three commercial kits were assessed. Such kits are marketed primarily as offering high quality gDNA from procedures with reduced manipulations (giving time savings) and increased safety by removing the requirement for phenol-chloroform extraction. The three kits selected were based on different principles, though all initially utilised a cell lysis step including a cell lysis buffer and proteinase K.

Contaminating RNA was removed with RNaseA treatment (see 2.5.1.1.3 Preparation of RibonucleaseA (RNaseA), page 49) the specifics of which varied between protocols.

Nucleon (Scotlab) is based on a patented resin that in combination with sodium perchlorate and chloroform removes protein and cellular debris. Though the quality of the gDNA was acceptable, physical limitations on the amount of tissue that could

be handled resulted in relatively small yields which would have been insufficient for the downstream requirements without multiple preparations from each tail.

Puregene (Flowgen) is based on a protein precipitation buffer, which produces an insoluble pellet of protein and cell debris from which the DNA is separated by removing the supernatant in which it is dissolved. This system proved to be inconsistent in the quality of the gDNA produced.

The QIAamp Tissue kit (Qiagen) is based on a patented spin column system in which gDNA is first absorbed onto the membrane allowing the removal of proteins in the flow-through followed by a change in buffering that results in the elution of gDNA from the membrane. This system proved to give consistently high yields of undegraded, easily digestible gDNA with a high molecular weight (Figure 8, page 83) and was selected for routine preparations.

3.2.1 QuiAMP gDNA extraction

Frozen mouse tail samples of approximately 0.5cm were finely chopped and added to 180 μ l of buffer ATL and 20 μ l of proteinase K (see 2.5.1.1.4 Preparation of proteinase K, page 49) in a sterile 1.5ml eppendorf and vortexed. Tail samples were incubated at 55⁰C with brief vortexing every ~20 mins until well digested. This period varied with the age of the mouse between approximately 1 and 5 hrs. Digested samples were spun at 12,000g for 15 minutes to sediment the tissue debris, after which 180 μ l of supernatant was removed to a fresh sterile eppendorf. To the supernatant 20 μ l of 20mg μ l⁻¹ RNaseA was added followed by a brief vortex and 2 mins incubation at room temperature. A mixture of 200 μ l buffer AL with 210 μ l alcohol was added to each sample and the whole volume spun through a column to bind the gDNA to the membrane and extract the protein. This was followed by two washes in buffer AW to remove final traces of protein from the membrane. The gDNA was eluted in buffer AE at 70⁰C. Pre-heated buffer (200 μ l) was added to the column and the assembly incubated at 70⁰C for 5 minutes before the buffer was spun through the column. The importance of this incubation as compared with centrifugation immediately following the addition of the warmed buffer was assessed and found to significantly increase the final yield. This step was repeated to give a final volume of 400 μ l. Yields varied with the age of the mouse but were between ~60-140 μ g with an OD_{260/280} of >1.7 (see 2.5.1.3 Quantification of nucleic acid, page 50). Samples were stored at -20⁰C.

3.3 PCR genotyping

All the transgenes could be identified specifically by PCR with the appropriate primer pairs (see below). This system, however, did not differentiate between hemizygous and homozygous individuals. Gene dosage or zygosity was assessed by Southern blot analysis.

The core PCR protocol is described in 2.5.2.1 PCR core programme (page 52). The positions of the primer pairs for the specific transgenes is illustrated in Figure 9 (page 84). The sequence of the specific primers pairs and their PCR conditions are in Table 5 (page 85). Though all primer pairs have been described previously their behaviour was reassessed for this laboratory with regards to quantity of target, magnesium concentration and cycle assay to give conditions in which the presence of the transgene could be recognised reliably.

3.3.1 #66 and #72 mice

The only transgene specific sequence in the construct was a portion of the T7 promoter at the 3' end (see Figure 9, page 84). A T7 specific primer in conjunction with a primer from the 3' end of the murine PLP gene produces a PCR product of 250bp with both transgenes and was described by Readhead and others (1994). It was noted in preliminary experiments that the system was relatively easily overloaded with target. Therefore as the potential for false negatives existed, accurate quantification of the gDNA target for was important

To ensure consistent results all PCR runs included target from a wild type other than the transgenic background, a known transgene positive, a known transgene negative and a no target as controls. The PCR product is illustrated Figure 10 (page 86).

3.3.2 *PlpTag1* and *Dm20Tag2* mice

The transgenic status of the *Plptag1* and *Dm20tag2* minigene mice were assessed using primers described by Nadon *et al* (1994). The two transgenes generate products of different sizes (*Plptag1* 412bp; *Dm20tag1* 307bp) confirming the nature of the transgene in an individual mouse. Controls similar to those used for #66 and #72 mice were used. The PCR products obtained for each of the two transgenes is illustrated in Figure 10 (page 86).

3.3.3 *Plp^{lP}* carrier females

The *Plp* gene mutation underlying the *Plp^{lP}* phenotype results in the abolition of a *DdeI* restriction site at the 5' end of exon 5 (see Figure 11, page 87). This was used

to identify female carriers of the *Plp^p* allele by PCR using primers that span this region, followed by *DdeI* digestion of the product. The primers used were those described by Ikenaka *et al* (1988). The product of this primer pair is a discrete population thus 10µl aliquot of the PCR product was digested in a 12µl reaction with 6u *DdeI* (Life Technologies, Paisley) for 1 hr at 37⁰C and run out on a 2% agarose gel with a 10µl aliquot of undigested product. The resulting restriction profile is illustrated in Figure 11 (page 87).

3.4 Southern blot assessment of #66 and #72 transgene zygosity

Southern blotting was used both to confirm suspected zygosity (as assessed from a combination of phenotypic and pathological findings in conjunction with PCR) and in situations where there was no other information, other than PCR identification.

3.4.1 gDNA digestion

The goal of Southern analysis was to assess relative hybridisation signal intensities. To enhance such differences the quantity of gDNA digested was at the lower end of the detection range in this system (see 3.6 Discussion, page 82).

The fragment used for labelling was a *BamHI* digest and hence the gDNA was subjected to the same digest. Digests of 5µg were performed in 35µl volumes using *BamHI* (Life Technologies, Paisley) for 3 hrs at 37⁰C, at which point representative 0.5µg aliquots were gel-checked to assess the completeness of the digestion. A further indication of the complete digestion was the presence of satellite bands after gel electrophoresis of the digests (see Figure 5 page 54). Completed digests were stored at -20⁰C.

Southern blots were designed to include wild type and homozygous/hemizygous controls. All gDNA samples were processed as duplicates.

3.4.2 Southern transfer

See 2.5.3 Southern transfer, page 52

3.4.3 Hybridisation probes

A 2.5Kb *BamHI* fragment (termed B6), a sub-clone of COS901, was radiolabelled. The fragment used for hybridisation recognised a sequence including exon 1 of the

endogenous *Plp* gene and the transgenes (Figure 3, page 14) as described previously (Readhead *et al.*, 1994).

Probe preparation is described in 2.7.2 Radiolabelling (page 61). Probes were prepared with an activity in excess of 10^8 cpm μg^{-1} . Final probe concentration in the hybridisation buffer was $10\mu\text{g ml}^{-1}$ for probes 10^8 cpm μg^{-1} and $2\mu\text{g ml}^{-1}$ for probes $>10^9$ cpm μg^{-1} (Greenberg and Bender, 1997).

3.4.3.1 Interpretation

Comparisons of signal intensity between controls and unknowns was made to assess zygosity taking into account the relative gDNA loading as determined from the gel photograph. An example of the relative intensities of the various zygosity is shown in Figure 12 (page 88).

3.5 Breeding of transgenic mice and *Plp^{JP}* crosses

Mice were bred primarily in the animal house of the Veterinary Research Facility, University of Glasgow Veterinary School and also at the animal breeding facilities GMBH, Heidelberg. The particular animal house used in Glasgow is known to have evidence of MHV and picorna virus infection both of which have been associated with neurological disease in mice (see 1.3.1.1 Demyelination in mice due to viral infection, page 25), however, there has been no evidence of clinical disease during the period of the project. Mice bred at GMBH are specific pathogen free and had not been exposed to these viruses. There were no apparent differences in phenotype or pathology in the mice bred at the two facilities nor were there abnormalities in the wild type mice bred at Glasgow, suggesting that these viruses were not significant in the development of the phenotypes described below.

The four lines of transgenic mice were maintained by creating harems of transgenic positive animals that were genotyped by PCR as described above. In harems of #72, *Plptg1* and *Dm20tg2* occasional pairings included a breeding adult that was transgene negative to ensure that both hemizygous and homozygous offspring were bred. However, for #66 the early death meant that only hemizygous animals were suitable for breeding.

To produce offspring with the *Plp^{JP}* phenotype and carrying one of the transgenes harems of *Plp^{JP}* carrier females and transgene positive males were set up. Offspring were tail tipped at P10 and assessed for their transgenic status by PCR. This

breeding strategy could only result in transgene positive mice being hemizygous and samples were not assessed by Southern blot.

3.6 Discussion

The initial description of #66 and #72 mice by Readhead and others (1994) established the relationship between zygosity and the mutant phenotypes. With aspects of the pathology already outlined such details as phenotype and pathological findings could be used, in conjunction with PCR data, as internal controls to Southern blotting. Their experiments had also estimated the copy number associated with the #66 and #72 transgenic cassettes.

In this project the ambition for the Southern analysis was the determination of zygosity and thus experiments were not required for quantitative hybridisation analysis. It was considered unnecessary to achieve a quantitative analysis as the experimental design is more complex and is not easily achieved using autoradiography - the technology available (Darling and Brickell, 1994). Using a suitably labelled probe (10^8 - 10^9 dpm μg^{-1}) approximately 0.5pg of target DNA can be detected which for a single copy of a 500bp sequence, in the human genome, is equivalent to 3.3 μg of DNA (Brown, 1997). Consequently to emphasise hybridisation differences Southern analyses were performed at the lower limits of detection (5 μg) at which over saturation of the autoradiograph was less likely. This resulted in weak signals from wild type mice which was not considered significant as the status of these mice was identified by PCR. The ability to assess confidently differences in hybridisation were an important aspect of this project and of particular significance in assessing the zygosity of #72. Here the difference between hemizygous and homozygous is only 3 copies, and at the limits of resolution for this approach and as a consequence samples from mice in which identification was not clear cut were rejected for further study.

The technical requirements for accurate estimation of transgene copy number could not be fulfilled and this was not undertaken. There, however, exists the possibility for changes to occur to the transgenes. This includes changes in copy number and the present study does not address this specifically, other than by not observing changes in the established phenotypes. The late onset phenotype, which had not been noted previously, was observed in litters of mice in which the phenotype of homozygous mice was as expected.

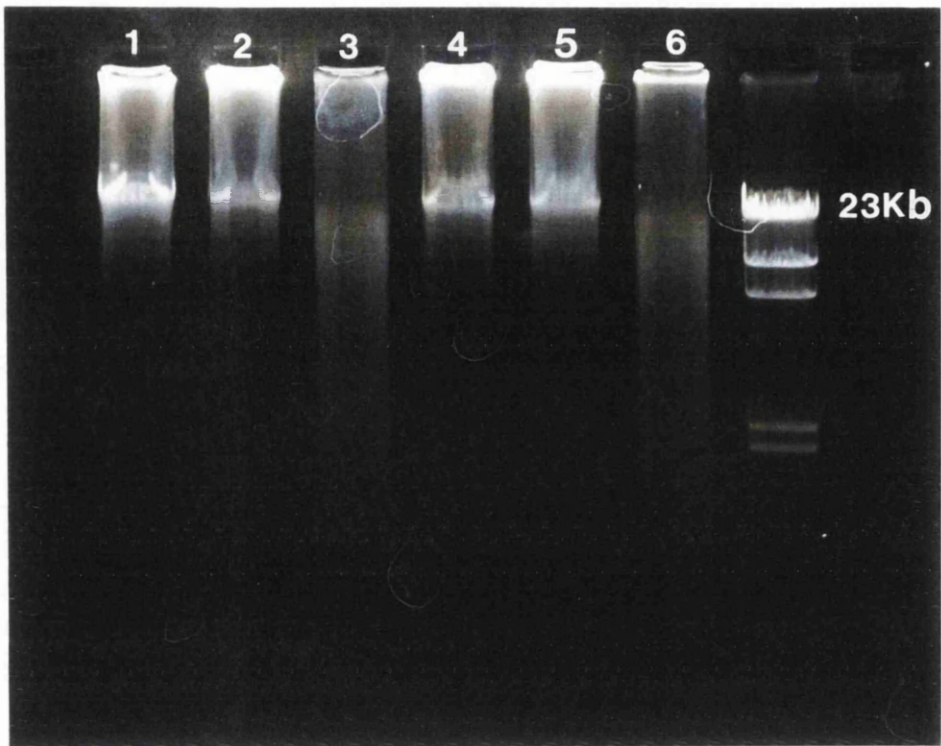
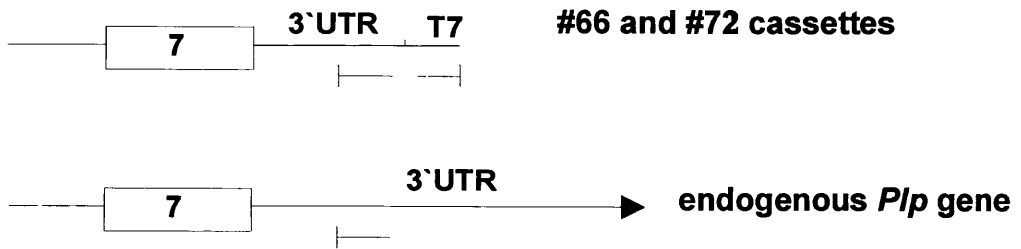
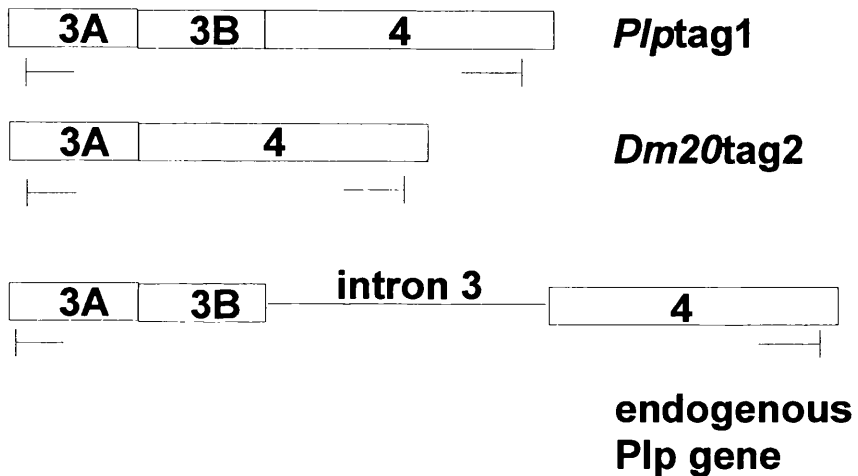


Figure 8. Assessment of the quality of gDNA extracted from fresh (lanes 1-3) and frozen (lanes 4-6) mouse tails with the QIAamp Tissue kit. Lanes: 1 and 4 gDNA incubated at room temperature; 2 and 5 incubated at 37⁰C in the presence of buffer and the absence of enzyme; 3 and 6 *Bam*HI digest at 37⁰C; 7 λ *Hind*III marker showing undigested gDNA as a tight population of molecular weight 23Kb. The frozen tail sample had been stored for 14 months at -20⁰C.



a)



b)

Figure 9. The position of primers (red sense, blue α sense) to produce a transgene specific product from genomic DNA to identify mice carrying the #66 / #72 transgene and *PlpTag1* and *Dm20Tag2* transgenes.

Genotype	Forward primer (5') sense	Reverse primer (3') anti-sense	Final MgCl ₂ concentration (mM)	Product length (bp)
#66 and #72	5'-CaggTgTTGAGTCTgATCTACACAAG-3'	5'-gCATAATACgACTCACTATAgggATC-3'	3	400
<i>Plp</i> and <i>Dm20</i>	5'-TCCATgCCTTCCAgTATgTCAATCT-3'	5'-TACATTCTggCgTCAGCACAgAgA-3'	3	412 <i>Plp</i> 307 <i>Dm20</i>
wild type <i>Plp</i> allele	5'-AgTCAATAgCTCCTTTgTTC-3'	5'-CACTCTTCTCATTCACTTACC-3'	3	258

Table 5. Summary of PCR primers used for the genotyping of transgenic and *Plp^{flp}* mice.

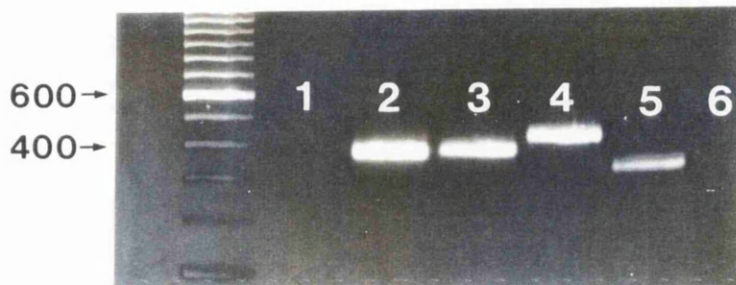


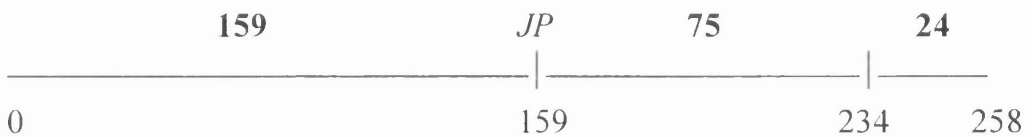
Figure 10. Products of PCR reactions used for identification of #66/#72, *Plp*Tag1 and *Dm20*Tag2 transgenes. Lane 1 wild type, lane 2 #66 (400bp), lane 3 #72 (400bp), lane 4 *Plp*Tag1 (412bp), lane 5 *Dm20*Tag2 (307bp), lane 6 wild type. PCR in lanes 1-3 was performed with the *Plp*-T7 primer pair and PCR in lanes 4-6 with the *Plp:Dm20* primer pair (see Table 5, Page 85). Marker 100bp ladder.

The *Plp^{jP}* mutation results in the loss of a *DdeI* restriction site at the intron 4/exon 5 boundary due to an a→g substitution. *DdeI* recognises the sequence C'TNAG

wild type sequence accttag/GT (lower case denotes intronic sequence)

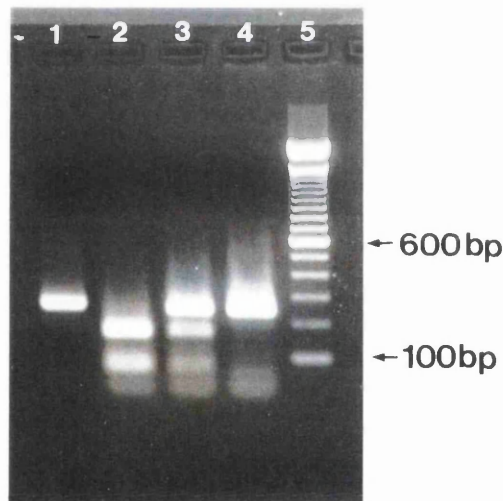
Plp^{jP} sequence atctt**gg**/GT (mutation in bold)

PCR product with *DdeI* sites (—|—) and restriction product sizes (bold)



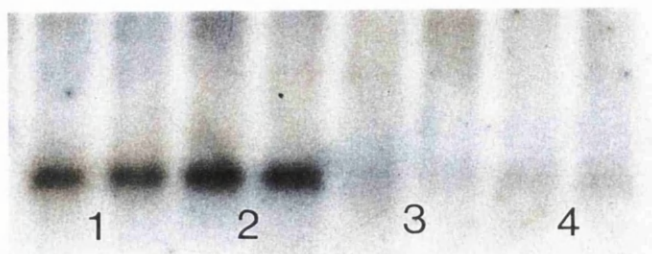
The mutated *DdeI* site is marked (*JP*).

a)

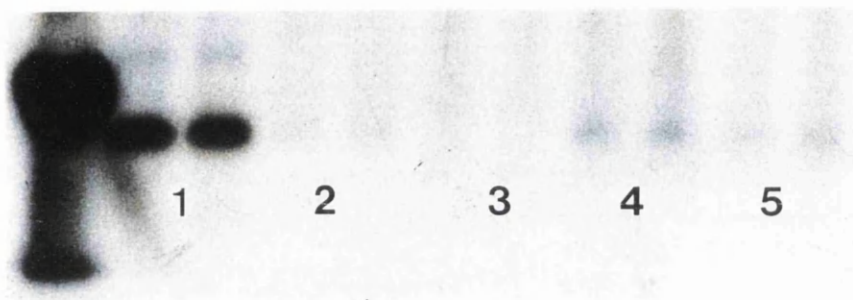


b)

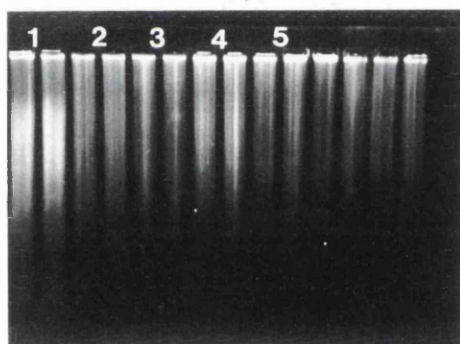
Figure 11. Identification of *Plp^{jP}* carrier females by PCR of gDNA and subsequent *DdeI* digest. a) explanation of how the loss of a *DdeI* restriction site can be used to identify the *Plp^{jP}* allele; b) gel showing: lane 1 undigested product, lane 2 wild female (both alleles digested), lane 3 *Plp^{jP}* heterozygote female with *Plp^{jP}* (undigested*) and wild type *Plp* alleles (digested), lane 4 *Plp^{jP}* male with one *Plp^{jP}* allele (undigested*) and lane 5 100bp ladder. *a 24bp fragment is produced



a)



b)



c)

Figure 12. Examples of autoradiographs of Southern blots using probe B6. All samples are run as pairs and lanes are numbered in pairs. a) #72 mice: lane 1 homozygous, lane 2 homozygous, lane 3 wild type and lane 4 hemizygous; b) #66 mice: lane 1 homozygous, lane 2 wild type, lane 3 wild type, lane 4 hemizygous and lane 5 hemizygous. Lanes 1 and 4 are relatively overloaded as can be seen in c) the gel photograph. The strong hybridisation signal to the left of lane 1 represents non-specific binding to the 100bp ladder.

4. Late onset neurodegeneration in mice hemizygous for the #66 and #72 transgenes

4.1 Background

At the inception of this project there was limited information concerning the effects of increased *Plp* gene dosage on mice hemizygous for the #66 and #72 transgenes. Specifically they had not been recognised as having an abnormal phenotype, in contrast to their homozygous littermates, though they were thought to be mildly dysmyelinated and have *Plp* mRNA levels greater than both homozygous and wild type mice in adulthood (Readhead *et al.*, 1994). Late onset disease had, however, been observed in *Dm20* minigene transgenic mice (Mastronardi *et al.*, 1993). A demyelinating phenotype was also observed in hemizygous 4e mice (Inoue *et al.*, 1996; Kagawa *et al.*, 1994). Thus it was considered that hemizygous #66 and #72 mice were potential candidates for developing neurological abnormalities.

Litters of hemizygous mice and their wild type littermates were allowed to age and observed for the development of phenotypic abnormalities. Neurological abnormalities developed in mice over about 12 months of age.

4.2 Aims

The aims of this work were to describe myelination in hemizygous mice, confirm the late-onset nature of the development of the neurological abnormalities and examine transcription of *Plp* and other selected genes in relation to the development of phenotypic abnormalities. Mice were sampled around the peak of myelination and time points representing early and late adulthood. Older mice with and without clinical signs were examined to assess the abnormalities associated with the development of neurological signs and in particular how the glial population were affected. The development of the neurological phenotype is associated with increased cellularity of the affected tissues. Though morphologically many of these cells appear to be microglia it has been speculated that in 4e mice (Inoue *et al.*, 1996) there may be an immune component, accordingly studies were undertaken to assess whether there is an associated T cell response.

4.3 Methods

The developmental studies were performed at P20 (peak of myelination) and P60 (early adulthood). Tissues were procured for glial cell quantification; myelin morphometry; assessment of the transcriptional output of the combined endogenous

and exogenous *Plp* genes and other myelin genes; assessment of the distribution of myelin proteins and other proteins; description of the extent of pathological change. Tissues from older transgenic mice with neurological signs and their non-transgenic (wild type) littermates were collected.

Glial cell counts were also undertaken in younger animals to characterise further the development of the glial cell population.

ISH for *Plp* gene transcripts was used to examine the oligodendrocyte population both during development and assess qualitatively the effects of the pathology on population numbers and *Plp* gene transcription.

As an indication of myelin gene transcription the steady state mRNA levels of the *Plp*, *Mobp* and *Mbp* genes were assessed by northern hybridisation in addition to RT-PCR determination of *Plp:Dm20* ratios.

4.3.1 Mouse breeding

The breeding and identification of #66 and #72 transgenic and wild type mice for these experiments is described in 3 Genotyping and breeding of transgenic mice, page 76.

4.3.2 Preparation of tissue

The preparation of tissues for resin and paraffin wax embedding, frozen sections and electronmicroscopy is described in 2.1 Tissue fixation and processing (page 43). The extraction of RNA is described in 2.5.1.2 The isolation and storage of RNA (page 49).

4.3.3 Histopathology

A survey of the nervous system was undertaken on 1µm resin sections stained with methylene blue/azur and on paraffin sections stained with H&E. The resin sections give excellent visualisation of myelin and cell morphology.

4.3.4 Immunocytochemistry

4.3.4.1 Immunostaining for myelin proteins

Immunostaining for myelin proteins (PLP/DM20, MBP, MAG) and GFAP was performed on both resin, paraffin embedded sections and frozen sections. The protocols are summarised in 2.9 Immunocytochemistry (page 68) and the details of the antibodies, link antibodies/fluorescent conjugates and their sources are presented

for the PAP technique in Table 3 (page 70) and Table 4 (page 71) for fluorescent techniques.

Protocols for microglial and T cell immunostaining are described below.

4.3.4.2 Immunostaining for microglia

Sections for immunostaining for microglia were prepared from mice perfused with periodate-lysine-paraformaldehyde fixative (2.1.1.3 Periodate-lysine-paraformaldehyde, page 43) and the tissues cryo-preserved with sucrose (2.2.3 Cryo-preservation, page 44). Details of the antibody, secondary antibodies and their sources are given in Table 6 (page 107).

Slides were thawed and allowed to dry. All incubations were carried out at room temperature. Endogenous peroxidase activity was quenched by immersing the sections in 0.3% hydrogen peroxidase for 20 mins. Sections were washed in PBS for 30 mins to remove embedding medium. Non-specific binding was blocked by incubating in 1% rabbit serum for 30 mins. Excess serum was blotted off and the sections incubated in the primary antibody, F4/80, for 60 mins. Excess antibody was removed by two 10 min washes in PBS. Sections were incubated in the biotinylated secondary antibody for 45 mins and washed for 30 mins in PBS. An avidin DH/biotinylated horseradish peroxidase system was used to label the immunocomplexes and these were visualised by incubating in DAB. Sections were osmicated in 0.1% osmium tetroxide to enhance chromogen intensity and washed thoroughly in water. Sections were counterstained, dehydrated and mounted in DPX.

4.3.4.3 Immunostaining for T cells

Sections for immunostaining for T cells were prepared from mice perfused with periodate-lysine-paraformaldehyde fixative and the tissues cryo-preserved (see above). Details of the antibodies, secondary antibodies and their sources are given in Table 6 (page 107).

Slides were immunostained for a small panel of T cell markers with the aim of identifying the presence of T cells. Due to the difficulty of producing suitable control CNS tissue splenic tissue was used as a control. Markers were chosen to identify the two broad categories of T cell - CD4 (“helper”) and CD8 (“killer”) cells. The panel also included CD45, a pan leukocyte marker that also identifies macrophage lineage cells including microglia, and CD3, a pan T cell marker.

Slides were thawed and allowed to dry. Sections were permeabilised with 0.1% Triton-X in PBS for 5 mins and washed in PBS. Non-specific binding was blocked with 10% rabbit serum in PBS for 30 mins. Excess serum was blotted off and the sections incubated with the primary antibodies in 2% rabbit serum over night at room temperature. Excess antibody was removed by washing in PBS for 5 mins. Incubation with the secondary antibody was for 45 mins and followed by a 5 min wash in PBS. An avidin DH/biotinylated horseradish peroxidase system was used to label the immunocomplexes and these were visualised by incubating in DAB (Fast DAB, Sigma) for 60 secs. Counterstaining was with Harris's haematoxylin for 1 min and the excess washed off in water. Sections were dehydrated and mounted in Micromount (Surgipath).

4.3.5 Myelin morphometry, ultrastructure of myelin and glial cells

Quantitative measurements of myelin thickness and density were made at P20 and P60 as described in 2.10 Morphometry (page 72). The data for axonal diameter and *g* value were pooled for the three genotypes of mice. The morphology of glial cells was examined at both these ages and also in aged mice.

4.3.6 Glial cell quantification

Total glial cell density was quantified as described in 2.10.1 Glial cell quantification (page 72).

4.3.7 Dead cell density

The density of dead cells in cervical cord white matter was quantified as described in 2.10.1.1.1 Dead cell density (page 73).

4.3.8 Transcript analysis

4.3.8.1 Northern analysis

These experiments were performed on total cellular RNA extracted from whole brain. The procedure of northern transfer is described in 2.5.4.2 Northern blotting (page 56). Hybridisation analysis was undertaken using labelled DNA fragments for the detection of message from the following genes: *Plp*, *Mobp* and *Mbp* (see Figure 13, page 108). PLP-1 is a 449bp fragment released from the plasmid PLP-p27 (Milner *et al.*, 1985) which recognises the three *Plp* gene message isoforms, with the major band being ~3Kb in the mouse. MOBP is a 1.3Kb fragment released from the plasmid pMMSV2 (this clone contains the cDNA for the 81aa protein isoform) (Montague *et al.*, 1997) which because it contains sequence common to all

Mobp message isoforms recognises 5 message species, with the most abundant species being 2.4Kb in the mouse. MBP is a 1400bp fragment released from the plasmid pSP64MBP (Mentaberry *et al.*, 1986) recognising a major band of ~5Kb.

The preparation of radiolabelled probes is described in 2.7 Preparation of radiolabelled probes (page 61). Equivalence of transfer was undertaken by routine methylene blue staining of northern filters and hybridisation with probe for murine 7S ribosomal RNA as a measure of invariant temporal expression. 7S is a 400bp fragment released from the plasmid pA6 (Balmain *et al.*, 1982) (see Figure 13, page 108).

4.3.8.2 Semi-quantitative RT-PCR for *Plp:Dm20* ratio

The cDNAs for these experiments was prepared from whole brain as described in 2.5.4.1.2 cDNA preparation (page 55). The protocol of these experiments is described in 2.5.4.1.3 RT-PCR (page 56). Experiments were performed using the *Plp* gene exon 2→4 primers (see Table 2, page 58). This primer pair produces separate products for the *Plp* and *Dm20* message isoforms as they encompass the 3B portion of exon 3, which is spliced out in the *Dm20* message isoform. Their use for semi-quantitative PCR for the assessment of the *Plp:Dm20* message isoform has previously established (Dickinson, 1995).

4.3.8.3 *In situ* hybridisation

In situ hybridisation studies of cervical spinal cord were performed at P20 and P60 with studies of cervical cord and brain in aged mice. Hybridisation was with the PLP-1 probe. The ISH technique is described in 2.8 *In situ* hybridisation (ISH) (page 62).

4.3.9 CNS protein analysis

Protein were extracted from whole brain and analysed by western blot (see 2.6 Analysis of proteins, page 60). Blots were immunostained for PLP/DM20 using the C-terminal antibody PLP226 (see Table 3, page 70).

4.4 Results

Unless otherwise stated hemizygous mice are compared to their non-transgenic litter mates (otherwise referred to as wild type).

4.4.1 Phenotypic characteristics

4.4.1.1 Growth

At P60 the body weights of hemizygous #66 and #72 mice were not significantly different from wild type ($p=0.9525$). However, the weight of hemizygous mice older than P300 was significantly less than that of wild type mice ($p=0.0001$) (Figure 14, page 109). Interpretation of this result must take into consideration that many, but not all, of the hemizygous mice were selected for sampling because they exhibited neurological abnormalities. There also likely to be an age related change in mouse body weight.

4.4.1.2 Neurological abnormalities

Hemizygous mice were phenotypically unremarkable for many months and they reproduced normally. Around 12-18 months of age progressive neurological signs developed, principally tremor and ataxia. Both sexes were affected. Affected mice became weak and appeared to have reduced grip strength. Seizures were a late feature in the progression of signs but probably important in the terminal stages of the phenotype. A consistent finding at post-mortem in mice with advanced neurological signs was a distended, full bladder implying urinary retention. Such mice also commonly had urine staining of the perineal region. Subjectively many animals with advanced disease had impaired vision.

4.4.2 Pathology of neurodegeneration

4.4.2.1 Nature of neurodegeneration

Hemizygous mice older than P60, with or without phenotypic signs, showed evidence of pathology, most obviously in their optic nerves (see 4.4.2.2 Distribution of lesions, page 96). Brains of affected mice showed varying degrees of hydrocephalus involving the lateral ventricles with the loss of myelin being obvious to the naked eye (see Figure 15, page 110). Light microscopy demonstrated diffuse vacuolation of both the grey and white matter, which could reach dimensions of 1mm or more, and was occasionally visible to the naked eye. Immunostaining and EM studies (data not shown) showed that these vacuoles arise from distension of the myelin sheath (Figure 17, page 114).

The affected regions were characterised by gliosis, demyelination and axonal degeneration. There was no inflammatory infiltrate or perivascular cuffing (with lymphocytes or neutrophils) and macrophages were not observed within the degenerating myelin. The dominant process varied between areas with

demyelination being predominant in the optic nerve and axonal degeneration being the primary process in the spinal cord.

Demyelination was associated with the formation of large loops of redundant myelin. Axonal degeneration was demonstrated by axonal swellings and frank Wallerian-type degeneration of the axon and myelin sheath. Degenerate myelinated axons were characterised by whorls of myelin debris and axonal fragments. There was no proximal/distal selectivity of fibre degeneration within a tract; for example corticospinal tracts were affected at all levels of the spinal cord. Loss of axons was implied from observing extensive areas of white matter consisting of astrocytic processes. Numerous reactive microglia were present in the more chronic lesions (see .

Light microscopy of the sciatic nerve and muscles of the hindlimb of aged hemizygous mice was unremarkable (data not shown).

4.4.2.2 Distribution of lesions

White matter changes were observed in all phenotypically affected animals, however, during myelination and early adulthood the CNS of the hemizygous mice was indistinguishable from that of wild type littermates. As the mice aged the development of lesions was notable for the tract specificity. Initially small fibre tracts are specifically targeted, as indicated by the early involvement of the optic nerve. Subtle abnormalities of myelin, which may represent early changes, are detectable in the optic nerve at P60, however, similar changes can also be occasionally detected in wild type optic nerve at the same age. By P120 optic nerve changes are well established. Ventral column abnormalities are not seen without concomitant abnormalities of the dorsal columns and optic nerves whilst abnormalities of the dorsal columns are observed in the absence of ventral column pathology. This suggests that the changes observed in the dorsal columns of the spinal cord involving the deeper regions of the lateral columns, fasciculus gracilis and corticospinal tracts at around P365, represent the next stage of progression. The larger fibres of the ventral funiculus and fasciculus cuneatus in the dorsal columns were spared, though occasional small diameter fibres were degenerating. The final stages of progression in the spinal cord involve the ventral columns. The development of neurodegeneration in the spinal cord is illustrated in Figure 16, pages 111-113.

The changes were progressive and associated with the eventual involvement of the majority of the CNS, including cerebellar and cerebral cortices, diencephalon, brain

stem, the ventral columns of the spinal cord and also the grey matter of the spinal cord.

4.4.3 Glial cell density

Total glial cell densities are presented in Figure 18, page 115.

The data suggests that at P20 the total glial cell density is significantly greater in #72 hemizygous mice ($p=0.0424$), whilst this difference is no longer apparent at P60 ($p>0.05$). In #66 mice the data suggests that the glial cell density is greater at P10 (wild type values = $225 \text{ cells mm}^{-2}$ and $232 \text{ cells mm}^{-2}$ and median hemizygous = $271 \text{ cells mm}^{-2}$) and is similar to wild type at P20 and P60. There is no significant differences between wild type and either of the lines of hemizygous mice at P60 ($p>0.05$).

Total white matter glial cell numbers are presented in Figure 19, page 116. Though white matter areas appear similar for hemizygous and wild type mice (see below) the increase in total glial cell numbers suggested by the increase total glial cell density is not as apparent.

A striking feature of aged hemizygous #66 and #72 mice is the gliosis affecting the degenerating white matter tracts. Morphologically, the predominant cells types appear to be microglia (Figure 20, page 117) and astrocytes. At P120 examination of degenerating tracts suggested an increased glial cell density but this is not strongly supported by the total glial cell density. However, at this time point the ventral columns are not affected by neurodegeneration.

4.4.4 Dead cell density

At P20 the dead cells density in cervical cord white matter in #66 and #72 hemizygous mice were not significantly different to wild type ($p>0.05$) (see Figure 21, page 118) with medians of: wild type 0.72 mm^{-2} , #66 0.48 mm^{-2} , #72 0.79 mm^{-2} .

4.4.5 Myelin morphometry

At P20 and P60 the area of the white matter, myelin volume and g ratio appear indistinguishable from wild type (see Figure 22, pages 114-119) and no statistically significant differences were detected. Myelin sheath thickness did not appear to differ between wild type and hemizygous mice at either P20 and P60 and there appears to be some accumulation of myelin between these two time points in hemizygous #72 mice.

4.4.6 Oligodendrocyte and axon ultrastructure

No abnormalities were observed in the oligodendrocytes of developing or young adult mice hemizygous for either #66 or #72 transgenes. The early changes of redundant myelin loops and distension of the inner tongue of oligodendrocytes in the optic nerve and spinal cord are shown in Figure 23 (page 121). In chronic lesions these were more extensive demyelination (principally in the optic nerve) and loss of axons, inferred from the increasing proportion of astrocytic processes, in the spinal cord (see Figure 24 pages 122-123). In aged animals with neurodegeneration the oligodendrocyte cell bodies and major processes remained morphologically unaffected, however, the adaxonal region of oligodendrocyte processes associated with non-degenerate fibres was often abnormal. Abnormalities ranged from distension with a granular amorphous material to vesicular degeneration. The abnormal features of oligodendrocytes from aged hemizygous oligodendrocytes are illustrated in Figure 25 (page 124).

4.4.7 Gene expression

4.4.7.1 Immunocytochemistry

Studies at P20 and P60 for PLP and MBP demonstrated the distribution and staining intensity of myelin proteins was indistinguishable from wild type (data not shown). In affected animals there was an obvious loss of myelin-associated proteins in areas of neurodegeneration (e.g. MBP Figure 26, page 125).

Immunostaining for phosphorylated neurofilaments (NF) showed the presence of axonal swellings in many regions particularly the ventral medulla, Purkinje cell axons (torpedoes) and in the white matter of the spinal cord (Figure 26, page 125). Smaller spheroids were also observed in some regions of the basal nuclei (caudate nucleus and putamen) and in the cerebral cortex. Subjectively the occurrence of axonal swellings increased with the severity of phenotypic signs. Occasional neuronal perikarya, particularly in the deep cerebellar and reticular formation nuclei, contained phosphorylated NF. Areas of demyelination showed a reduction in immunostaining inferring a loss of axons from the loss of phosphorylated epitopes. These axonal changes are illustrated in Figure 26 (page 125).

Staining for microglia demonstrated an increase in microglia in white matter tracts of the brain (Figure 27 page 127). The microglia in these tracts exhibited changes in morphology, including hypertrophy of the soma and a reduction in the length of processes, consistent with a change to an activated status (Gehrmann and Kreutzberg, 1995).

Immunostaining for CD45 showed a general increase in immunoreactivity in white matter tracts in the aged hemizygous #66 and #72 mice, whilst T cell specific immunostaining (CD3, CD4, CD8) was sparse, with occasional positive cells in the white matter. CD45 positive cells with the morphology of lymphocytes were also sparse suggesting that the hypercellularity was not due to B cell lymphocytes. The CD45 immunoreactivity is likely to represent immunostaining of the microglial processes. The features of immunostaining for T cells is presented in Figure 28, pages 129-130

The integrity of the periaxonal space is indicated by the presence of immunoreactivity for MAG. Immunostaining for MAG was deficient in regions containing degenerate or demyelinated fibres but present where fibres remained intact (Figure 26, page 125).

Immunostaining for GFAP indicates are consistent with an increase in astrocyte processes and probable reactive astrocytosis (Figure 26, page 125).

4.4.7.2 Transcript analysis

4.4.7.2.1 Northern hybridisation

Transcription of the myelin genes *Plp*, *Mobp* and *Mbp* was examined (Figure 29, page 131). Hybridisation to S7 ribosomal RNA was used as a control for invariant temporal expression. All bands conformed to the predicted sizes based on the positions relative to the 28 and 18S ribosomal markers (which are shown for the *Mbp* hybridisation, panel d). At all ages the steady state levels of *Plp* gene mRNA (panel a) and the other selected myelin genes (panels c and e) were greater than wild type, though at P20 in hemizygous #72 this increase is equivocal. This persisted even in animals that were in the terminal stages of the disease (panels a and c, lane 7). In #72 hemizygous mice at P20 and P60 (data not shown) *Plp* (panel a, lane 2) and *Mobp* (panel c, lane 3) transcript levels were only slightly greater than wild type whilst in aged animals they were equivalent to #66 mice (panels a and c, lane 4 wild type, lanes 5 and 6 #66, lane 7 #72).

4.4.7.2.2 *Plp:Dm20* ratio

The *Plp:Dm20* ratio were examined by RT-PCR using cyclophilin as a control for invariant temporal expression, the levels of which are reasonably constant across the spectrum of ages and genotypes (panel b (i) and (ii) Figure 29, page 131). The *Plp:Dm20* ratio was unaltered from that in wild type (lane 1 P20 and lane 4 aged) in myelinating and aged hemizygous mice (lane 2 #72 P20, lane 3 #66 P20, lane 5 #66

Late onset neurodegeneration in hemizygous mice

aged, lane 6 #72 aged). The amount of *Plp:Dm20* message was markedly increased in #66 hemizygous mice (lanes 3 and 5) at all ages whilst the increase in #72 hemizygous mice was at P20 is equivocal. These findings were consistent with the northern hybridisation data.

4.4.7.2.3 *In-situ* studies

At P20 (data not shown) and P60 hemizygous mice adequate numbers of *Plp* gene expressing cells are present. In aged mice the oligodendrocyte population of the of the brain and spinal cord (data not shown) were qualitatively equivalent to, if not greater than wild type, with the signal per cell also being equivalent or possibly increased (Figure 30, page 133). The distribution of positive cells was indistinguishable from wild type and was predominantly in the white matter regions.

4.4.7.3 Myelin proteins

In aged hemizygous mice there was a variable increase in both protein isoforms (Figure 29, page 131). These changes perhaps reflect the variable nature of the phenotype. However, the PLP:DM20 protein isoform ratio appears to be unaltered from wild type.

4.4.8 Summary

The morphological development of the myelin sheath in hemizygous #66 and #72 mice was essentially indistinguishable from their wild type litter mates. The only observed difference was an increase in total glial cell density during myelination in hemizygous mice.

The late onset neurological phenotype was related to progressive demyelination and axonal degeneration. The distribution of pathology showed a marked predilection for small diameter fibres with larger diameter fibres becoming involved only in the later stages.

At all ages examined, including mice in the terminal stages, the expression of myelin genes was greater than in wild type (P20 hemizygous #72 requires further characterisation to confirm an increase in *Plp* gene transcription). Subjectively oligodendrocyte numbers were maintained in animals with neurodegeneration (and possibly increased) and likewise the production of *Plp/Dm20* message by individual oligodendrocytes was maintained.

Oligodendrocyte cell bodies and major processes were morphologically normal at all ages. However, in aged hemizygous mice there were abnormalities of the

adaxonal region in which there was accumulation of abnormal cytoplasm in the inner tongue.

There was no evidence of the neurodegeneration being due to a primary inflammatory event though there was a microglial and astrocytic response to the neurodegenerative process. Though lesions were hypercellular, cells with the morphology of lymphocytes represented a very small proportion of the total population and there was a very sparse T cell infiltrate. There was no perivascular cuffing, a common finding with acute inflammation where cells are attracted from the circulation. Macrophages were not observed within the myelin sheath, another common feature of inflammatory demyelination.

4.5 Discussion

The data presented in this chapter demonstrates that normal myelin development and myelin maintenance can be achieved in the face of the upregulated myelin gene transcription found in the #66 and #72 hemizygous mice. However, in the long term this is associated with perturbations of not only the myelin sheath but also of axons. The phenotype is different to that in mice homozygous for these transgenes, which is characterised by dysmyelination (see 5.6 Discussion, page 144). However, demyelination and axonal degeneration also develop in homozygous #66 and #72 mice superimposed on their dysmyelinated background, and with an accelerated time course (see 5.6 Discussion, page 144).

Late onset demyelination has now been described in other examples of *Plp* gene or minigene transgenic mice (see 1.4.2.4 Evidence that increased *Plp* gene dosage affects myelination, page 38). The relationship between gene dosage, transcription and protein levels is complex and increased copies of a gene do not necessarily result in a predictable increase in gene transcription. In my studies the hemizygous #66 mice have a greater level of steady state mRNA than their homozygous littermates (see Figure 53, page 194). In hemizygous #66 mice the increased gene dosage is reflected in an raised steady state levels of *Plp* message which persists throughout life. In hemizygous #72 mice myelin gene transcription increases with age implying a change in myelin gene regulation or mRNA stability. *In situ* hybridisation studies suggest some increase in oligodendrocyte numbers in aged hemizygous animals but this not of the same magnitude of the increase in message levels, suggesting that the increase observed in bulk brain RNA is due to an increase in transcription or mRNA stability. This is supported by an apparent increase in signal intensity per cell on *in-situ* studies. Quantification of *in-situ* studies in

relation to both cell numbers and transcript level is complex due to the profound effects of many aspects of the procedure on the final autoradiograph. Increased levels of *Plp* transcripts are associated with an elevation in the steady state levels of message for other myelin genes (*Mbp* and *Mobp*) suggesting a change in the coordinate expression of myelin genes. The effect of *Plp* gene copy number on other myelin genes has not been well described though in hemizygous 4e mice *Mbp* mRNA is reported to be reduced at P19, though this may be related to the reduced number of oligodendrocytes (Kagawa *et al.*, 1994). Increased myelin production, due to increased oligodendrocyte activity, is seen in mice with increased copies of IGF-1 and is not associated with a neurological phenotype (Carson *et al.*, 1993). The data presented here flags the possibility that other genes involved in myelin elaboration and maintenance, not examined here, may also have had their pattern of expression altered. The significance of the apparent upregulation of other myelin genes in the development of neurodegeneration in the hemizygous #66 and #72 mice is uncertain.

A predominant feature of the phenotype is a gliosis due to increased numbers of astrocytes and microglia. The significance of these cell types in the development of the lesions is uncertain. Astrocytosis is a common feature of many of the myelin mutants (see 1.3.2.1 Animal models page 26) and is thought to be a secondary phenomenon (Bignami and Dahl, 1995). Astrocytes are known to have many functions including the secretion of cytokines and involvement in antigen presentation. Microgliosis, in the absence of lymphocyte infiltration, is now thought to be evidence of chronic inflammation within the CNS (Perry, 1994). Little is known about the state of microglia in aged mice, however, in aged rats they exist in a comparatively upregulated state and it has been postulated this may exacerbate the response to inflammatory stimuli (Perry *et al.*, 1993). A demyelinating phenotype was observed in transgenic mice over-expressing interleukin-3 (IL-3) in which there was a marked microgliosis, but the pathological features described were distinct from those observed in hemizygous #66 and #72 mice and involved microglia/macrophages invading myelin with the axons remaining largely unaffected (Chiang *et al.*, 1996).

The significance of the apparent increase in total glial cell density in developing hemizygous #66 and #72 mice is uncertain. Sampling at other earlier time points would help confirm its presence and determine its magnitude. Quantification of the nature of the cell types involved is complicated by the difficulty of confidently assessing cell type at younger ages (Skoff, 1990), one approach would be the quantification of ISH to identify *Plp* gene transcribing cells, though accurate quantification can be difficult to achieve. Another is the use of oligodendrocyte

specific immunostaining (Carson *et al.*, 1993). The dead cell density in both types of mice at P20 was indistinguishable from wild type, though potentially it may be elevated at younger ages. An increase in total glial cell density is also seen in developing homozygous #66 and #72 mice, which is associated with a probable increase in dead cell density (see 5.6 Discussion, page 144).

Demyelination affected primarily tracts composed of small diameter axons. The loss of myelin occurs in the presence of a apparently adequate numbers of oligodendrocytes, which even in the most extreme manifestation of the phenotype continue to transcribe myelin genes. The cell bodies and major process were morphologically unaffected though there were abnormalities of the adaxonal cytoplasm, not present in younger animals. It is uncertain whether this age-related change represents a primary perturbation of the oligodendrocyte/axon interface or is a result of the demyelinating process. Accumulations of cytoplasmic elements in the adaxonal region is a non-specific phenomenon occurring in the “dying-back oligodendrogliopathy” which can occur following the administration of exogenous toxins (Blakemore, 1972), is seen as a late sequel to MAG deficiency (Lassmann *et al.*, 1997) and has also been described in inflammatory demyelinating lesions (Ludwin, 1997), however, a dying-back oligodendrogliopathy does not necessarily result in axon degeneration. The dying-back oligodendropathy may indicate primary oligodendrocyte dysfunction though changes in the soma are minimal and indicates how cells with extensive transport and cytoskeletal functions are vulnerable to injury (Ludwin, 1997). Vacuolation of myelin is also a non-specific finding associated with a number of aetiologies and may be associated with minimal oligodendrocyte abnormalities (Blakemore, 1972). Myelin vacuolation and redundant loops of myelin is a feature of mice with extra copies of the *Cnp* gene (Gravel *et al.*, 1996) and in HIV-1 transgenic mouse a vacuolar myelopathy is seen in spinal cord (Goudreau *et al.*, 1996). Demyelination primarily affected small diameter axons.

In tracts affected by demyelination many myelin sheaths exhibit focal myelin thickening and loops of redundant myelin. The aetiopathogenesis of these aberrant myelin structures is uncertain. They could potentially reflect a number of derangements of myelin and/or the axon including: perturbations of myelin turnover; unravelling of the myelin sheath and axonal atrophy. Of these possibilities investigations into myelin turnover would be the most straight forward to pursue. Axonal atrophy as an event proceeding myelin loss does not seem likely from the initial morphometric analysis of the ventral columns. Investigations would require following the distribution of axon diameters as the phenotype progressed and as discussed below this would be complicated by its very variable nature.

The axonal degeneration also affects small diameter axons. The axonal pathology in the hemizygous #66 and #72 mice includes Wallerian-type degeneration and the development of axonal swellings (or spheroids). It is also possible that previously demyelinated axons also degenerate although their detection is problematical. Axonal degeneration and swelling is not generally a significant feature of the dysmyelinating *Plp* gene mutants though it is described in *Plp⁰* and *md-rat*, and also in *qk* and *Mbp^{shi}* mice, though in these later mutants it involves the accumulation of different organelles (Rosenfeld & Friedrich, Jr. 1983; Hirano *et al.*, 1969). Immunocytochemistry shows the axonal swellings contain phosphorylated NFs and the accumulation of NFs was confirmed by electronmicroscopy. The development of axonal swellings is a non-specific finding and probably implies perturbations in axonal transport of NF proteins. It has been suggested that in myelin mutants axonal swellings are a result of myelin deficiency (Rosenfeld & Friedrich, Jr. 1983) but this would not appear to be the case in the hemizygous transgenic mice (they are also not a feature of the dysmyelinating homozygous #66 mice, which are lacking in myelin). The accumulation of NFs may result in axonal dysfunction as suggested for motor neurone disease (Lee *et al.*, 1994) and could contribute to the neurological phenotype.

The relationship between demyelination and axonal degeneration in the hemizygous #66 and #72 mice is not clear. It is well recognised that the development and integrity of the axon and its myelinating glial cell are interdependent (De Waegh *et al.*, 1992; Kirkpatrick & Brady, 1994; Sánchez *et al.*, 1996; Aguayo *et al.*, 1979). Axons do not necessarily degenerate following acute loss of myelin although in chronic demyelination associated with MS plaques axonal loss may be significant (Ferguson *et al.*, 1997; McDonald, 1994). Affected hemizygous #66 and #72 mice contain profiles of degenerating myelin typical of those found in Wallerian-type degeneration. This suggests degeneration of an axon with a previously intact myelin sheath, indicating that prior demyelination is not necessary for axonal degeneration. However, it is less easy to recognise degeneration of a demyelinated axon which will be phagocytosed rapidly, leaving little evidence of its previous existence. The presence of marked astrocytic scars and reduced axon numbers in tracts where demyelination is known to occur suggests that demyelinated axons have degenerated. It is therefore probable that axonal degeneration occurs in the hemizygous mice both with and without prior demyelination.

The very specific nature of the pathology is intriguing. It not only affects fibres of a specific diameter but also exhibits a temporally related, tract specific nature implying heterogeneity within the white matter of the CNS. The heterogeneity of CNS myelin has been described with differences between regions of brain and also

between brain and spinal cord (Norton and Cammer, 1984) and immunocytochemistry suggests there is a difference in the amounts of the PLP/DM20 protein isoforms present in myelin of large and small fibres (Hartman *et al.*, 1982). Morphological heterogeneity of the oligodendrocyte population is well recognised, with different subtypes being typical of different regions of the CNS (Wood and Bunge, 1984), although the relative contributions of axon and oligodendrocyte to the morphology of the mature cell remains unresolved (Szuchet, 1995). Butt *et al.* (1995) have demonstrated both biochemical and morphological differences between oligodendrocytes myelinating small and large diameter axons. It is therefore possible that the distribution of pathology in hemizygous #66 and #72 mice reflects differences between sub-groups of the oligodendrocyte population. Interestingly, the pattern of demyelination/degeneration is similar to that of dysmyelination seen in homozygous #66 mice with the later myelinating tracts being the most susceptible (Readhead *et al.*, 1994).

Abnormalities of the levels of myelin proteins have been described in *Dm20* minigene mice and our data shows that they are perturbed in aged #66 and #72 hemizygous mice. In the *Dm20* minigene transgenic mice abnormalities of the myelin proteins developed before the onset of a recognisable phenotype (Johnson *et al.*, 1995). The PLP/DM20 protein isoforms in #66 and #72 mice are indistinguishable from wild type during myelination (data not shown) but show a variable increase in aged mice. Currently there are no data on how these changes are related to the progression of the phenotype. Interestingly, changes occur in MBP cationicity in the *Dm20* minigene mice, a finding also observed in MS (Johnson *et al.*, 1995), showing that the abnormalities of myelin composition extend to other myelin proteins. However, these changes may reflect a consequence of demyelination.

Further characterisation of the neurodegenerative process in hemizygous #66 and #72 mice would be complicated by the apparently large variation in the progression of the phenotype rendering the interpretation of information gathered at specific time points difficult. The investigation of these mice using more sensitive parameters to gauge the development of neurodegeneration may be helpful in discerning the sequence of events.

In conclusion the data presented in this chapter confirms that mice hemizygous for the #66 and #72 transgenes develop a late onset neurodegenerative disorder. The observation that apparently normal myelination is achieved in mice with high levels of *Plp* and other myelin gene transcripts suggest that the relationship between *Plp* gene dosage, levels of expression and perturbations of myelination is more complex

Late onset neurodegeneration in hemizygous mice

than purely an increase in transcriptional output. The reasons for the crisis in phenotypic signs in affected mice, which develop relatively rapidly in relation to the prolonged period during which degeneration is known to be occurring, is unknown, but a potential factor is the microgliosis. The mechanism of neurodegeneration is unknown but it is likely that that the demyelination and axonal degeneration are the result of related but different processes.

Primary antibody	Dilution	Source	Link
F4/80 (microglia)	1:20	Serotec	biotinylated rabbit anti-rat (1:100)
CD4 (Tcell) (YTS177 + YTA3.1)*	1:2 hybridoma supernatant	S.Cobbald, University of Oxford	biotinylated rabbit anti-rat (1:100)
CD3 (T cell) KT3.1*	neat hybridoma supernatant	American Tissue Culture Collection (source of hybridoma)	biotinylated rabbit anti-rat (1:100)
CD8 (Tcell) YTS169*	1:500 hybridoma supernatant	S.Cobbard, University of Oxford	biotinylated rabbit anti-rat (1:100)
CD45 (Tcell)	1:20	Serotec	biotinylated rabbit anti-rat (1:100)

Table 6. Antibodies, dilutions, sources and links used in immunostaining for microglia and T cells in mice hemizygous for #66 and #72 transgenes (* denotes clone). The PAP complex used with all antibodies was Vectastain ABC (Vector) and all links were sourced from Vector.

Late onset neurodegeneration in hemizygous mice

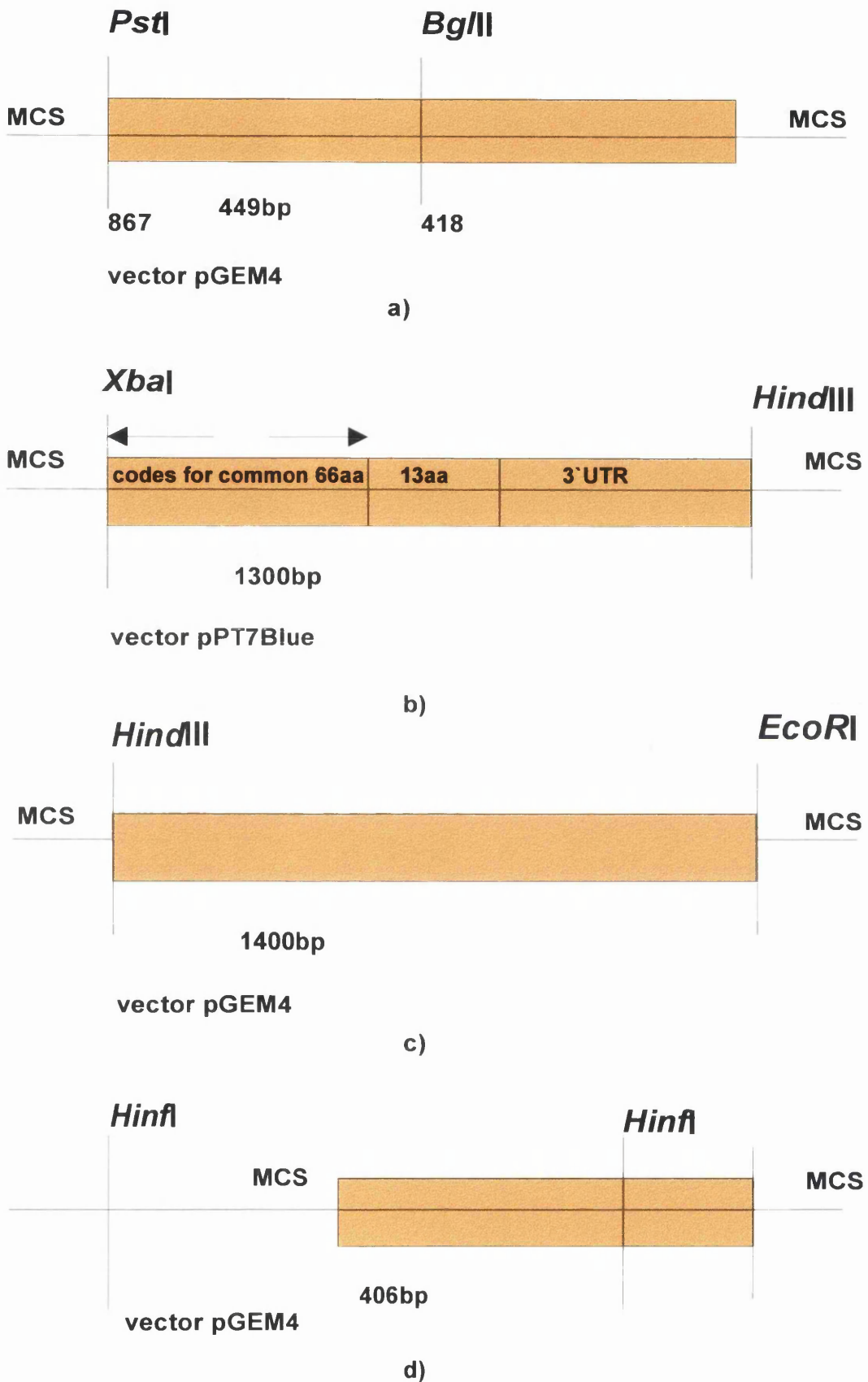


Figure 13. Schematic diagram of digests for the liberation of DNA fragments used for northern hybridisation. a) PLP-1; b) MOBP; c) MBP; d) 7S

Late onset neurodegeneration in hemizygous mice

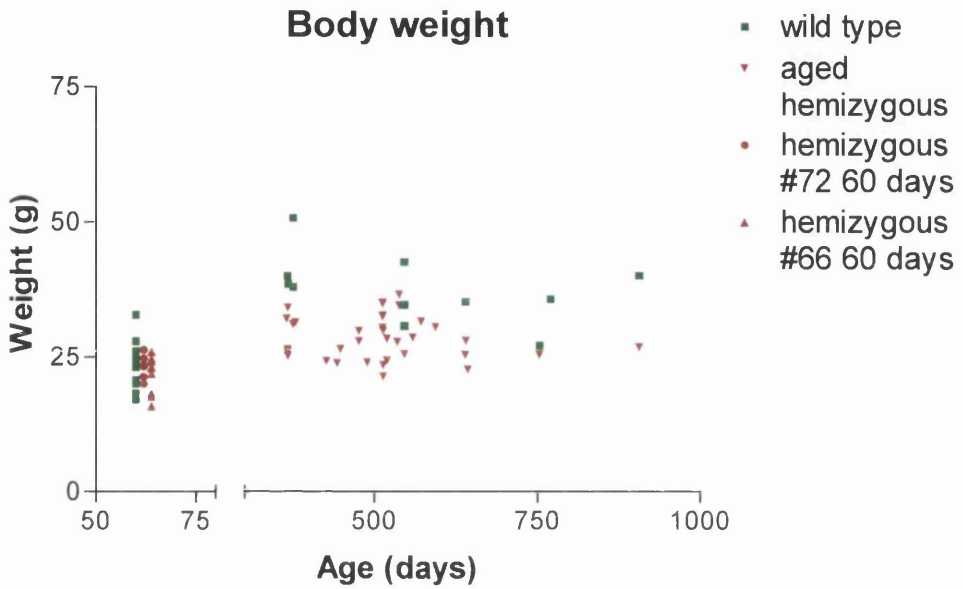
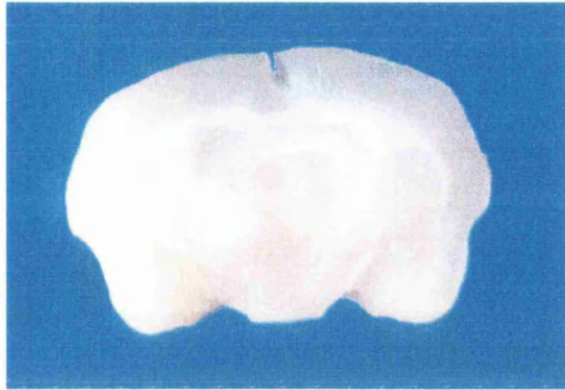
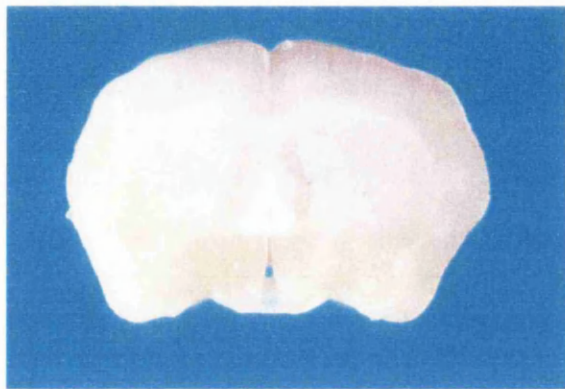


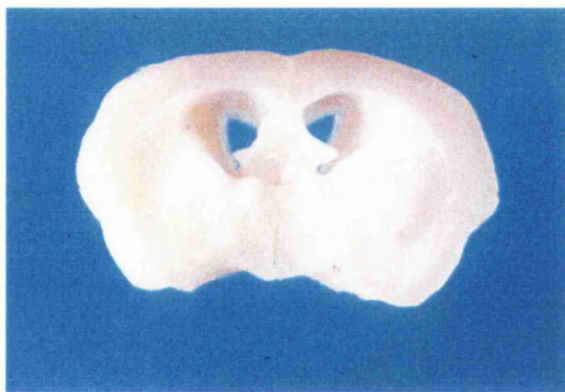
Figure 14. Body weight of mice hemizygous for #66 and #72 transgenes at P60 and affected aged mice greater than P300 compared to wild type.



a)

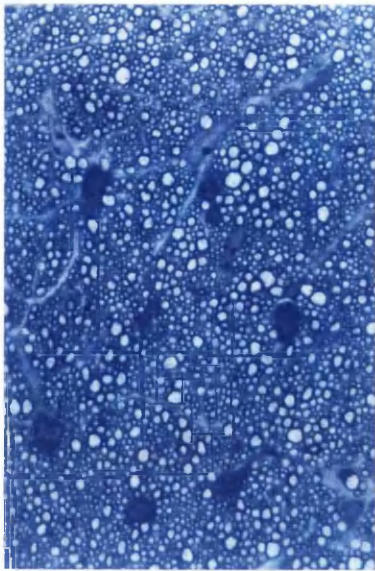


b)

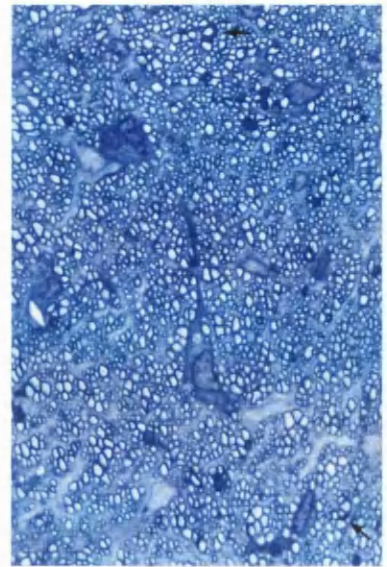


c)

Figure 15. Transverse sections of brain from aged wild type and hemizygous #66 and #72 mice. a) wild type (P578); b) #66 (P448) ataxia and apathetic; c) #72 (P663) apathetic. These gross sections illustrate loss of white matter (b) and (c) and hydrocephalus (c) in aged hemizygous mice.

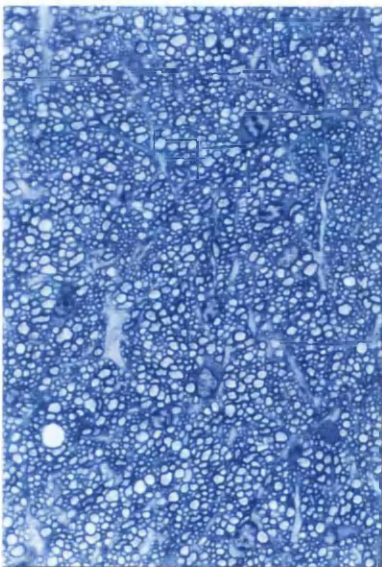


(i)

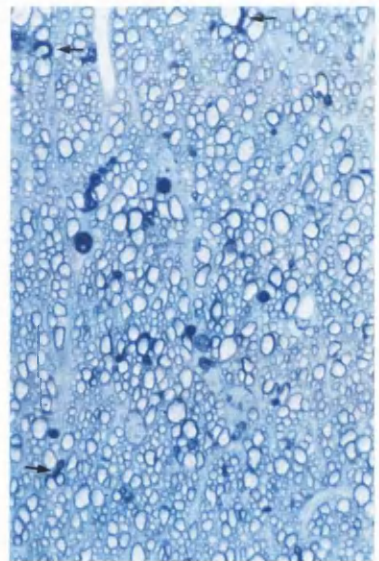


(ii)

a)



(i)



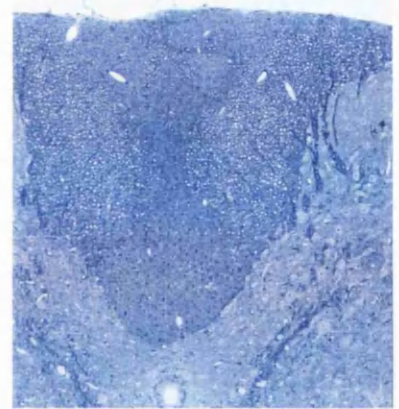
(ii)

b)

Figure 16. Tract specific distribution of lesions in the development of demyelination in #66 and #72 hemizygous mice. a) P60 optic nerve (i) wild type (x990) (ii) hemizygous (#66) (x990); b) P120 optic nerve (i) wild type (750) (ii) hemizygous (#72) (x990). At P60 occasional abnormal myelin sheaths are observed in hemizygous mice (→) whilst at P120 there is obvious demyelination in the optic nerves of hemizygous mice, with loops of redundant myelin being a common feature (↔).

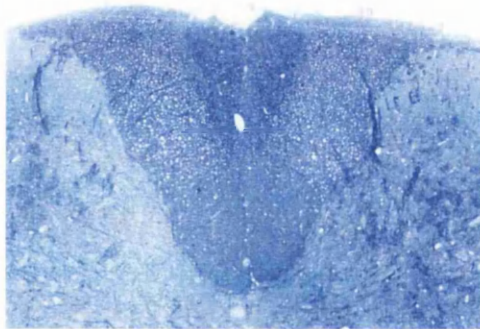


(i)

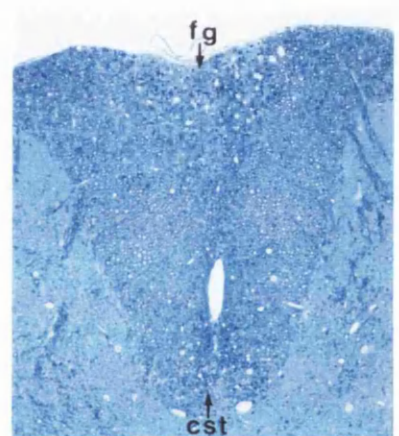


(ii)

c)



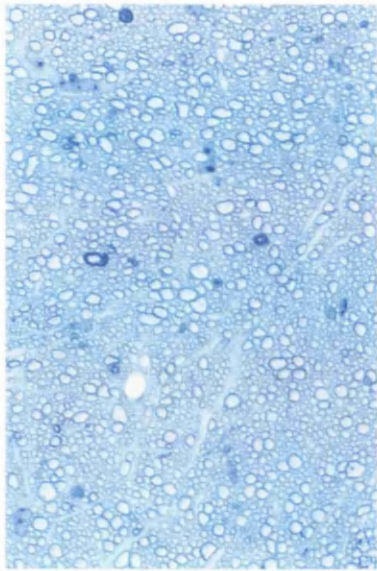
(i)



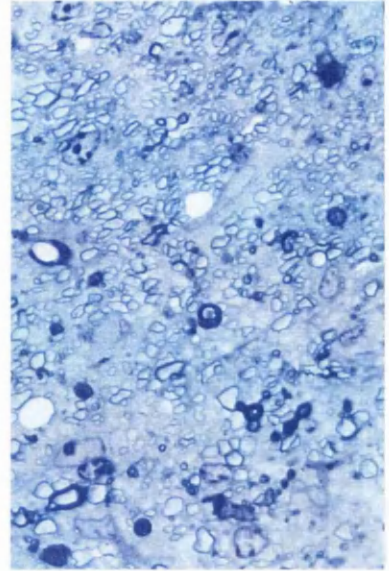
(ii)

d)

Figure 16 (continued). Tract specific distribution of lesions in the development of demyelination in #66 and #72 hemizygous mice. c) P120 dorsal columns spinal cord (i) wild type (x150) (ii) hemizygous (#72) (x99). d) dorsal columns (i) wild type (P365) (x75) (ii) hemizygous (P578, #72) (x99). At P120 the dorsal columns are unaffected. In older animals there is degeneration affecting the dorsal columns with abnormalities primarily affecting the fasciculus gracilis (fg) and the corticospinal tracts (cst).

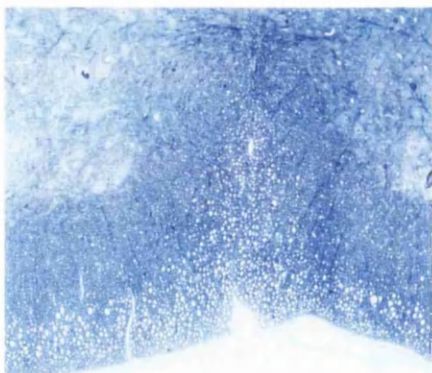


(i)

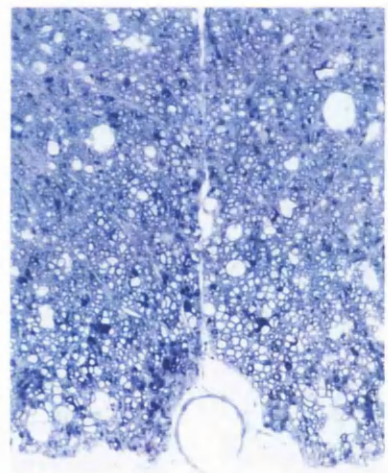


(ii)

e)



(i)



(ii)

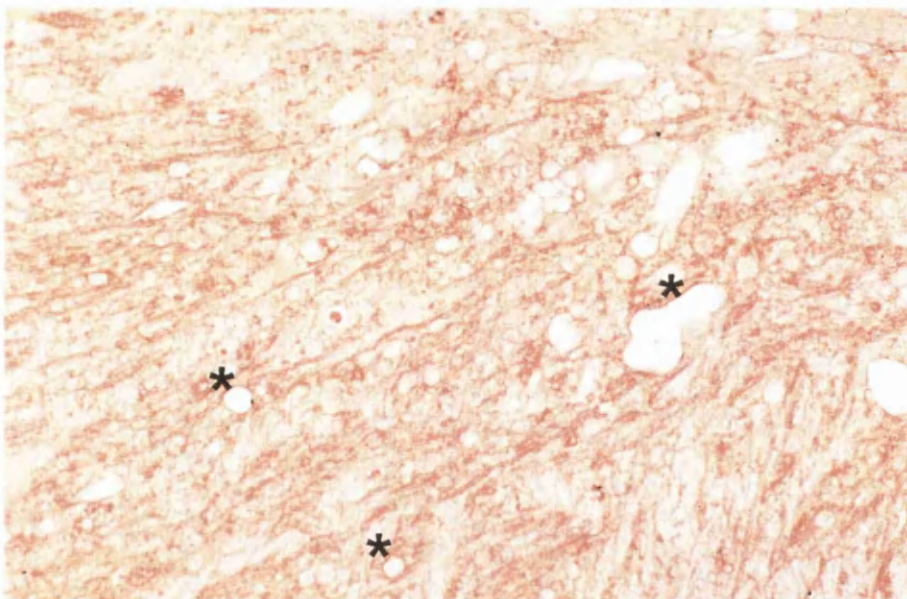
f)

Figure 16 (continued). Tract specific distribution of lesions in the development of demyelination in #66 and #72 hemizygous mice. (e) demyelination of optic nerve in mouse with degeneration affecting optic nerve and dorsal and ventral columns of the spinal cord (i) wild type (P365) (x990) (ii) hemizygous (#66, P489) (x990); (f) ventral column demyelination (i) wild type (P365) (x75) (ii) hemizygous (#66, P489) (x75). Eventually all white matter tracts examined showed evidence of neurodegeneration, with the ventral columns being amongst the last to be involved in the spinal cord.

Late onset neurodegeneration in hemizygous mice



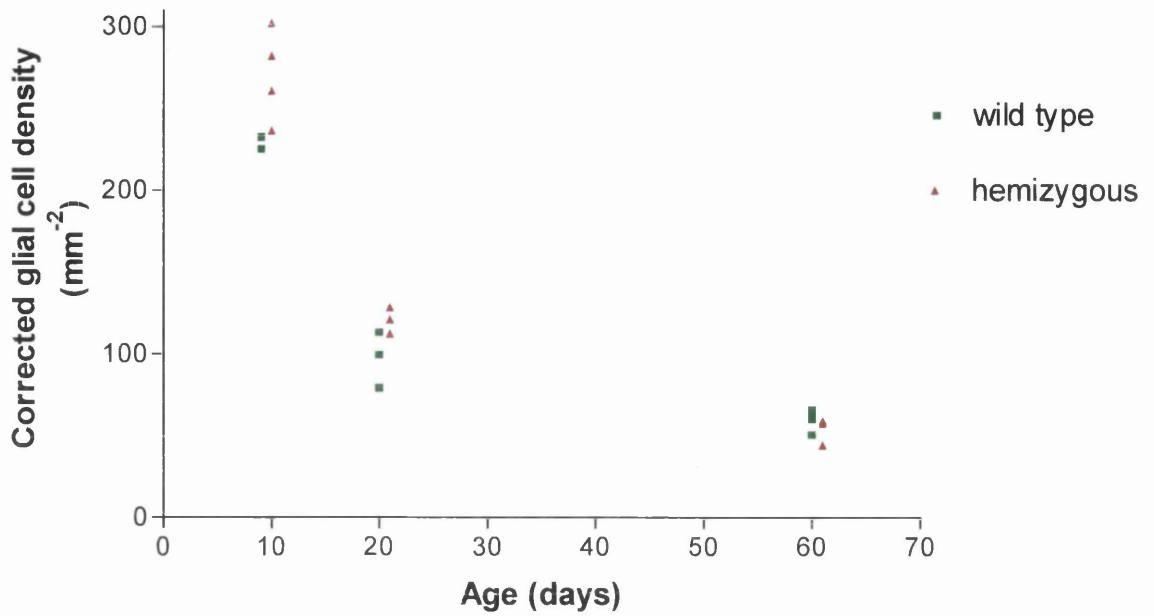
(a)



(b)

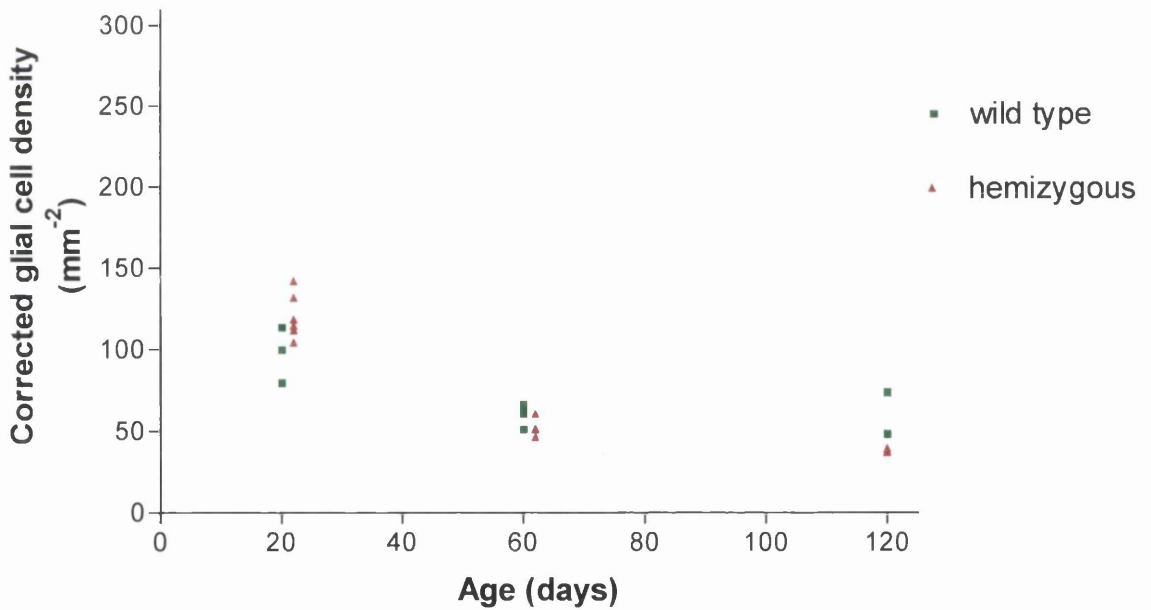
Figure17. Vacuolation of the grey and white matter in a hemizygous #72 mouse stained for PLP/DM20. a) transverse brain section including corpus callosum and optic nerve (PLP₂₂₆) (x9.9); b) PLP₂₂₆ immunostaining (*) of vacuolation showing that the wall of the vacuole contains PLP (x150).

Hemizygous #66



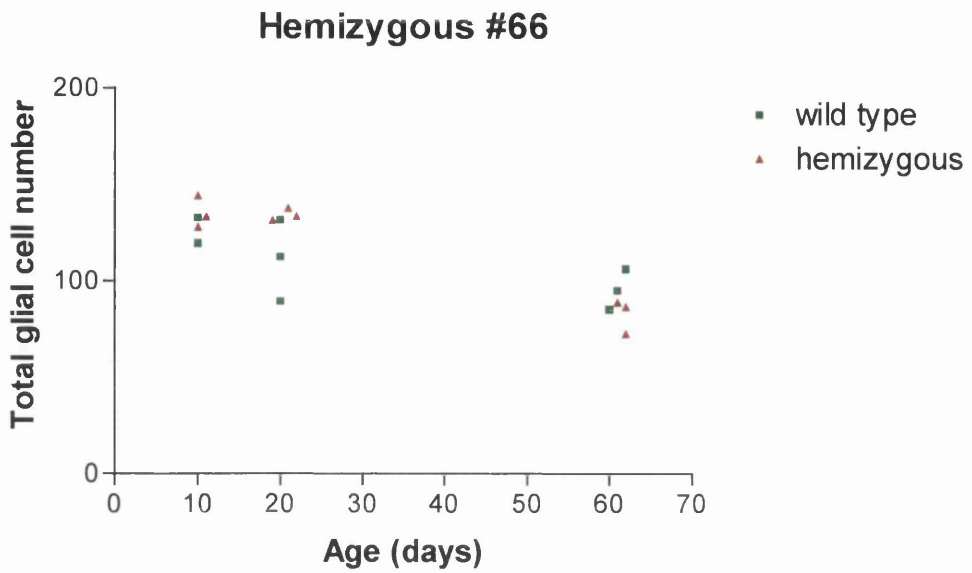
a)

Hemizygous #72

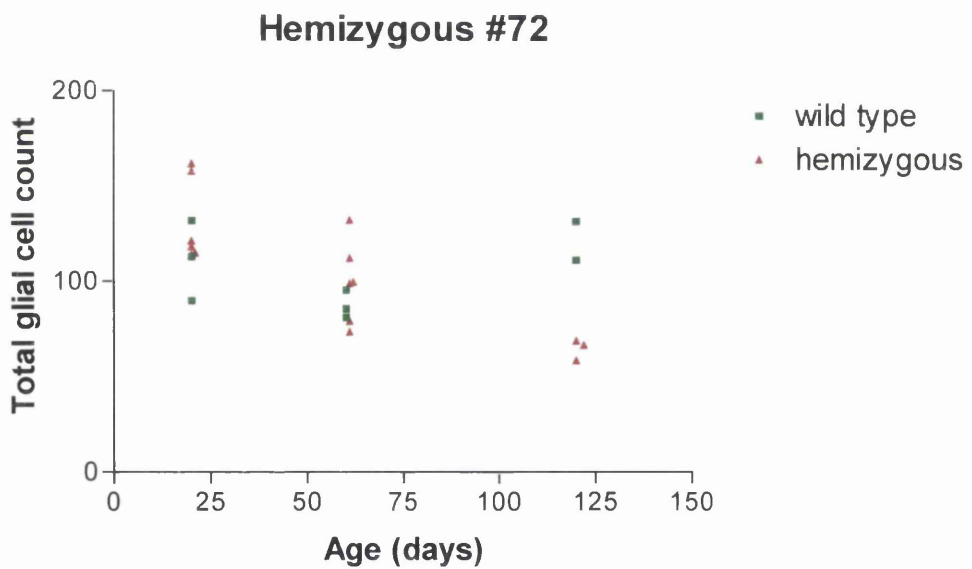


b)

Figure 18. Corrected total glial cell density in cervical cord white matter (segment C2) in #66 and #72 hemizygous mice compared with wild type. a) #66; b) #72.



(a)



(b)

Figure 19. Corrected white matter total glial cell count in cervical cord white matter (segment C2) in hemizygous #66 and #72 mice with wild type. a) #66; b) #72.

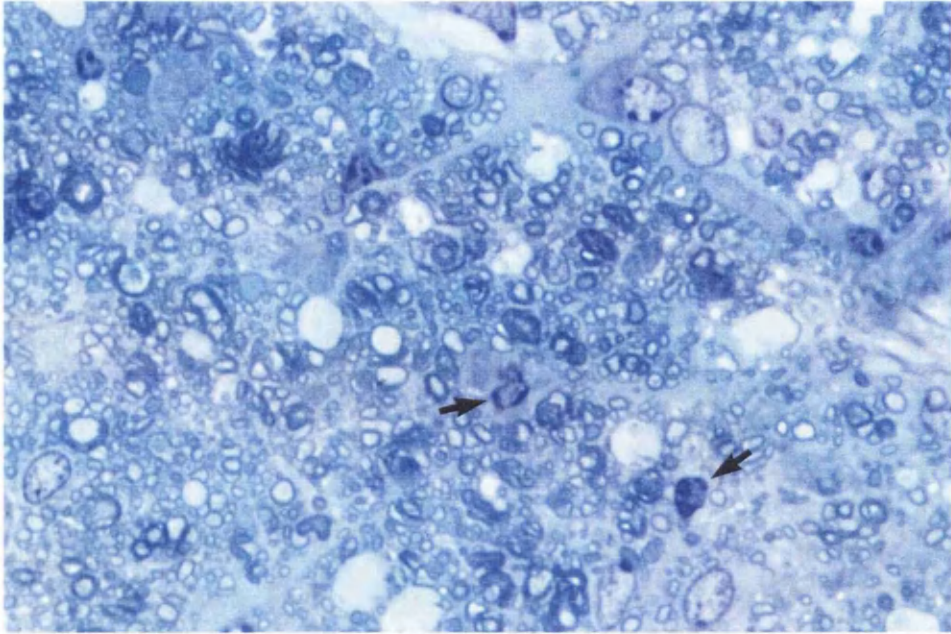


Figure 20. Microglia in area of neurodegeneration in aged hemizygous mouse (#72, P578) (x990). Corticospinal tracts of the cervical cord (C2). (↔) cells with microglial morphology.

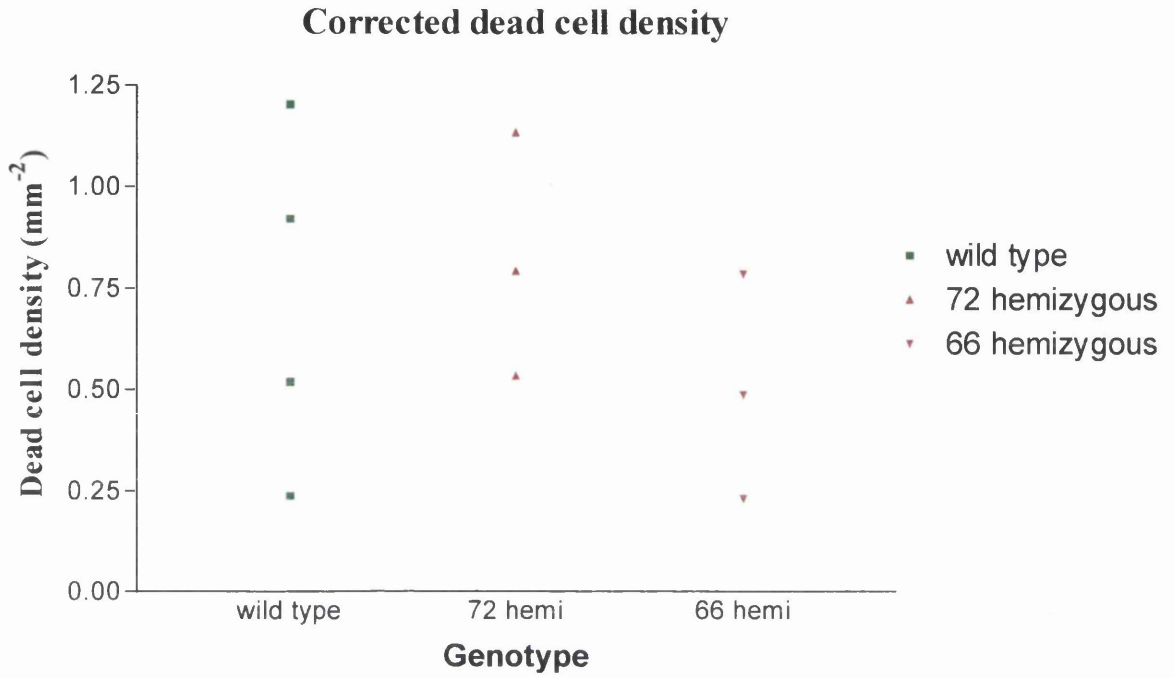
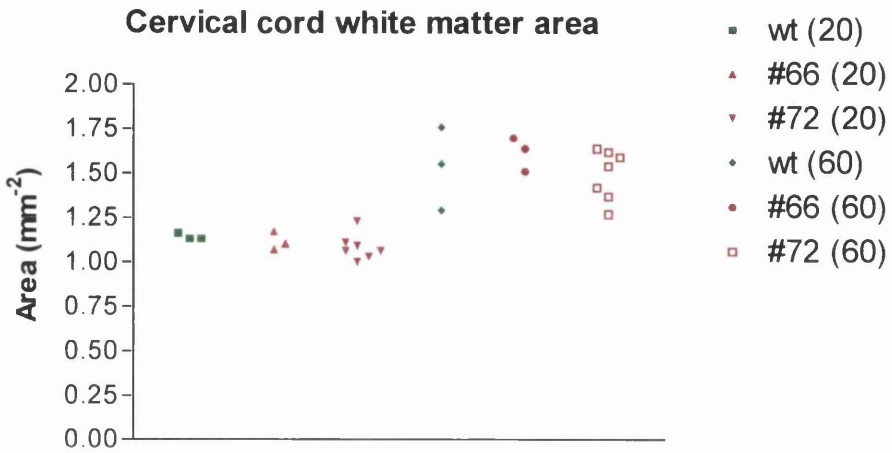
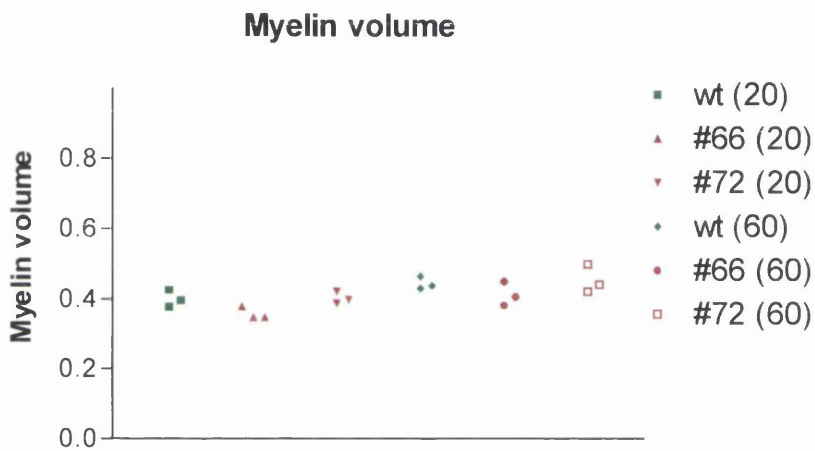


Figure 21. Dead cell densities in the white matter of cervical cord in 20 day hemizygous #66 and #72 mice and their wild type litter mates.

Late onset neurodegeneration in hemizygous mice



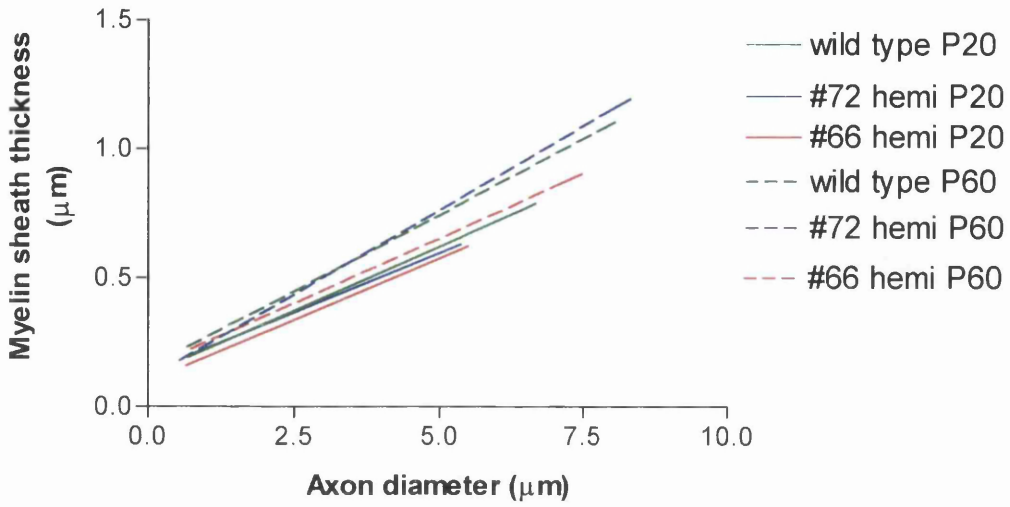
a)



b)

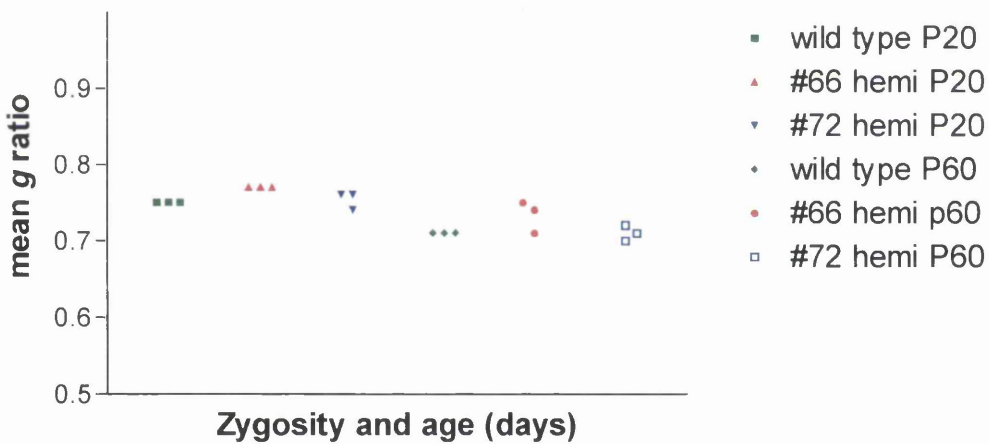
Figure 22. Morphometric analysis of myelin in the cervical cord of hemizygous #66 and #72 mice at P20 and P60. a) white matter area; b) myelin volume.

Myelin thickness vs axon diameter P20 and P60



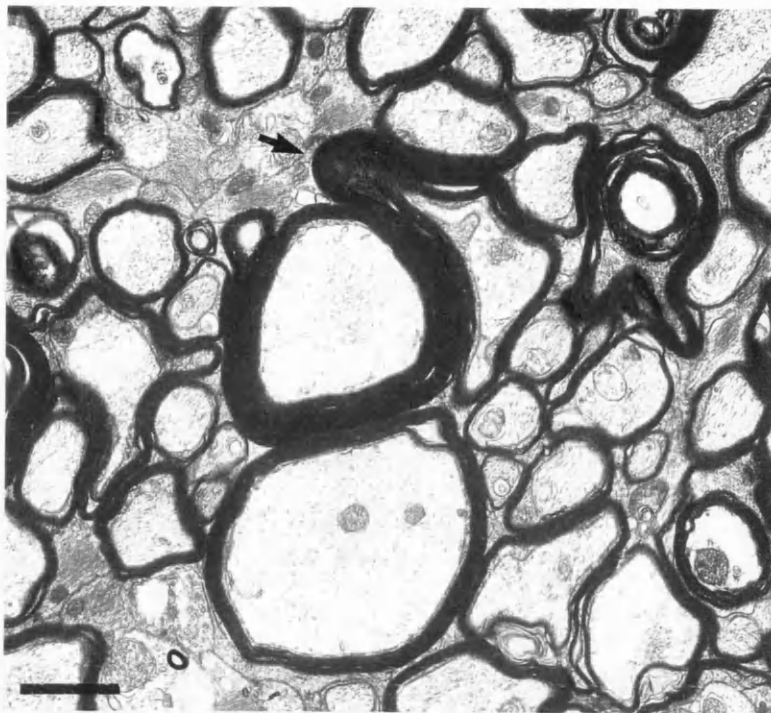
c)

mean g ratio at P20 and P60

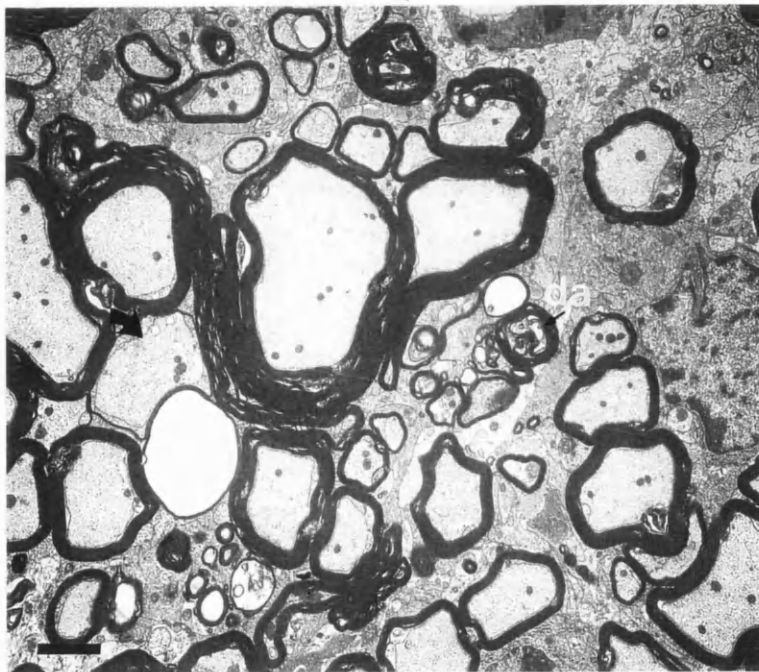


d)

Figure 22 (continued). Morphometric analysis of myelin in the cervical cord of hemizygous #66 and #72 mice at P20 and P60. c) myelin sheath thickness; d) mean g ratio.



a)



b)

Figure 23. Electronmicrograph of the early changes associated with hemizyosity for the #66 and #72 transgenes. a) optic nerve (#72, P120) showing redundant myelin loops (↔) (scale bar 1 μ m); b) ventral columns of spinal cord (#72, P583) showing redundant myelin loops, a demyelinated axon (↔) and a degenerating axon (da) (scale bar 2 μ m). In both tracts many sheaths are unaffected and there is little apparent loss of myelin.

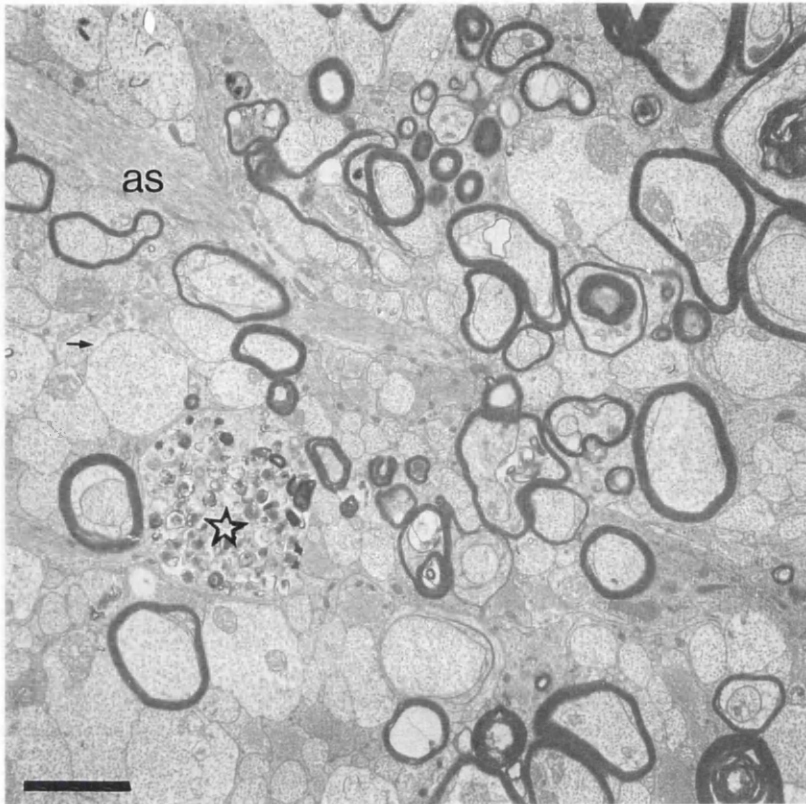


Figure 24. Electronmicrograph of the late changes associated with hemizyosity for the #66 and #72 transgenes. a) optic nerve (#66 P372). Many axons are demyelinated (→) and there is an increase in astrocytic processes (as). A demyelinated swollen axon is present, which contains many dense bodies (☆) (scale bar 1 μ m).

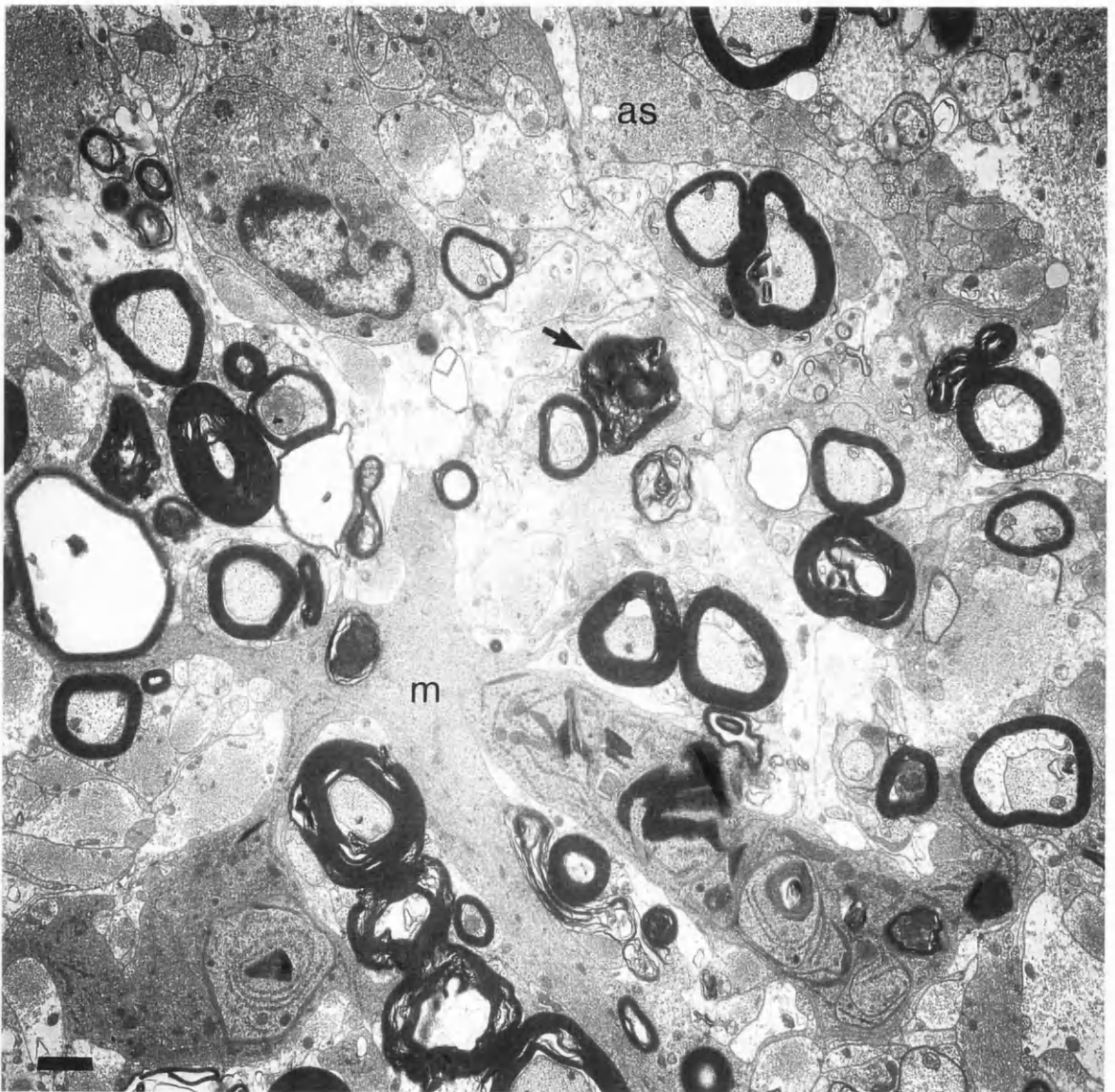
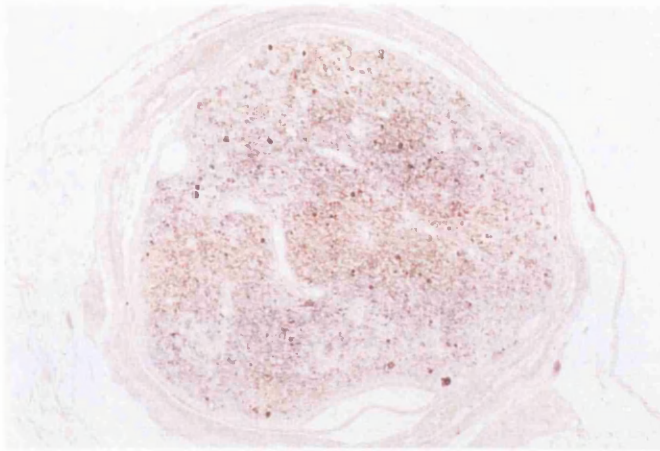


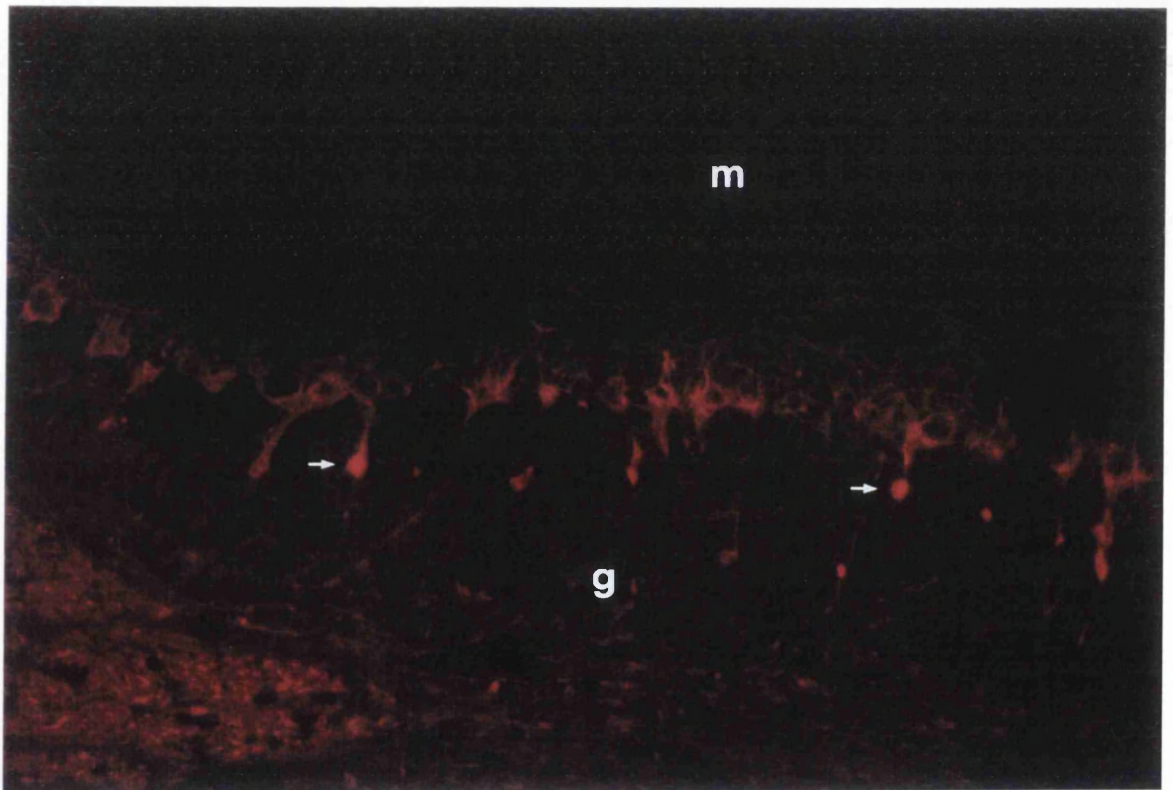
Figure 24 (continued). Electronmicrograph of the late changes associated with hemizyosity for the #66 and #72 transgenes. b) area from the fasciculus gracilis of a chronic lesion in a hemizygous #72 (P583) mouse showing increase in astrocyte processes (as), activated microglia (m) and a loss of axons. Degenerating fibres are present (→) (scale bar 2 μ m).



Figure 25. Electronmicrograph of the abnormalities of the inner tongue of an oligodendrocyte from a mouse hemizygous for the #66 transgene (P372). There is distension with a granular material (g). The periaxonal space appears intact (scale bar 1 μ m).



(a)

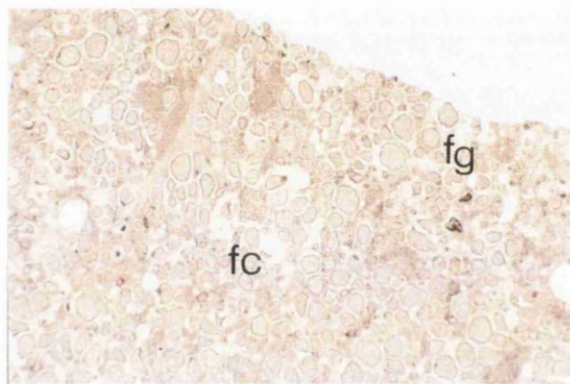


(b)

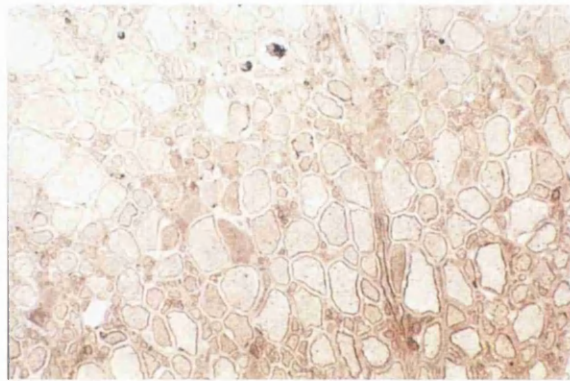
Figure 26. Immunostaining for myelin proteins and phosphorylated NF-H (SMI-31) in areas of neurodegeneration in aged hemizygous #66 and #72 mice. a) reduction in PLP/DM20 (PLP₂₂₆) in the optic nerve (#66, P448); b) cerebellar cortex showing molecular layer (m) and granule cell layer (g) with intervening Purkinje cells immunostained for SMI-31, the Purkinje cell axons exhibit numerous torpedo swellings (→).



c)

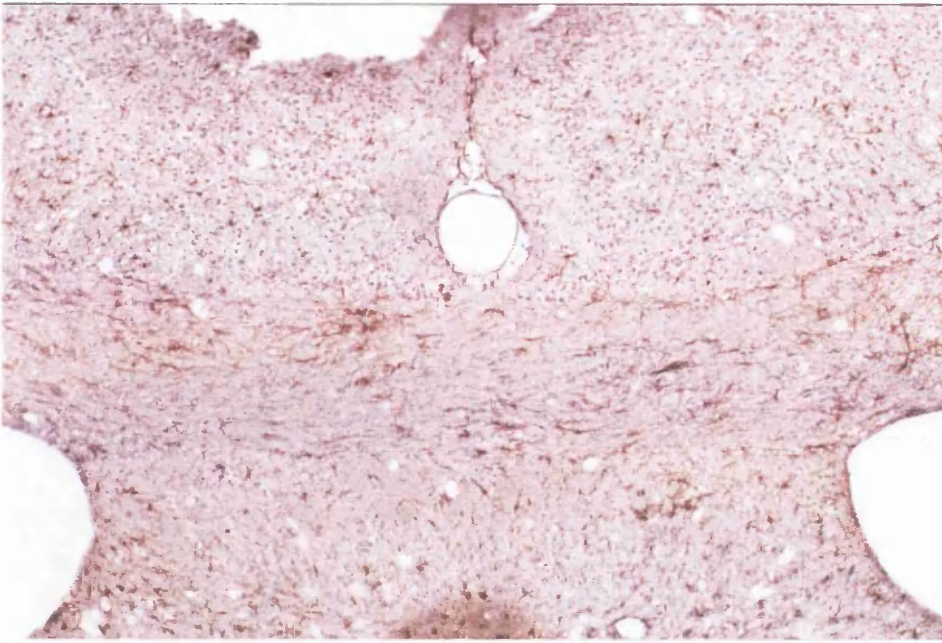


d)

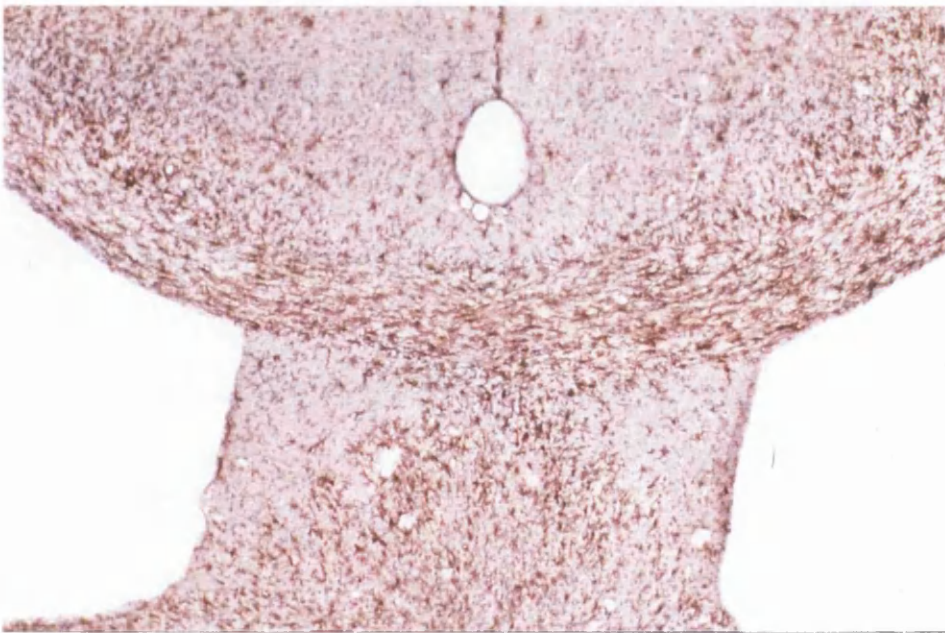


e)

Figure 26 (continued). Changes in the immunostaining for myelin proteins and phosphorylated NF-H (SMI-31) in areas of neurodegeneration in aged hemizygous #66 and #72 mice. c) thoracic cord showing loss of immunostaining in the degenerating corticospinal tracts (\rightarrow); d) dorsal columns at the junction of fasciculus gracilis (fg) and fasciculus cuneatus (fc) immunostained for MAG demonstrating the integrity of the periaxonal space; e) ventral columns of same mouse immunostained for MAG. Immunostaining for MAG is lost in areas with axonal degeneration (fg) but retained in areas where myelinated fibres are intact. In the ventral columns, which are unaffected, all fibres have a normal MAG positive periaxonal space.



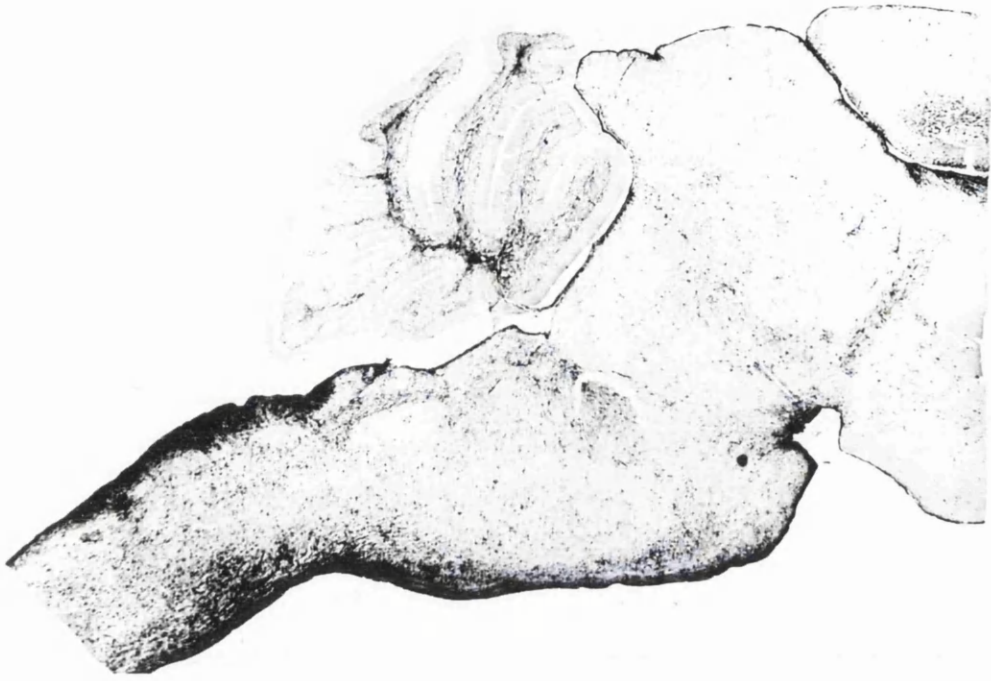
(i)



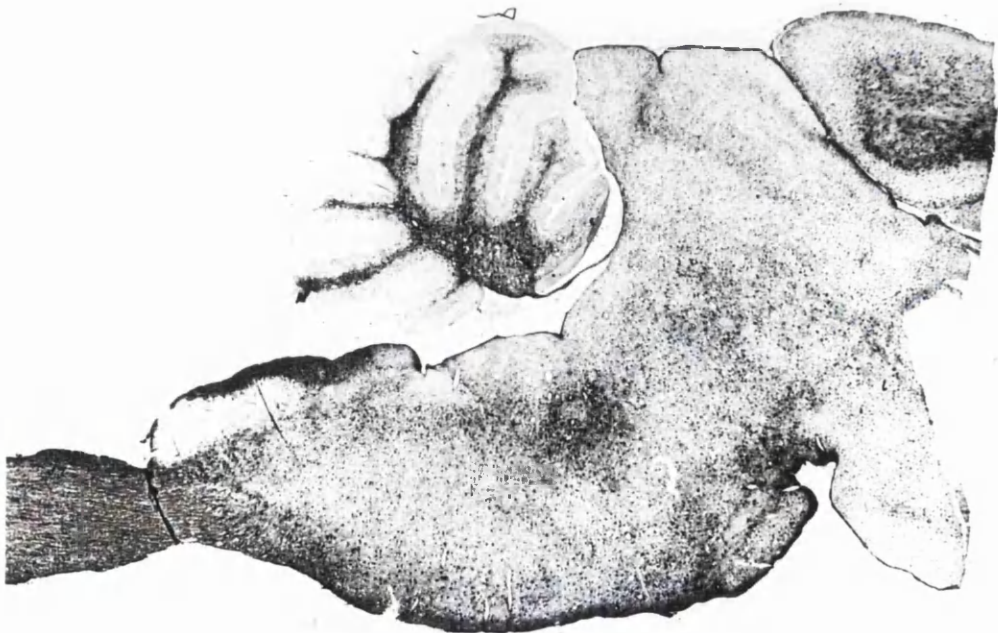
(ii)

a)

Figure 14. Microgliosis and astrocytosis in aged mice hemizygous for #66 and #72 transgenes. a) F4/80 staining for microglia i) corpus callosum in wild type (P770) (x75); ii) microgliosis in corpus callosum of aged hemizygous mouse (#72, P572) (x75).



(i)



(ii)

(b)

Figure 27 (continued). b) sagittal section of brain immunostained with GFAP for astrocytic processes. (i) wild type (P546) (x10); (ii) aged hemizygous (P365) (x10).

Late onset neurodegeneration in hemizygous mice

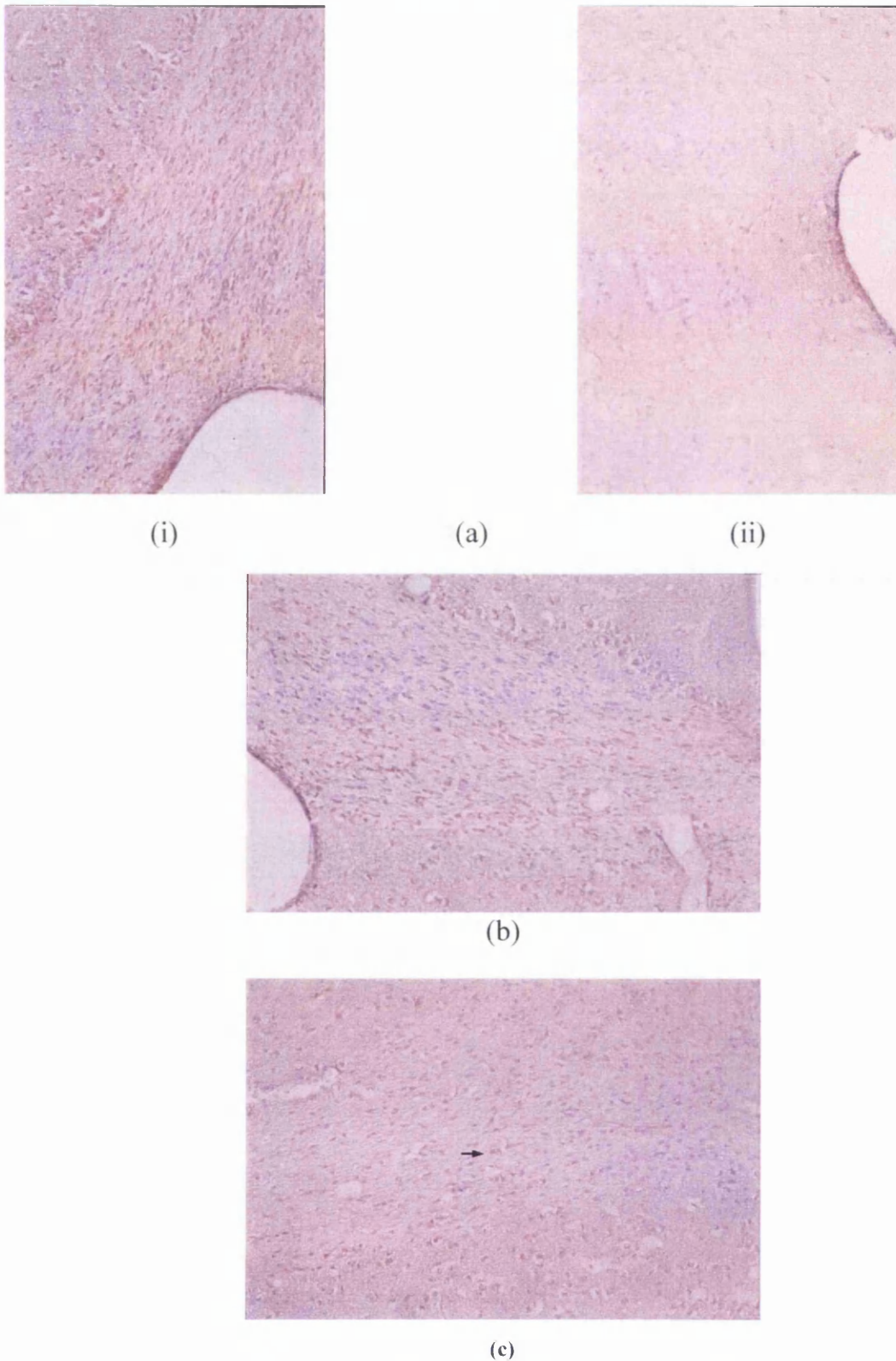
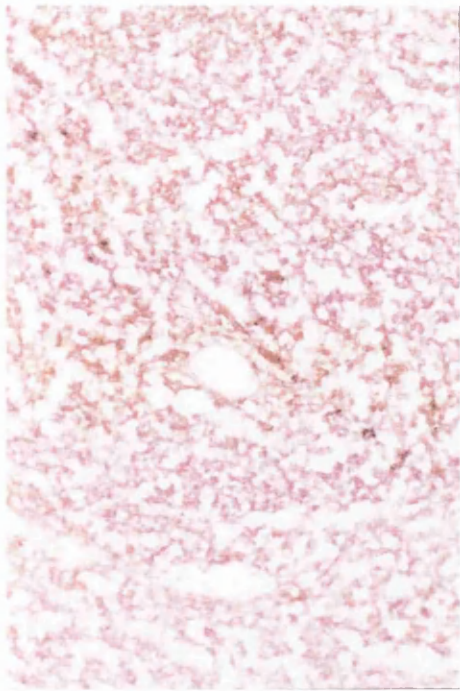
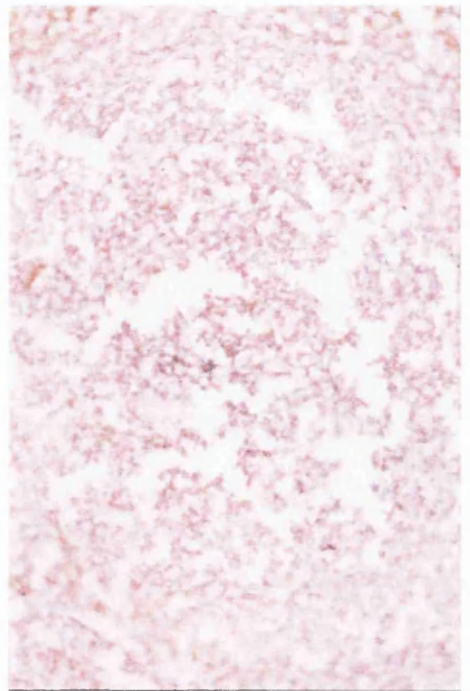


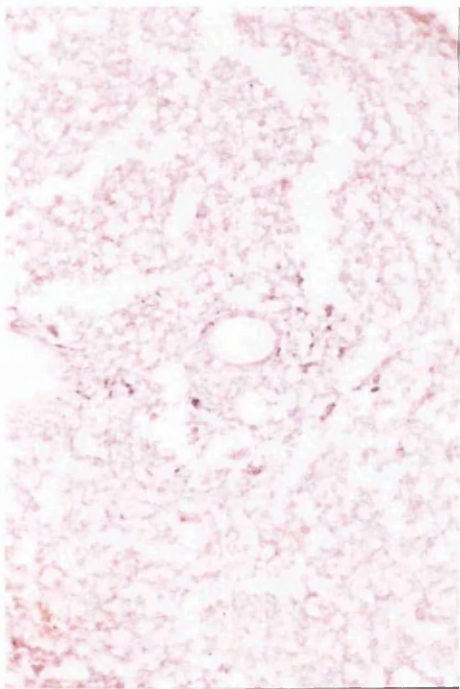
Figure 28. T cells in the brain of mice hemizygous for the #72 transgene. a) CD45 immunostaining showing general increase in immunoreactivity in the corpus callosum of aged hemizygous #72 mouse (P572) (i) compared to wild type (P770) (ii); b) CD8 immunostaining of corpus callosi with no immunoreactive cells; c) CD3 immunostaining of corpus callosum with occasional positive cells (→) (all x50).



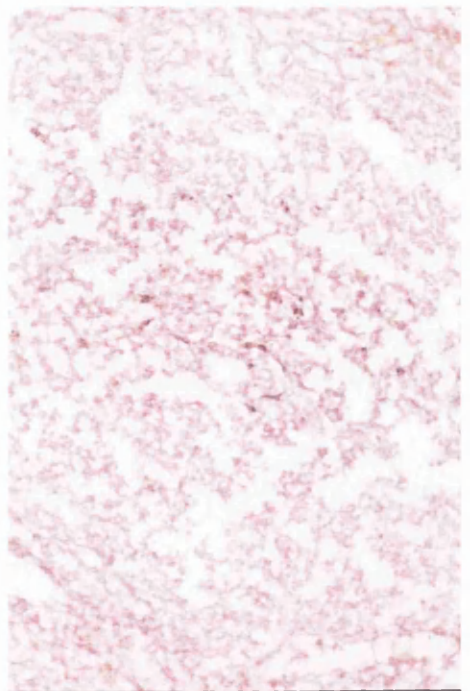
(i)



(ii)



(iii)



(iv)

Figure 28 (continued). d) immunostaining of the “T” cell region of the spleen as positive control for T cell antibodies (i) CD45, (ii) CD3, (iii) CD4 and (iv) CD8 (all x50).

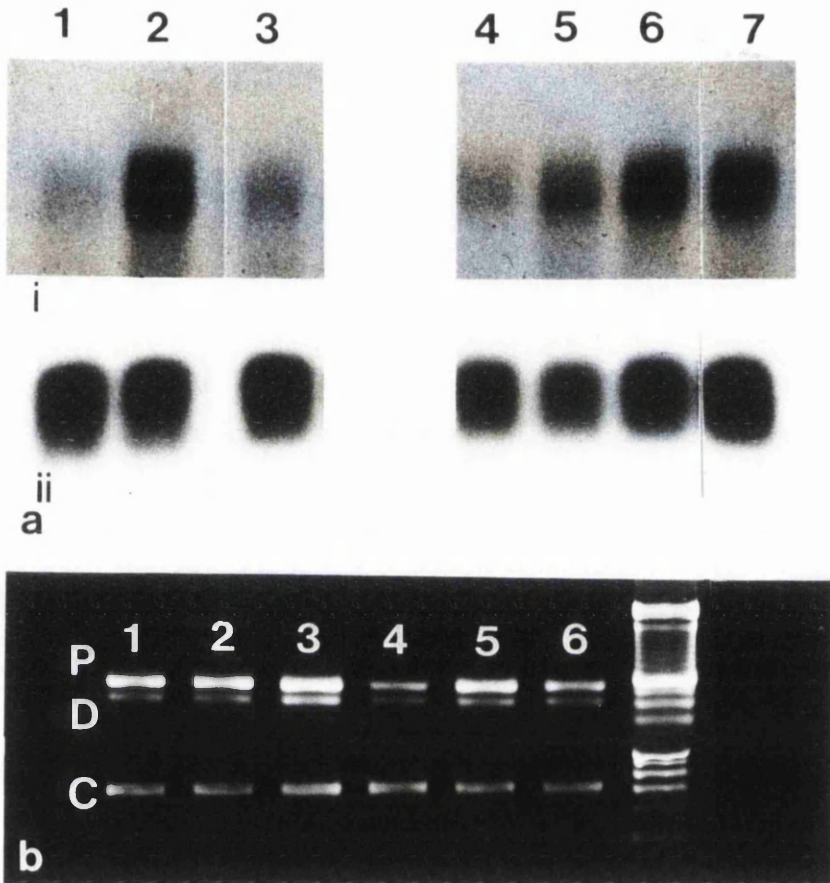


Figure 29. Expression of myelin genes in 20 day and aged mice and their wild type littermates showing autoradiographs of northern hybridisation, RT-PCR and western analysis. a) northern hybridisation with PLP-1 (i) and 7S (ii) at P20 (lane 1 wild type , lane 2 #66 and lane 3 #72) and in aged hemizygous mice (lane 4 aged wild type (P735), lane 5 #66 (P514, no overt phenotypic signs), lane 6 #66 (P546, neurological abnormalities) and lane 7 #72 (P753, moribund, terminal seizure); b) RT-PCR showing *Plp:Dm20* ratios at P20 (lane 1 wild type, lane 2 #72 and lane 3 #66) and in aged mice (lane 4 aged wild type (P546), lane 5 #66 (P514) and lane 6 (P546) *Plp* (P), *Dm20* (D) and cyclophilin.

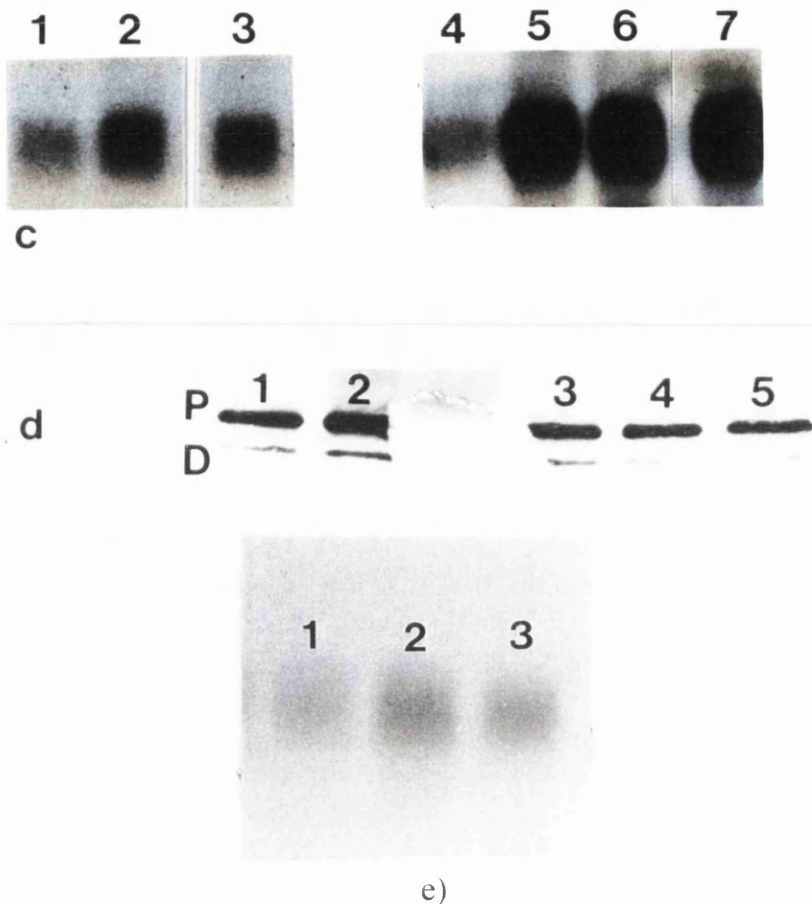


Figure 29 (continued). Expression of myelin genes in 20 day and aged mice and their wild type littermates showing autoradiographs of northern hybridisation, RT-PCR and western analysis. c) northern hybridisation for MOBP at P20 (lane 1 wild type, lane 2 #66 and lane 3 #72) and in aged mice (lane 4 wild type (P546), lane 5 #66 (P514, no overt phenotypic signs), lane 6 #66 (P546, neurological abnormalities) and lane 7 #72 (P753, neurological abnormalities); d) western analysis of protein extracted from whole brain immunostained for PLP/DM20 (PLP₂₂₆) lane 1 #66 (P513, no phenotypic abnormalities), lane 2 #66 (P538, mild neurological signs), lane 3 #72 (P546, no phenotypic abnormalities), lane 5 wild type (P546), lane 6 wild type (P546); e) northern hybridisation aged mice for MBP lane 1 wild type (P753), lane 2 #66 (P514) and lane 3 (P644);

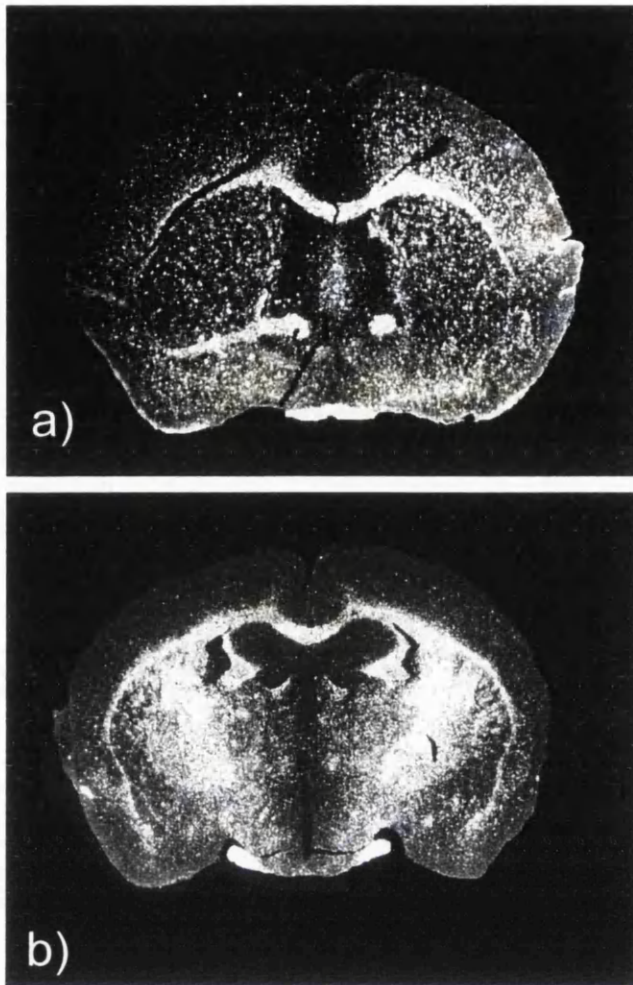


Figure 30. *In-situ* hybridisation (PLP-1) of transverse sections of brains from hemizygous mice at a) P60 (#66) (x10) and b) aged (P754) (x10). At both P60 and in the aged brain there are apparently adequate numbers of cells expressing *Plp/Dm20* message isoforms, with a possible increase in the number of expressing cells and message per cell in the aged animal.

5. Dysmyelination and demyelination in mice homozygous for #66 and #72 transgene cassettes

5.1 Background

In the first offspring generated from the #66 foundation animals it was observed unexpectedly that a proportion of the mice exhibited a neurological phenotype (Readhead *et al.*, 1994). Affected mice had a tremor from the time of ambulation, quickly developed seizures, had stunted growth and died prematurely. Histopathological examination showed severe dysmyelination. The frequency of affected individuals within litters, in conjunction with Southern hybridisation analysis for *Plp* gene copy number, demonstrated that affected mice were homozygous for the transgene. It is this dysmyelinating phenotype, related to increased *Plp* gene dosage, that was the basis for this project.

It was subsequently shown that #72 homozygous mice also exhibited dysmyelination but more subtle in nature and that they also eventually developed seizures and died prematurely (compared to their non-transgenic littermates), but at a greater age than homozygous #66 mice.

5.2 Aims

The mechanism underlying the abnormalities in myelination observed in these lines of transgenic mice was unknown but their contrasting phenotypes suggested differences in the underlying cellular pathology. This study describes mice homozygous for #66 or #72 transgenes, with particular reference to the CNS glial cell population and the expression of myelin proteins. Unless otherwise stated homozygous animals are compared to their non-transgenic litter mates (also referred to as wild type).

Two time points were selected for more detailed study: P20 representing the period of peak myelination; P60 representing the adult state which is also around the point of death in homozygous #66 mice. #72 mice were also studied at P120, at which point neurological abnormalities were established in some, but not all, mice.

5.3 Methods

The methods used are summarised in 4.3 Methods (page 90). References to the location of detailed descriptions of particular techniques are also given there.

5.4 Results for homozygous #72 transgenic mice

5.4.1 Phenotypic characteristics

5.4.1.1 Growth

Male and female mice varied noticeably in body weight and as sample sizes were small the values for body weight are presented for each sex. Subjectively, #72 homozygous mice were indistinguishable from their wild type and hemizygous litter mates and at P60 body weight of homozygotes was equivalent to wild type (Figure 31, page 148).

5.4.1.2 Neurological abnormalities

Homozygous #72 mice lived free from gross neurological abnormalities until well into adulthood. Onset of disease was usually indicated by seizures, which were progressive in frequency and duration; ataxia and weight loss were also noted. Death was also usually as a result of seizure activity. The onset of disease was very variable with neurological abnormalities becoming apparent between P60 to P140.

5.4.2 Neuropathology

Dysmyelination and the development of demyelination in homozygous #72 mice is illustrated in Figure 32, pages 149-152. Dysmyelination was evident in all white matter tracts examined at P20, with generalised thinning of myelin sheaths. Though the great majority axons in the optic nerve and corticospinal tracts were ensheathed there were occasional naked fibres. At P20 infrequent myelin sheaths in the optic nerve exhibited focal myelin thickening; by P60 demyelination and axonal swellings were apparent and by P120 the optic nerve was largely demyelinated. The dorsal columns of the spinal cord had a heterogeneous appearance at all ages studied, with the most affected areas being the corticospinal tracts. At P20 these tracts contained a number of naked axons with occasional focal thickenings of myelin sheaths. At P60 these abnormalities were more extensive and by P120 there was extensive demyelination of the corticospinal tracts with occasional axonal swellings. The ventral columns appeared virtually unaffected until P120 by which time there were abundant abnormalities of myelin sheaths with focal myelin thickenings and the formation of redundant loops of myelin.

The development of pathology in the brain was not examined.

5.4.3 Glial cell density

The data for corrected total glial cell density is presented in Figure 33, page 153. There is a trend for an increase in glial cell density during myelination which appears to decrease with time, until at P60 values are similar to wild type. At P20 there is a significant difference between homozygous and wild type ($p=0.0286$) which is not present at P60 ($p>0.05$). In homozygous #72 mice at P120 the cell densities, which were performed in the ventral columns, are similar to wild type. However, in the dorsal column tracts affected by neurodegeneration there is a subjective increase in cells with the morphology of microglia.

5.4.4 Dead cell density

The dead cell density in cervical cord at P20 was estimated to be approximately 4x greater than wild type (Figure 35, page 155). (median wild type = 0.72cells mm^{-2} and #72 = 2.6 cells mm^{-2}). Though this is not significant ($p=0.0571$) the p value suggests that further data points might confirm this difference.

5.4.5 Myelin morphometry

The data for myelin morphometry in homozygous #72 mice is presented in Figure 36, pages 156-158. The white matter area appears to be reduced compared to wild type at both P20 (wild type median = 1.13mm^{-2} and #72 = 0.99mm^{-2}) and P60 (median wild type = 1.57mm^{-2} and #72 = 1.37mm^{-2}) but does, however, appear to increase with age. Myelin sheaths are thin, being approximately 70% the thickness of wild type at P20 and 80% at P60. The apparent increase in myelin sheath thickness with age is reflected in an apparent increase in the myelin volume, however, by P60 they have not apparently attained an equivalent thickness to that in the wild type at P20. The apparent reduction in myelin thickness is associated with an apparent increase in the mean g ratio. None of these differences are statistically significant.

5.4.6 Ultrastructure of oligodendrocytes and myelin

The myelin in homozygous #72 mice was compacted normally with a recognisable MDL and double IPL (see Figure 37, page 159).

At P20 (Figure 38, page 160) and P60 (Figure 39, page 161) apparently normal and abnormal oligodendrocytes were observed within the ventral columns. The primary abnormality was the presence of vacuolar structures, which had an appearance similar to those observed in homozygous #66 mice (see 5.5.6 Ultrastructure of oligodendrocytes and myelin, page 142 and Figure 40, page 163). In areas of

demyelination abnormalities of the oligodendrocyte inner tongue were observed, similar to those seen in aged hemizygous #66 and #72 mice (see 4.4.6 Oligodendrocyte and axon ultrastructure (page 98) and Figure 25, page 124).

5.4.7 Gene expression

5.4.7.1 Immunocytochemistry

Immunostaining for myelin proteins (PLP/DM20 and MBP) demonstrated a reduction in immunostaining, particularly in the more dramatically affected small fibre tracts, commensurate with the reduction in myelin observed on methylene blue/azur II sections. An example of immunostaining for MBP in a homozygous #72 mouse at P60 is given in Figure 43 (page 168). Immunostaining with SMI-31 demonstrated axonal swellings in affected tracts (Figure 43, page 168).

5.4.7.2 Transcript analysis

5.4.7.2.1 Northern hybridisation

Transcription of the myelin genes *Plp* and *Mobp* were examined at P20 (Figure 44, page 169). *Plp* mRNA steady state levels were approximately equivalent to wild type (panel a) whilst the message levels for *Mobp* (panel b) were marginally elevated.

5.4.7.2.2 RT-PCR for *Plp:Dm20* ratio

The *Plp:Dm20* ratio was examined by RT-PCR using cyclophilin as a control for invariant temporal expression, the levels of which are reasonably constant across the spectrum of ages and genotypes (panel c (i) and (ii) Figure 44, page 169). The *Plp:Dm20* ratio was equivalent to wild type (lane 1) at P20 (lane 3) and P60 (lane 6). The total PCR product was, however, elevated compared to wild type at both P20 and P60. This supports the finding for the *Plp* northern hybridisation experiment that *Plp* gene transcription is not reduced at P20 (lane 3) and suggests that the same is likely to be true for P60. However, it emphasises that further experiments are required to clarify the relative levels of *Plp* gene transcription in wild type and homozygous #72 mice. This may represent a difference in sensitivity between the two experimental approaches. The findings in hemizygous mice where *Mobp* and *Mbp* gene transcription were elevated in conjunction with increased *Plp* gene transcription (4.4.7.2.1 Northern analysis, page 99) suggests that this may be the case in homozygous #72 mice (as it is for homozygous #66 mice - see 5.5.7.2.1 Northern hybridisation, page 142).

5.4.7.3 *In situ* hybridisation studies

In-situ studies using the PLP-1 probe demonstrated a similar number of oligodendrocytes in white matter regions at P20 (data not shown). However, at P60 there was an apparent reduction in positive cells, seen in the region of the corticospinal tracts, suggesting a possible loss of oligodendrocytes (Figure 45, page 170).

5.4.8 Summary of the phenotype of homozygous #72 mice

Homozygous #72 mice are dysmyelinated but the degree of perturbation is insufficient to induce the gross neurological abnormalities observed in homozygous #66 mice and other dysmyelinating mutants. However, older mice exhibit progressive neurological disease and premature death (as compared to their hemizygous and wild type litter mates).

Myelination appears to commence at a similar time to wild type, myelin sheaths are thinner but have a normal periodicity, and myelin continues to accumulate into adulthood. *Plp* gene transcription is not reduced at P20 or P60 and may possibly be increased. The ratio of the *Plp:Dm20* message isoforms appears to be similar to wild type. Myelin is lost in older animals with the pattern of demyelination being a feature of tracts containing small diameter axons. Demyelination is progressive, initially affecting the optic nerve, followed by small fibre tracts of the dorsal columns (e.g. corticospinal tracts), lateral columns and the smaller diameter axons of the ventral columns. Myelin loss is associated with the development of focal thickening and redundant loops of myelin. There is no evidence of remyelination in affected tracts. In areas of myelin loss there is an axonopathy. Demyelinated swollen axons are also occasionally observed with the axoplasm containing dense bodies. Abnormal oligodendrocytes contain vacuolar structures, some of which may represent autophagic vacuoles although not all oligodendrocytes have obvious abnormalities.

Myelination is associated with a gliosis and subjectively the onset of disease is also associated with a gliosis in affected tracts related to an increase in microglia. *In-situ* hybridisation studies indicate that the abnormalities observed are not due to a lack of oligodendrocytes.

5.5 Results for homozygous #66 transgenic mice

5.5.1 Phenotypic characteristics

5.5.1.1 Growth

On examination of litters of #66 mice those with the phenotypic characteristics of homozygosity for the transgene appeared subjectively to be smaller than their wild type litter mates. However, the pooling of data from multiple litters and the corresponding differences related to litter size etc. (see 2.13 Growth of mice, page 75) obscures this. This trend is apparent at P60, as male and female mice vary noticeably in body weight and as sample sizes were small the values for body weight are presented for each sex (Figure 31, page 148).

5.5.1.2 Neurological abnormalities

Homozygous mice were identifiable from the time of ambulation as they had a tremor associated with movement. The time of onset of seizure activity was variable. Observation of the mice suggested the frequency and duration of seizures increased with age and eventually animals became moribund. Older animals were less active. Death occurred between approximately P40 and P70.

5.5.2 Neuropathology

Dysmyelination and demyelination in homozygous #66 mice is illustrated in Figure 32, pages 149-152. Dysmyelination was evident in all tracts at P10 with a reduction in the number of myelinated axons and the thickness of the myelin sheaths. At P10 there were very few myelinated fibres in the optic nerve and though this had increased subjectively by P20 the number of myelinated sheaths was still reduced compared to wild type. However, at P60 there was virtually no myelin present and any remaining myelin sheaths showed evidence of focal thickening and formation of myelin loops. At P10 the dorsal columns, particularly the corticospinal tracts had very few myelinated fibres, though the proportion appeared to have increased by P20. At P60 the proportion of myelinated fibres appeared to have decreased compared to P20, the corticospinal tracts were largely demyelinated and abnormal myelin sheaths were common. Subjectively, a higher proportion of axons were myelinated in the ventral columns as compared to the dorsal columns at all ages examined. The proportion of myelinated fibres in the ventral columns increased subjectively between P10 and P60, though by P60 there were fibres exhibiting focal thickenings and loops of redundant myelin.

Dysmyelination and demyelination in homozygous mice

Subjectively there was an increase in cells with the morphology of astrocytes and microglia compared to wild type in the white matter. The proportion of both types of cell appeared to increase with age.

The development of pathology in the brain was not studied.

5.5.3 Total glial cell density

The data for total glial cell density is presented in Figure 33, page 153. The trend at all ages is for a greater glial cell density in homozygous #66 mice. Though the differences at P20 and P60 are not significantly different from wild type the p values ($p=0.1$ and $p=0.1333$ respectively) suggest that further data points are likely to confirm this increase in total glial cell density in homozygous mice as being significant. This apparent increase in total glial cell density became less marked with age. However, the total glial cell numbers in white matter were reduced (Figure 34, page 154), probably reflecting the reduction in white matter area (see below).

5.5.4 Dead cell density

Dead cell densities in the white matter of the cord were apparently elevated in homozygous #66 mice to approximately 6x wild type at P20 (Figure 35, page 155). (median wild type = $0.72 \text{ cells mm}^{-2}$ and the two data points for #66 homozygous = 4.1 and $5.7 \text{ cells mm}^{-2}$). This difference is not statistically significant

5.5.5 Myelin morphometry

The data for myelin morphometry for homozygous #66 mice is presented in Figure 36 (pages 156-158). The white matter area was apparently reduced at both P20 (median wild type = 1.13 mm^{-2} and #66 = 0.86 mm^{-2}) and P60 (median wild type = 1.57 mm^{-2} and the two data points for #66 = 0.95 mm^{-2} and 1.04 mm^{-2}). There is little evidence of the increase in myelin sheath thickness that appears to occur in #72 mice and myelin sheaths are approximately 60% the thickness of wild type at P20. The apparent increase in mean myelin volume suggest an increase in the amount of myelin between P20 and P60, though more data points would be required to establish this.. Two possible events would lead to an increase in myelin volume, an increase in myelin thickness which seems unlikely, or an increase in the proportion of myelinated axons. The mean g ratio appears to be increased at both P20 and P60 in comparison to wild type, consistent with the thin myelin sheaths.

5.5.6 Ultrastructure of oligodendrocytes and myelin

The earliest time point examined by EM was P3, an age before the major upregulation of the production of myelin proteins. The most striking abnormalities of the oligodendrocytes were abundant vacuolar structures in most areas of the cytoplasm, of which there were two groups distinguished by the thickness of their walls (Figure 40, page 163 cf. P3 wild type Figure 41, page 165). The thicker walled structures probably represent autophagic vacuoles, whilst the nature of the thinner walled structures is uncertain. The presence of autophagic vacuoles implies abnormal protein turnover. Similar changes were present in the oligodendrocytes of P10 mice (Figure 42, page 166-167) and older mice (Figure 38, page 160).

5.5.7 Gene expression

5.5.7.1 Immunocytochemistry

Immunostaining for myelin proteins (PLP/DM20 and MBP) demonstrated a reduction in immunostaining, particularly in the more dramatically affected small fibre tracts, commensurate with the reduction in myelin observed on methylene blue/azur II sections. Examples of immunostaining for MBP in a homozygous #66 mice at P60 and #72 at P70 is given in Figure 43 (page 168). GFAP immunostaining demonstrated an increase in immunoreactivity consistent with the apparent increase in astrocytes as described by Readhead *et al* (1994) (data not shown).

5.5.7.2 Transcript analysis

5.5.7.2.1 Northern hybridisation

Transcription of the myelin genes *Plp* and *Mobp* was examined at P20 and P60 for *Plp* and P60 for *Mobp* (see Figure 44, page 169). At P20 *Plp* mRNA steady state levels were marginally increased compared to wild type (panel a lanes 1 and 2) whilst at P60 they were equivalent to wild type (panel a lanes 5 and 6). At P60 *Mobp* mRNA levels were equivalent to wild type (panel b lanes 3 and 4).

5.5.7.2.2 RT-PCR for *Plp:Dm20* ratio

The *Plp:Dm20* ratio was examined by RT-PCR using cyclophilin as a control for invariant temporal expression, the levels of which are reasonably constant across the spectrum of ages and genotypes (panel c (i) and (ii) Figure 44, page 169). The *Plp:Dm20* ratio was equivalent to wild type at P60. However, at P20 there is a reduction in the intensity in the band representing the *Plp* message isoform relative to wild type whilst the *Dm20* band is of similar intensity (panel c (i) lanes 1 and 2).

Dysmyelination and demyelination in homozygous mice

Total product appears to be reduced compared to wild type, primarily because of the reduction in the *Plp* isoform band. Though this does support the increase in *Plp* gene transcription suggested by the *Plp* northern hybridisation other such hybridisation experiments (not shown) do support an increase in *Plp* gene transcription in #66 P20 homozygous mice. This conflict in levels as assessed by these different approaches may reflect a difference in sensitivity (see 5.6 Discussion, page 144).

5.5.7.3 *In-situ* studies

In-situ studies using the PLP-1 probe demonstrated a similar number of oligodendrocytes in white matter regions at P20 (data not shown). However, at P60 there was an apparent reduction in positive cells, seen in the region of the corticospinal tracts, suggesting a possible loss of oligodendrocytes (Figure 45, page 170).

5.5.8 Summary of the phenotype of homozygous #66 mice

Homozygous #66 mice are severely dysmyelinated with many naked axons and any myelin sheaths formed are abnormally thin. The neurological phenotype is progressive and the mice die prematurely compared to their hemizygous and wild type littermates.

The onset of myelination is possibly delayed with the proportion of myelinated fibres increasing between P10 and P20. The perturbation in the formation of myelin sheaths appears to be more profound in small fibre tracts. Between P20 and P60 the proportion of myelinated fibres appears to decrease in tracts with a proportion of small diameter axons e.g. the optic nerve. At P20 *Plp* gene transcription appears to be elevated although there is a change in ratio of the transcripts with a reduction in the *Plp* message isoform. There is an apparent increase in total glial cell density in the developing CNS white matter, the nature of which has yet to be confirmed but many of these cells have the morphological appearance of oligodendrocytes. In P60 mice the glial cell population subjectively contains an increased proportion of microglia.

Demyelination occurs in older mice and is most predominant in tracts composed of small fibres e.g. the optic nerve and corticospinal tracts.

5.6 Discussion

The data presented in this chapter confirms that mice homozygous for the #66 or #72 transgenes are dysmyelinated. The evidence for this is the development of abnormally thin myelin sheaths and the apparent increase in the incidence of amyelinated axons. There is a marked difference in the degree to which they are affected which presumably contributes to the difference in the severity of their phenotypes, with #66 mice having a more severe perturbation in myelin development. Though not formally documented in this chapter, subjectively there is a difference in the degree of dysmyelination between tracts with late myelinating, predominantly small fibre tracts being the most affected.

Homozygosity for both the #66 and #72 transgenes is associated with an increase in total glial cell density during myelination. The data indicate that this is probably greatest early in myelination with cell numbers declining to around wild type levels at P20, the peak of myelination in wild type mice, though further data points would be required to be confident of this. An increase in glial cell density during myelination is a feature of many, but not all, *Plp* gene mutants but is not prominent in mutations affecting other myelin genes. In *Plp^{ΔP}* mice this has been demonstrated to include increased oligodendrocyte precursor proliferation (Hernández *et al.*, 1997). Immaturity of the glial cell population results in an altered *Plp:Dm20* message isoform ratio, with a decrease in *Plp* dominance (Nadon & Duncan, 1996; Tosic *et al.*, 1994). Similarly an increase in the proportion of immature cells within the oligodendroglial population might be expected to alter the *Plp:Dm20* ratio. This was observed in homozygous #66 but not #72 mice, suggesting differences in the dynamics of oligodendrocyte population differentiation. The factors driving this increase in total glial cell density is unknown but amyelinated axons *per se* are unlikely to be responsible, as there are many amyelinated axons in non-*Plp* gene mutants.

The increase in total glial cell density seen in affected *Plp* gene mutants is associated with increased oligodendroglial cell death, with the incidence broadly correlating with the severity of the hypomyelination (Skoff, 1995). Increased cell death in affected *Plp* gene mutants appears to be due to apoptosis, with cells exhibiting classic morphological changes, however Skoff (1995) has suggested that there may be subtle differences in the mechanism of apoptosis in the immature oligodendrocytes of the *Plp^{ΔP}* mouse. Increased cell death is a feature of both homozygous #66 and #72 mice at P20, however, *in-situ* studies indicate that an adequate number of oligodendrocytes is present. Interestingly a relationship of increased cell death and increased severity of dysmyelination is present in the #66

Dysmyelination and demyelination in homozygous mice

and #72 mice. This is in contrast to homozygous *4e* mice, which in common with *Plp^{lP}* mice have a reduction in mature oligodendrocytes but apparently adequate numbers of precursors (Kagawa *et al.*, 1994). Homozygous #66 mice may lose some oligodendrocytes as they age. The nature of the glial cell population during the development of transgenic mice expressing the *Dm20* minigene is not described but would be interesting as the DM20 protein isoform is speculated to play a role in oligodendrocyte development and there is evidence that it might be elevated in *Plp* gene transgenic mice (see below).

Dysmyelination in homozygous #66 and #72 occurs despite an apparently adequate numbers of oligodendrocytes (as identified by PLP-1 ISH). The oligodendrocyte populations of homozygous #66 and #72 mice are, however, compromised in their ability to elaborate and maintain myelin (see below). Though not formally investigated in this project there is a probably a delay in myelination in homozygous #66 mice. Delayed myelination has been described in the less severely affected *Plp* gene mutants *Plp^{lP-rsh}* mice and *Pt* rabbit (Tosic *et al.*, 1993; 221). Possible explanations for a delay is a failure to generate sufficient oligodendrocytes competent to myelinate axons or a reduction in the rate of myelin production by individual oligodendrocytes.

Oligodendroglial cells of homozygous #66 and #72 mice have ultrastructural abnormalities during development, that become less apparent with age. These are observed during the pre-myelination differentiation phase and during the major elaboration of myelin. They are much less striking in adults. The changes seen (e.g. autophagic vacuoles) are indicative of abnormal protein trafficking. This may indicate that the oligodendrocytes of these mice have compromised intracellular transport systems that show evidence of abnormalities only during high demand.

It is intriguing that at the peak of myelination the combined transcriptional output of the exogenous and endogenous *Plp* genes in homozygous #66 and #72 mice is not only very similar to each other but very similar to wild type, though there are major differences in the progress of myelination. *In-situ* hybridisation studies and total glial cell counts suggest that oligodendrocyte numbers are probably also similar suggesting that the transcriptional output of individual oligodendrocytes is probably at least equivalent to wild type, if not marginally increased. This points to a post-transcriptional effect on *Plp* gene expression. It is possible that it is the ability to produce myelin rather than PLP/DM20 protein isoforms that is the principle derangement, as it is known that reasonable amounts of myelin can be elaborated in the complete absence of these proteins (Klugmann *et al.*, 1997; Boison & Stoffel,

Dysmyelination and demyelination in homozygous mice

1994). Though there is evidence of abnormalities in ultrastructural elements involved in protein transport there is no conclusive evidence that it is blocked.

The finding of apparently adequate levels of *Plp* gene transcription in #66 and #72 mice is superficially contradictory to the findings in homozygous *4e* mice where at P19 there is a marked fall in mRNA levels. However, other evidence points to these mice having a reduced population of mature oligodendrocytes and the change in *Plp* gene transcription on an individual cell basis is less certain. This illustrates that levels of steady state mRNA based on tissue samples in relation to the activity in individual cells must be interpreted with a degree of caution. In this project the steady state levels for the mRNAs of *Plp* and other myelin genes has been equated to oligodendrocyte numbers as estimated by *in situ* hybridisation and cell counting. Whether the small increases in steady state mRNA levels for the *Plp* gene suggested for homozygous #66 and #72 mice is a result of increased cell numbers remains unresolved. The magnitude of this has not been fully established with variations occurring between the different experimental methods. In the initial description of the #66 and #72 mice a radioactive PCR method in conjunction with phosphoimaging documented a 50% increase over wild type in *Plp* gene transcription in homozygous #66 mice at P60 (Readhead *et al.*, 1994). This serves to illustrate the differences in sensitivities of experimental procedures and how this can be significant when examining relatively small differences. More accurate quantification of the various cell types, an estimation of the maturity of the population and further characterisation of the magnitude of any elevation in transcription would be required to resolve this.

The development of demyelination superimposed on dysmyelination was unrecognised as a feature of #66 and #72 mice before the studies presented here were undertaken. This is of particular interest in the light of the late-onset demyelination in hemizygous #66 and #72 mice. In homozygous #72 mice the late-onset demyelination rather than their mild dysmyelination would appear to be the significant factor in development of a neurological phenotype and probably contributes to their early death. In older homozygous #72 mice the abnormalities of the inner oligodendrocyte tongue are similar in nature to those in aged hemizygous #66 and #72 mice.

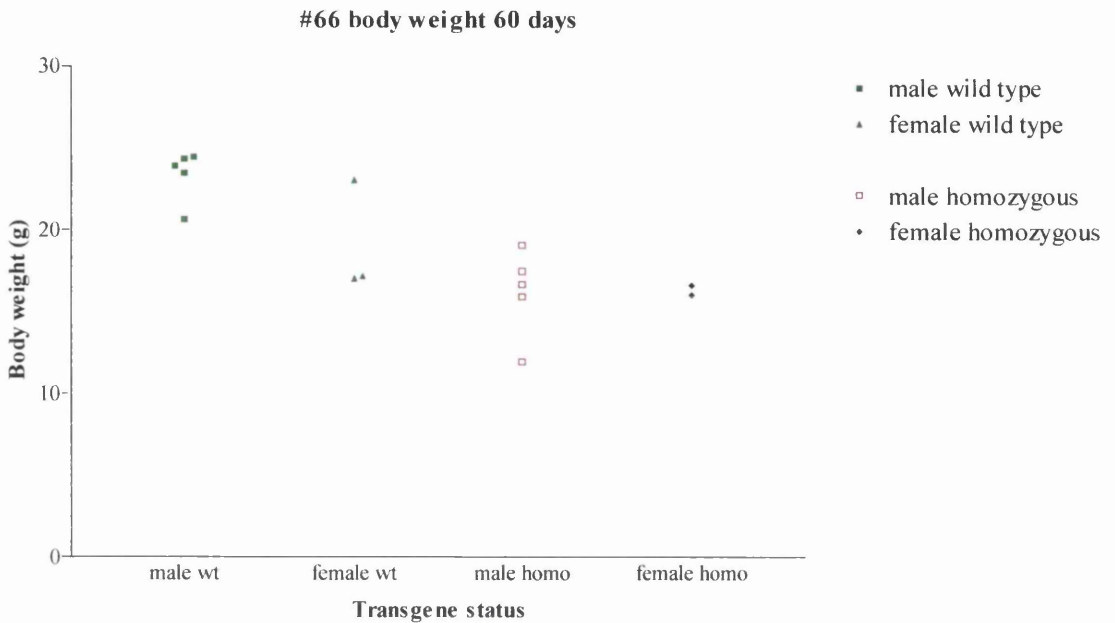
The data presented here support the concept that increased *Plp* gene dosage is associated with dysmyelination. However, the mechanism by which increased dosage of this gene has such devastating effects remains elusive. These studies on the homozygous #66 and #72 mice suggest that it is not a reduction in *Plp* gene transcription during myelination which is the underlying reason for dysmyelination,

Dysmyelination and demyelination in homozygous mice

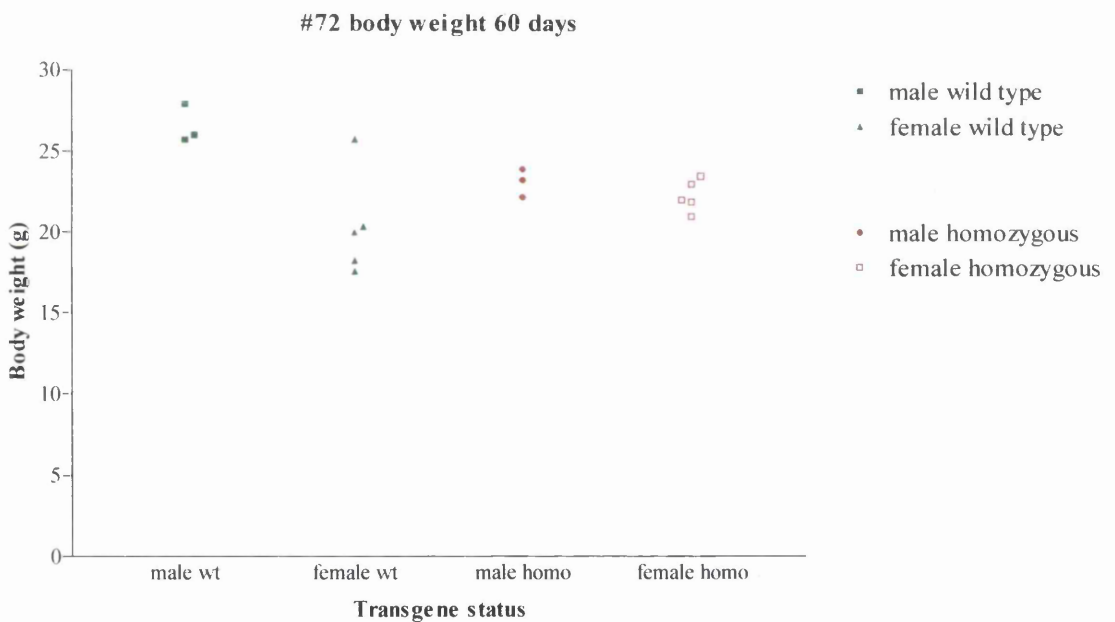
with both types of mice having steady state mRNA levels around that of wild type. The magnitude of increase in steady state mRNA levels in the two types of homozygous mouse is probably fairly similar and is therefore unlikely to be responsible for the perturbation of myelination, indeed far greater levels were found in the hemizygous (particularly #66) mice (see Figure 53, page 194).

In conclusion, the reason for the dysmyelination observed in homozygous #66 and #72 mice remains unelucidated. However, these studies do suggest that a potentially fruitful area of further investigation lies in the early development of the oligodendrocyte population.

Dysmyelination and demyelination in homozygous mice



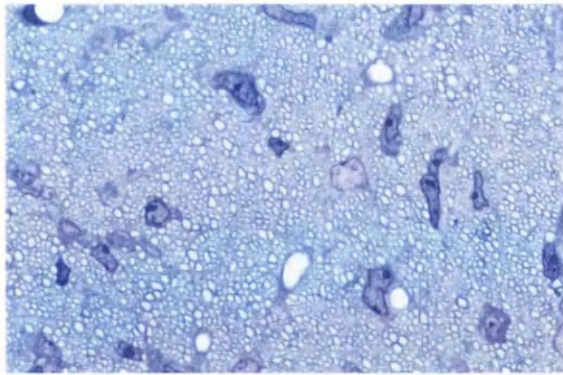
a)



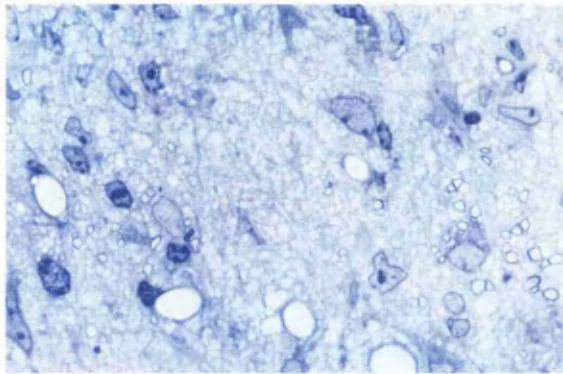
b)

Figure 31. Body weights of homozygous #66 and #72 mice and wild type at 60 days. The trend is for homozygous #66 (a) mice to be smaller than wild type whilst homozygous #72 mice (b) appear to be similar to wild type.

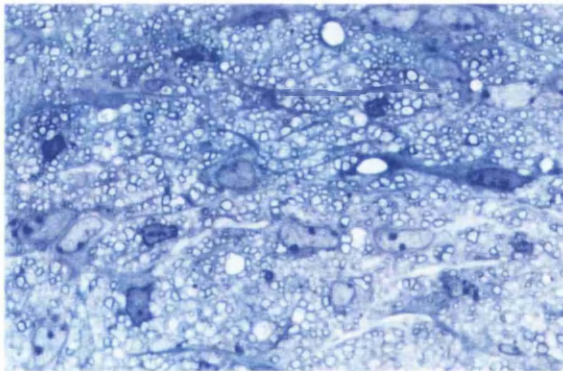
Dysmyelination and demyelination in homozygous mice



(i)



(ii)

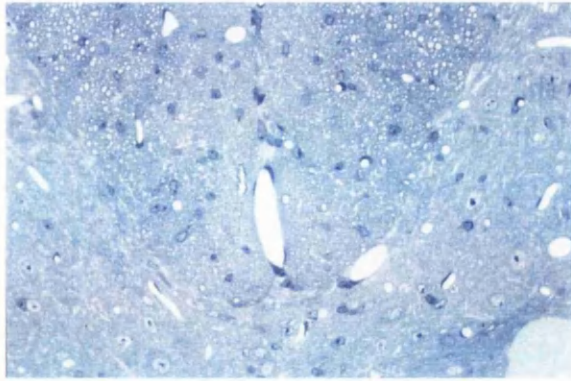


(iii)

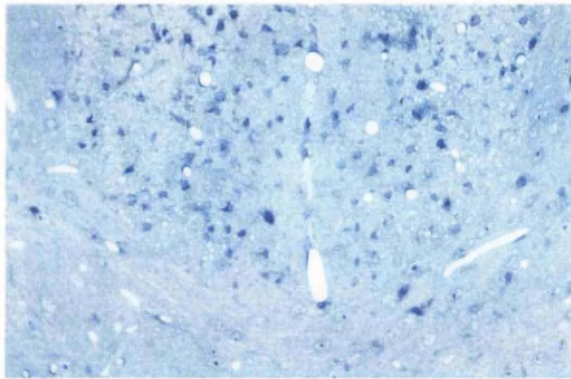
a)

Figure 32. Abnormalities of myelination in homozygous #66 and #72 mice. a) P20 optic nerve (i) wild type (ii) #66 (iii) #72. Optic nerves from homozygous mice are hypomyelinated, with thin myelin sheaths, amyelinated fibres and a gliosis. These abnormalities are more profound in #66 mice (all x990).

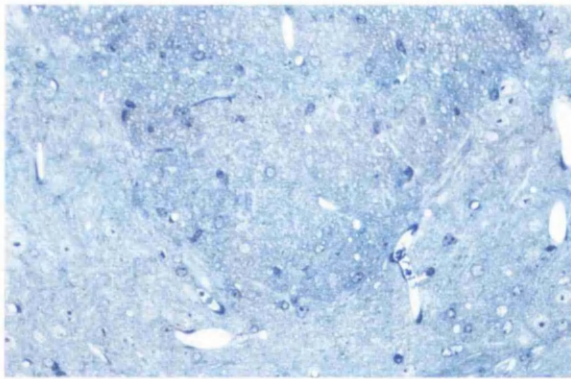
Dysmyelination and demyelination in homozygous mice



(i)



(ii)

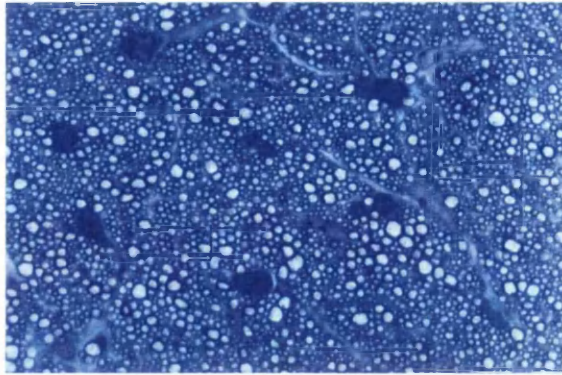


(iii)

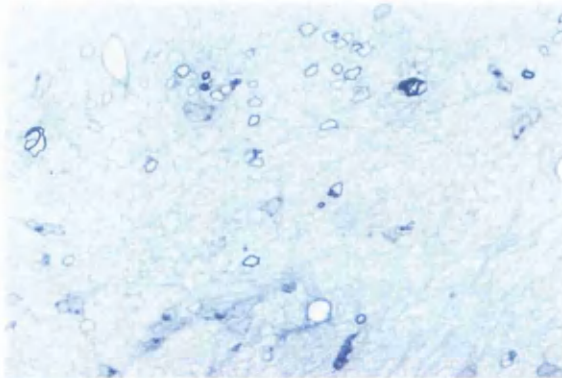
b)

Figure 32 (continued). Abnormalities of myelination in homozygous #66 and #72 mice. b) dorsal columns at P20 (i) wild type (ii) #66 (iii) #72. Both homozygous mice are hypomyelinated, though the degree varies between tracts and #66 mice are more profoundly affected (all x90).

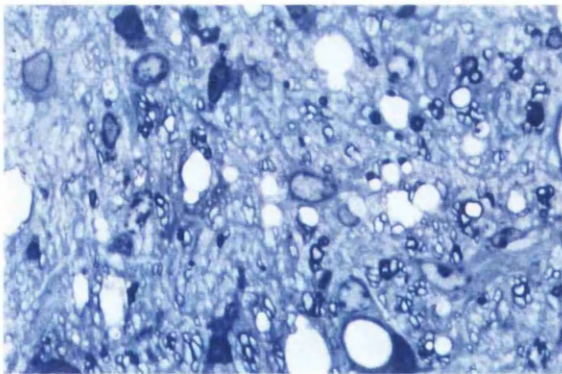
Dysmyelination and demyelination in homozygous mice



(i)



(ii)

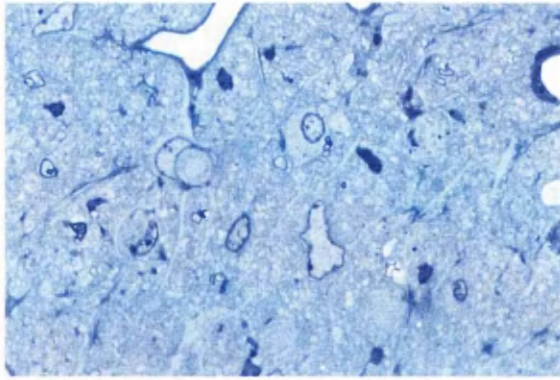


(iii)

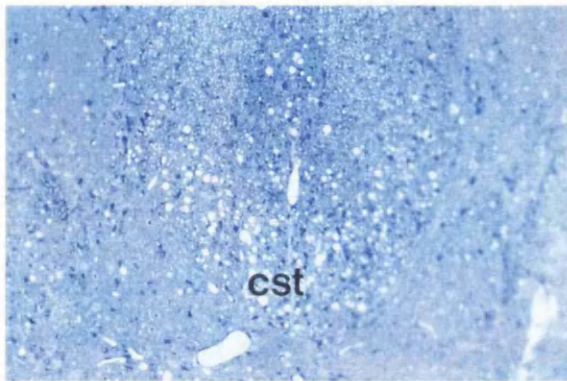
c)

Figure 32 (continued). Abnormalities of myelination in homozygous #66 and #72 mice. c) P60 optic nerve (i) wild type (ii) #66 (iii) #72. The optic nerves from both homozygous mice are profoundly hypomyelinated. Subjectively, in #72 optic nerve there is a reduction in the proportion of myelinated fibres and some myelin sheaths exhibit focal thickening and redundant myelin. #66 optic nerve remains profoundly hypomyelinated and myelin sheaths exhibit similar abnormalities to those observed in #72 mice (all x990).

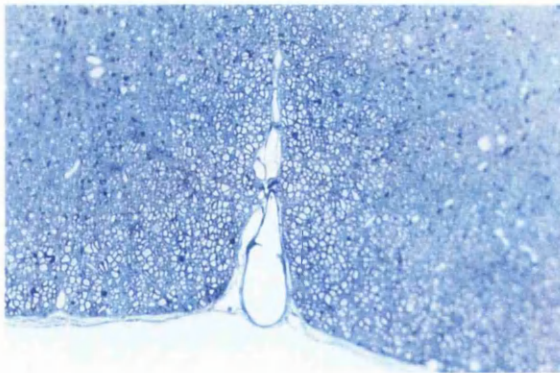
Dysmyelination and demyelination in homozygous mice



(i)



(ii)

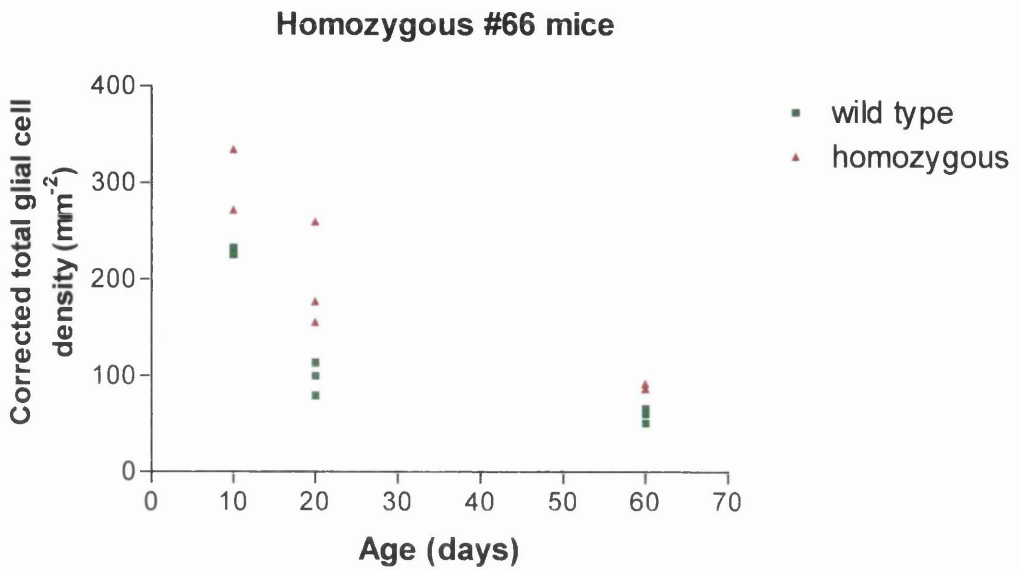


(iii)

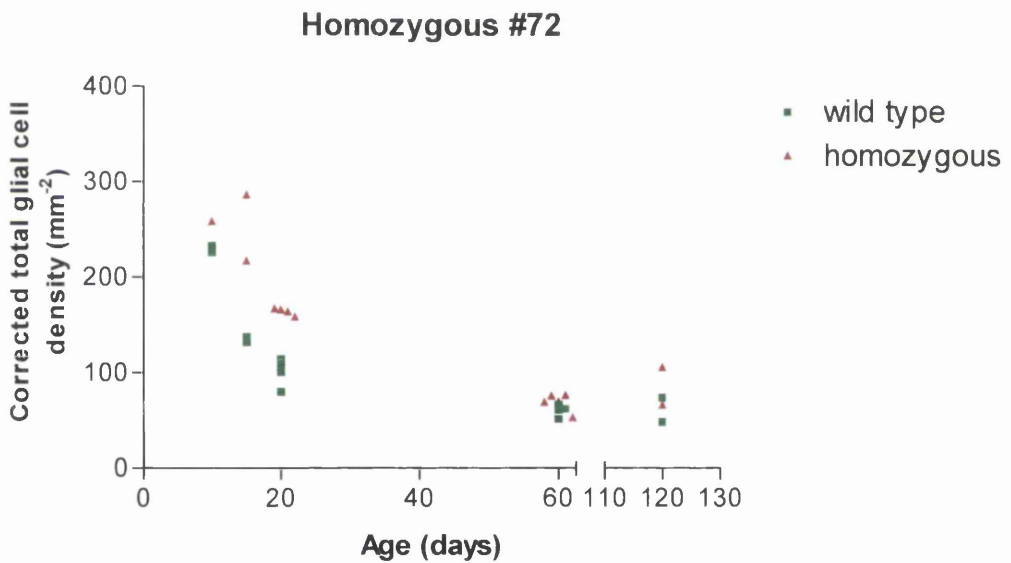
d)

Figure 32 (continued). Abnormalities of myelination in homozygous #66 and #72 mice. d) P120 homozygous #72 (i) optic nerve (x990) (ii) dorsal columns (x150) (iii) ventral columns (x150). At P120 optic nerve is demyelinated and the dorsal and ventral columns show demyelination, which is more profound in the dorsal columns. Pathology in the dorsal columns exhibits a tract specific nature (e.g. the corticospinal tracts (cst) are particularly affected).

Dysmyelination and demyelination in homozygous mice



a)

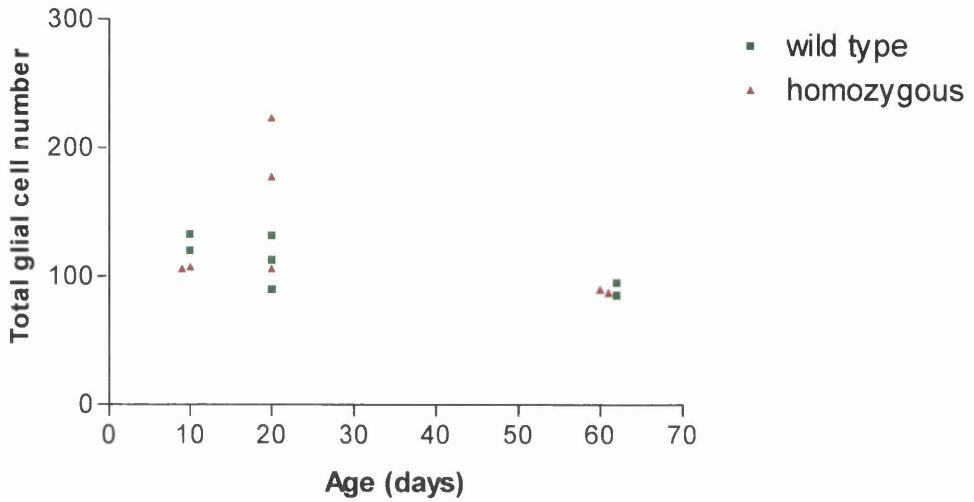


b)

Figure 33. Total glial cell density in homozygous #66 and # 72mice. a) #72; b) #66. The trend is for an increase in total glial cell density during myelination.

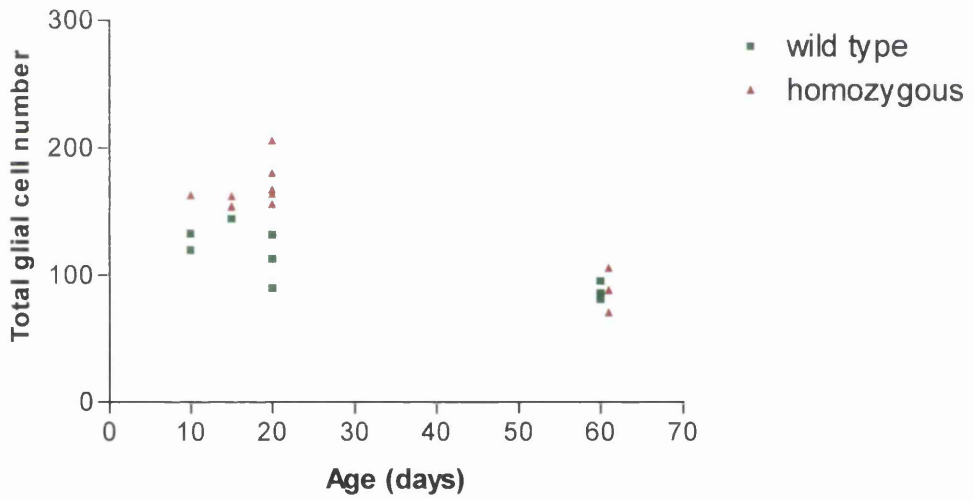
Dysmyelination and demyelination in homozygous mice

Homozygous #66



a)

Homozygous #72



b)

Figure 34. Total glial cell numbers in white matter in homozygous #66 and #72 mice. a) #72; b) #66.

Dysmyelination and demyelination in homozygous mice

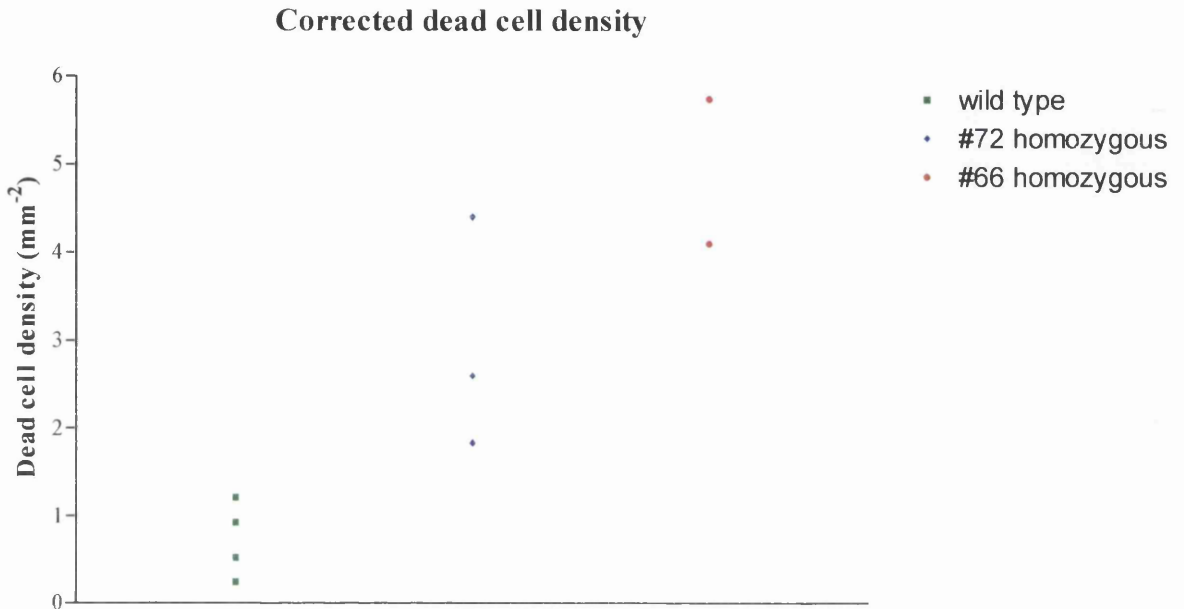
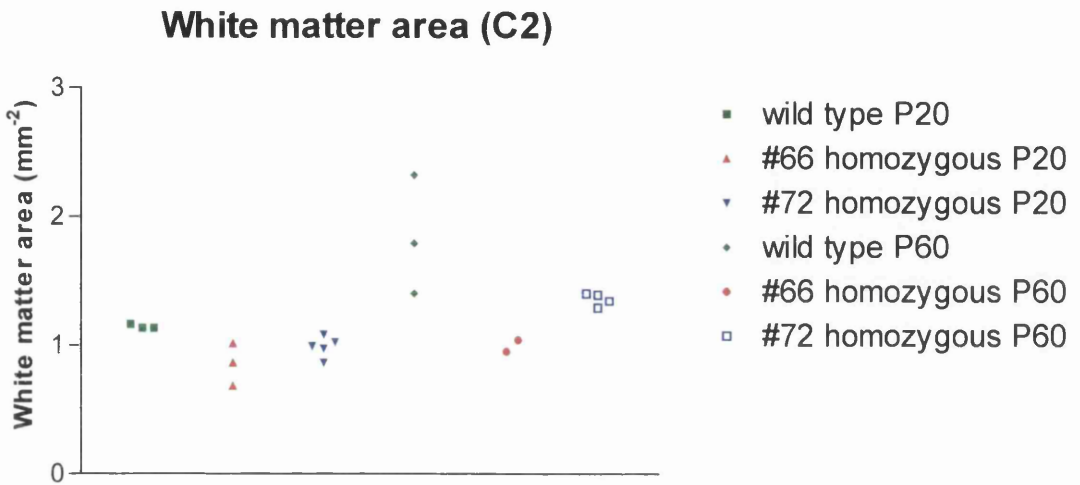
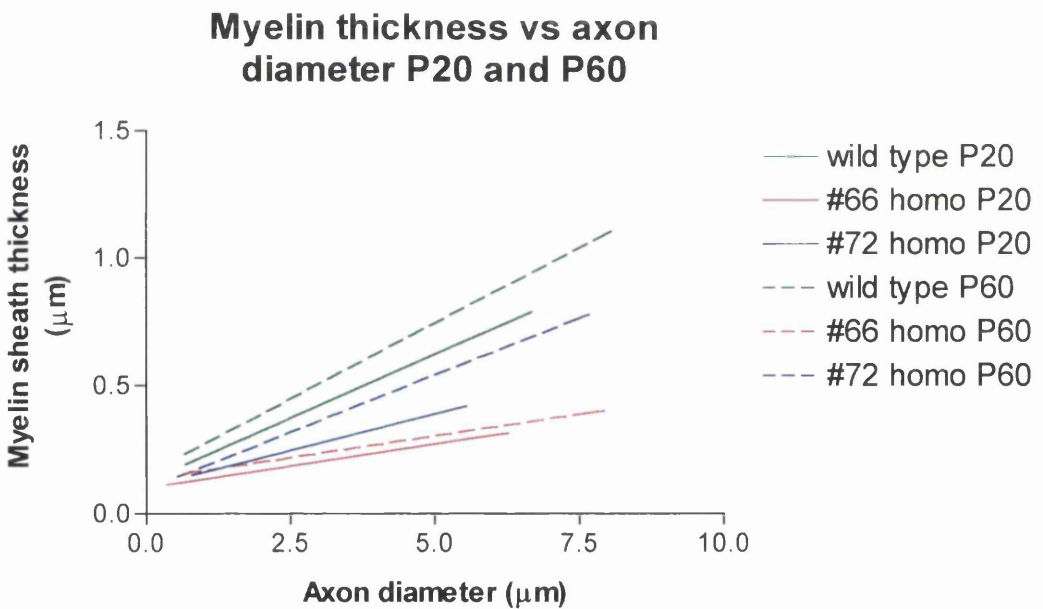


Figure 35. Estimates of dead cells in cervical cords of #66 and #72 homozygous mice at P20.

Dysmyelination and demyelination in homozygous mice



a)



b)

Figure 36. Myelin morphometry in #66 and #72 homozygous mice at P20 and P60. a) white matter area; b) myelin sheath thickness.

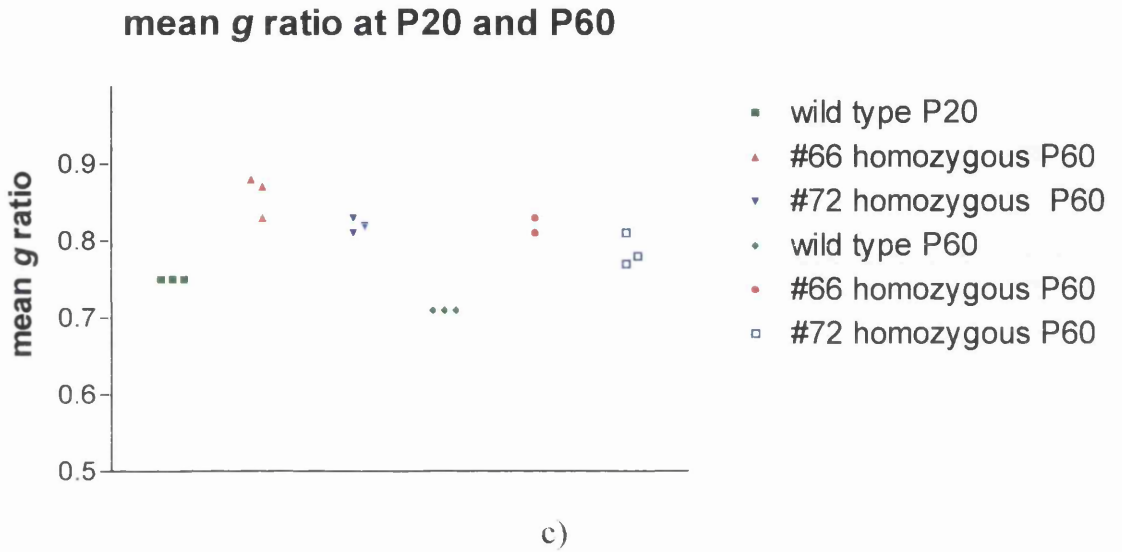


Figure 36 (continued). Myelin morphometry in #66 and #72 homozygous mice at P20 and P60. c) mean g ratio at P20 and P60.

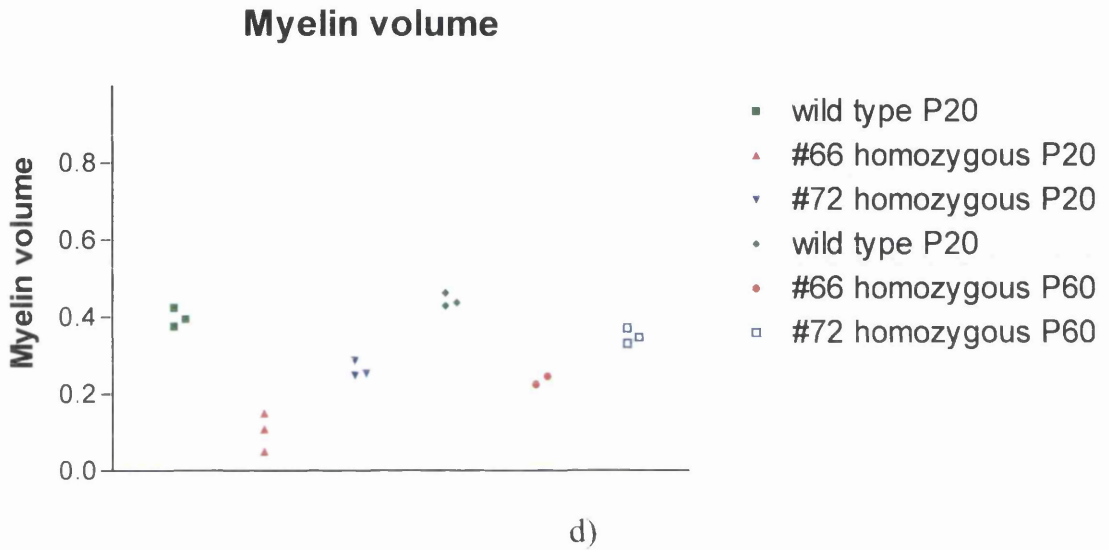


Figure 36 (continued). Myelin morphometry in #66 and #72 homozygous mice at P20 and P60. d) myelin volume.

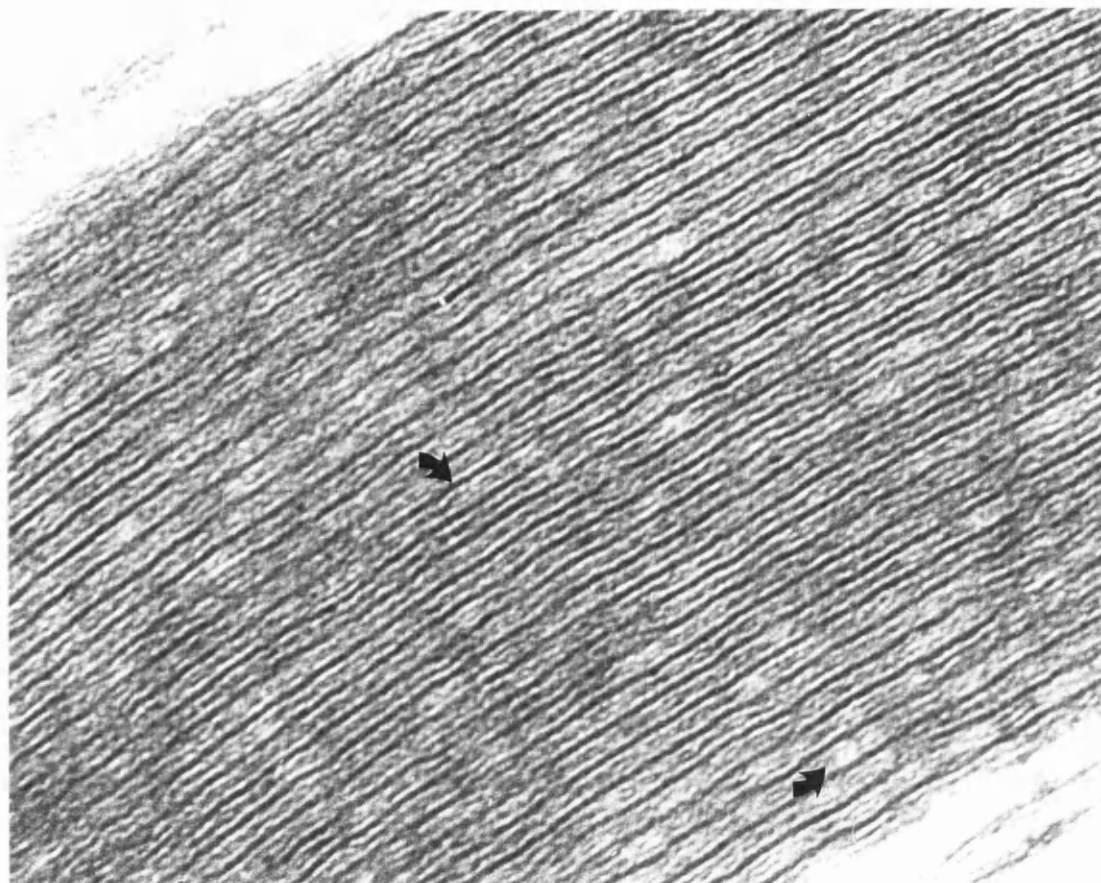
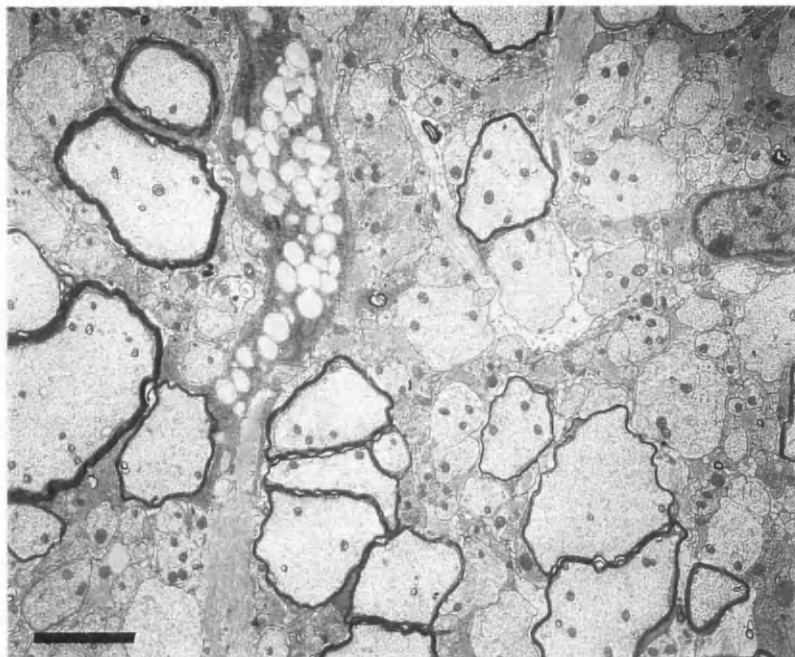
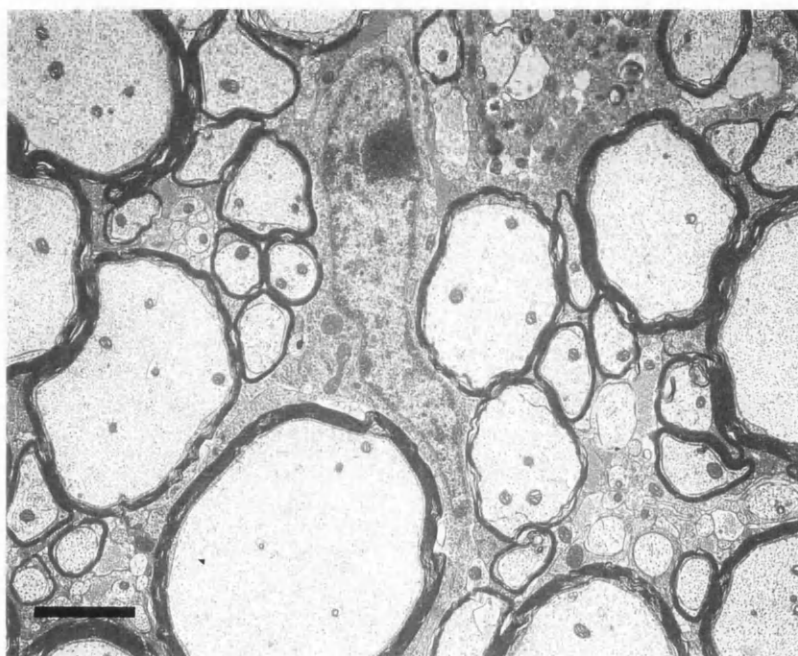


Figure 37. Electronmicrograph of the ultrastructure of myelin from the ventral columns of a homozygous #72 mouse. There is a compacted lamellar structure with the MDL (↖) and the double IPL (↗) (scale bar 0.1 μ m)

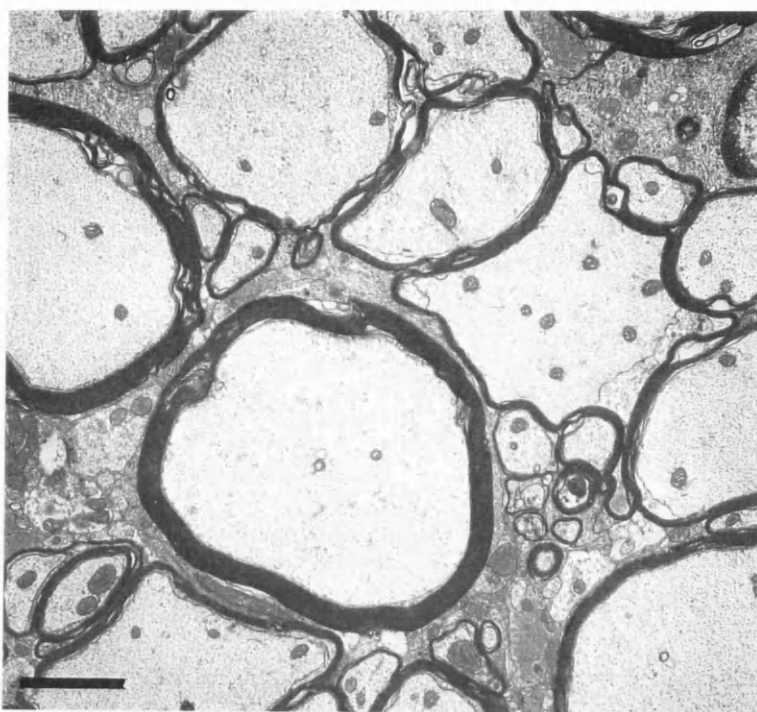


(a)

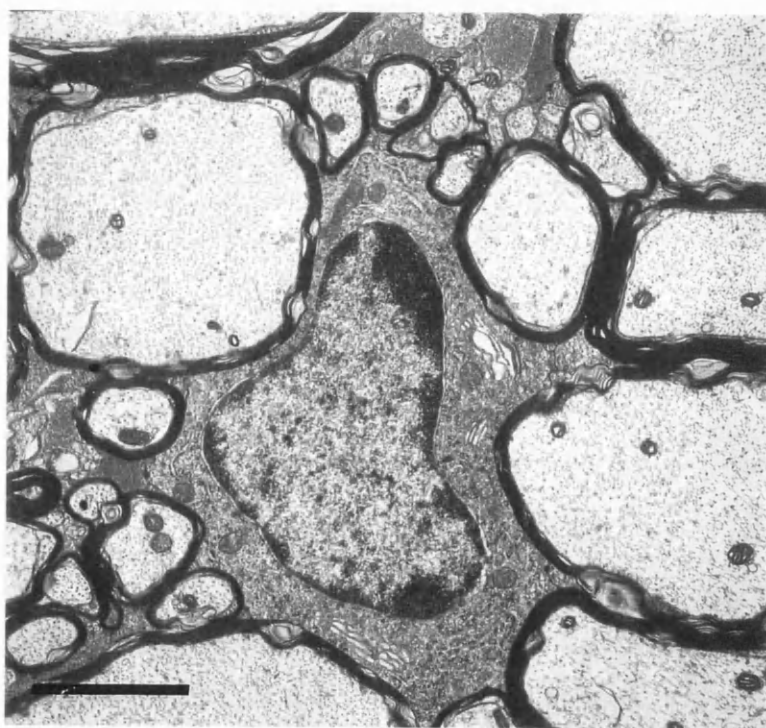


(b)

Figure 38. Electronmicrograph of spinal cord white matter at P20: (a) homozygous #66 (scale bar $2\mu\text{m}$) , (b) homozygous #72 (scale bar $2\mu\text{m}$). The majority of axons in the #66 homozygous mouse are amyelinated with any myelin sheaths being thin whilst in homozygous #72 mice the majority of axons are myelinated, albeit with sheaths of reduced thickness. A microglial cell (mc) in the homozygous #66 contains many phagosomes, contents unknown.

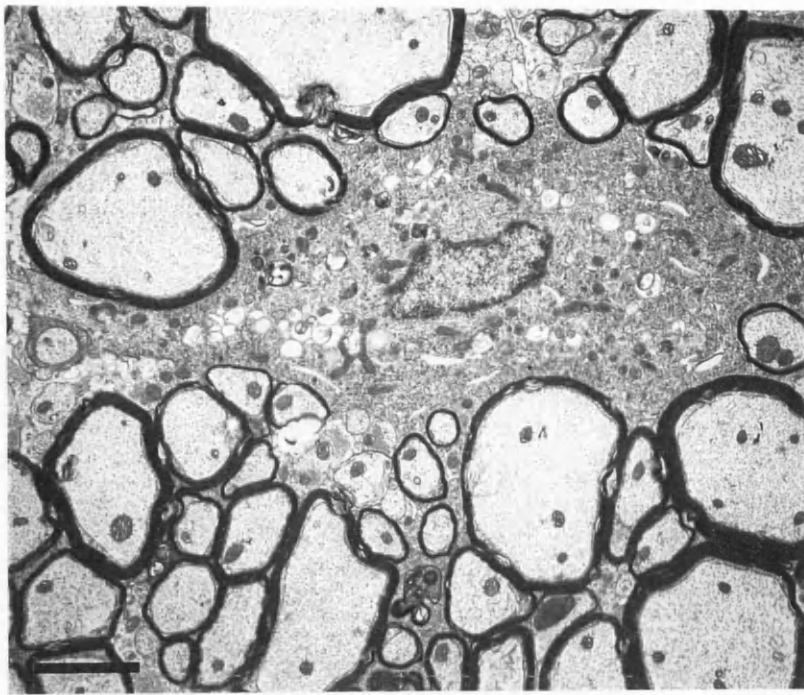


(a)

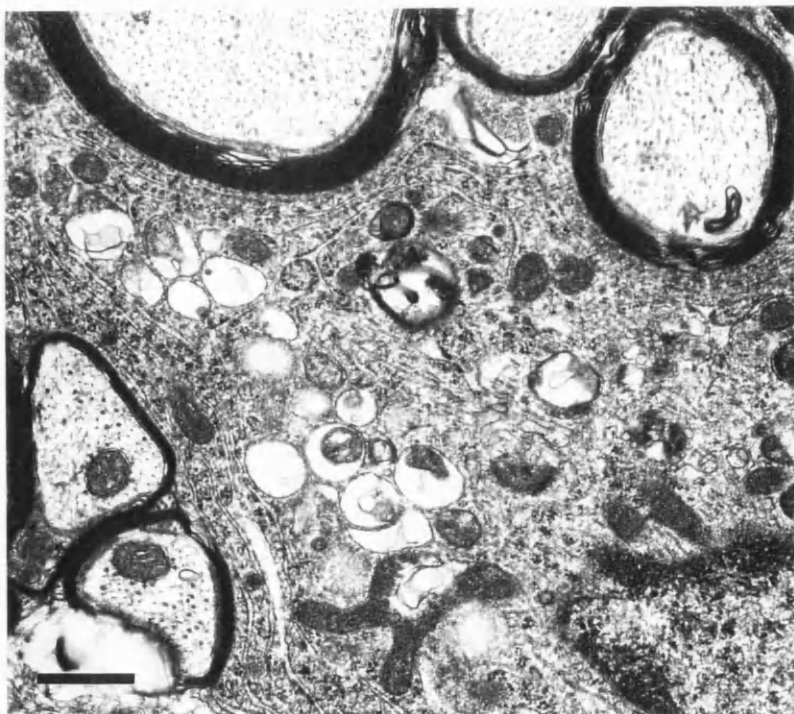


(b)

Figure 39. Electronmicrographs of spinal cord white matter at P60 in #72 homozygous mice. a) the majority of axons are myelinated though myelin is thin. The degree of hypomyelination is variable between fibres (scale bar $2\mu\text{m}$); b) the cytoplasm of some oligodendrocytes appears normal (scale bar $1\mu\text{m}$).

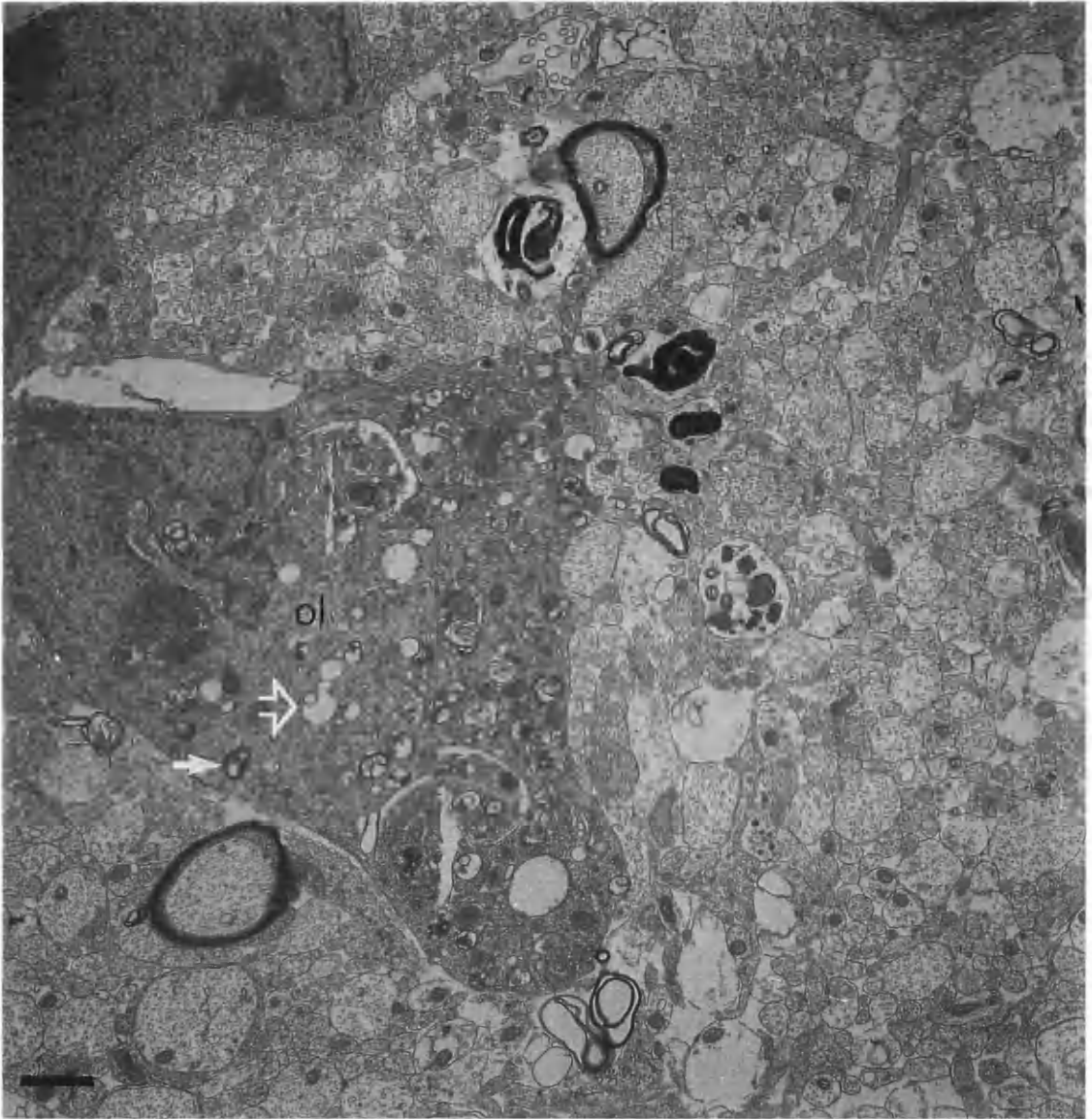


(c)



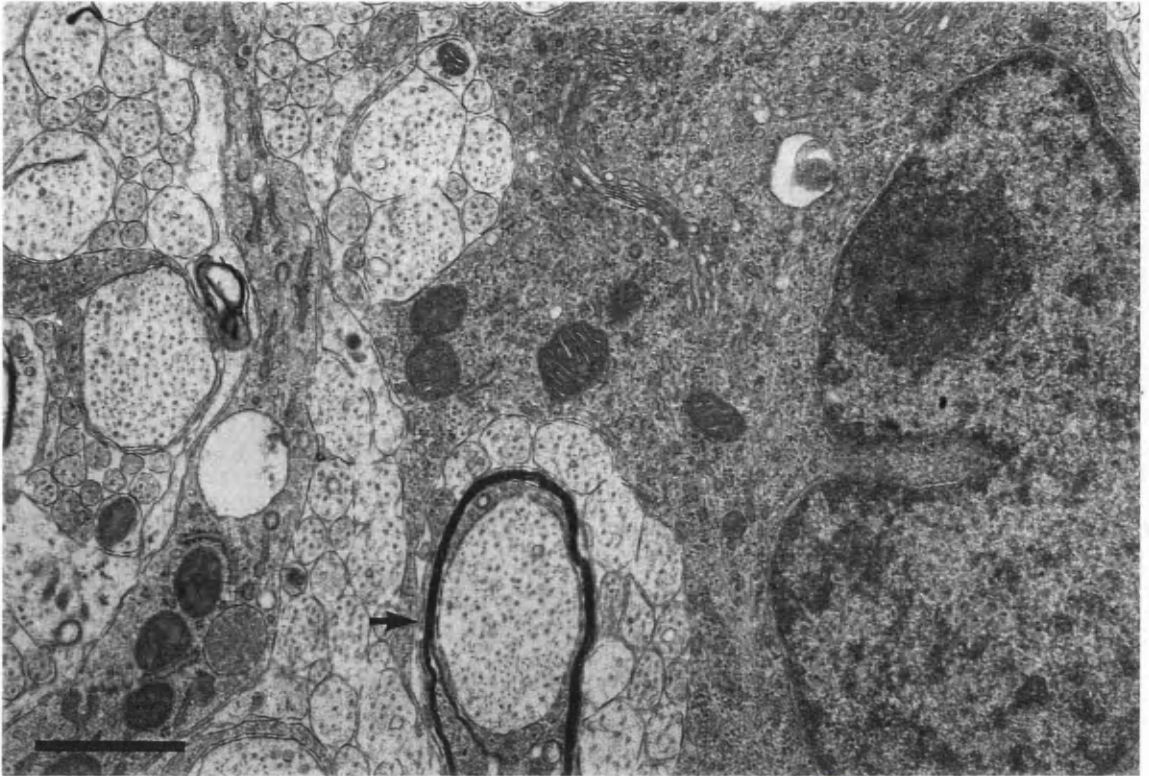
(d)

Figure 39 (continued). Electronmicrograph of spinal cord white matter at P60 in #72 homozygous mouse. c) other oligodendrocytes in the same area of white matter have vacuolar structures in the cytoplasm (scale bar $2\mu\text{m}$) d) same oligodendrocyte at a higher magnification (scale bar $1\mu\text{m}$).



(a)

Figure 40. Electronmicrograph of spinal cord white matter of a homozygous #66 (P3) mouse (c.f. wild type Figure 41, page 165). a) Occasional myelin sheaths are present. The cytoplasm of an oligodendrocyte (ol) is striking for the numerous vesicular bodies present. These appear to be of two types: relatively thick walled structures (↔), which probably represent autophagic vacuoles, and thinner walled structures, the nature of which is unknown (↪) (scale bar 1 μ m).



(b)

Figure 40 (continued). Electronmicrograph of spinal cord white matter of a homozygous #66 (P3) mouse. b) this higher magnification electronmicrograph shows an area of cytoplasm that is relatively unaffected. The RER is relatively normal. An oligodendrocyte process is in the early stages of wrapping an axon (→) (scale bar 1 μ m).

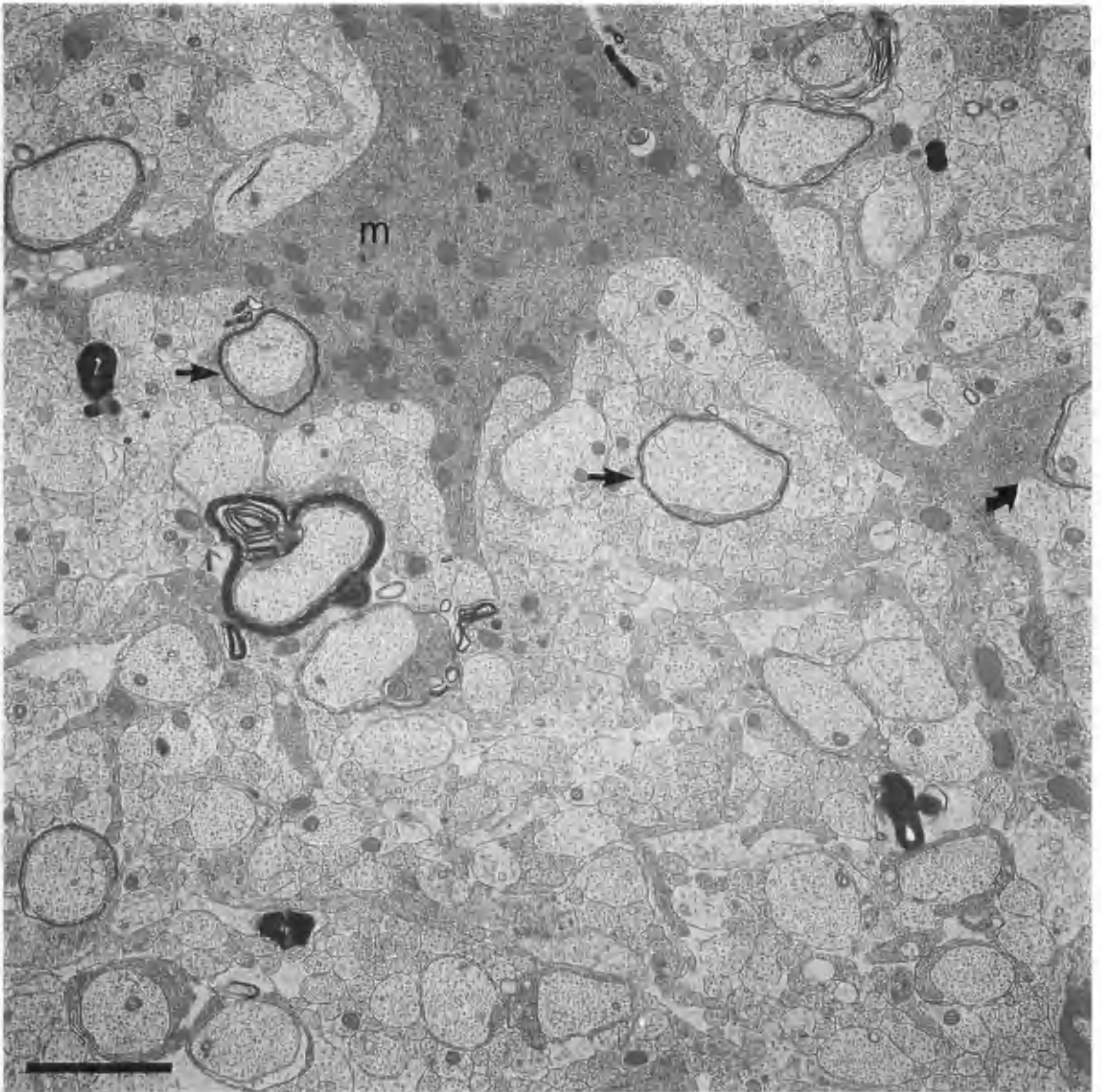
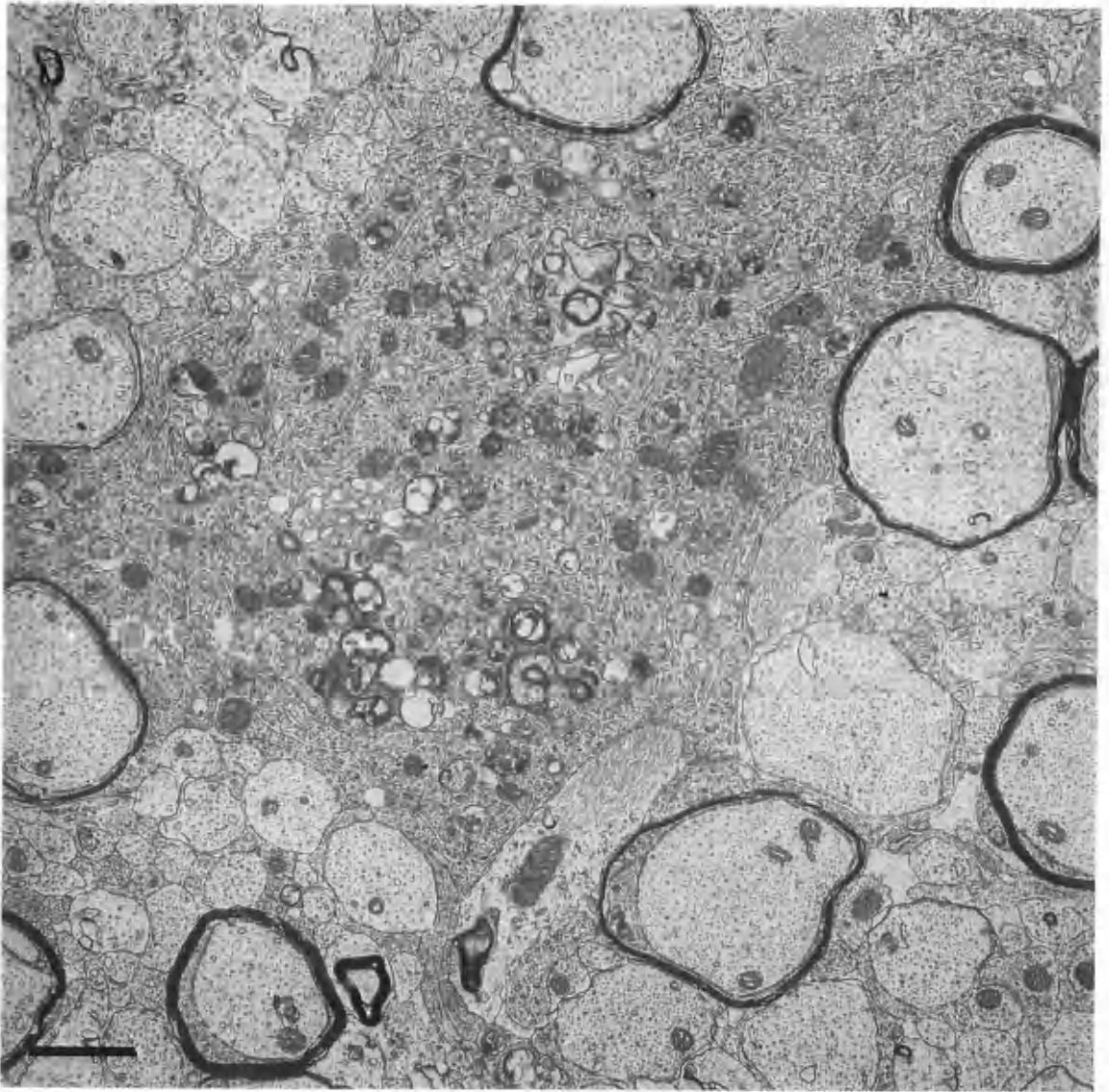
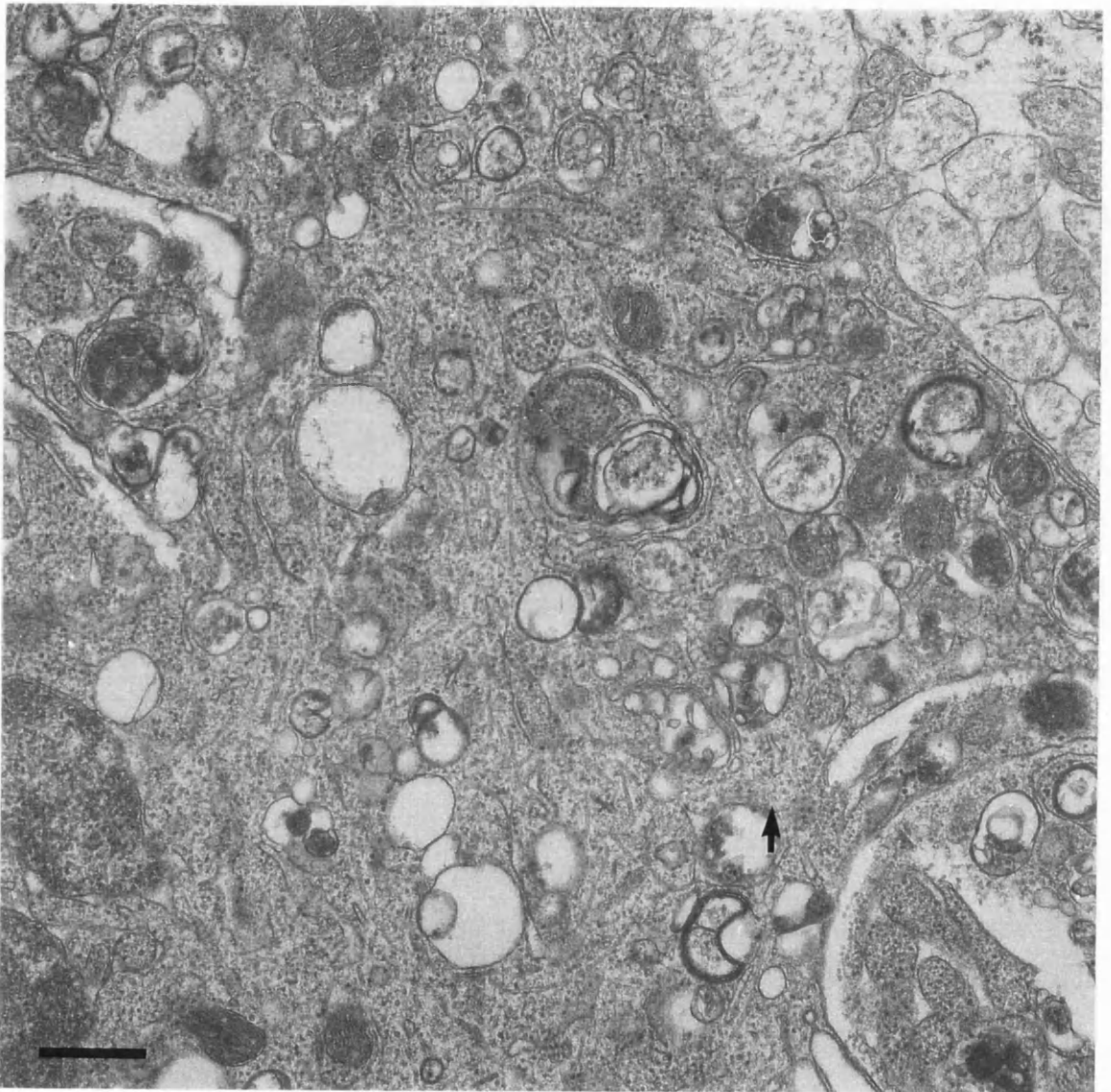


Figure 41. Electronmicrograph of spinal cord white matter of a wild type (P3) mouse (scale bar 1 μ m). Thin myelin sheaths are present (↔) though the majority of axons are naked. Oligodendrocyte processes are wrapping axons (↗). The relatively homogeneous cytoplasm contains some structures (e.g. mitochondria (m)).



(a)

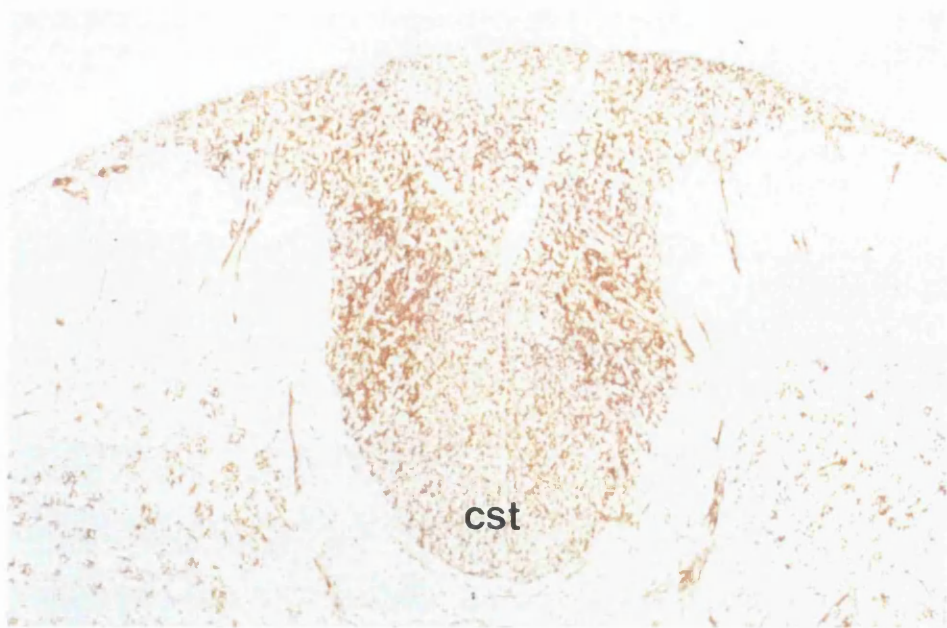
Figure 42. Ultrastructure of developing (P10) homozygous #66 oligodendrocyte and myelin. a) thin myelin sheaths are present but the majority of axons remain naked. The vacuolar structures in oligodendrocyte cytoplasm noted at P3 are still present (scale bar 1 μ m).



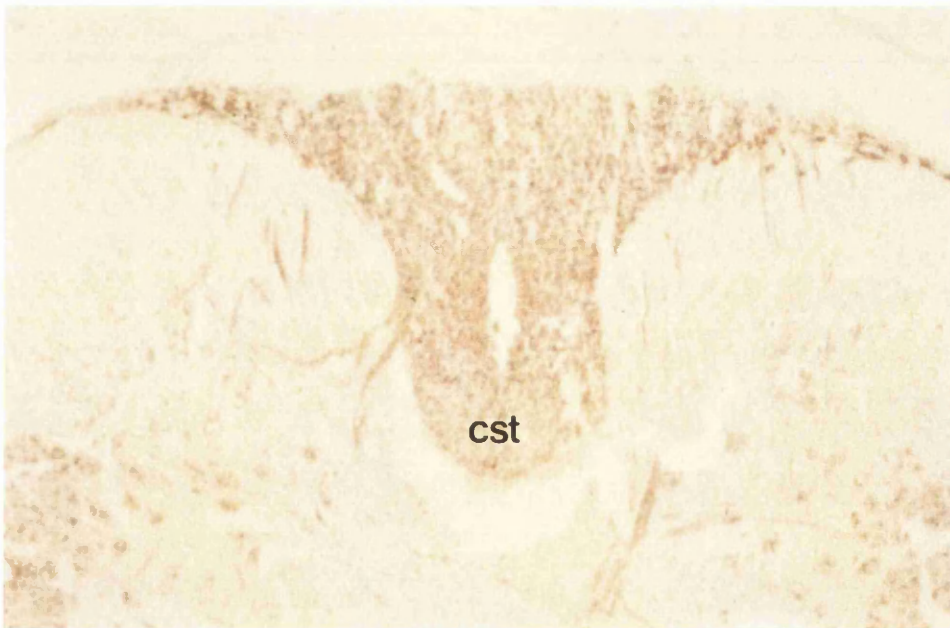
(b)

Figure 42 (continued). Ultrastructure of developing (P10) homozygous #66 oligodendrocyte and myelin. b) higher magnification of the cytoplasm shows the cisternal structure of the RER is severely disrupted with the ribosomes showing displacement (→) (scale bar 0.5 μ m).

Dysmyelination and demyelination in homozygous mice

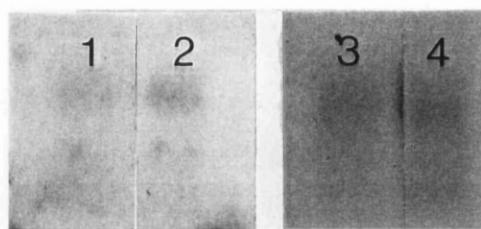


a)

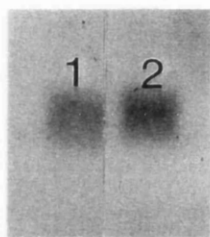


b)

Figure 43. MBP immunostaining showing reduced immunoreactivity at P60 in thoracic cord reflecting the reduced amount of myelin present. a) homozygous #66 (P60); b) homozygous #72 (P70). The reduced immunostaining is particularly evident in tracts containing predominantly small fibres e.g. the corticospinal tracts (cst) (both x75).



a)



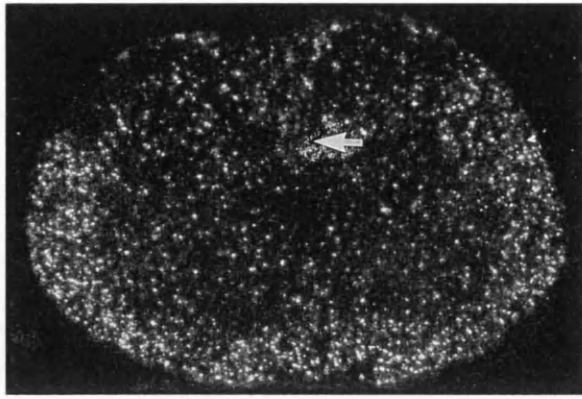
b)



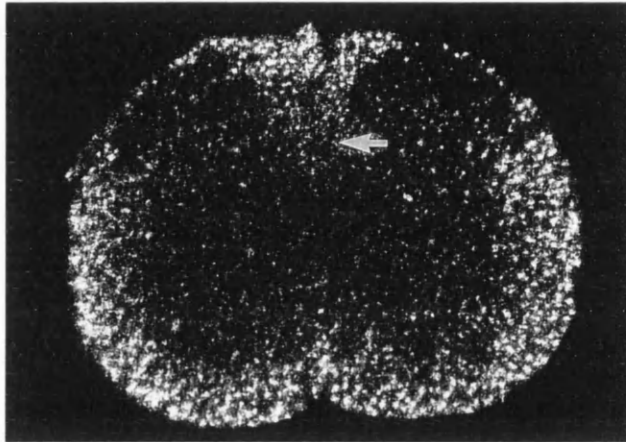
c)

Figure 44. Transcription of the *Plp* (PLP-1) and *Mobp* genes in homozygous #66 and #72 mice at P20. a) northern hybridisation with PLP-1: #66 lane 1 wild type, lane 2 homozygote, #72 lane 3 wild type, lane 4 homozygote; b) northern hybridisation with MOBP-1: #72 lane 1 wild type, lane 2 homozygote; c) RT-PCR for *Plp: Dm20* ratios (i) primers *Plp* gene exon 2→4 P20 lane 1 wild type, lane 2 #66, lane 3 #72 P60 lane 4 wild type, lane 5 #66 and lane 6 #72 (ii) primers cyclophilin lanes 1-6 as above.

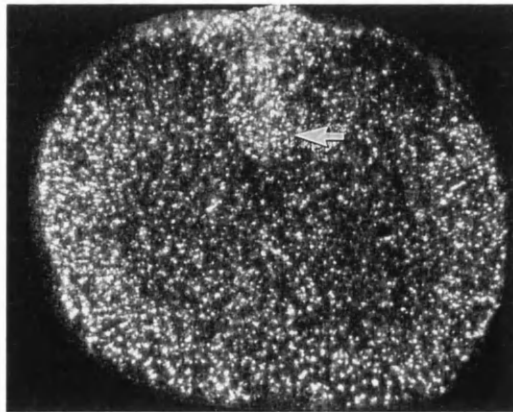
Dysmyelination and demyelination in homozygous mice



a)



b)



c)

Figure 45. *In-situ* hybridisation with PLP-1 of cervical cord from homozygous #66 and #72 mice and wild type at P60. a) #66; b) #72; c) wild type (all x30). The numbers of positive cells appear similar to wild type in both groups of transgenic mice, with the exception of the spinocerebellar tracts, where the number of positive cells appears to be reduced (→), and the dorsal columns in general in #66 mice.

6. Expression of *P/p* transgenes in the peripheral nervous system

6.1 Background

The compact myelin of the central and peripheral nervous systems share many features but differ in a number of respects, including their protein composition. P₀, the major constituent protein of PNS myelin is absent from the CNS. Although PLP and DM20 are present in Schwann cells it is generally accepted they are not incorporated into PNS myelin (1.2.1.2 Comparison of CNS and PNS myelin page 4). It is known, however, that the *Plp* gene is both transcribed and translated in NMFSC and MFSC with the *Dm20* mRNA being the dominant message isoform (1.2.3.3 Expression of the *Plp* gene in the PNS page 23). Immunocytochemistry demonstrates the presence of protein in the paranodes and Schmidt-Lanterman incisures of both the MFSC and NMFSC. Differential staining with antibodies recognising both polypeptides or only PLP, suggest that DM20 is present in all these locations. PLP staining appears restricted to the perinuclear region of the MFSCs and is absent from NMFSCs (Griffiths *et al.*, 1995). PLP and/or DM20 proteins have, however, been demonstrated in the peripheral myelin of other genera (see 1.2.2.1.1 Phylogenetic evolution of the *Plp* gene page 13) and both have been observed to co-localise with the P₀ (PLP in amphibia and DM20 in bony fish). In evolutionary terms PLP/DM20 appears to have replaced P₀ in the CNS but not in the PNS. It has been proposed that the lack of PLP/DM20 in the myelin of mammalian PNS is due to specific exclusion by Schwann cells (Puckett *et al.*, 1987). It has recently reported that the PLP/DM20 protein isoforms are present in normal rabbit PNS myelin (Tosic *et al.*, 1996).

The function of the *Plp* gene products in the PNS is unknown, and thus it is uncertain whether their transcription underlies a specific function or represents an evolutionary legacy. Studies on the regulation of the *Plp* gene in the PNS suggest that the gene is uncoupled from the co-ordinated expression of the PNS myelin genes (Dickinson, 1995; Kamholz *et al.*, 1992; Stahl *et al.*, 1990). The use of an alternative transcription start site compared to the CNS is consistent with a different cohort of *trans* factors in the Schwann cell, though the regulatory significance of this is uncertain (Kamholz *et al.*, 1992). The apparent normality of the PNS in *Plp* gene mutants and *Plp* gene knockout mice is not suggestive of a pivotal function for this gene in the development and function of PNS myelin.

The work presented in this chapter was stimulated by the unexpected observation of positive immunostaining for the PLP/DM20 protein isoforms in the ventral nerve roots of spinal cord from homozygous #72 mice.

6.2 Aims

The initial aim was to confirm that the PLP/DM20 immunostaining observed in the PNS of the #72 homozygous mice was due to the insertion of the PLP/DM20 protein isoforms into the peripheral myelin and that it was influenced by Schwann cells.

The availability of a range of *Plp* transgenes (#72, #66, *Plptg1* and *Dm20tg2*) afforded the possibility of examining the behaviour of constructs encoding for the two proteins both in conjunction and individually in the PNS environment. To facilitate this a *Plp⁰* background was used as the level of endogenous *Plp* gene activity is low and the gene transcripts and products can be distinguished from full length gene products. The antibodies directed against the PLP-CT do not react with *Plp⁰* proteins.

6.3 Methods

Double immunostaining was used to assess whether the PLP polypeptides co-localise with P₀, the major protein in PNS myelin. With the lack of an antibody specific to DM20 its presence or absence is inferred from the differential pattern of staining with the PLP-CT and PLP-specific antibodies.

Transplantation techniques were used to confirm that incorporation of the PLP/DM20 protein isoforms into PNS myelin is a property of #72 homozygous MFSC rather than a result of axonal signalling. A graft of sciatic nerve anastomosed in a transected nerve serves as a scaffold for the regrowing proximal axons which are myelinated by the transplanted Schwann cells (Aguayo *et al.*, 1977). Nude mice are used as recipients to minimise the problems associated with tissue rejection.

RT-PCR technology was chosen to investigate the transcription of transgenes as it is possible to examine the ratios of *Plp* and *Dm20* mRNA as well as the overall level of transcription. An approach that would require the breeding of smaller numbers of mice than would be required for the northern hybridisation approach. An alternative technique would have been an RNase protection assay, which as a direct assay of message levels (Mason *et al.*, 1993). Experiments were designed to confirm

transgene transcription and to investigate the relative levels of transcription in the #72 hemi and homozygous mice in comparison to their wild type littermates.

Electron microscopy was used to ascertain whether the incorporation of the PLP/DM20 protein isoforms altered the ultrastructure of the peripheral myelin.

6.3.1 Mouse breeding

The breeding and identification of animals for these experiments is described in 3 Genotyping and breeding of transgenic mice page 76. Mice were killed at 21 days, as the *Plp^{lP}* mutation is lethal by about 4 to 5 weeks, with the exception of nude mouse transplant recipients (see below).

6.3.2 Immunocytochemistry

Tissues were harvested and fixed as described in 2.1 Tissue fixation and processing (page 43). Tissues for extraction of RNA were removed immediately into liquid nitrogen.

Both frozen and paraffin wax sections of cervical cord, sciatic nerve and cauda equina were used for immunocytochemistry. Immunostaining for myelin is better visualised using paraffin wax sections although cytoplasmic staining around myelin is lost using such preparations. Cytoplasmic immunoreactivity is retained in frozen tissue sometimes making it difficult to distinguish from staining of the myelin. For this reason both methods were used to determine the localisation of PLP/DM20.

Sciatic nerve preparations were teased in PBS to separate fibres and facilitate visualisation of the distribution of immunoreactivity along fibres (Griffiths *et al.*, 1995).

Tissues were immunostained for PLP-CT, PLP-specific, P₀ and SMI-31 antibodies using indirect Immunofluorescence. Techniques are described in 2.9.1.2 Immunofluorescence (page 69) and the details of individual antibodies are given in Table 4 (page 71). Double staining of tissues was undertaken to demonstrate localisation of the PLP/DM20 protein isoforms relative to axonal or Schwann cell components.

6.3.3 Transplant studies

Donor homozygous #72 mice were killed and the sciatic nerves removed into sterile PBS. Recipient nude mice were anaesthetised with halothane, the sciatic nerve transected, and a 5mm portion of #72 sciatic was anastomosed into the gap. Ethilon

(14/0) sutures were used to maintain the graft's position and for later orientation. Mice were killed 60 days following transplantation and perfused with paraformaldehyde (2.1 Tissue fixation and processing page 43). Both sciatic nerves were removed and embedded in paraffin wax. A control experiment was performed using a non-transgenic littermate as the donor of sciatic nerve.

6.3.4 Ultrastructure of myelin

Sciatic nerve and lumbar nerve root were removed from 60 day old homozygous #72 mice perfused with Karnovsky's modified fixative and the tissue prepared for EM (2.1 Tissue fixation and processing page 43) to examine the morphology of myelin and Schwann cells.

6.3.5 Transcript analysis by RT-PCR

The ambitions of the RT-PCR experiments were two-fold: a) to confirm the transcription of the transgenes in *Plp^{ΔP}* sciatic nerves; b) to examine the transcriptional output from the combined endogenous and exogenous *Plp* genes in wild type mice complemented with genomic transgenes.

The low yields of RNA from murine sciatic nerves necessitated the pooling of tissue, usually 2-8 pairs of nerves. The preparation of RNA is described in 2.5.1.2 The isolation and storage of RNA page 49. The preparation of cDNA is described in 2.5.4.1.2 cDNA preparation, page 55.

6.3.5.1 Identifying transgene activity on a *Plp^{ΔP}* background

To highlight transgene expression on the *Plp^{ΔP}* background required development of a primer pair that would produce a product exclusively from transgene-derived message. In experiments described in previous chapters the *Plp:Dm20* ratios were examined using a primer pair spanning exons 2→4. which also produce product from a *Plp^{ΔP}* cDNA. As exon 5 is not transcribed in *Plp^{ΔP}* (see page 26) a primer pair was designed with one primer upstream of exon 3 (in exon 2) with the reverse primer within exon 5 (2.5.4.1.1 Design of novel PCR primers, page 55).

6.3.5.2 Semi-quantitative RT-PCR of #72 mice

These experiments were undertaken on the wild type background at 21 days. The exon 2→4 primers were used for this experiment (2.5.4.1.3 RT-PCR page 56).

6.4 Results

6.4.1 Immunocytochemistry

The myelin of wild type peripheral nerves immunostains strongly for P₀ but not with PLP-CT or PLP-specific antibodies. In teased sciatic nerve preparations there is staining of the SLIs and paranodes of MFSC and the cytoplasm of NMFSC with the PLP-CT antibody. This distribution of PLP/DM20 and P₀ immunostaining in wild type mice is illustrated in Figure 46 (pages 181-182). It has been shown previously that staining of the cytoplasmic components with PLP-specific antibody is weak, and limited to the perinuclear region, and that the predominant protein isoform in Schwann cells is DM20 (Griffiths *et al.*, 1995). In marked contrast to wild type, the peripheral myelin of homozygous #72 mice stains strongly with PLP-CT and PLP-specific antibodies and co-localises with P₀ staining (Figure 47, page 183). Additionally, the cytoplasmic staining with the PLP-CT antibody is retained in the transgenic mice

When expressed on a *Plp1P* background the genomic transgenes (#66 and #72) produce an appearance similar to that in homozygous #72 animals with PLP/DM20 immunostaining co-localising with P₀ and strong immunoreactivity in the cytoplasmic regions of the MFSC and NMFSC (Figure 48, pages 184-186). In contrast, expression of the *Plptg1* in the *Plp1P* background results in a more uniform staining of the myelinated fibres making the cytoplasmic domains less prominent. Paraffin wax sections immunostained with PLP-CT and PLP-specific antibodies indicate that it is the PLP protein isoform that is present in the myelin sheath (Figure 49, page 187). Complementation with the *Dm20tg2* transgene results in immunostaining of the cytoplasmic domains of myelinated fibres only (Figure 48, pages 184-186), with no reactivity for the DM20 protein isoform in myelin (Figure 49, page 187).

6.4.2 Nerve transplantation study

Grafts from transgenic or wild type mice anastomosed into the sciatic nerves of nude mice were readily reinnervated by host axons resulting in myelination of the graft and distal stump. When the donor Schwann cells are derived from a #72 homozygous transgenic mouse the myelin in the graft immunostains with the PLP-CT antibody, whereas the distal stump remains negative. This confirms that the incorporation of the PLP/DM20 protein isoforms into myelin is a function of the transgenic Schwann cells (Figure 50, page 188).

6.4.3 Morphology

The ultrastructure of peripheral myelin containing PLP, from #72 mice shows no differences from wild type at 60 days (Figure 51 page 189). The IPL and MDL are normally compacted and subjectively the periodicity of the IPL and MDL appeared unaltered. The relationship between myelin thickness and axon diameter appeared to be unaltered. No evidence of abnormality was detected in the Golgi apparatus or RER of the Schwann cells from transgenic animals.

6.4.4 RT-PCR

The RT-PCR data is presented in Figure 52, page 190.

The dominance of the *Dm20* message, in wild type sciatic nerve, is maintained in sciatic tissue from #72 transgenic mice and when this transgene is expressed on the *Plp^{flp}* background. Semi-quantitative RT-PCR demonstrates that the incorporation of the PLP protein into peripheral myelin of #72 homozygous and hemizygous mice is associated with increased levels of *Plp* gene transcript, though the *Plp:Dm20* ratio is probably unaltered. The levels of transcription appear similar for the hemizygous and homozygous states. The level of transcription of the *P0* gene appears unaltered in the #72 transgenic mice. The *Plptg1* and *Dm20tg2* transgenes were transcribed in the sciatic nerves of *Plp^{flp}/Y* mice producing the single expected message isoform.

6.5 Discussion

The consensus that the PLP/DM20 protein isoforms are not present in PNS myelin stems from the inability to detect it immunocytochemically, both in tissue sections and by western blots. It is possible, however, that this methodology is insufficiently sensitive, as suggested by the work of Agrawal and Agrawal (1991) where a radioactive labelling technique identified PLP/DM20 in rat PNS myelin. However, this work has not been corroborated. It is also possible that different species may incorporate the polypeptides to different levels, thus producing further variation in results.

These studies confirm the original supposition that mice transgenic for the #72 transgene incorporate PLP and/or DM20 in the myelin of their PNS. The implication from the experiments using transgenes expressing only a single isoform on the *Plp^{flp}* background, is that PLP is incorporated into myelin. This challenges the current consensus that products of the *Plp* gene are found only in the cytoplasmic domains of Schwann cells.

The assertion that the PLP protein isoform is incorporated into the peripheral myelin is based on co-localisation of immunoreactivity with P₀, known to be present in PNS myelin. The orientation of PLP within the myelin membrane is unknown but the preservation of immunoreactivity suggests that certain epitopes are preserved. Exact localisation of PLP within the myelin structure would require more detailed analysis, a potential technique being immunogold staining and examination by electronmicroscopy (Mastronardi *et al.*, 1993). It is known that both the PLP and DM20 protein isoforms can coexist with P₀ in PNS myelin in other genera, without disrupting the lamellar structure. My observations show that this is also possible in the mammalian PNS. P₀ is thought to be largely responsible for the periodicity of PNS myelin (Martini *et al.*, 1995; Giese *et al.*, 1992; Lemke *et al.*, 1988) and is proposed to have a larger extracellular domain than the PLP/DM20 protein isoforms. It is probable therefore that PLP is thus prevented from forming its normal structural associations by the increased distance between extracellular surfaces in PNS myelin.

The incorporation of the PLP protein isoform into PNS myelin appears to be a dose related phenomenon. The level of endogenous *Plp* gene transcription in the Schwann cells of #72 transgenic mice is augmented by the presence of transgenes resulting in increased total level of *Plp* transcripts. Thus the lack of the PLP protein isoform in normal PNS myelin appears to be as a result of low levels of production rather than specific exclusion. It may be that this is related to the use of a different transcription start site in the PNS, which is not part of the co-ordinated programme of myelination and is transcribed at a low level. Different *trans*-factors are operating in the Schwann cell compared to the oligodendrocyte. The incorporation of the PLP/DM20 protein isoforms into the myelin-like figures in P₀ knockout mice is interesting as it implies that the entry of these proteins into PNS myelin may also depend on the relative quantities of other myelin proteins. The disruption of the IPL in these P₀ deficient mice not only confirms the role of P₀ in the IPL of the PNS but suggests that the incorporated PLP/DM20 protein isoforms are either not present in sufficient quantities to replace the absent P₀ or are incapable of its functional replacement.

One of the potential problems with the expression of transgenes is activity outwith the normal tissue range leading to aberrant effects. The expression of these transgenes in the PNS would not be considered ectopic as this tissue normally expresses the *Plp* gene. In the CNS of hemizygous #72 mice, increased steady state levels of *Plp* message are associated with increases in the transcriptional levels of other myelin genes (see 4.3.8.1 Northern analysis, page 93). Interestingly, the levels of *P₀* gene transcription are unaltered in the transgenic PNS, which concurs with the

idea that in the PNS *Plp* gene transcription is uncoupled from the regulation of the other myelin genes (Griffiths *et al.*, 1995).

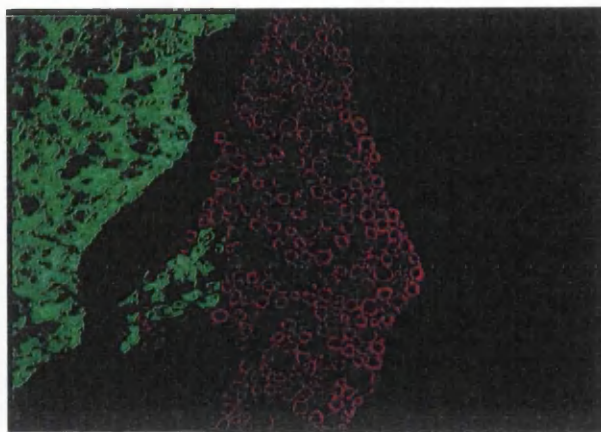
The expression of the genomic transgenes on the *Plp^Δ/Y* background with the consequent production of PLP/DM20 protein confirms that these transgenes are capable of altering the mutant phenotype. In the CNS the activity of the mutant *Plp^Δ* gene interferes with transgene activity (Schneider *et al.*, 1995) and it was a concern that a similar effect might be observed in the PNS. At the time these experiments were performed the preferred background of a true null *Plp* gene background was unavailable. The lack of apparent effect of the *Plp^Δ* allele on transgene activity in Schwann cells is interesting but perhaps unsurprising, in that endogenous gene activity might be expected to be low and that the any potential negative effects would be swamped by transgene activity. The results of the experiments with the genomic transgenes confirmed that the *Plp^Δ/Y* background was a reasonable environment to study the separate *Plp* and *Dm20* cDNA transgenes.

The two protein isoforms were targeted differently, with only the *Plptg1* transgene producing incorporation of protein into the myelin. However, both protein isoforms were found in the cytoplasmic domains. The implication of these findings is that the PLP protein isoform can be transported within the cell and be inserted into PNS myelin in the absence of DM20. As discussed in 7 General discussion (page 191) the evidence from transfection studies on intracellular trafficking of the two protein isoforms have produced conflicting results. However, none of these studies have been on myelinating cells and these *in vivo* studies suggest that the myelinating environment may influence trafficking. My studies also corroborate the observations in some transfection studies that PLP can be transported to cell membranes in the absence of DM20 (Schedl *et al.*, 1996; Gow *et al.*, 1994) (Dr P. Montague personal communication). However, my studies conflict with cell transfection experiments in which DM20 has also been transported to the membrane. It may well be that DM20 is handled differently in myelinating cells and cell lines. Evidence from a *Plp-LacZ* mouse suggests that the first 13 amino acid residues are sufficient for targeting of PLP protein to myelin (Wight *et al.*, 1993), but the results presented here suggest that this general response may be modified by other signals within the PLP and DM20 protein isoforms, possibly residing in the 35 amino acid PLP-specific region. The properties conferred on PLP by this segment result in differences in inositol hexakisphosphate binding, a protein possibly involved in vesicular transport (Yamaguchi *et al.*, 1996). A further possibility is that the tertiary structure adopted by PLP is beneficial to transport and incorporation in myelin. These studies support the hypothesis of differential targeting of the two

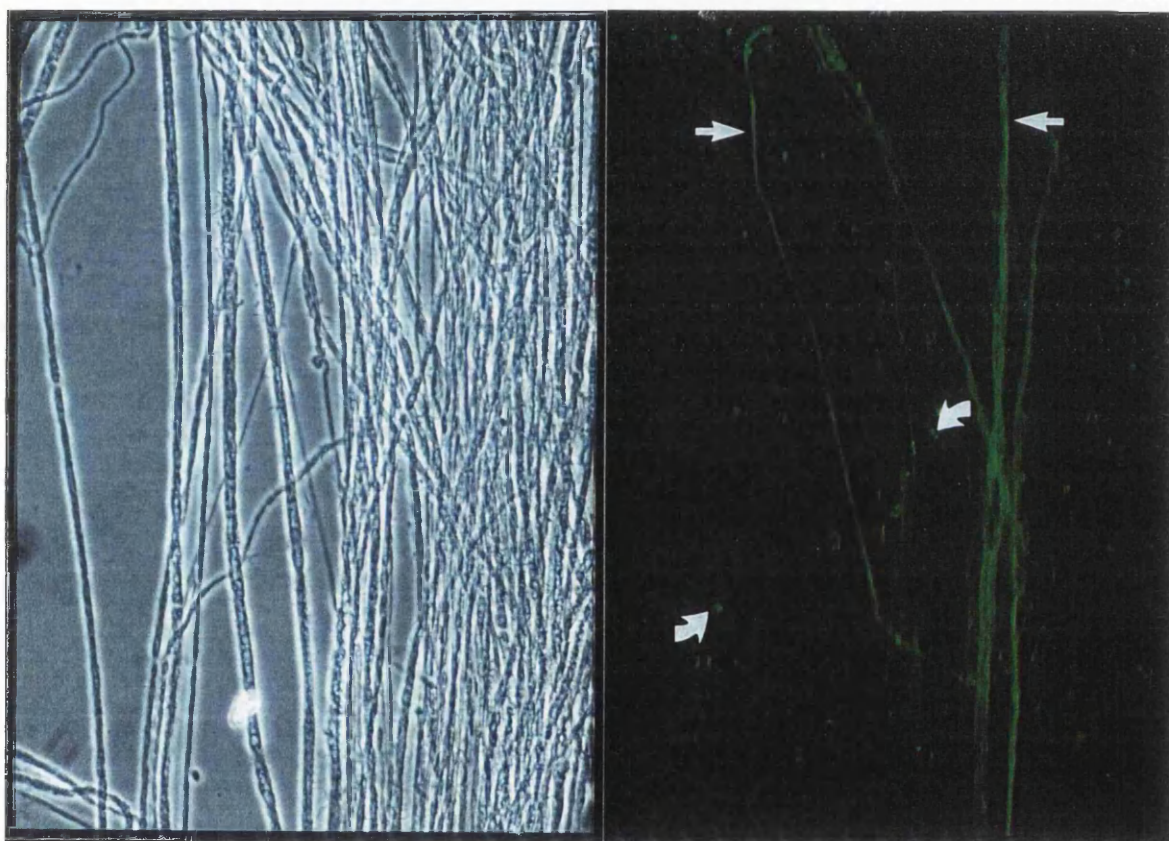
Plp gene products and suggest the possibility of this occurring in oligodendrocytes, though any extrapolation from Schwann cell to oligodendrocyte should be made with great caution.

The present study shows that the two *Plp* gene products, particularly DM20, are enriched in uncompact cytoplasmic domains of the MFSC. This is a region where a number of adhesion or adhesion related molecules, not all specific to Schwann cells, accumulate, such as certain integrins, ankyrin, spectrin and connexin 32 (Colman *et al.*, 1996; Scherer, 1996). It is also a region rich in MAG, which is excluded from compact myelin, and is thought to act as a heterophilic adhesion molecule between axon and Schwann cell (Montague and Griffiths, 1997). The intense staining of these regions probably reflects the presence of protein, probably DM20, in the plasma membranes and transport vesicles. The functional significance of this cytoplasmic localisation of DM20 in myelinated fibres is unknown. DM20 *per se* does not appear to be essential for the development and maintenance of the peripheral nerves, as indicated by their apparent normality in mice with missense and null mutations of the *Plp* gene.

In conclusion these studies have addressed the expression of the *Plp* gene in the other myelinating cell type, the Schwann cell, and indicate that the lack of the PLP and DM20 protein isoforms in peripheral myelin is not due to exclusion but rather to the low level of gene expression in this cell type. The use of specific minigenes containing specific cDNAs that generate the individual protein isoforms allows investigation of the targeting of these individual isoforms in this myelinating environment. The results demonstrate that PLP can be incorporated into myelin whilst DM20 appears to be targeted to cytoplasmic domains, regions that are populated with proteins having cell adhesion and pore formation properties. The differential targeting of the PLP and DM20 protein isoforms also implies that myelinating cells may handle these two protein isoforms differently, which is pertinent to the heterogeneity of disease seen with *Plp* gene mutations (see 7 General discussion page, 191).



(a)



(i)

(ii)

Figure 46. PLP/DM20 and P₀ immunostaining in wild type CNS and PNS. a) a merged confocal image of paraffin section of spinal cord with a ventral root showing PLP/DM20 (green) staining in the CNS and P₀ (red) in the PNS; b) (i) bright field of teased sciatic nerve preparation (x56) (ii) immunofluorescence showing immunoreactivity for PLP/DM20 in the MFSC localised at the Schmidt-Lanterman incisures (↘) and paranodes (↗) whilst the NMFSC appear as bright green bands (→) (x56).

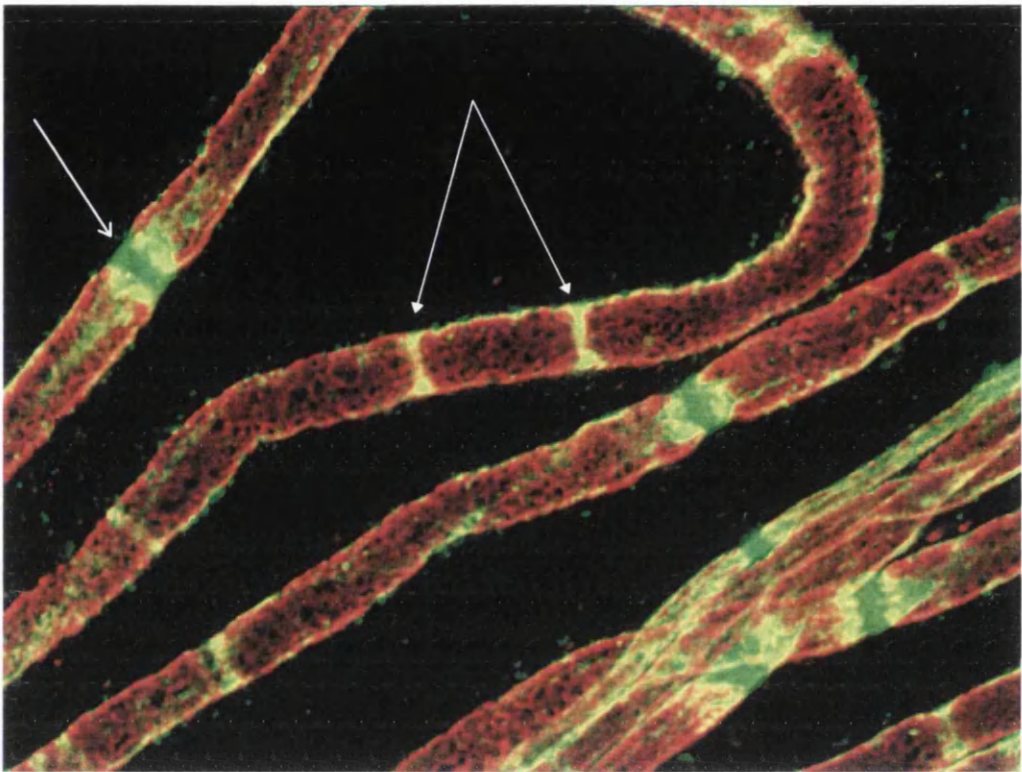
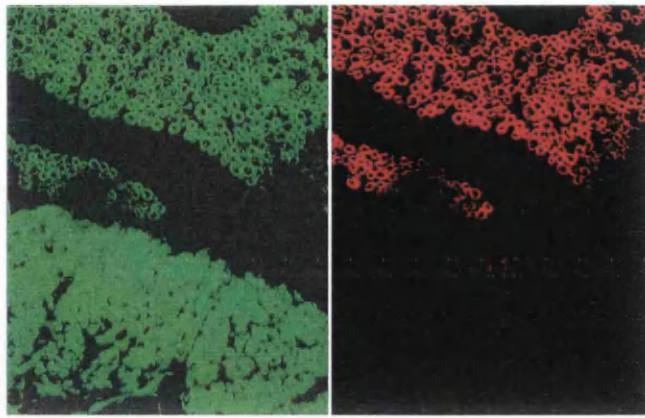
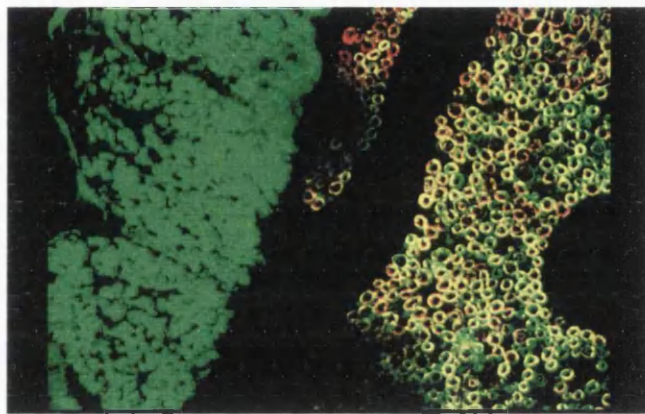


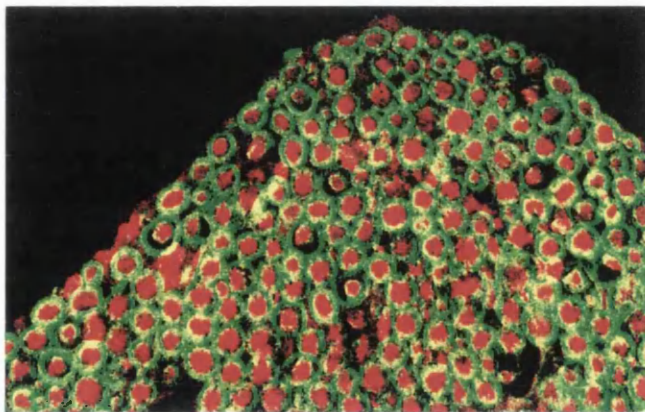
Figure 46 (continued). PLP/DM20 and P₀ immunostaining in wild type CNS and PNS. c) merged confocal image of a teased sciatic nerve preparation double stained for PLP/DM20 (green) and P₀ (red) emphasising that in wild type sciatic nerve the two proteins localise to different domains. The paranodes (open arrow) and Schmidt-Lanterman incisures (closed arrow) immunostain for PLP-CT, which is also present in the thin outer layer of Schwann cell cytoplasm surrounding the myelin sheath.



a)

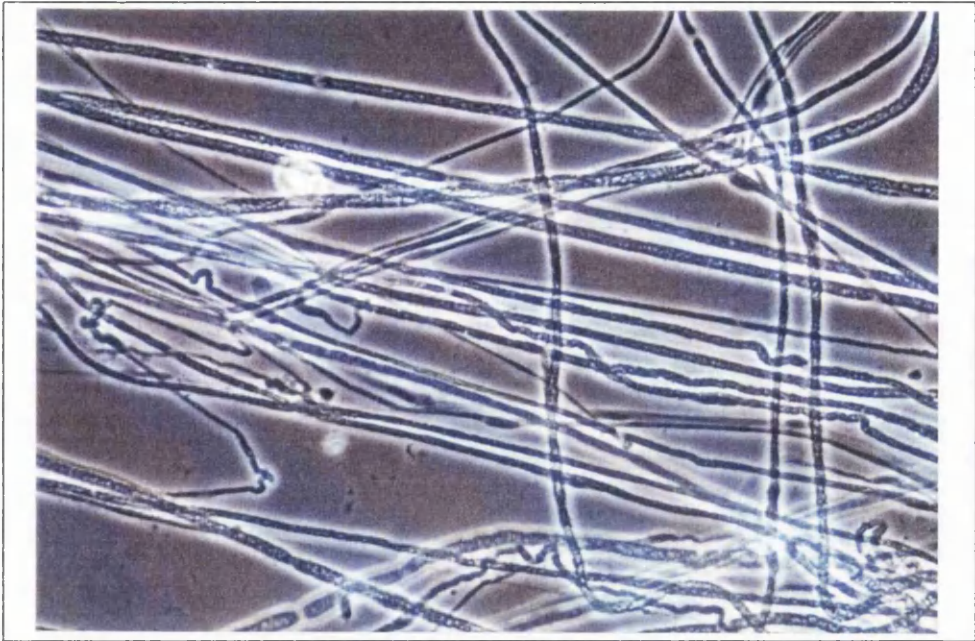


b)



c)

Figure 47. Immunostaining of PNS myelin in a homozygous #72 mouse. a) unmerged confocal images of a paraffin section of spinal cord (sc) and ventral nerve root (vr) double stained for P₀ (red) (i) and PLP/DM20 (green) (ii); b) merged confocal image of (a) with the co-localisation of PLP/DM20 and P₀ showing as yellow; c) merged confocal image of a paraffin section double stained for PLP/DM20 (green) and SMI (red) showing the PLP/DM20 in the myelin. The slight gap separating axon and myelin is probably a fixation artefact.



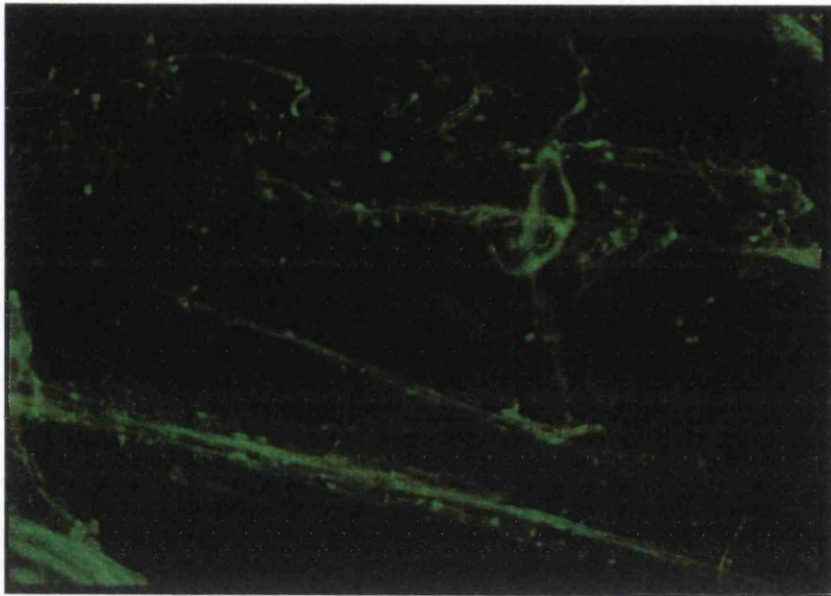
(i)



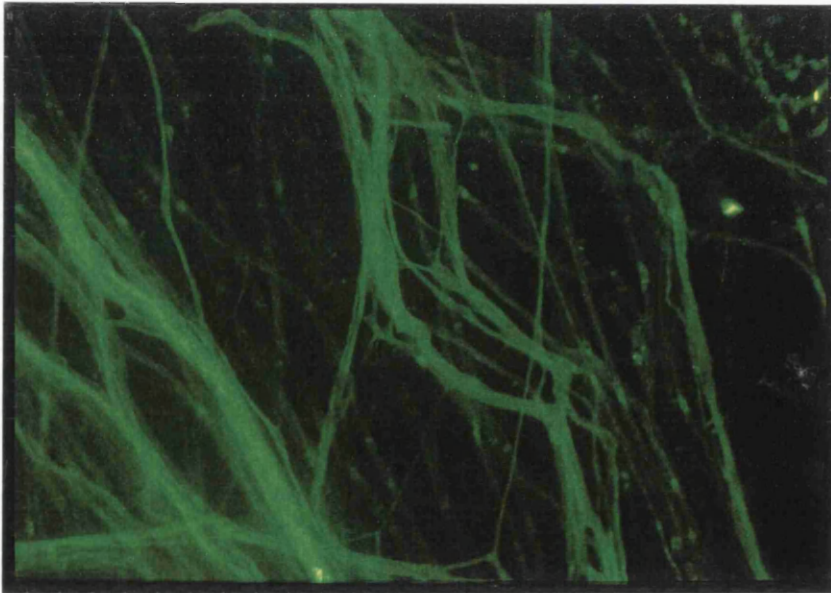
(ii)

a)

Figure 48. The distribution of *Plp* transgene-derived PLP/DM20 (green) proteins in the *Plp^{Dp}/Y* PNS. a) (i) teased *Plp^{Dp}* sciatic preparation (x56) (ii) same field immunostained for PLP/DM20.



(i)



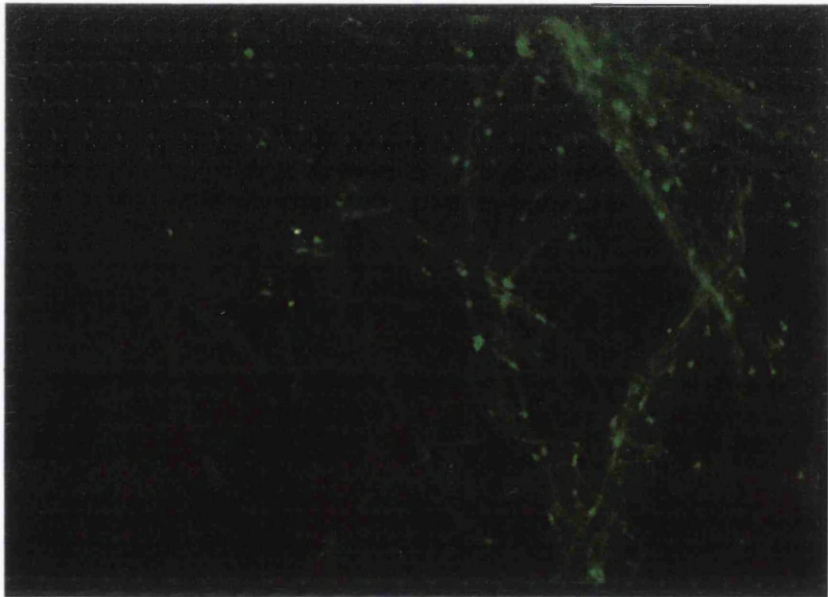
(ii)

b)

Figure 48 (continued). The distribution of *Plp* transgene-derived PLP/DM20 (green) proteins in the *Plp^{pl}/Y* PNS. b) (i) #66 with immunoreactivity of the cytoplasmic domains of MFSC and NMFSC, giving a similar pattern to wild type (x56) (ii) #72 exhibiting a similar pattern to #66 (x56).



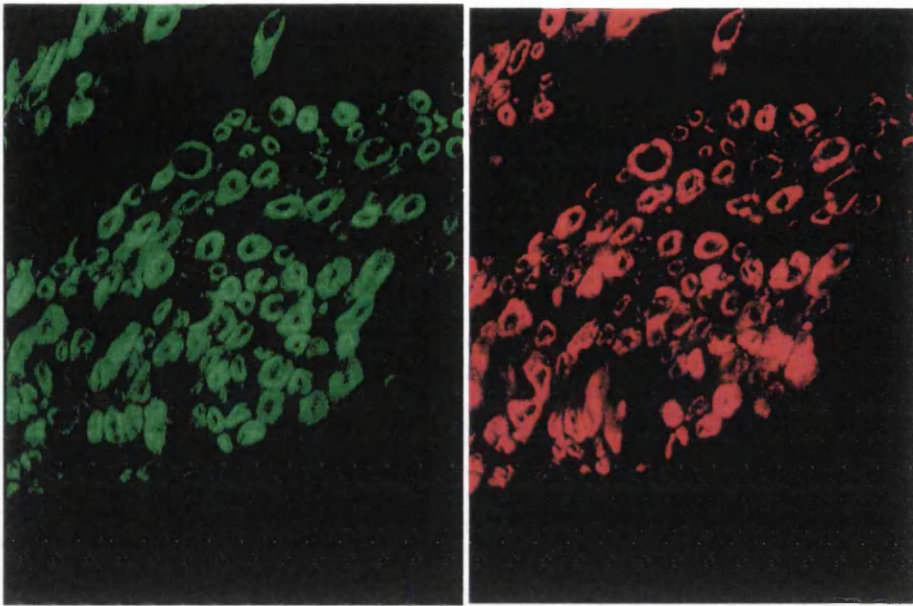
(iii)



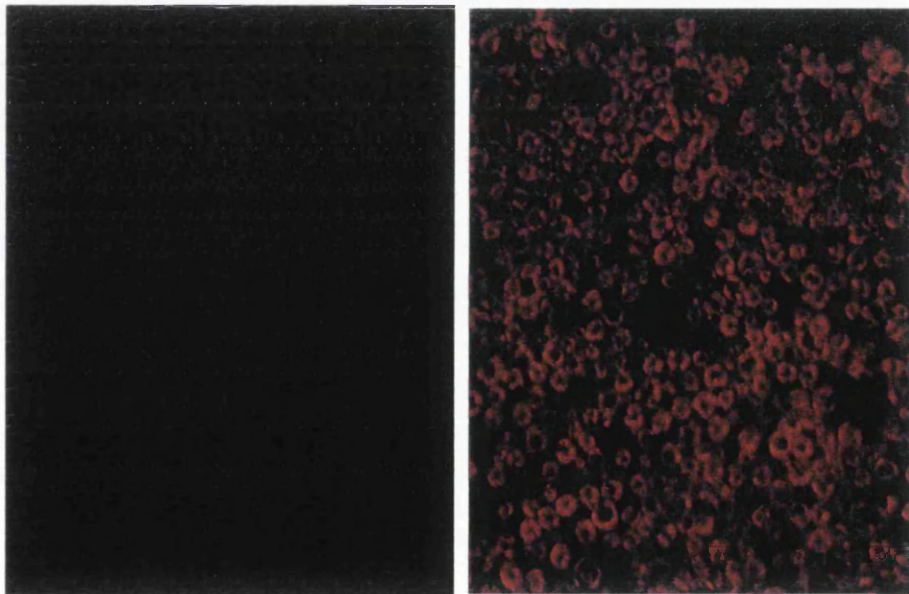
(iv)

b)

Figure 48 (continued). The distribution of *Plp* transgene-derived PLP/DM20 (green) proteins in the *Plp^{fl/y}* PNS. (iii) complemented with a *PlpTag1* transgene shows a more uniform immunoreactivity of nerve fibres though still with immunostaining of the cytoplasmic regions (x112) (iv) complemented with a *Dm20Tag2* transgene exhibits cytoplasmic immunostaining in myelinated fibres only (x56).

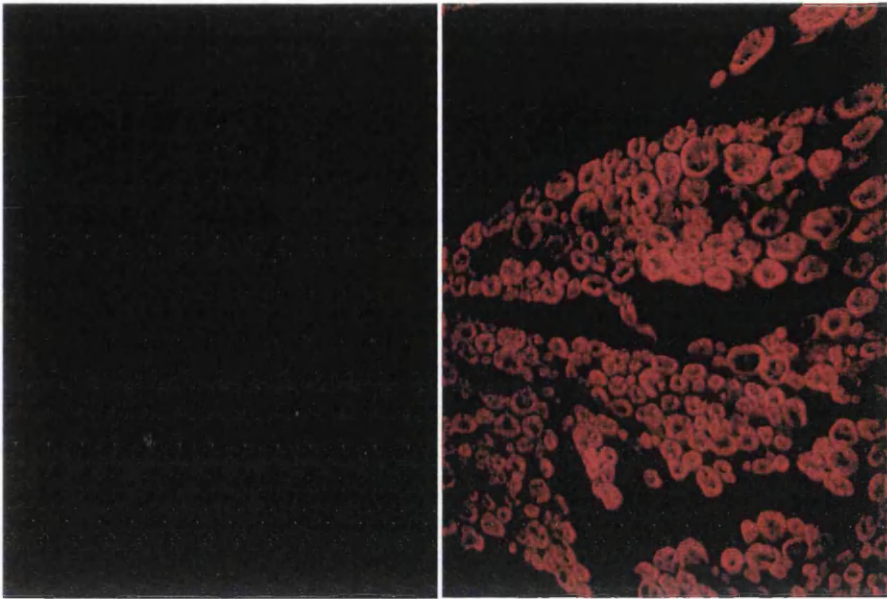


a)

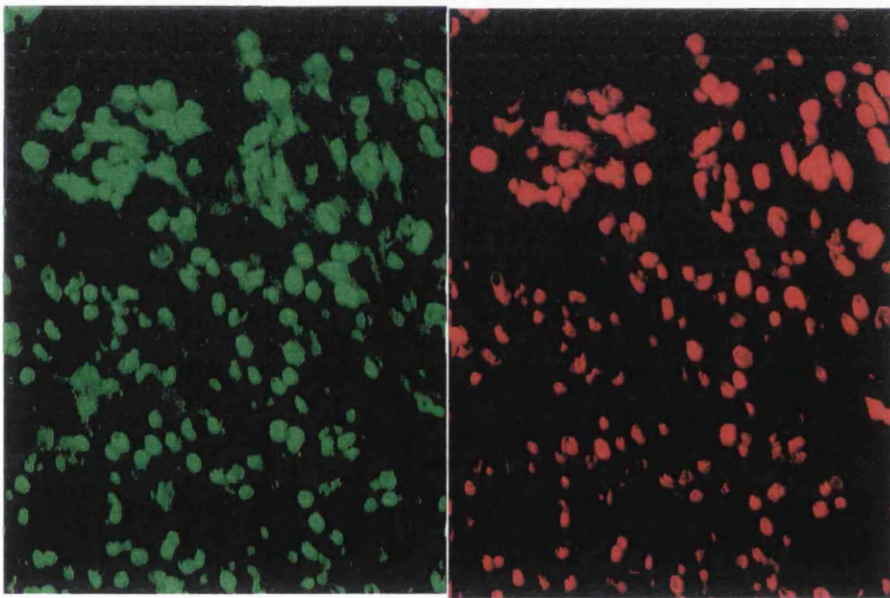


b)

Figure 49. The *PlpTag1* transgene facilitates the incorporation of PLP into PNS myelin whilst the *Dm20Tag2* transgene does not appear to facilitate the incorporation of DM20 into myelin. Unmerged confocal images of paraffin sections of sciatic nerve double stained for PLP/DM20 (green) and P₀ (red). a) *Plp^{pl}/Y* mouse complemented with the *PlpTag1* transgene showing PLP/DM20 immunoreactivity of myelin; b) *Plp^{pl}/Y* mouse complemented with the *Dm20Tag2* transgene showing the lack of PLP/DM20 immunoreactivity in myelin.



(a)



(b)

Figure 50. Unmerged confocal images of paraffin sections of sciatic nerve from a nude mouse that received a graft of sciatic nerve from a homozygous #72 mouse, double stained for PLP/DM20 (green) and P₀ (red). a) region distal to the graft where remyelination has been achieved by host Schwann cells. The myelin is P₀ positive and PLP/DM20 negative; b) region of the graft, showing remyelination where the myelin contains both P₀ and PLP/DM20.

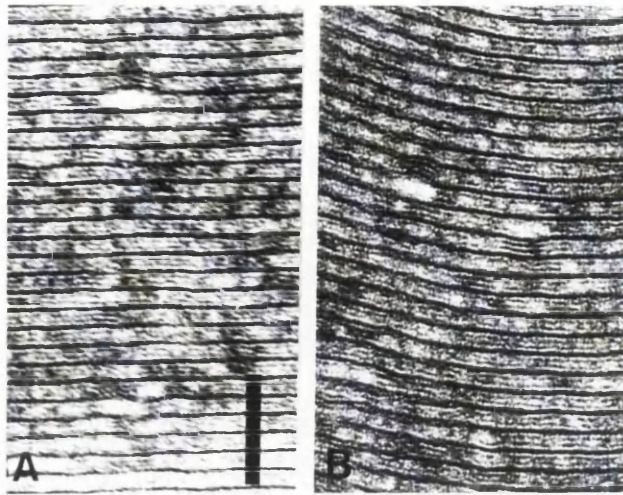


Figure 51. Electronmicrographs of PNS myelin sheaths from the ventral nerve roots of a wild type mouse and a homozygous #72 litter mate at 60 days. Both sheaths show normal major dense lines and double intraperiod lines. a) wild type; b) homozygous #72. (scale bar = 0.1 μ m).

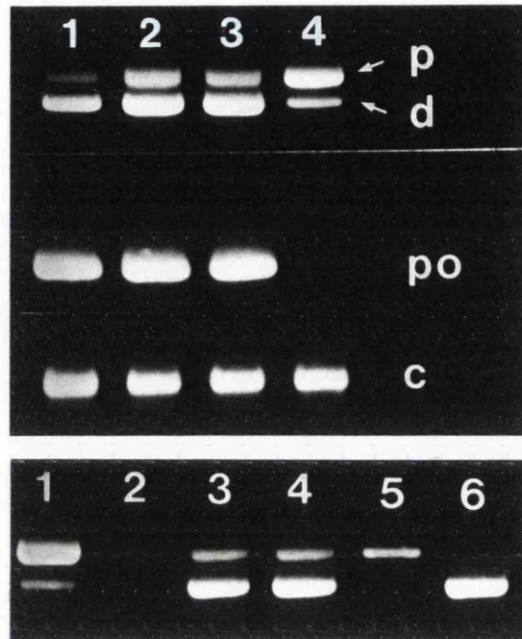


Figure 52. RT-PCR data illustrating the behaviour of *Plp* transgenes on a wild type and *Plp*^{jp} backgrounds. All samples represent P20. a) *Plp* gene exon 2→4 primers have been used to assess *Plp:Dm20* ratios (p and d), P₀ primers (po) and cyclophilin (c). Lane 1 sciatic nerve from wild type; lane 2 sciatic nerve from hemizygous #72; lane 3 sciatic nerve from homozygous #72; brain from wild type. Sciatic nerves from the transgenic mice show increased intensity of both bands relative to wild type but maintain the *Dm20* dominance. b) RT-PCR products from *Plp*^{jp} mice expressing various transgenes. *Plp* gene exon 2→5 primers were used to demonstrate the presence of transgene derived transcripts. Lane 1 brain from wild type; lane 2 brain from *Plp*^{jp}; lane 3 sciatic nerve from wild type; lane 4 sciatic nerve from *Plp*^{jp} harbouring #72 transgene; lane 5 sciatic nerve from *Plp*^{jp} mouse harbouring *Plp* minigene; lane 6 sciatic nerve from *Plp*^{jp} mouse harbouring *Dm20* minigene.

7. General discussion

The material presented in this thesis concerns the effects of extra copies of the wild type *Plp* gene on the development and maintenance of the axon/oligodendrocyte unit. The data presented support the concept that increased *Plp* gene dosage can influence both these processes. The picture that emerges is of a complex relationship between gene dosage and the phenotype with extra copies of the wild type *Plp* gene being associated with both dysmyelination (see 5 Dysmyelination and demyelination in mice homozygous for #66 and #72 transgene cassettes, page 134) and demyelination and with axonal abnormalities (see 4 Late onset neurodegeneration in mice hemizygous for the #66 and #72 transgenes, page 89). Further, the data show that demyelination occurs in the already dysmyelinated homozygous #66 and #72 mice, suggesting that though both processes are a result of increased gene dosage they are due to perturbations of separate aspects of the oligodendrocyte\axon relationship. The purpose of this general discussion is to examine the relationship between gene dosage and the effects on myelination and myelin maintenance in the light of the data presented and how these relate to the phenotypes observed with other *Plp* gene mutations.

However, before examining the aspects of gene dosage which may be related to dysmyelination it is worth considering whether there is any concern that the products of the transgenes differ from those of the wild type *Plp* gene. The constructs used carry all the known coding sequence and have been demonstrated to produce a protein that immunostains with a PLP-C-terminal antibody, thus demonstrating a full length polypeptide. It is present in CNS myelin suggesting that it can adopt a suitable conformation to be incorporated. For both transgenic cassettes the authors recloned the transgenes from their transgenic mice and demonstrated that the sequence was unaltered. As discussed in 1.2.1.3.2.1 The myelin proteolipid protein (page 5) there is no functional assay for the PLP and DM20 protein isoforms which would be useful in confirming the status of the transgene products. However, the transgenes are capable of preventing the axonopathy that develops in *Plp* knockout mice (Griffiths, personal communication), thus suggesting the products are functionally active. Considering these observations there is no reason to believe that the nature of transgene derived PLP and DM20 protein isoforms is different from wild type or is in itself detrimental.

The relationship between gene copy, transgene zygosity and phenotype for transgenic mice with extra copies of the *Plp* gene is complex. As discussed in 1.4.1 Expression of cloned genes (page 34) the relationship between copy number and transgene activity cannot be assumed to be a direct function of the number of copies in transgenic cassettes, though position-independent/copy dependent activity can be

achieved by the inclusion of the appropriate regulatory regions. Thus, though the relationship between gene copy number and phenotype observed with the homozygous #66 and #72 mice is suggestive of increasing gene dosage being deleterious it must be seen in the light of known problems associated with transgene regulation and it is possible that the different site of integration contributes to the more extreme nature of the #66 transgene. Interestingly, in the hemizygous state the #66 transgene is not demonstrably different in its effects to the #72 cassette. In #66 and #72 mice dysmyelination is related to zygosity rather than gene copy number. This relationship between zygosity and dysmyelination is also observed in the *4e* mice (Kagawa *et al.*, 1994). The increase in copy number required to produce abnormalities of myelination in man is a single extra copy.

The dysmyelination observed in conjunction with increased gene copy number is often loosely referred to as "gene over expression", however, this term is rather imprecise and does not address at which stage in the multistep process of eukaryotic gene transcription, translation and product transport the abnormalities are thought to be occurring. It is more fruitful to examine the available evidence for the different stages of gene expression. Dysmyelination in #66 and #72 mice occurs in the presence of apparently adequate numbers of oligodendrocytes. Though *4e* mice and some human cases are reported to be deficient in oligodendrocytes the observations in #66 and #72 mice implies that though lack of sufficient mature oligodendrocytes may impair myelination, probably in the number of internodes formed, it is not the primary reason for the thin myelin sheath.

Estimation of the steady state mRNA levels for the *Plp* and other myelin genes suggest a post-transcriptional pathway affecting myelination. There is no evidence that dysmyelination is due to increased transcriptional levels in myelinating cells. At 20 days hemizygous #66 and #72 mice are myelinating normally yet the levels of *Plp* message are elevated compared to the dysmyelinated homozygous mice and wild type mice (Figure 53, page 194). In homozygous *4e* mice dysmyelination is associated with decreased levels of *Plp* mRNA; however, there is also a decreased mature oligodendrocyte population.

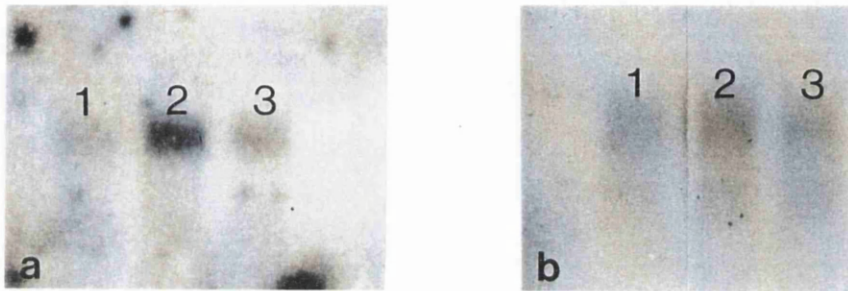


Figure 53. Northern hybridisation analysis of *Plp* gene transcription in #66 and #72 mice at P20. A comparison of wild type, hemizygous and homozygous mice. Panel a) #66: lane 1 wild type, lane 2 hemizygous, lane 3 homozygous; panel b) #72: lane 1 wild type, lane 2 hemizygous, lane 3 homozygous.

These studies have only addressed *Plp* gene transcription at two time points and do not directly consider the circumstances during development. It is postulated that the DM20 protein isoform may play a role in glial cell development (see 1.2.2.2 Developmental expression of the *Plp* gene in the CNS, page 15). Studies in 4*e* mice show that transgene activity in the embryonic mouse reflects gene dosage more directly, implying high levels of *Dm20* message isoform during this possibly sensitive stage may result in a compromised oligodendrocyte population. Ultrastructural studies of developing oligodendrocytes from homozygous #66 mice show abnormalities present from an early stage. Further, more detailed studies with serial electronmicrographs, would be required to determine whether these changes were restricted to myelinating oligodendrocytes. The presence of autophagic vacuoles indicates abnormal protein turnover and could represent the elimination of proteins from the periphery of the cell. Studies of glial cell densities and the likely increase in the incidence of cell death suggest that in homozygous mice the dynamics of the developing glial cell population are altered. Labelling experiments with ³H thymidine would be required to establish the nature of the cell types involved, though subjectively this would appear to involve the oligodendrocyte population. Whilst an increased ratio of *Dm20* relative to *Plp* message isoforms has been described in one human pedigree (Carango *et al.*, 1995) a number of studies involving *Dm20* minigenes have failed to create a dysmyelinating model (see 1.4.2.4 Evidence that increased *Plp* gene dosage affects myelination, page 38). It has been suggested that a stoichiometric relationship between the PLP and DM20 protein isoforms may be disrupted by imbalance of the two proteins leading to instability of the myelin formed (Hodes & Dlouhy, 1996). Tissue culture experiments show that PLP and DM20 protein isoforms can be transported and inserted into myelin independently, suggesting that the proposed precise stoichiometric relationship may not exist.

Examination of the steady state mRNA data for the #66 and #72 mice shows that extra copies of the *Plp* gene in these mice influence the co-ordinate control of the CNS myelin genes Figure 53 (page 194) but not the PNS myelin genes (see 6.4.4 RT-PCR, page 177). This raises the question of contribution of other genes to the observed phenotype. The development of oligodendrocytes and the formation of myelin represent the contributions of a myriad of closely co-ordinated genes coding for myelin proteins and many other products associated with cell contact, protein transport, etc. It is entirely possible that changes in the developmental profile of related genes contributes to the phenotype. The point of development at which this may be significant may also be very specific. For instance transgenic mice carrying extra copies of the *Cnp* gene are abnormally myelinated and there is evidence that

over-expression of the *Cnp* gene interferes with the development of oligodendrocyte/axonal contact early in myelin formation (Gravel *et al.*, 1996). Interestingly increased gene dosage of the *Cnpase* gene also influences the transcription of other myelin genes, including the *Plp* gene.

As described in 1.2.2.1.1 Phylogenetic evolution of the *Plp* gene (page 13) the *Plp* gene is a member of the larger DM family of genes, which generally have yet to be ascribed functions. The relationship of their products to those of the *Plp* gene have not been elucidated, however, there are minimal changes in the profile of M6a in the *Plp* gene knockout mouse (Klugmann *et al.*, 1997). Membership of a gene family does not imply that products of family members can necessarily substitute for one another. However, the possibility arises that if these genes are involved in the co-ordinated programme of myelin gene transcription that their function may be disrupted in *Plp* mutants.

The extra copies of the *Plp* gene associated with PMD and the #66,#72 and 4*e* mice all contain non-coding sequences, varying in length, that are of significance in *Plp* gene transcription and other myelin genes (1.4.2.3.1 *Plp* transgenic mice with extra copies of the wild type *Plp* gene (page 37) and 1.2.3 Regulation of *Plp* gene expression and co-ordinate expression of the myelin genes (page 16)). The increased population of *cis*-elements potentially offers increased competition for *trans* factors within a cell. It is known that disease can be related to *trans* factor deficiency and that the levels of *trans* factors can be critical at certain times of development as the associated diseases tend to represent abnormalities of development (Engelkamp & van Heyningen, 1996). Model systems for assessing the toxic effects of regulatory genes have been developed in yeast (Daniel, 1996). The lengths of 5' non-coding sequence varies between #66/72 mice and 4*e* mice but whether the extra 5' sequence in 4*e* mice includes significant extra sequences that contribute to the severity of the phenotype as argued by Ikenaka and Kakawa (1995) is debatable, considering the other factors influencing transgene activity. Extra copies of 5' sequence are also present in the *Lac-z* fusion transgenic mice (Wight *et al.*, 1993) and the *Plp* and *Dm20* minigene mice (1.4.2.4 Evidence that increased *Plp* gene dosage affects myelination, page 38) none of which show evidence of dysmyelination, suggesting that homozygosity for these 5' regulatory sequences alone is not sufficient to induce dysmyelination.

Do *Plp* gene duplications and the other mutations of *Plp* share a common pathogenesis? The investigation of naturally occurring and engineered models of *Plp* gene mutation have demonstrated that a dysmyelinating phenotype is associated with mutation events of quite different natures. A number of authors have

attempted to identify whether there is a relationship between mutation and phenotype in PMD (e.g. Hodes & Dlouhy, 1996). This task is complicated by the relatively small number of cases, (there is only one example of the same mutation occurring in separate human pedigrees), and the influence of varying genetic background resulting in noticeable heterogeneity within and between families. The effects of other loci on phenotype present problems in linking specific mutations to phenotypic changes (Erickson, 1996), however, some patterns do emerge in such a study of PMD. Complete deletions, of which at least two are recorded, and mutations affecting only the 3B portion of PLP are related to relatively mild clinical abnormalities. Also the only mutation shared by a human pedigree and a animal model (*Plp^{jP}-rsh*) exhibits relatively mild phenotypic signs in both species (Kobayashi *et al.*, 1994). Whether there is a “duplication phenotype” as seen with PMP22 in peripheral neuropathies (see 1.3.2.4 Hereditary motor and sensory neuropathies (HMSN) of the PNS, page 34) is uncertain (Hodes & Dlouhy, 1996). The outbred human population shows that modifying loci can have a significant impact on the development of phenotype. The animal models of *Plp* mutation are usually studied on stable in-bred populations and thus variation in phenotype is less apparent (interestingly *Pt* rabbit is described as having a noticeably variable phenotype, with the worst affected animals selected for the description of the pathology (Tosic *et al.*, 1993)). However, both the *Plp^{jP}* and *Plp^{jP}-rsh* alleles exhibit variation in phenotype when bred onto different genetic backgrounds (Griffiths, unpublished observations).

However, this variation in phenotype with mutation does suggest that there are potentially a number of mechanisms leading to a similar endpoint. Investigation of the relationship between mutation and phenotype in relation to the *Plp* gene is further complicated as the two protein isoforms exhibit different developmental profiles and probably have different functions. This is underlined by mutations in exon 3B showing that a normal DM20 protein can positively influence development of myelination even in the face of a mutated PLP protein.

Mutations inducing a change in the protein structure and disrupting postulated protein-protein interactions (see 1.2.2.1.1 Phylogenetic evolution of the *Plp* gene, page 13) might well be expected to influence the properties of the PLP and DM20 protein isoforms. Studies of some animal models indicate that protein transport is perturbed with abnormalities primarily affecting the RER, probably due to abnormal protein folding (Gow *et al.*, 1994). It has been suggested that in *Plp^{jP}* the abnormal proteins are in some way toxic to the oligodendrocyte (Schneider *et al.*, 1995). However, this is questioned by observations that oligodendrocyte death appears to occur before major production of the PLP/DM20 protein isoforms (Vermeesch *et*

al., 1990). Additionally, transplant (Lachapelle, 1995) and cell culture studies (Knapp *et al.*, 1996) show that myelinating abilities of *Plp^{jp}* oligodendrocytes are influenced by their environment. Transfection studies have shown that mutant PLP and DM20 proteins are abnormally distributed suggesting perturbations of trafficking and membrane insertion. Interestingly, positive correlations can be made between phenotypic severity and the ability of mutant proteins to reach the cell surface and enter the endocytic pathway (Thomson *et al.*, 1997; Gow & Lazzarini, 1996; Gow *et al.*, 1994). In these studies mutations associated with the most severe phenotypes resulted in both PLP and DM20 being retained in the RER whilst with mutations associated with milder phenotypes DM20, but not PLP, passed to the cell membrane. These studies demonstrate clearly that the changes in protein structure associated with mutation affects protein transport and can induce the RER changes that are observed in some mutants. The observations are used to argue quite strongly for protein trafficking perturbations being a major contributor to the phenotypic findings in PMD and animals models (Gow & Lazzarini, 1996; Gow *et al.*, 1994). However, it is not surprising that altered proteins are abnormally translocated and the significance of these effects in relation to dysmyelination (Schedl *et al.*, 1996) remains to be determined.

The severe disruption of myelin and myelination seen with mutations affecting the strongly conserved putative transmembrane regions highlights the sensitivity of this structure to change. However, mutants such as *Plp^{jp-rsh}* and the knockout mice in which there is relatively mild disease and no abnormal phenotype respectively, suggest that disruption of the IPL alone is not the reason for the severe phenotypes associated with some *Plp* gene mutations. The developmental profile of *Plp* gene expression implies that PLP and DM20 have different roles during development and myelin formation (1.2.2.2 Developmental expression of the *Plp* gene in the CNS, page 15). *Dm20* transcripts are maximal during the pre-myelination phase of oligodendrocyte development and have also been detected in PNS glia (where the *Plp* gene does not appear to be part of the co-ordinated transcription programme of myelin genes (Griffiths *et al.*, 1995)), embryonic neural cells (Ikenaka *et al.*, 1992) and cardiac myocytes at about 0.1-0.2% of the levels in the brain (Campagnoni *et al.*, 1992). In cardiac myocytes there is evidence of developmental regulation. Recently, both message and product have been demonstrated in the human foetal thymus, spleen and testis (message only) confirming expression in non-glial tissue (Pribyl *et al.*, 1996). Mutant animals such as *Plp^{jp-rsh}* and *Pt* rabbit in which glial cell death and hypomyelination are uncoupled (usually both features of *Plp* gene mutant animals) illustrate that mutations can selectively affect these two features of oligodendrocyte biology (see 1.3.2.1 Animal models, page 26).

Molecular studies of the human *Plp* gene and relevant animal models indicate the range of phenotypes associated with mutation is considerably greater than previously recognised. This illustrates the potential value of animal models in furthering the understanding of disease in conditions where rarity contributes to difficulties of collating information and provides pointers to features that should be examined carefully. For example, though SPG2 is probably a demyelinating disease (Hodes & Dlouhy, 1996) nothing is known about the development of myelin in these cases; however, the transgenic model suggests that it may be relatively normal and that the disease may be more complicated than demyelination alone, as the transgenic mice exhibit an axonopathy. PMD, essentially a dysmyelinating disorder, is described as progressive in some cases. Although some of this clinical deterioration may be due to dysmyelination (myelination in man continues into the second decade) there is indication from the #66 and #72 transgenic mice that demyelination may also be occurring, contributing to the progression of the disease.

Another aspect of this project has expanded the understanding of the *Plp* gene in the PNS. The work described in 6 Expression of *Plp* transgenes in the peripheral nervous system (page 171) shows that myelinating Schwann cells handle PLP and DM20 protein isoforms differently. Though caution should be exercised in extrapolating from Schwann cell to oligodendrocyte it implies that there is a signal within the PLP-specific region that can be used for differentiating between the two protein isoforms. As described above tissue culture experiments and *in vivo* observations (Schedl *et al.*, 1996) have shown that for several mutations of the *Plp* gene, protein trafficking and membrane insertion of the DM20 isoform are less affected than that of the cognate PLP isoform. This observation of successful DM20 transport is more noticeable for the mutations associated with the less severe phenotypes and may be a contributing factor to the less severe nature of disease in these mutants.

In conclusion the work presented in this thesis has illustrated that increased dosage of the *Plp* gene affects myelin during both development and maintenance and shows a parallel between the experimental models and the spectrum of disease associated with *PLP* gene duplications in man. The mechanisms underlying the deleterious effects of *Plp* gene duplication remain unelucidated and this work suggests they are likely to be complex and may involve perturbations in the expression of other genes.

8. Appendix

8.1 Fixatives

8.1.1 Buffered neutral formaldehyde, 4% (BNF)

For 1L of fixative:

40% formaldehyde (Merck)	100ml
tap water	900ml
sodium di-hydrogen phosphate	4g
di-potassium hydrogen phosphate	8g

8.1.2 Karnovsky`s modified fixative (paraformaldehyde/glutaraldehyde 4%/5%)

For 500ml “strong fix”:

8% formaldehyde	250ml
25% glutaraldehyde	100ml
0.08M cacodylate buffer pH7.2	mix formaldehyde and glutaraldehyde and make up to 500ml
calcium chloride	250mg

Filter and store at 4⁰C for a maximum of ~14 days.

8% formaldehyde: 20g paraformaldehyde + 250ml distilled water; heat to 65⁰C; add 1M NaOH to clear the solution; cool to 4⁰C.

0.08M cacodylate buffer: add 17.12g sodium cacodylate buffer to 1l and adjust pH to 7.2.

8.1.3 Periodate-lysine-paraformaldehyde

For 1L of fixative:

lysine monohydrochloride	13.7g in 375ml distilled water
sodium hydrogen phosphate	1.8g in 100ml distilled water
	mix to give 475ml at pH7.4
paraformaldehyde	20g in 200ml distilled water

store at 4⁰C until required, overnight if required

Mix buffered lysine and paraformaldehyde and make up volume to 1L with 0.1M phosphate buffer. Add 2.14g sodium periodate and allow to dissolve. Use immediately.

8.2 Tissue processing protocols

8.2.1 Paraffin wax processing

Solutions used for preparation of tissue for paraffin blocks:

- 1) 70% methylated spirit / 5% phenol 2 hrs
- 2) 90% methylated spirit / 5% phenol 2 hrs
- 3) methylated spirit 2 hrs
- 4) ethanol / 5% phenol x3
2 hrs
1 hr
1 hr
- 5) 1% celloidin in methyl benzoate* 4 hrs
- 6) xylene 1 hr (x3)
- 7) paraffin wax x2 7 hrs

*celloidin was obtained as Necoloidine (Merk) and considered as a 100% solution (1ml in 100ml benzyl benzoate).

8.2.2 Resin processing

Processing involved the following solutions:

1)	isotonic cacodylate buffer	40C	50 mins
2)	1% osmium tetroxide in cacodylate buffer	room temperature	2 hrs
3)	isotonic cacodylate buffer	room temperature	30 mins
4)	50% ethanol	40C	5 mins
5)	50% ethanol	40C	10 mins
6)	70% ethanol	40C	5 mins
7)	70% ethanol	40C	10 mins
8)	80% ethanol	40C	5 mins
9)	80% ethanol	40C	10 mins
10)	90% ethanol	40C	5 mins
11)	90% ethanol	40C	10 mins
12)	ethanol	40C	20 mins
13)	ethanol	40C	20 mins
14)	propylene oxide	room temperature	15 mins
15)	propylene oxide	room temperature	15 mins
16)	1:3 resin*:propylene oxide	room temperature	13 hrs
17)	1:2 resin:propylene oxide	room temperature	6 hrs
18)	1:2 resin:propylene oxide	room temperature	18 hrs

19) resin 30⁰C 4 hrs

* resin composition page 204.

isotonic sodium cacodylate buffer: 16.05g sodium cacodylate, 3.8g sodium chloride, 0.055g calcium chloride, 0.102g magnesium chloride + distilled water to 1000ml; adjust topH7.2 - 7.3

Processed samples were embedded in resin filled silicone moulds and left to polymerise overnight at 60⁰C.

8.3 Mounting media

8.3.1 Araldite resin

30g	araldite CY212	resin
25.2g	dodecanyl succinic anhydride (DDSA)	hardener
1.2ml	2,4,6-tri-dimethylaminomethyl-phenol (DMP 30)	accelerator
1.0ml	di-butyl phthalate	plasticiser

8.4 Staining protocols and stains

8.4.1 Haematoxylin and eosin

Sections were passed through the following solutions:

1)	xylene	2 min
2)	absolute alcohol	2 min
3)	methyalted spirit	2 min
4)	water	2 min
5)	Lugols iodine	1 min
6)	water	1 min

7)	5% sodium thiosulphate	1 min
8)	water	
9)	Mayer`s haematoxylin*	10 mins
10)	1% acid alcohol	3 dips
11)	water	2 mins
12)	Scot`s tap water substitute*	1 min
13)	water	2 mins
14)	methyated spirit	10 secs
15)	saturated alcoholic eosin	2 mins
16)	methyated spirit	2 mins
17)	absolute alcohol	2 mins
18)	histoclear	2 mins
19)	xylene	5 mins

* details page 205.

8.4.2 haematoxylin

1)	water	2 mins
2)	Mayer`s haematoxylin	50 secs
3)	water	wash off excess haematoxylin
4)	Scot`s tap water substitute	30 secs

8.4.3 Staining of tissues for electronmicroscopy

- | | | |
|----|--|--------------|
| 1) | saturated uranyl acetate in
50% ethanol | 5-15
mins |
| 2) | 50% ethanol | rinse |
| 3) | 50% ethanol | rinse |
| 4) | distilled water | rinse x 2 |
| 5) | air dry | |
| 6) | Reynold's lead citrate*
(Sodium hydroxide
moistened chamber) | 5-10
mins |
| 7) | 1M sodium hydroxide | rinse x 3 |
| 8) | distilled water | rinse x 5 |

*details page 207.

8.4.3.1.1 Mayer's haematoxylin:

1.0g haematoxylin

10.0g potassium alum

0.2g sodium iodate

made up in 1l distilled water. Bring to boiling point and allow to cool over night and add:

1.0g citric acid

50g chloral hydrate

8.4.3.1.2 Scot's tap water:

3.5g sodium bicarbonate

20.0g magnesium sulphate

in 1l distilled water.

8.4.3.1.3 Methylene blue / azur II:

1% methylene blue

1% azur II

1% borax

in distilled water.

8.4.3.1.4 Reynold's lead citrate:

1.33g lead nitrate

1.76g sodium citrate

each dissolved in 15ml distilled water for 1min vigorous shaking followed by occasional shaking for the next 30 mins. Clear with 8.0ml 1M sodium hydroxide and make up to final volume of 50ml with distilled water (final pH12).

8.4.3.2 methylene blue

0.15g methylene blue

50ml 3M sodium acetate

made up to 500ml in DW to give 0.03% (w/v) methylene blue. Check pH5.2.

8.5 Buffers

8.5.1 Tris buffered saline

3g Tris base

8g sodium chloride

0.2g potassium chloride

Dissolve in 800ml DW, adjust pH to 7.4 with hydrochloric acid and make up to 1l with DW. This give final concentrations of 25mM Tris pH7.4, 136mM sodium chloride, 2.6mM potassium chloride.

8.5.1.1 Phosphate buffered saline

8g sodium chloride

0.2g potassium chloride

1.44g di-sodium hydrogen phosphate

0.2g potassium hydrogen phosphate

Dissolve in 800ml DW, adjust pH to 7.4 with hydrochloric acid and make up to 1l with DW.

8.5.2 Gel running buffer

8.5.2.1 Tris acetate EDTA buffer x10

0.04M Tris acetate, 0.001M EDTA.

48.4g Tris base

11.4ml glacial acetic acid

20ml 0.5 MEDTA

made up to 1L in DW.

8.5.2.2 MOPS x10

Sodium MOPS 0.2M, sodium acetate 50mM and 10mM EDTA pH7.0

23.1g sodium MOPS

3.4g sodium acetate

10ml 0.5M EDTA

3.55ml acetic acid

made up to 500ml with DW. Autoclaved, which results in light green colouration, and stored at 4°C.

8.5.2.3 Northern denaturing buffer

formamide 20.3µl

MOPSx10 4.16µl

40% formaldehyde 6.66µl

Total volume 31.12µl

This buffer was made up as a master mix to ensure accurate pipetting. Added to 10µl of RNA sample.

8.5.3 SSC (Sodium chloride / sodium citrate) x20

3M sodium chloride / 0.3M sodium citrate

1753g sodium chloride

882g sodium citrate

made up to 10l with DW.

8.5.4 TE

10mM Tris pH8.0, 1mM EDTA

500µl 1M Tris pH8.0

100µl 0.5M EDTA

8.6 Loading dyes

8.6.1.1 6x buffer for TAE conditions

30% glycerol (Sigma); 0.25% bromophenol blue; 0.25% xylene cyanol FF (Sigma).

8.6.1.2 Northern loading dye

50% glycerol (Sigma); 1mM EDTA; 0.25% bromophenol blue; 0.25% 0.25% xylene cyanol FF (Sigma).

8.7 Bacteriological media

8.7.1 Luria-Bertani medium

10g tryptone (Oxid)

5g yeast extract (Oxid)

10g sodium chloride

Make up to 1l in DW and adjust to pH7.0 using ~0.2ml 5N sodium hydroxide. Sterilise by autoclaving for 20 mins at 15lb in². Store at 4°C.

8.7.2 SOC medium

20g tryptone (Oxid)

5g yeast extract (Oxid)

0.5g sodium chloride

Make up to 970ml in DW, add 10ml 250mM potassium chloride and adjust to pH7.0 using ~0.2ml 5N sodium hydroxide. Autoclave for 20 mins at 15lb in². Cool to <60⁰C and add 20ml filter sterilised 1M glucose solution.

9. Abbreviations:

Abbreviation	Full name
aa	amino acid
APES	3-aminopropyltriethoxy-silane
BAER	brain stem evoked response
CMT1A	Charcot-Marie-Tooth disease 1A
CGT	UDP-galactose:ceramide galactosyl-transferase
CNP	2',3'-cyclic nucleotide 3'-phosphodiesterase
CNS	central nervous system
CST	cranial sympathetic trunk
DAB	3,4,4',4',-tetraminobiphenyl hydrochloride
DEPC	di-ethyl pyrocarbonate
DM20	the small isoform of the PLP gene
DMD	Duchenne muscular dystrophy
DNA	de-oxyribo nucleic acid
dNTP	deoxynucleotides
DSD	Dejerine-Stottas disease
DTT	dithiothreitol
DW	distilled, deionised water
EDTA	Ethylene-di-amine-tetra-acetate
EM	electronmicroscopy
EMG	electromyography
ES	embryonic stem
FITC	fluoroscein isothiocyanate

gDNA	genomic DNA
GFAP	glial fibrillary acidic protein
H and E	haematoxylin and eosin
HNPP	hereditary neuropathy with liability to pressure palsies
HMSN	hereditary motor and sensory neuropathy
HSP	hereditary spastic paraplegias
IGF-1	insulin-like growth factor 1
IL-3	interleukin-3
IP	intraproduct line
ISH	<i>in-situ</i> hybridisation
<i>Lcam1</i>	neural cell adhesion molecule L1
L-MAG	large isoform of myelin associated glycoprotein
MAG	myelin associated glycoprotein
MASA	mental retardation, Apraxia, shuffling gait, adducted thumb
MBP	myelin basic protein
MDL	major dense line
min(s)	minute(s)
MFSC	myelin forming Schwann cell
MHV	murine hepatitis virus
NMFSC	non-myelin forming Schwann cell
MOBP	myelin-oligodendrocyte basic protein
MOSP	myelin/oligodendrocyte specific protein
MOPS	3-(N-morpholino) propanesulphonic acid
MS	multiple sclerosis
MyT1	Myelin transcription factor 1
NF	neurofilament
NGS	normal goat serum

NO	nitric oxide
NSE	neurone-specific enolase
P	post natal age (days)
PAP	peroxidase anti-peroxidase
PCR	polymerase chain reaction
PLP	proteolipid protein
PMD	Pelizaeus-Merzbacher disease
PMP22	peripheral myelin protein gene 22
Pol II	RNA polymerase II
RER	rough endoplasmic reticulum
RNA	ribonucleic acid
RNAaseA	RibonucleaseA
rpm	revolutions per minute
ROS	reactive oxygen species
RS	rabbit serum
SLI	Scmidt-Lanterman incisure
snRNP	small nucleur ribnonucleoprotein
S-MAG	small isoform of myelin associated glycoprotein
SPG1	spastic paraplegia gene locus 1
SPG2	spastic paraplegia gene locus 2
SSC	standard sodium citrate buffer
STAR protein	signal transduction and activator of RNA
STW	sterile distilled, deionised water
TAE buffer	Tris acetate EDTA buffer
TBS	Tris buffered saline
THR	thyroid hormone receptor
TLCK	N α -p- tosyl-L-lysine chloro-methyl ketone
TMEV	Theiler`s murine encephaloyelitis virus

TXR

Texas red

UV

ultra violet

10. References

- AGRAWAL, H.C. & AGRAWAL, D. (1991) Proteolipid protein and DM-20 are synthesized by Schwann cells, present in myelin membrane, but they are not fatty acylated. *Neurochemical Research* **16**, 855-858.
- AGUAYO, A.J., BRAY, G.M. & PERKINS, S.C. (1979) Axon-Schwann cell relationships in neuropathies of mutant mice. *Annals of the New York Academy of Sciences* **317**, 512-531.
- AGUAYO, A.J., KASARJIAN, J., SKAMENE, E., KONGSHAVN, P. & BRAY, G.M. (1977) Myelination of mouse axons by Schwann cells transplanted from normal and abnormal human nerves. *Nature* **268**, 753-755.
- ALLEN I.V., KIRK J. (1997) The anatomical and molecular pathology of multiple sclerosis. In *Molecular biology of multiple sclerosis* (edited by RUSSELL, W.C.), pp. 9-22. Chichester: John Wiley & Sons Ltd.
- ARMSTRONG, R.C., KIM, J.G. & HUDSON, L.D. (1995) Expression of myelin transcription factor I (MyTI), a "zinc-finger" DNA-Binding protein, in developing oligodendrocytes. *Glia* **14**, 303-321.
- BALMAIN, A., KRUMLAUF, R., VASS, J.K. & BIRNIE, G.D. (1982) Cloning and characterisation of the abundant cytoplasmic 7S RNA from mouse cells. *Nucleic Acids Research* **10**, 4259-4277.
- BARRES, B.A., LAZAR, M.A. & RAFF, M.C. (1994) A novel role for thyroid hormone, glucocorticoids and retinoic acid in timing oligodendrocyte development. *Development* **120**, 1097-1108.
- BELMONT, J.W. (1996) Genetic control of X inactivation and processes leading to X-inactivation skewing. *Am J Hum Genet* **58**, 1101-1108.
- BENJAMINS, J.A., STUDZINSKI, D.M. & SKOFF, R.P. (1994) Analysis of myelin proteolipid protein and F₀ ATPase subunit 9 in normal and *jimpy* CNS. *Neurochemical Research* **19**, 1013-1022.
- BERNDT, J., KIM, J.G. & HUDSON, L.D. (1992) Identification of *cis*-regulatory elements in the myelin proteolipid protein (PLP) gene. *Journal of Biological Chemistry* **267**, 14730-14737.
- BIGNAMI A., DAHL D. (1995) Gliosis. In *Neuroglia* (edited by KETTENMANN, H., RANSOM, B.R.), pp. 843-858. Oxford: Oxford University Press.

- BIRNBOIM, H.C. & DOLY, J. (1979) A rapid alkaline extraction procedure for screening recombinant plasmid DNA. *Nucleic Acids Research* **7**, 1513-1523.
- BIZZOZERO, O.A. & GOOD, L.K. (1991) Rapid metabolism of fatty acids covalently bound to myelin proteolipid protein. *Journal of Biological Chemistry* **266**, 17092-17098.
- BLAKEMORE, W.F. (1972) Observations on oligodendrocyte degeneration, the resolution of status spongiosus and remyelination in cuprizone intoxication in mice. *Journal of Neurocytology* **1**, 413-426.
- BLAKEMORE, W.F. (1984) The response of oligodendrocytes to chemical injury. *Acta Neurologica Scandinavica* **70 (suppl 100)**, 33-38.
- BOESPFLUG-TANGUY, O., MIMAULT, C., MELKI, J., CAVAGNA, A., GIRAUD, G., PHAM-DINH, D., DASTUGUE, B., DAUTIGNY, A. & PMD CLINICAL GROUP, (1994) Genetic homogeneity of Pelizaeus-Merzbacher disease: Tight linkage to the proteolipoprotein locus in 16 affected families. *Am J Hum Genet* **55**, 461-467.
- BOISON, D. & STOFFEL, W. (1994) Disruption of the compacted myelin sheath of axons of the central nervous system in proteolipid protein-deficient mice. *Proceedings of the National Academy of Sciences USA* **91**, 11709-11713.
- BONNEAU, D., ROZET, J.-M., BULTEAU, C., BERTHIER, M., METTEY, R., GIL, R., MUNNICH, A. & LE MERRER, M. (1993) X-linked spastic paraplegia (SPG2): clinical heterogeneity at a single locus. *J Med Genet* **30**, 381-384.
- BRADLEY, W.G. & JENKISON, M. (1973) Abnormalities of peripheral nerves in murine muscular dystrophy. *Journal of the Neurological Sciences* **18**, 227-247.
- BRONSTEIN, J.M., POPPER, P., MICEVYCH, P.E. & FARBER, D.B. (1996) Isolation and characterization of a novel oligodendrocyte-specific protein. *Neurology* **47**, 772-778.
- BROWN, M.C., BESIO MORENO, M., BONGARZONE, E.R., COHEN, P.D., SOTO, E.F. & PASQUINI, J.M. (1993) Vesicular transport of myelin proteolipid and cerebroside sulfates to the myelin membrane. *Journal of Neuroscience Research* **35**, 402-408.

- BROWN T. (1997) Preparation and analysis of DNA. In *Current protocols in molecular biology* (edited by AUSUBEL, F.M.), New York: John Wiley and Sons Ltd.
- BRUYN, G.W., WEENINK, H.R., BOTS, G.T.A.M., TEEPEN, J.L.J.M. & VAN WOLFEREN, W.J.A. (1985) Pelizaeus-Merzbacher disease (The Lowenberg-Hill type). *Acta Neuropathologica (Berlin)* **67**, 177-189.
- BUNGE R.P., FERNANDEZ-VALLE C. (1995) Basic biology of the Schwann cell. In *Neuroglia* (edited by KETTENMANN, H., RANSOM, B.R.), pp. 44-57. Oxford: Oxford University Press.
- BUTT, A.M., IBRAHIM, M., RUGE, F.M. & BERRY, M. (1995) Biochemical subtypes of oligodendrocyte in the anterior medullary velum of the rat as revealed by the monoclonal antibody Rip. *Glia* **14**, 185-197.
- CAMBI, F., TANG, X.M., CORDRAY, P., FAIN, P.R., KEPPEN, L.D. & BARKER, D.F. (1996) Refined genetic mapping and proteolipid protein mutation analysis in X-linked pure hereditary spastic paraplegia. *Neurology* **46**, 1112-1117.
- CAMP, C.D. & LOWENBERG, K. (1941) An american family with pelizaeus-Merzbacher disease. *Archives of Neurology and Psychiatry* **45**, 261-264.
- CAMPAGNONI, A.T. (1988) Molecular biology of myelin proteins from the central nervous system. *Journal of Neurochemistry* **51**, 1-14.
- CAMPAGNONI, C.W., GARBAY, B., MICEVYCH, P., PRIBYL, T., KAMPF, K., HANDLEY, V.W. & CAMPAGNONI, A.T. (1992) DM20 mRNA splice product of the myelin proteolipid protein gene is expressed in the murine heart. *Journal of Neuroscience Research* **33**, 148-155.
- CARANGO, P., FUNANAGE, V.L., QUIROS, R.E., DEBRUYN, C.S. & MARKS, H.G. (1995) Overexpression of DM20 messenger RNA in two brothers with Pelizaeus-Merzbacher disease. *Annals of Neurology* **38**, 610-617.
- CARSON, M.J., BEHRINGER, R.R., BRINSTER, R.L. & MCMORRIS, F.A. (1993) Insulin-like growth factor I increases brain growth and central nervous system myelination in transgenic mice. *Neuron* **10**, 729-740.
- CHARRON, G., GUY, L.G., BAZINET, M. & JULIEN, J.P. (1995) Multiple neuron-specific enhancers in the gene coding for the human neurofilament light chain. *Journal of Biological Chemistry* **270**, 30604-30610.

- CHIANG, C.S., POWELL, H.C., GOLD, L.H., SAMIMI, A. & CAMPBELL, I.L. (1996) Macrophage microglial-mediated primary demyelination and motor disease induced by the central nervous system production of interleukin-3 in transgenic mice. *Journal of Clinical Investigation* **97**, 1512-1524.
- CHOMCZYNSKI, P. & SACCHI, N. (1987) Single-step method of RNA isolation by acid guanidinium-thiocyanate-phenol-chloroform extraction. *Annals of Biochemistry* **162**, 156-159.
- CLARK, A.J., BISINGER, P., BULLOCK, D.W., DAMAK, S., WALLACE, R., WHITELAW, C.B.A. & YULL, F. (1994) Chromosomal position effects and the modulation of transgene expression. *Reproduction Fertility and Development* **6**, 589-598.
- COETZEE, T., FUJITA, N., DUPREE, J., SHI, R., BLIGHT, A., SUZUKI, K. & POPKO, B. (1996) Myelination in the absence of galactocerebroside and sulfatide: Normal structure with abnormal function and regional instability. *Cell* **86**, 209-219.
- COLMAN D.R., DOYLE J.P., D'URSO D., KITAGAWA K., PEDRAZA L., YOSHIDA M., FANNON A.M. (1996) Speculations on myelin sheath evolution. In *Glial Cell Development: basic principles and clinical relevance* (edited by JESSEN, K.R., RICHARDSON, W.D.), pp. 85-100. Oxford: BIOS Scientific Publishers Limited.
- COLMAN, D.R., KREIBICH, G., FREY, A.B. & SABATINI, D.D. (1982) Synthesis and incorporation of myelin polypeptides into CNS myelin. *Journal of Cell Biology* **95**, 598-608.
- COOK, J.L., IRIAS-DONAGHEY, S. & DEININGER, P.L. (1992) Regulation of rodent myelin proteolipid protein gene expression. *Neuroscience Letters* **137**, 56-60.
- COX, K.H., DELEON, D.V., ANGERER, L.M. & ANGERER, R.C. (1984) Detection of mRNAs in sea urchin embryos by in situ hybridization using asymmetric RNA probes. *Developmental Biology* **101**, 485-502.
- CREMERS, F.P.M., PFEIFFER, R.A., VAN DE POL, T.J.R., HOFKER, M.H., KRUSE, T.A., WIERINGA, B. & ROPERS, H.H. (1987) An interstitial duplication of the X chromosome in a male allows physical fine mapping of probes from the Xq13-q22 region. *Human Genetics* **77**, 23-27.

- CUNLIFFE-BEAMER T.L., LES E.P. (1987) The laboratory mouse. In *The UFAW handbook on the care and management of laboratory animals* (edited by POOLE, T.), pp. 275-308. Harlow: Longman Scientific and Technical.
- CUZNER, M.L. & NORTON, W.T. (1996) Biochemistry of demyelination. *Brain Pathology* **6**, 231-242.
- DANIEL, J. (1996) Measuring the toxic effects of high gene dosage on yeast cells. *Molecular General Genetics* **253**, 393-396.
- DANIELSON, P.E., FORSS-PETTER, S., BROW, M.A., CALAVETTA, L., DOUGLASS, J., MILNER, R.J. & SUTCLIFFE, J.G. (1988) p1B15: a cDNA clone of the rat mRNA encoding cyclophilin. *DNA* **7**, 261-267.
- DARLING D.C., BRICKELL P.M. (1994) Electrophoresis of RNA and northern blotting. In *Nucleic acid blotting: the basics* (edited by DARLING, D.C., BRICKNELL, P.M.), pp. 45-60. Oxford: IRL Press.
- DE ANGELIS, D.A. & BRAUN, P.E. (1996) 2',3'-cyclic nucleotide 3'-phosphodiesterase binds to actin-based cytoskeletal elements in an isoprenylation-independent manner. *Journal of Neurochemistry* **67**, 943-951.
- DE WAEGH, S.M., LEE, V.M.-Y. & BRADY, S.T. (1992) Local modulation of neurofilament phosphorylation, axonal caliber, and slow axonal transport by myelinating Schwann cells. *Cell* **68**, 451-463.
- Dickinson, P.J. (1995) Developmental expression of the proteolipid protein gene in the nervous system. Faculty of Veterinary Medicine, University of Glasgow, p83.
- DICKINSON, P.J., FANARRAGA, M.L., GRIFFITHS, I.R., BARRIE, J.A., KYRIAKIDES, E. & MONTAGUE, P. (1996) Oligodendrocyte progenitors in the embryonic spinal cord express DM-20. *Neuropathology and Applied Neurobiology* **22**, 188-198.
- DICKINSON, P.J., GRIFFITHS, I.R., BARRIE, J.A., KYRIAKIDES, E., POLLOCK, G.S., BARNETT, S.C., BARRIE, J.M. & POLLOCK, G.F. (1997) Expression of the *dm-20* isoform of the *plp* gene in olfactory nerve ensheathing cells: evidence from developmental studies. *Journal of Neurocytology* **26**, 181-189.
- DIEHL, H., SCHAICH, M., BUDZINSKI, R. & STOFFEL, W. (1986) Individual exons encode the integral membrane domains of human proteolipid protein. *Proceedings of the National Academy of Sciences USA* **83**, 9807-9811.

- DIJKSTRA, C.D., DE GROOT, C.J.A. & HUITINGA, I. (1992) The role of macrophages in demyelination. *Journal of Neuroimmunology* **40**, 183-188.
- DOYLE, J.P. & COLMAN, D.R. (1993) Glial-neuron interactions and the regulation of myelin formation. *Current Opinion in Cell Biology* **5**, 779-785.
- DUBOIS-DALCQ, M., BEHAR, T., HUDSON, L.D. & LAZZARINI, R.A. (1986) Emergence of three myelin proteins in oligodendrocytes cultured without neurons. *Journal of Cell Biology* **102**, 384-392.
- DUNCAN, I.D., HAMMANG, J.P., GODA, S. & QUARLES, R.H. (1989) Myelination in the jimpy mouse in the absence of proteolipid protein. *Glia* **2**, 148-154.
- DUNCAN, I.D., HAMMANG, J.P. & TRAPP, B.D. (1987) Abnormal compact myelin in the myelin-deficient rat: absence of proteolipid protein correlates with a defect in the intraperiod line. *Proceedings of the National Academy of Sciences USA* **84**, 6287-6291.
- EBERSOLE, T.A., CHEN, Q., JUSTICE, M.J. & ARTZT, K. (1996) The *quaking* gene product necessary in embryogenesis and myelination combines features of RNA binding and signal transduction proteins. *Nature Genetics* **12**, 260-265.
- ELLIS, D. & MALCOLM, S. (1994) Proteolipid protein gene dosage effect in Pelizaeus-Merzbacher disease. *Nature Genetics* **6**, 333-334.
- ENGELKAMP, D. & VAN HEYNINGEN, V. (1996) Transcription factors in disease. *Curr Opin Genet Dev* **6**, 334-342.
- ERICKSON, R.P. (1996) Mouse models of human genetic disease: Which mouse is more like a man? *BioEssays* **18**, 993-998.
- FANNON, A.M., MASTRONARDI, F.G. & MOSCARELLO, M.A. (1994) Isolation and identification of proteolipid proteins in *jimpy* mouse brain. *Neurochemical Research* **19**, 1005-1012.
- FERGUSON, B., MATYSZAK, M.K., ESIRI, M.M. & PERRY, V.H. (1997) Axonal damage in acute multiple sclerosis lesions. *Brain* **120**, 393-399.
- FOLCH, J. & LEES, M. (1951) Proteolipids, a new type of tissue lipoproteins. *Journal of Biological Chemistry* **191**, 807-817.

- FRAHER, J.P. (1992) The CNS-PNS transitional zone of the rat. Morphometric studies at cranial and spinal levels. *Progress in Neurobiology* **38**, 261-316.
- FRAICHARD, A., CHASSANDE, O., BILBAUT, G., DEHAY, C., SAVATIER, P. & SAMARUT, J. (1995) In vitro differentiation of embryonic stem cells into glial cells and functional neurons. *Journal of Cell Science* **108**, 3181-3188.
- FUJIWARA K. (1994) Mouse hepatitis virus. In *Virus infections of rodents and langomorphs* (edited by OSTERHAUS, A.D.M.E.), pp. 249-257. Amsterdam: Elsevier Science BV.
- GAO, F.B., DURAND, B. & RAFF, M. (1997) Oligodendrocyte precursor cells count time but not cell divisions before differentiation. *Current Biology* **7**, 152-155.
- GARDINIER, M.V., MACKLIN, W.B., DINIAK, A.J. & DEININGER, P.L. (1986) Characterization of myelin proteolipid mRNAs in normal and jimpy mice. *Mol Cell Biol* **6**, 3755-3762.
- GEHRMANN J., KREUTZBERG G.W. (1995) Microglia in experimental neuropathology. In *Neuroglia* (edited by KETTENMANN, H., RANSOM, B.R.), pp. 883-904. Oxford: Oxford University Press.
- GHANDOUR, M.S. & SKOFF, R.P. (1988) Expression of galactocerebroside in developing normal and jimpy oligodendrocytes *in situ*. *Journal of Neurocytology* **17**, 485-498.
- GIESE, K.P., MARTINI, R., LEMKE, G., SORIANO, P. & SCHACHNER, M. (1992) Mouse *P0* gene disruption leads to hypomyelination, abnormal expression of recognition molecules, and degeneration of myelin and axons. *Cell* **71**, 565-576.
- GOUDREAU, G., CARPENTER, S., BEAULIEU, N. & JOLICOEUR, P. (1996) Vacuolar myelopathy in transgenic mice expressing human immunodeficiency virus type 1 proteins under the regulation of the myelin basic protein gene promoter. *Nature Medicine* **2**, 655-661.
- GOUT, O., DE SANTO, R., ARNHEITER, H., HUDSON, L.D. & DUBOIS-DALCQ, M. (1991) A transgenic tag for tracking transplanted glial cells. *Society for Neuroscience Abstracts* **17**, 157.9 (Abstract).
- GOW, A., FRIEDRICH, V.L., JR. & LAZZARINI, R.A. (1994) Many naturally occurring mutations of myelin proteolipid protein impair its intracellular transport. *Journal of Neuroscience Research* **37**, 574-583.

- GOW, A., FRIEDRICH, V.L., JR. & LAZZARINI, R.A. (1994) Intracellular transport and sorting of the oligodendrocyte transmembrane proteolipid protein. *Journal of Neuroscience Research* **37**, 563-573.
- GOW, A., GRAGEROV, A., GARD, A.L., COLMAN, D.R., LAZZARINI, R.A. & GARD, A. (1997) Conservation of topology, but not conformation, of the proteolipid proteins of the myelin sheath. *Journal of Neuroscience* **17**, 181-189.
- GOW, A. & LAZZARINI, R.A. (1996) A cellular mechanism governing the severity of Pelizaeus-Merzbacher disease. *Nature Genetics* **13**, 422-428.
- GRAVEL, M., PETERSON, J., YONG, V.W., KOTTIS, V., TRAPP, B. & BRAUN, P.E. (1996) Overexpression of 2',3'-cyclic nucleotide 3'-phosphodiesterase in transgenic mice alters oligodendrocyte development and produces aberrant myelination. *Molecular and Cellular Neuroscience* **7**, 453-466.
- GREENBERG M.E., BENDER T.P. (1997) Preparation and analysis of RNA. In *Current protocols in molecular biology* (edited by AUSUBEL, F.M.), New York: John Wiley and Sons Ltd.
- GREER, J.M., DYER, C.A., PAKASKI, M., SYMONOWICZ, C. & LEES, M.B. (1996) Orientation of myelin proteolipid protein in the oligodendrocyte cell membrane. *Neurochemical Research* **21**, 431-440.
- GRIFFITHS, I.R., DICKINSON, P. & MONTAGUE, P. (1995) Expression of the proteolipid protein gene in glial cells of the post-natal peripheral nervous system of rodents. *Neuropathology and Applied Neurobiology* **21**, 97-110.
- GRINSPAN, J., WRABETZ, L. & KAMHOLZ, J. (1993) Oligodendrocyte maturation and myelin gene expression in PDGF-treated cultures from rat cerebral white matter. *Journal of Neurocytology* **22**, 322-333.
- HARDING, A.E. (1983) Classification of the hereditary ataxias and paraplegias. *Lancet* **1**, 1151-115.
- HARTMAN, B.K., AGRAWAL, H.C., AGRAWAL, D. & KALMBACH, S. (1982) Development and maturation of central nervous system myelin: comparison of immunohistochemical localization of proteolipid protein and basic protein in myelin

and oligodendrocytes. *Proceedings of the National Academy of Sciences USA* **79**, 4217-4220.

HARVEY C., ECCLES S.J., HENTSCHEL C.C.G. (1992) Expression of genes in mammalian cells. In *Transgenesis: applications of genetic transfer* (edited by MURRAY, J.A.H.), pp. 131-153. Chichester: John Wiley and Sons Ltd.

HAYASHI, S. (1978) Acetylation of chromosome squashes of *Drosophila melanogaster* decreases the background in autoradiographs from hybridization with ¹²⁵I-labelled RNA. *Journal of Histochemistry and Cytochemistry* **36**, 677-679.

HERNANDEZ, J.M.V., DALMAU, I., GONZALEZ, B. & CASTELLANO, B. (1997) Abnormal expression of the proliferating cell nuclear antigen (PCNA) in the spinal cord of the hypomyelinated jimpy mutant mice. *Brain Research* **747**, 130-139.

HIRANO, A., SAX, D.S. & ZIMMERMAN, H.M. (1969) The fine structure of the cerebella of jimpy mice and their "normal" litter mates. *Journal of Neuropathology and Experimental Neurology* **28**, 388-400.

HODES, M.E., DEMYER, W.E., PRATT, V.M., EDWARDS, M.K. & DLOUHY, S.R. (1995) Girl with signs of Pelizaeus-Merzbacher disease heterozygous for a mutation in exon 2 of the proteolipid protein gene. *American Journal of Medical Genetics* **55**, 397-401.

HODES, M.E. & DLOUHY, S.R. (1996) The proteolipid protein gene: double, double, ... and trouble. *Am J Hum Genet* **59**, 12-15.

HODES, M.E., PRATT, V.M. & DLOUHY, S.R. (1993) Genetics of Pelizaeus-Merzbacher disease. *Developmental Neuroscience* **15**, 383-394.

HOLZ, A., SCHAEREN-WIEMERS, N., SCHAEFER, C., POTT, U., COLELLO, R.J. & SCHWAB, M.E. (1996) Molecular and developmental characterization of novel cDNAs of the myelin-associated oligodendrocytic basic protein. *Journal of Neuroscience* **16**, 467-477.

HUDSON, L.D., FRIEDRICH, V.L., JR., BEHAR, T., DUBOIS-DALCQ, M. & LAZZARINI, R.A. (1989) The initial events in myelin synthesis: orientation of proteolipid protein in the plasma membrane of cultured oligodendrocytes. *Journal of Cell Biology* **109**, 717-727.

- HUDSON L.D., KO N., KIM J.G. (1996) Control of myelin gene expression. In *Glial Cell Development: basic principles and clinical relevance* (edited by JESSEN, K.R., RICHARDSON, W.D.), pp. 101-121. Oxford: Bios Scientific Publishers.
- HUDSON L.D., NADON N.L. (1992) Amino acid substitutions in proteolipid protein that cause dysmyelination. In *Myelin: Biology and Chemistry* (edited by MARTENSON, R.E.), pp. 677-702. Boca Raton: CRC Press.
- HUDSON, L.D., PUCKETT, C., BERNDT, J., CHAN, J. & GENIC, S. (1989) Mutation of the proteolipid protein gene PLP in a human X chromosome-linked myelin disorder. *Proceedings of the National Academy of Sciences USA* **86**, 8128-8131.
- HUXLEY, C., PASSAGE, E., MANSON, A., PUTZU, G., FIGARELLA-BRANGER, D., PELLISSIER, J.F. & FONTÉS, M. (1996) Construction of a mouse model of Charcot-Marie-Tooth disease type 1A by pronuclear injection of human YAC DNA. *Human Molecular Genetics* **5**, 563-569.
- IKENAKA, K., FURUICHI, T., IWASAKI, Y., MORIGUCHI, A., OKANO, H. & MIKOSHIBA, K. (1988) Myelin proteolipid protein gene structure and its regulation of expression in normal and *jimpy* mutant mice. *Journal of Molecular Biology* **199**, 587-596.
- IKENAKA, K. & KAGAWA, T. (1995) Transgenic systems in studying myelin gene expression. *Developmental Neuroscience* **17**, 127-136.
- IKENAKA, K., KAGAWA, T. & MIKOSHIBA, K. (1992) Selective expression of DM-20, an alternatively spliced myelin proteolipid protein gene product, in developing nervous system and in non-glial cells. *Journal of Neurochemistry* **58**, 2248-2253.
- INOUE, K., OSAKA, H., SUGIYAMA, N., KAWANISHI, C., ONISHI, H., NEZU, A., KIMURA, K., KIMURA, S., YAMADA, Y. & KOSAKA, K. (1996) A duplicated *PLP* gene causing Pelizaeus-Merzbacher disease detected by comparative multiplex PCR. *Am J Hum Genet* **59**, 32-39.
- INOUE, Y., KAGAWA, T., MATSUMURA, Y., IKENAKA, K. & MIKOSHIBA, K. (1996) Cell death of oligodendrocytes or demyelination induced by overexpression of proteolipid protein depending on expressed gene dosage. *Neuroscience Research* **25**, 161-172.

- JANZ, R. & STOFFEL, W. (1993) Characterization of a brain-specific Sp 1-like activity interacting with an unusual binding site within the myelin proteolipid protein promoter. *Biol Chem Hoppe Seyler* **374**, 507-517.
- JAQUET, V., GOW, A., TOSIC, M., SUCHANEK, G., BREITSCHOPF, H., LASSMANN, H., LAZZARINI, R.A. & MATTHIEU, J.M. (1996) An antisense transgenic strategy to inhibit the myelin oligodendrocyte glycoprotein synthesis. *Molecular Brain Research* **43**, 333-337.
- JOHNSON, R.S., RODER, J.C. & RIORDAN, J.R. (1995) Over-expression of the DM-20 myelin proteolipid causes central nervous system demyelination in transgenic mice. *Journal of Neurochemistry* **64**, 967-976.
- JOUET, M., ROSENTHAL, A., ARMSTRONG, G., MACFARLANE, J., STEVENSON, R., PATERSON, J., METZENBERG, A., IONASESCU, V., TEMPLE, K. & KENWRICK, S. (1994) X-linked spastic paraplegia (SPG1), MASA syndrome and X-linked hydrocephalus result from mutations in the *L1* gene. *Nature Genetics* **7**, 402-407.
- KAGAWA, T., IKENAKA, K., INOUE, Y., KURIYAMA, S., TSUJII, T., NAKAO, J., NAKAJIMA, K., ARUGA, J., OKANO, H. & MIKOSHIBA, K. (1994) Glial cell degeneration and hypomyelination caused by overexpression of myelin proteolipid protein gene. *Neuron* **13**, 427-442.
- KAMHOLZ, J., SESSA, M., SCHERER, S., VOGELBACKER, H., MOKUNO, K., BARON, P., WRABETZ, L., SHY, M. & PLEASURE, D. (1992) Structure and expression of proteolipid protein in the peripheral nervous system. *Journal of Neuroscience Research* **31**, 231-244.
- KERNER, A.L. & CARSON, J.H. (1984) Effect of the jimpy mutation on expression of myelin proteins in heterozygous and hemizygous mouse brain. *Journal of Neurochemistry* **43**, 1706-1715.
- KIDD, G.J., HAUER, P.E. & TRAPP, B.D. (1990) Axons modulate myelin protein messenger RNA levels during central nervous system myelination in vivo. *Journal of Neuroscience Research* **26**, 409-418.
- KIRCHHOFF, F., OHLEMEYER, C. & KETTENMANN, H. (1997) Expression of myelin-associated glycoprotein transcripts in murine oligodendrocytes. *Neuroscience* **78**, 561-570.

- KIRKPATRICK, L.L. & BRADY, S.T. (1994) Modulation of the axonal microtubule cytoskeleton by myelinating Schwann cells. *Journal of Neuroscience* **14**, 7440-7450.
- KITAGAWA, K., SINOWAY, M.P., YANG, C., GOULD, R.M. & COLMAN, D.R. (1993) A proteolipid protein gene family: Expression in sharks and rays and possible evolution from an ancestral gene encoding a pore-forming polypeptide. *Neuron* **11**, 433-448.
- KLUGMANN, M., SHWAB, M., PÜHLHOFER, A., SCHNEIDER, A., ZIMMERMANN, F., GRIFFITHS, I.R. & NAVE, K. (1997) Assembly of CNS myelin in the absence of proteolipid protein. *Neuron* **18**, 59-70.
- KNAPP, P.E. (1996) Proteolipid protein: Is it more than just a structural component of myelin. *Developmental Neuroscience* **18**, 297-308.
- KNAPP, P.E., BENJAMINS, J.A. & SKOFF, R.P. (1996) Epigenetic factors up-regulate expression of myelin proteins in the dysmyelinating jimpy mutant mouse. *Journal of Neurobiology* **29**, 138-150.
- KNAPP, P.E. & SKOFF, R.P. (1993) Jimpy mutation affects astrocytes: Lengthening of the cell cycle in vitro. *Developmental Neuroscience* **15**, 31-36.
- KOBAYASHI, H., GARCIA, C.A., ALFONSO, G., MARKS, H.G. & HOFFMAN, E.P. (1996) Molecular genetics of familial spastic paraplegia: A multitude of responsible genes. *Journal of the Neurological Sciences* **137**, 131-138.
- KOBAYASHI, H., HOFFMAN, E.P. & MARKS, H.G. (1994) The *rumpshaker* mutation in spastic paraplegia. *Nature Genetics* **7**, 351-352.
- KOLLIAS G., GROSVELD F. (1992) The study of gene regulation in transgenic mice. In *Transgenic animals* (edited by GROSVELD, F., KOLLIAS, G.), pp. 79-98. London: Academic Press Limited.
- KONOLA, J.T., YAMAMURA, T., TYLER, B. & LEES, M.B. (1992) Orientation of the myelin proteolipid protein C-terminus in oligodendroglial membranes. *Glia* **5**, 112-121.
- KRONQUIST, K.E., CRANDALL, B.F., MACKLIN, W.B. & CAMPAGNONI, A.T. (1987) Expression of myelin proteins in the developing human spinal cord: cloning and sequencing of human proteolipid protein cDNA. *Journal of Neuroscience Research* **18**, 395-401.

- LACHAPELLE, F. (1995) Glial transplants: An *in vivo* analysis of extrinsic and intrinsic determinants of dysmyelination in genetic variants. *Brain Pathology* **5**, 289-299.
- LASSMANN, H., BARTSCH, U., MONTAG, D. & SCHACHNER, M. (1997) Dying-back oligodendroglipathy: A late sequel of myelin-associated glycoprotein deficiency. *Glia* **19**, 104-110.
- LAURSEN, R.A., SAMIULLAH, M. & LEES, M.B. (1984) The structure of bovine brain myelin proteolipid and its organization in myelin. *Proceedings of the National Academy of Sciences USA* **81**, 2912-2916.
- LEE, M.K., MARSZALEK, J.R. & CLEVELAND, D.W. (1994) A mutant neurofilament subunit causes massive, selective motor neuron death: Implications for the pathogenesis of human motor neuron disease. *Neuron* **13**, 975-988.
- LEES M.B., BROSTOFF S.W. (1984) Proteins of myelin. In *Myelin* (edited by MORELL, P.), pp. 197-224. New York: Plenum Press.
- LEFEBVRE, V., ZHOU, G., MUKHOPADHYAY, K., SMITH, C.N., ZHANG, Z., EBERSPAECHER, H., ZHOU, X., MAITY, S.N. & DE CROMBRUGGHE, B. (1996) An 18-base pair sequence in the mouse pro α 1(II) collagen gene is sufficient for expression in cartilage and binds nuclear proteins that are selectively expressed in chondrocytes. *Mol Cell Biol* **16**, 4512-4523.
- LEMKE, G., LAMAR, E. & PATTERSON, J. (1988) Isolation and analysis of the gene encoding peripheral myelin protein zero. *Neuron* **1**, 73-83.
- LINDSEY J.R., BOORMAN G.A., COLLINS M.J., HSU C., VAN HOOSIER G.L., WAGNER J.E. (1991) Central nervous system. In *Infectious diseases of rats and mice* (edited by LINDSEY, J.R., BOORMAN, G.A., COLLINS, M.J., HSU, C., VAN HOOSIER, G.L., WAGNER, J.E.), pp. 223-230. Washington: National Acedemy Press.
- LIPTON H.L., ROZHON E.J., BANDYOPADHYAY P. (1994) Picornavirus infections. In *Virus infections of rodents and langomorphs* (edited by OSTERHAUS, A.D.M.E.), pp. 373-385. Amsterdam: Elsevier Science BV.
- LOWENBERG, K. & HILL, T.S. (1933) Diffuse sclerosis with preserved myelin islands. *Archives of Neurology and Psychiatry* **29**, 1232-1245.

- LUDWIN S.K. (1995) Pathology of the myelin sheath. In *The axon* (edited by WAXMAN, S.G., KOCSIS, J.D., STYS, P.K.), pp. 412-437. Oxford: Oxford University Press.
- LUDWIN, S.K. (1997) The pathobiology of the oligodendrocyte. *Journal of Neuropathology and Experimental Neurology* **56**, 111-124.
- MACKLIN, W.B., BRAUN, P.E. & LEES, M.B. (1982) Electroblot analysis of the myelin proteolipid protein. *Journal of Neuroscience Research* **7**, 1-10.
- MACKLIN, W.B., CAMPAGNONI, A.T., DEININGER, P.L. & GARDINIER, M.V. (1987) Structure and expression of the mouse proteolipid protein gene. *Journal of Neuroscience Research* **18**, 383-394.
- MACKLIN, W.B., GARDINIER, M.V., OBESO, Z.O., KING, K.D. & WIGHT, P.A. (1991) Mutations in the myelin proteolipid protein gene alter oligodendrocyte gene expression in jimpy and jimpy^{msd} mice. *Journal of Neurochemistry* **56**, 163-171.
- MARTINI, R., MOHAJERI, M.H., KASPER, S., GIESE, K.P. & SCHACHNER, M. (1995) Mice doubly deficient in the genes for P0 and myelin basic protein show that both proteins contribute to the formation of the major dense line in peripheral nerve myelin. *Journal of Neuroscience* **15**, 4488-4495.
- MASON P.J., ENVER T., WILKINSON D., WILLIAMS J.G. (1993) Assay of gene transcription *in vivo*. In *Gene transcription* (edited by HAMES, B.D., HIGGINS, S.J.), pp. 5-64. Oxford: IRL Press.
- MASTRONARDI, F.G., ACKERLEY, C.A., ARSENAULT, L., ROOTS, B.I. & MOSCARELLO, M.A. (1993) Demyelination in a transgenic mouse: A model for multiple sclerosis. *Journal of Neuroscience Research* **36**, 315-324.
- MATTEI, M.G., ALLIEL, P.M., DAUTIGNY, A., PASSAGE, E., PHAM-DINH, D., MATTEI, J.F. & JOLLES, P. (1986) The gene encoding for the major brain proteolipid (PLP) maps on the q-22 band of the human X chromosome. *Human Genetics* **72**, 352-353.
- MAYCOX, P.R., ORTUÑO, D., BURROLA, P., KUHN, R., BIERI, P.L., ARREZO, J.C. & LEMKE, G. (1997) A transgenic mouse model for human hereditary neuropathy with liability to pressure palsies. *Molecular and Cellular Neuroscience* **8**, 405-416.

- MCDONALD, W.I. (1994) Rachele Fishman-Matthew Moore Lecture. The pathological and clinical dynamics of multiple sclerosis. *J Neuropathol Exp Neurol* **53**, 338-343.
- MENTABERRY, A., ADESNIK, M., ATCHISON, M., NORGDARD, E.M., ALVAREZ, F., SABATINI, D.D. & COLMAN, D.R. (1986) Small basic proteins of myelin from central and peripheral nervous systems are encoded by the same gene. *Proceedings of the National Academy of Sciences USA* **83**, 1111-1114.
- MILNER, R.J., LAI, C., NAVE, K., LENOIR, D., OGATA, J. & SUTCLIFFE, J.G. (1985) Nucleotide sequence of two mRNAs for rat brain myelin proteolipid protein. *Cell* **42**, 931-939.
- MIMAUT, C., CAILLOUX, F., GIRAUD, G., DASTUGUE, B. & BOESPFLUG-TANGUY, O. (1995) Dinucleotide repeat polymorphism in the proteolipoprotein (PLP) gene. *Human Genetics* **96**, 236-
- MINUK, J. & BRAUN, P.E. (1996) Differential intracellular sorting of the myelin-associated glycoprotein isoforms. *Journal of Neuroscience Research* **44**, 411-420.
- MITCHELL, L.S., GILLESPIE, C.S., MCALLISTER, F., FANARRAGA, M., KIRKHAM, D., KELLY, B., BROPHY, P.J., GRIFFITHS, I.R., MONTAGUE, P. & KENNEDY, P.G.E. (1992) Developmental expression of the major myelin protein genes in the CNS of the X-linked hypomyelinating mutant rumpshaker. *Journal of Neuroscience Research* **33**, 205-217.
- MONTAGUE, P., DICKINSON, P.J., MCCALLION, A.S., STEWART, G.J., SAVIOZ, A., DAVIES, R.W., KENNEDY, P.G.E., GRIFFITHS, I.R. (1997) Developmental expression of the murine *Mobp* gene. *Journal of Neuroscience Research* [In Press]
- MONTAGUE P., GRIFFITHS I.R. (1997) Molecular biology of the glia: components of myelin-PLP and minor myelin proteins. In *Molecular Biology of Multiple Sclerosis* (edited by RUSSELL, W.C.), pp. 55-69. Chichester: J.Wiley & Sons.
- NADON, N.L., ARNHEITER, H. & HUDSON, L.D. (1994) A combination of PLP and DM20 transgenes promotes partial myelination in the jimpy mouse. *Journal of Neurochemistry* **63**, 822-833.

- NADON, N.L. & DUNCAN, I.D. (1996) Molecular analysis of glial cell development in the canine 'shaking pup' mutant. *Developmental Neuroscience* **18**, 174-184.
- NAKAJIMA, K., IKENAKA, K., KAGAWA, T., ARUGA, J., NAKAO, J., NAKAHIRA, K., SHIOTA, C., KIM, S.U. & MIKOSHIBA, K. (1993) Novel isoforms of mouse myelin basic protein predominantly expressed in embryonic stage. *Journal of Neurochemistry* **60**, 1554-1563.
- NANCE, M.A., PRATT, V.M., BOYADJIEV, S., TAYLOR, S., HODES, M.E. & DLOUHY, S.R. (1993) Adult-onset neurological disorder in a Pelizaeus-Merzbacher disease carrier mother (abstract). *Am J Hum Genet* **53**, 1745 (Abstract).
- NAVE, K., BLOOM, F.E. & MILNER, R.J. (1987) A single nucleotide difference in the gene for myelin proteolipid protein defines the *jimpy* mutation in mouse. *Journal of Neurochemistry* **49**, 1873-1877.
- NAVE, K., LAI, C., BLOOM, F.E. & MILNER, R.J. (1987) Splice site selection in the proteolipid protein (PLP) gene transcript and primary structure of the DM-20 protein of central nervous system myelin. *Proceedings of the National Academy of Sciences USA* **84**, 5665-5669.
- NAVE K., SCHNEIDER A., READHEAD C., GRIFFITHS I.R., PÜHLHOFER A., BARTHOLOMÄ A., GRAF S., KEIFER B. (1993) Molecular biology and neurogenetics of the proteolipid protein. In *A multidisciplinary approach to myelin diseases* (edited by SALVATI, S.), New York: Plenum Press.
- NAVE K.-A. (1996) Myelin-specific genes and their mutations in the mouse. In *Glial Cell Development. Basic Principles and Clinical Relevance* (edited by JESSEN, K.R., RICHARDSON, W.D.), pp. 141-164. Oxford: Bios.
- NAVE, K.-A. & LEMKE, G. (1991) Induction of the myelin proteolipid protein (PLP) gene in C6 glioblastoma cells: Functional analysis of the PLP promoter. *Journal of Neuroscience* **11**, 3060-3069.
- NORTON W.T., CAMMER W. (1984) Isolation and characterization of myelin. In *Myelin* (edited by MORELL, P.), pp. 147-196. New York and London: Plenum Press.
- NYBERG-HANSEN, R. (1964) The location and termination of tectospinal fibers in the cat. *Experimental Neurology* **9**, 212-227.

- ORIAN, J.M., MITCHELL, A.W.S., MARSHMAN, W.E., WEBB, G.C., AYERS, M.M., GRAIL, D., FORD, J.H., KAYE, A.H. & GONZALES, M.F. (1994) Insertional mutagenesis inducing hypomyelination in transgenic mice. *Journal of Neuroscience Research* **39**, 604-612.
- OTTERBACH, B., STOFFEL, W. & RAMAEKERS, V. (1993) A novel mutation in the proteolipid protein gene leading to Pelizaeus-Merzbacher disease. *Biol Chem Hoppe Seyler* **374**, 75-83.
- PARMANTIER, E., CABON, F., BRAUN, C., D'URSO, D., MÜLLER, H.W. & ZALC, B. (1995) Peripheral myelin protein-22 is expressed in rat and mouse brain and spinal cord motoneurons. *Eur J Neurosci* **7**, 1080-1088.
- PEDRAZA, L., FIDLER, L., STAUGAITIS, S.M. & COLMAN, D.R. (1997) The active transport of myelin basic protein into the nucleus suggests a regulatory role in myelination. *Neuron* **18**, 579-589.
- PERRY V.H. (1994) Macrophages and microglia in diseases of the CNS. In *Macrophages and the nervous system* (edited by PERRY, V.H.), pp. 87-101. Austin: R.G. Landes.
- PERRY, V.H., MATYSZAK, M.K. & FEARN, S. (1993) Altered antigen expression of microglia in the aged rodent CNS. *Glia* **7**, 60-67.
- POPOT, J.-L., DINH, D.P. & DAUTIGNY, A. (1991) Major myelin proteolipid: The 4- α -helix topology. *Journal of Membrane Biology* **120**, 233-246.
- PRATT, V.M., BOYADJIEV, S., DLOUHY, S.R., SILVER, K., DER KALOUSTIAN, V.M. & HODES, M.E. (1995) Pelizaeus-Merzbacher disease in a family of Portuguese origin caused by a point mutation in exon 5 of the proteolipid protein gene. *American Journal of Medical Genetics* **55**, 402-404.
- PRIBYL, T.M., CAMPAGNONI, C., KAMPF, K., HANDLEY, V.W. & CAMPAGNONI, A.T. (1996) The major myelin protein genes are expressed in the human thymus. *Journal of Neuroscience Research* **45**, 812-819.
- PUCKETT, C., HUDSON, L.D., ONO, K., BENECKE, J., DUBOIS-DALCQ, M. & LAZZARINI, R.A. (1987) Myelin-specific proteolipid protein is expressed in myelinating Schwann cells but is not incorporated into myelin sheaths. *Journal of Neuroscience Research* **18**, 511-518.

- QUARLES R.H., COLMAN D.R., SALZER J.L., TRAPP B.D. (1992) Myelin-associated glycoprotein: structure-function relationships and involvement in neurological diseases. In *Myelin: biology and chemistry* (edited by MARTENSON, R.E.), pp. 413-448. Boca Ranton: CRC Press Inc.
- RAFF, M.C., MIRSKY, R., FIELDS, K.L., LISAK, R.P., DORFMAN, S.H., SILBERBERG, D.H., GREGSON, N.A., LIEBOWITZ, S. & KENNEDY, M.C. (1978) Galactocerebroside is a specific marker for oligodendrocytes in culture. *Nature* **274**, 813-816.
- RAINE C.S. (1984) Morphology of myelin and myelination. In *Myelin* (edited by MORELL, P.), pp. 1-50. New York: Plenum Press.
- RASKIND, W.H., WILLIAMS, C.A., HUDSON, L.D. & BIRD, T.D. (1991) Complete deletion of the proteolipid protein gene (PLP) in a family with X-linked Pelizaeus-Merzbacher disease. *Am J Hum Genet* **49**, 1355-1360.
- READHEAD, C., POPKO, B., TAKAHASHI, N., SHINE, H.D., SAAVEDRA, R.A., SIDMAN, R.L. & HOOD, L. (1987) Expression of a myelin basic protein gene in transgenic shiverer mice: correction of the dysmyelinating phenotype. *Cell* **48**, 703-712.
- READHEAD, C., SCHNEIDER, A., GRIFFITHS, I.R. & NAVE, K. (1994) Premature arrest of myelin formation in transgenic mice with increased proteolipid protein gene dosage. *Neuron* **12**, 583-595.
- REMAHL, S. & HILDEBRAND, C. (1990) Relation between axons and oligodendroglial cells during initial myelination. I. The glial unit. *Journal of Neurocytology* **19**, 313-328.
- RICHARDSON W.D., PRINGLE N.P., YU W.-P., COLLARINI E.J., HALL A. (1997) Origins and early development of oligodendrocytes. In *Glial cell development: basic principles and clinical relevance* (edited by JESSEN, K.R., RICHARDSON, W.D.), pp. 53-70. Oxford: Bios Scientific Publishers.
- RODRIGUEZ, M., PRAYOONWIWAT, N., HOWE, C. & SANBORN, K. (1994) Proteolipid protein gene expression in demyelination and remyelination of the central nervous system: A model for multiple sclerosis. *J Neuropathol Exp Neurol* **53**, 136-143.

- ROGERS K.R., VOUYIOUKLIS D.A., BROPHY P.J. (1997) Molecular cell biology of oligodendrocytes. In *Molecular biology of multiple sclerosis* (edited by RUSSELL, W.C.), pp. 23-36. Chichester: John Wiley & Sons Ltd.
- ROSENBLUTH J. (1995) Pathology of demyelinated and dysmyelinated axons. In *The axon* (edited by WAXMAN, S.G., KOCSIS, J.D., STYS, P.K.), pp. 391-411. Oxford: Oxford University Press.
- ROSENFELD, J. & FRIEDRICH, V.L., JR. (1983) Axonal swellings in jimpy mice: does lack of myelin cause neuronal abnormalities? *Neuroscience* **10**, 959-966.
- SAUGIER-VEBER, P., MUNNICH, A., BONNEAU, D., ROZET, J.-M., LE MERRER, M., GIL, R. & BOESPFLUG-TANGUY, O. (1994) X-linked spastic paraplegia and Pelizaeus-Merzbacher disease are allelic disorders at the proteolipid protein locus. *Nature Genetics* **6**, 257-262.
- SANCHEZ, I., HASSINGER, L., PASKEVICH, P.A., SHINE, H.D. & NIXON, R.A. (1996) Oligodendroglia regulate the regional expansion of axon caliber and local accumulation of neurofilaments during development independently of myelin formation. *Journal of Neuroscience* **16**, 5095-5105.
- SCHEDL, A., ROSS, A., ENGELKAMP, D., RASHBASS, P., VAN HEYNINGEN, V. & HASTIE, N.D. (1996) Influence of PAX6 gene dosage on development: overexpression causes severe eye abnormalities. *Cell* **86**, 71-82.
- SCHERER, S.S. (1996) Molecular specializations at nodes and paranodes in peripheral nerve. *Microsc Res Tech* **34**, 452-461.
- SCHERER, S.S., BRAUN, P.E., GRINSPAN, J., COLLARINI, E., WANG, D. & KAMHOLZ, J. (1994) Differential regulation of the 2',3'-cyclic nucleotide 3'-phosphodiesterase gene during oligodendrocyte development. *Neuron* **12**, 1363-1375.
- SCHERER, S.S., VOGELBACKER, H.H. & KAMHOLZ, J. (1992) Axons modulate the expression of proteolipid protein in the CNS. *Journal of Neuroscience Research* **32**, 138-148.
- SCHLIESS, F. & STOFFEL, W. (1991) Evolution of the myelin integral membrane proteins of the central nervous system. *Biol Chem Hoppe Seyler* **372**, 865-874.
- SCHNEIDER, A., GRIFFITHS, I.R., READHEAD, C. & NAVE, K.-A. (1995) Dominant-negative action of the jimpy mutation in mice complemented with an

autosomal transgene for myelin proteolipid protein. *Proceedings of the National Academy of Sciences USA* **92**, 4447-4451.

SCHNEIDER, A., MONTAGUE, P., GRIFFITHS, I.R., FANARRAGA, M., KENNEDY, P.G.E., BROPHY, P.J. & NAVE, K. (1992) Uncoupling of hypomyelination and glial cell death by a mutation in the proteolipid protein gene. *Nature* **358**, 758-761.

SCHWAB, M.E. & BARTHOLDI, D. (1996) Degeneration and regeneration of axons in the lesioned spinal cord. *Physiological Reviews* **76**, 319-370.

SEREDA, M., GRIFFITHS, I.R., PÜHLHOFER, A., STEWART, H., ROSSNER, M.J., ZIMMERMANN, F., MAGYAR, J.P., SCHNEIDER, A., HUND, E., MEINCK, H.M., *ET AL.* (1996) A transgenic rat model of Charcot-Marie-Tooth disease. *Neuron* **16**, 1049-1060.

SHIOTA, C., IKENAKA, K. & MIKOSHIBA, K. (1991) Developmental expression of myelin protein genes in dysmyelinating mutant mice: Analysis by nuclear run-off transcription assay, in situ hybridization, and immunohistochemistry. *Journal of Neurochemistry* **56**, 818-826.

SINOWAY, M.P., KITAGAWA, K., TIMSIT, S., HASHIM, G.A. & COLMAN, D.R. (1994) Proteolipid protein interactions in transfectants: Implications for myelin assembly. *Journal of Neuroscience Research* **37**, 551-562.

SKOFF, R.P. (1982) Increased proliferation of oligodendrocytes in the hypomyelinated mouse mutant-jimpy. *Brain Research* **248**, 19-31.

SKOFF, R.P. (1990) Gliogenesis in rat optic nerve: astrocytes are generated in a single wave before oligodendrocytes. *Developmental Biology* **139**, 149-168.

SKOFF, R.P. (1995) Programmed cell death in the dysmyelinating mutants. *Brain Pathology* **5**, 283-288.

SKOFF, R.P. & GHANDOUR, M.S. (1995) Oligodendrocytes in female carriers of the jimpy gene make more myelin than normal oligodendrocytes. *Journal of Comparative Neurology* **355**, 124-133.

SMITH, R. (1992) The basic protein of CNS myelin: Its structure and ligand binding. *Journal of Neurochemistry* **59**, 1589-1608.

- SMITH, R., COOK, J. & DICKENS, P.A. (1984) Structure of the proteolipid protein extracted from bovine central nervous system myelin with nondenaturing detergents. *Journal of Neurochemistry* **42**, 306-313.
- SNIPES, G.J. & SUTER, U. (1995) Molecular anatomy and genetics of myelin proteins in the peripheral nervous system. *Journal of Anatomy* **186**, 483-494.
- SOBEL, R.A., GREER, J.M., ISAAC, J., FONDREN, G. & LEES, M.B. (1994) Immunolocalization of proteolipid protein peptide 103-116 in myelin. *Journal of Neuroscience Research* **37**, 36-43.
- SORG, B.A., AGRAWAL, D., AGRAWAL, H.C. & CAMPAGNONI, A.T. (1986) Expression of myelin proteolipid protein and basic protein in normal and dysmyelinating mutant mice. *Journal of Neurochemistry* **46**, 379-387.
- SORG, B.A., SMITH, M.M. & CAMPAGNONI, A.T. (1987) Developmental expression of the myelin proteolipid protein and basic protein mRNA in normal and dysmyelinating mutant mice. *Journal of Neurochemistry* **49**, 1146-1154.
- STAHL, N., HARRY, J. & POPKO, B. (1990) Quantitative analysis of myelin protein gene expression during development in the rat sciatic nerve. *Molecular Brain Research* **8**, 209-212.
- STOFFEL, W., HILLEN, H. & GIERSIEFEN, H. (1984) Structure and molecular arrangement of proteolipid protein of central nervous system myelin. *Proceedings of the National Academy of Sciences USA* **81**, 5012-5016.
- STOFFEL, W., HILLEN, H., SCHRODER, W. & DEUTZMANN, R. (1983) The primary structure of bovine brain myelin lipophilin (proteolipid apoprotein). *Hoppe-Seyler's Zeitschrift fuer Physiologische Chemie* **364**, 1455-1466.
- STURROCK, R.R. (1983) In *Problems of glial identification and quantification in the ageing central nervous system* (edited by CREVOS-NAVARR, J.; SARKANDER, I.H.), pp. 179-209. New York: Raven Press.
- SUN, N., GRZYBICKI, D., CASTRO, R.F., MURPHY, S. & PERLMAN, S. (1995) Activation of astrocytes in the spinal cord of mice chronically infected with a neurotropic coronavirus. *Virology* **213**, 482-493.
- SUTER, U. (1997) Myelin: Keeping nerves well wrapped up. *Current Biology* **7**, R21-R23.

- SUTER, U. & SNIPES, G.J. (1995) Peripheral myelin protein 22: Facts and hypotheses. *Journal of Neuroscience Research* **40**, 145-151.
- SZUCHET S. (1995) The morphology and structure of oligodendrocytes and their functional implications. In *Neuroglia* (edited by KETTENMANN, H., RANSOM, B.R.), pp. 23-43. Oxford: Oxford University Press.
- TETZLOFF, S.U. & BIZZOZERO, O.A. (1993) Proteolipid protein from the peripheral nervous system also contains covalently bound fatty acids. *Biochemical and Biophysical Research Communications* **193**, 1304-1310.
- THOMAS, P.K., KING, R.H.M., SMALL, J.R. & ROBERTSON, A.M. (1996) The pathology of Charcot-Marie-Tooth disease and related disorders. *Neuropathol Appl Neurobiol* **22**, 269-284.
- THOMSON, C.E., MONTAGUE, P., JUNG, M., NAVE, K., GRIFFITHS, I.R. (1997) Phenotypic severity of murine *Plp* mutants reflects *in vivo* and *in vitro* variations in transport of PLP isoproteins. *Glia* [In Press]
- TIMSIT, S., MARTINEZ, S., ALLINQUANT, B., PEYRON, F., PUELLES, L. & ZALC, B. (1995) Oligodendrocytes originate in a restricted zone of the embryonic ventral neural tube defined by DM-20 mRNA expression. *Journal of Neuroscience* **15**, 1012-1024.
- TIMSIT, S.G., BALLY-CUIF, L., COLMAN, D.R. & ZALC, B. (1992) DM-20 mRNA is expressed during the embryonic development of the nervous system of the mouse. *Journal of Neurochemistry* **58**, 1172-1175.
- TOSIC, M., DOLIVO, M., AMIGUET, P., DOMANSKA-JANIK, K. & MATTHIEU, J.-M. (1993) Paralytic tremor (*pt*) rabbit: A sex-linked mutation affecting proteolipid protein-gene expression. *Brain Res* **625**, 307-312.
- TOSIC, M., DOLIVO, M., DOMANSKA-JANIK, K. & MATTHIEU, J.-M. (1994) Paralytic tremor (*pt*): A new allele of the proteolipid protein gene in rabbits. *Journal of Neurochemistry* **63**, 2210-2216.
- TOSIC, M., GOW, A., DOLIVO, M., DOMANSKA-JANIK, K., LAZZARINI, R.A. & MATTHIEU, J.M. (1996) Proteolipid/DM-20 proteins bearing the paralytic tremor mutation in peripheral nerves and transfected Cos-7 cells. *Neurochemical Research* **21**, 423-430.

- TRAPP B.D. (1990) Distribution of myelin protein gene products in actively-myelinating oligodendrocytes. In *Cellular and Molecular Biology of Myelination* (edited by JESERICH, G., ALTHAUS, H.A., WAEHNELDT, T.V.), pp. 59-79. Berlin: Springer-Verlag.
- TRAPP, B.D. (1990) Myelin-associated glycoprotein: location and potential functions. *Annals of the New York Academy of Sciences* **605**, 29-43.
- TRAPP, B.D., NISHIYAMA, A., CHENG, D. & MACKLIN, E. (1997) Differentiation and death of premyelinating oligodendrocytes in developing rodent brain. *Journal of Cell Biology* **137**, 459-468.
- TROFATTER, J.A., DLOUHY, S.R., DEMYER, W., CONNEALLY, P.J. & HODES, M.E. (1989) Pelizaeus-Merzbacher disease: tight linkage to proteolipid protein gene exon variant. *Proceedings of the National Academy of Sciences USA* **86**, 9427-9430.
- TSUNEISHI, S., TAKADA, S., MOTOIKE, T., OHASHI, T., SANNO, K. & NAKAMURA, H. (1991) Effects of dexamethasone on the expression of myelin basic protein, proteolipid protein, and glial fibrillary acidic protein genes in developing rat brain. *Developmental Brain Research* **61**, 117-123.
- VELA, J.M., DALMAU, I., GONZALEZ, B. & CASTELLANO, B. (1996) The microglial reaction in spinal cords of jimpy mice is related to apoptotic oligodendrocytes. *Brain Res* **712**, 134-142.
- VERMEESCH, M.K., KNAPP, P.E., SKOFF, R.P., STUDZINSKI, D.M. & BENJAMINS, J.A. (1990) Death of individual oligodendrocytes in *jimpy* precedes expression of proteolipid protein. *Developmental Neuroscience* **12**, 303-315.
- WAEHNELDT, T.V. & MALOTKA, J. (1989) Presence of proteolipid protein in coelocanth brain myelin demonstrates tetrapod affinities and questions a chondrichthyan association. *Journal of Neurochemistry* **52**, 1941-1943.
- WAEHNELDT, T.V., MATTHIEU, J.-M. & JESERICH, G. (1986) Major central nervous system myelin glycoprotein of the African lungfish (*Protopterus dolloi*) cross reacts with myelin proteolipid protein antibodies, indicating a close phylogenetic relationship with amphibians. *Journal of Neurochemistry* **46**, 1387-1391.
- WAXMAN S.G., BLACK J.A. (1995) Axoglial interactions at the cellular and molecular levels in central nervous system myelinated fibers. In *Neuroglia* (edited

by KETTENMANN, H., RANSOM, B.R.), pp. 587-610. Oxford: Oxford University Press.

WEIMBS, T. & STOFFEL, W. (1992) Proteolipid protein (PLP) of CNS myelin: Positions of free, disulfide-bonded, and fatty acid thioester-linked cysteine residues and implications for the membrane topology of PLP. *Biochemistry* **31**, 12289-12296.

WIGHT, P.A., DUCHALA, C.S., READHEAD, C. & MACKLIN, W.B. (1993) A myelin proteolipid protein-LacZ fusion protein is developmentally regulated and targeted to the myelin membrane in transgenic mice. *Journal of Cell Biology* **123**, 443-454.

WILKINS, A.S. (1990) Position effects, methylation and inherited epigenetic states. *BioEssays* **12**, 385-386.

WILKINSON, H.J., BAILES, J.A. & MCMAHON, A.P. (1987) Expression of the proto-oncogene interleukin-1 is restricted to specific neural cells in the developing mouse embryo. *Cell* **50**, 79-88.

WILLARD H.F. (1995) The sex chromosomes and X inactivation. In *The metabolic and inherited basis of inherited disease* (edited by SCRIVER, C.R., BEAUDET, A.L., SLY, W.S.), pp. 719-737. New York: McGraw-Hill.

WILLARD, H.F. & RIORDAN, J.R. (1985) Assignment of the gene for myelin proteolipid protein to the X chromosome: implications for X-linked myelin disorders. *Science* **230**, 940-942.

WILLIAMS, B.P., READ, J. & PRICE, J. (1991) The generation of neurons and oligodendrocytes from a common precursor cell. *Neuron* **7**, 685-693.

WILLIAMS M.A. (1977) Stereological techniques. In *Practical Methods in Electron Microscopy. Vol. 6. Quantitative Methods in Biology* (edited by GLAUERT, A.M.), pp. 5-84. Amsterdam: North Holland.

WOOD P., BUNGE R.P. (1984) The biology of the oligodendrocyte. In *Oligodendroglia* (edited by NORTON, W.T.), pp. 1-46. New York: Plenum Press.

WRIGHT, M.D. & TOMLINSON, M.G. (1994) The ins and outs of the transmembrane 4 superfamily. *Immunol Today* **15**, 588-594.

YAMAGUCHI, Y., IKENAKA, K., NIINOBE, M., YAMADA, H. & MIKOSHIBA, K. (1996) Myelin proteolipid protein (PLP), but not DM-20, is an

- inositol hexakisphosphate-binding protein. *Journal of Biological Chemistry* **271**, 27838-27846.
- YAMAMOTO, Y., MIZUNO, R., NISHIMURA, T., OGAWA, Y., YOSHIKAWA, H., FUJIMURA, H., ADACHI, E., KISHIMOTO, T., YANAGIHARA, T. & SAKODA, S. (1994) Cloning and expression of myelin-associated oligodendrocytic basic protein. A novel basic protein constituting the central nervous system myelin. *Journal of Biological Chemistry* **269**, 31725-31730.
- YAN, Y., LAGENAUR, C. & NARAYANAN, V. (1993) Molecular cloning of M6: Identification of a PLP/DM20 gene family. *Neuron* **11**, 423-431.
- YAN, Y.M., NARAYANAN, V. & LAGENAUR, C. (1996) Expression of members of the proteolipid protein gene family in the developing murine central nervous system. *Journal of Comparative Neurology* **370**, 465-478.
- YANAGISAWA, K., MÖLLER, J.R., DUNCAN, I.D. & QUARLES, R.H. (1987) Disproportional expression of proteolipid protein and DM-20 in the X-linked, dysmyelinating shaking pup mutant. *Journal of Neurochemistry* **49**, 1912-1917.
- YANAGISAWA, K. & QUARLES, R.H. (1986) Jimpy mice: quantitation of myelin-associated glycoprotein and other proteins. *Journal of Neurochemistry* **47**, 322-325.
- YU, W.-P., COLLARINI, E.J., PRINGLE, N.P. & RICHARDSON, W.D. (1994) Embryonic expression of myelin genes: Evidence for a focal source of oligodendrocyte precursors in the ventricular zone of the neural tube. *Neuron* **12**, 1353-1362.
- ZAHLER, A.M. & ROTH, M.B. (1995) Distinct functions of SR proteins in recruitment of U1 small nuclear ribonucleoprotein to alternative 5' splice sites. *Proceedings of the National Academy of Sciences USA* **92**, 2642-2646.
- ZHU, W., WIGGINS, R.C. & KONAT, G.W. (1994) Glucocorticoid-induced upregulation of proteolipid protein and myelin-associated glycoprotein genes in C6 cells. *Journal of Neuroscience Research* **37**, 208-212.

